



The
University
Of
Sheffield.

The activity of the TGF beta superfamily in prostate cancer and the formation of bone metastases

Thesis submitted for the degree of doctor of philosophy by

Huda Faisal AL-Shaibi

**Supervised by
Dr. Colby Eaton
Prof. Tim Skerry
Prof. Jalaluddin Awlia
Prof. Mohammed Ardawi**

**Department of Human Metabolism
Medical School**

April 2015

Summary

Introduction: Bone metastasis is a key event responsible for the progression and morbidity in prostate cancer patients. Interactions between prostate cancer cells and the bone microenvironment facilitate survival of tumour cells and alter bone turnover, a process that enhances growth of metastases in this site. This study aimed to test the hypothesis that tumour derived TGF β signaling regulates the differentiation/growth of osteoblastic lineage cells and promotes survival and growth of prostate cancer cells in bone. **Findings:** In initial studies I showed that factors produced by prostate cancer (PC3RFP) cells increased the proliferation and suppressed the differentiation of osteoblastic cells (SaOS2 cells). I showed that interactions between prostate cancer and osteoblastic cells affected the expression of TGF- β superfamily genes in the latter. Noggin, a BMP antagonist was expressed and secreted by PC3RFP cells but expressed at very low levels by SaOS2 when these cells were grown alone. This pattern changed when SaOS2 cells were treated with PC3RFP conditioned media, with strong induction of Noggin being demonstrated. Silencing Noggin in PC3 cells removed the effects of conditioned medium on the growth of SaOS2 cells, while media containing recombinant Noggin stimulated growth. Together these studies identify Noggin as an important regulator of osteoblast lineage cells that can be either directly secreted by tumour cells or induced in the bone cells by factors derived from prostate cancer cells. The latter is an important, novel finding of this study.

Xenograft experiments to test the role of Noggin on tumour colonization were inconclusive however; immunohistochemistry showed that in tibiae of tumour bearing mice, strong Noggin protein staining was found on the bone surface and in bone lining cells in close proximity to tumour foci.

Conclusion: These studies suggest that tumour derived/induced Noggin may play a role in suppression of osteoblast differentiation in prostate cancer bone metastases.

Acknowledgments

In the name of Allah, the most Gracious, the most Merciful. Thanks be to Allah for giving me the strength and the blessing to complete this thesis.

I would first like to thank my supervisor, Dr Colby Eaton, for his supervision, patience, continuous support and unlimited encouragement throughout my period of study. Many thanks are also due to my co-supervisors Prof. Tim Skerry, Prof. Jalal Aldine Aazm jalal and Prof. Mohammed Ardawi. I would also like to thank Prof. Peter Croucher for giving me the opportunity to work in his department in Sheffield.

I truly appreciate and would like to sincerely thank every member of the Human Metabolism Department at the University of Sheffield who offered me help or assistance along the way. Most notably I would like to thank Dr Clive Buckle for all his guidance in the gene expression analysis studies and Dr Julia Hough for her instruction in the lentiviral work described in this thesis. I would also like to thank Mrs Orla Gallagher, Mrs Anne Fowles, Dr Ning Wang, Mrs Susan Newton and Mrs Kay Hopkinson who all gave me support and guidance in various other aspects of my research in Sheffield.

My thanks are extended to the members of King Fahad Research Center, Joint Supervision Program (JSP) and the Center of Excellence in Genomic Medicine Research (CEGMR) Particularly Dr Farid Ahmad, Manal AL-Otibi, Fatma Kadi, Manal Shaabad, Maha AL-quaiti, ALjowhara Khelif and Mr Zaki Assouli for their help and unwavering support.

My appreciation and thanks extends to Dr Marco G. Cecchini from the Urology Research Laboratory University of Bern, Switzerland for his kind gift PC3-Noggin KD clone 14 and PC3-mock clone 4 cells that were used in some studies undertaken in Sheffield.

I would also like to thank my colleagues Zara, Osama and Freyja for their help and support during many difficult periods over the duration of my study and thesis preparation

Finally, I wish to dedicate this work to the memory of my late father Faisal, and to my Mother Amal who's prayers and support throughout my journey gave me the strength to pursue my dream to its realization.

My heartfelt appreciation goes to my husband Mohammed with out his love and support I would not have been able to finish this thesis. I would also like to thank my children Abdulrahman, Sara, Malik and Khaled, my brothers Dr Khaled, Dr Mohammed and my sister Dr Khairiah and my Friends Ulfat, Asma, Hind, Rana, Rania and Hadeel for their unlimited encouragement to persevere and complete this study.

Declaration

The work presented in this thesis was carried out by the candidate, with the following exceptions: processing of tissue samples for immune-histochemistry and scoring was performed by Mrs Orla Gallagher¹ and Mrs Anne Fowles¹; work with mice in the animal house was performed by Mrs Anne Fowles¹ and Dr Ning Wang¹; Flow cytometry and cell sorting was performed by Mrs Susan Newton¹, Mrs Kay Hopkinson¹ and Dr. Farid Ahmad².

¹Department of Human metabolism, University of Sheffield, Sheffield, UK;

²Center of Excellence In Genomic Medicine, King Abdulaziz University, Jeddah, Saudi Arabia.

Table of Contents

Summary.....	I
Acknowledgments.....	II
Declaration.....	IV
List of Figures.....	XIV
List of Tables.....	XVIII
List of Abbreviation.....	XIX
Chapter 1 Introduction and Background.....	1
1.1 General structure and function of bone.....	1
1.1.1 Bone cells.....	1
1.1.2 Osteoblasts.....	2
1.1.3 Bone lining cells.....	2
1.1.4 Osteocytes.....	2
1.1.5 Osteoclasts.....	3
1.1.6 Bone modeling and Remodling.....	3
1.2 Epidemiology of prostate cancer.....	6
1.2.1 Prostate cancer and Bone metastases.....	7
1.3 The transforming growth factor beta (TGF- β) superfamily and its signaling pathway	8
1.3.1 TGF- β structure.....	9
1.3.2 TGF- β function.....	10
1.3.3 Bone morphogenetic proteins (BMP) structure.....	10
1.3.4 BMP function.....	11
1.3.5 BMP antagonist Noggin structure.....	12
1.3.6 Noggin function	13
1.3.7 The TGF- β superfamily signaling pathway	13

1.4 The role TGF- β plays in different mechanisms.....	20
1.4.1 Apoptosis.....	20
1.4.2 Epithelial-mesenchymal transition and migratory responses.....	22
1.4.3 Cell proliferation	23
1.4.4 Matrix regulation	24
1.4.5 Cell differentiation	24
1.4.6 Tumour mediated immunosuppression	24
1.5 TGF- β superfamily expression and activities in prostate cancer and survival....	25
1.6 Bone microenvironment in tumour growth: a “vicious cycle”... ..	27
1.7 Growth factors as mediators of the bone microenvironment.....	28
1.8 The role of TGF- β in the initiation of bone metastases	29
1.9 Modulation of the TGF- β signaling as a strategy to suppress the formation of the bone metastases.....	32
1.10 Aim of the study	34
Chapter 2 Material and Method.....	36
2.1 Tissue culture materials and disposable equipment.....	36
2.2 Tissue culture techniques.....	36
2.2.1 Cell lines.....	36
2.2.2 Maintaining and sub-culturing of cell lines.....	37
2.2.3 Cell harvesting by trypsinisation.....	38
2.2.4 Thawing and freezing of the cells.....	38
2.2.4.1 Freezing cells.....	38
2.2.4.2 Thawing cells.....	38
2.2.5 Cell counting using Beckman Coulter Vi-cell ^{XR} Cell Viability Analyzer.....	38

2.3 Molecular techniques.....	39
2.3.1 Materials and disposable equipment used for RNA extraction.....	39
2.3.2 RNA extraction from cells using Qiagen RNAeasy Mini Kit.....	40
2.3.3 Quantification of RNA.....	41
2.3.4 Analyzing the RNA integrity using the RNA 6000 Nano Bioanalyzer Kit.....	41
2.3.5 Reverse Transcription and cDNA production.....	43
2.3.6 Quantitative real time PCR.....	44
2.4 Western blot.....	44
2.4.1 Protein extraction using Radio-Immunoprecipitation Assay (RIPA) buffer.....	46
2.4.2 Bicinchoninic acid (BCA) protein assay.....	46
2.4.3 Sample preparation.....	47
2.4.4 Sodium-Dodecyl-Sulphate Poly-Acrylamid Gel Electrophoresis (SDS-PAGE).....	47
2.4.5 Protein transfer	48
2.4.6 Immuno-detection of Noggin on western blots.....	49
2.4.7 Antibody stripping and membrane re-probing.....	50
2.5 Cell sorting using flow cytometry BD FACS Aria	50
2.6 Statistical analysis.....	50
Chapter 3 General characterization of cell lines and assessment of the effects of prostate cancer cells on osteoblastic cell proliferation and differentiation..	51
3.1 Introduction	51
3.2 Materials and methods.....	53
3.2.1 Materials and disposable equipment.....	53
3.2.2 Generating growth curves.....	53

3.2.3 Generating serum titration curves.....	53
3.2.4 Generating condition media from PC3RFP cells.....	54
3.2.5 Challenging the SaOS2 cell with the condition media (CM)	54
3.2.6 Analysis of the effect of condition media (CM) on the proliferation of osteoblastic cell lines.....	54
3.2.7 Differentiating MG63 by using differentiation media.....	55
3.2.8 Analysing the effects of condition media on the proliferation of differentiated MG63.....	55
3.2.9 Analysis of the effects of condition media and co-culture on the differentiation of osteoblastic cell lines.....	55
3.2.9.1 Alkaline phosphatase activity assay.....	56
3.2.9.2 PicoGreen assay.....	57
3.2.9.3 Alizarin red staining.....	58
3.2.9.4 Differentiation gene expression (Runx2, Osterix and COL1A).....	59
3.3 Results.....	60
3.3.1 Characterization of osteoblastic cell lines.....	60
3.3.2 Characterization of the PC3RFP prostate cancer cell line.....	61
3.3.3 Studies of the effect of various conditioned media concentrations on the growth of osteoblastic cell lines.....	62
3.3.4 Studies of the effects of conditioned media on the proliferation of osteoblastic cell lines.....	62
3.3.5 Differentiating MG63 cells by using differentiation media.....	64
3.3.6 Assessment of the effects of conditioned media on the proliferation of differentiated MG63.....	64
3.3.7 Assessment of the effect of CM and co-culture on the differentiation of osteoblastic cell lines.....	65

3.3.7.1 Analysis of alkaline phosphatase activity in osteoblasts.....	65
3.3.7.2 Analysis of mineralisation measured by alizarin red staining in osteoblastic cell lines.....	70
3.3.7.3 Expression of osteoblast differentiation genes COL1A, Osterix and Runx2 in osteoblastic cell lines.....	73
3.4 Discussion.....	76
3.4.1 Cells growth characterisation.....	76
3.4.2 The effect of prostatic cancer cells on the proliferation and differentiation of osteoblast cells.....	76
Chapter 4 Comparative gene expression profiles for the TGF-β superfamily in human prostatic cancer and osteoblastic cell lines grown alone and in direct/indirect contact.....	80
4.1 Introduction.....	80
4.2 Material and method.....	84
4.2.1 Materials and disposable equipment.....	84
4.2.2 Identifying the ability of PC3RFP to form colonies when seeded over osteoblast cell lines.....	84
4.2.3 Real-time RT-PCR using TaqMan Express tm plates to evaluate TGF- β superfamily gene expression in prostate cancer cell line and osteosarcoma cell lines.....	86
4.2.4 Real-time RT-PCR using TaqMan Express tm plates to evaluate TGF- β superfamily gene expression in co-cultured cells	87
4.2.5 Analysis of Noggin protein concentrations in PC3RFP condition media by ELISA.....	87
4.2.6 Further analysis of the effects of PC3RFP-CM and co-culture on Noggin expression in osteoblast cell lines using QRT-PCR.....	90
4.2.7 Immunofluorescence detection of Noggin in co-culture and in osteoblast grown in PC3RFP-CM.....	90

4.2.8 Detection of Noggin protein in co-cultures and in osteoblasts treated with PC3RFP-CM by using flow cytometry.....	92
4.2.8.1 Preparation of cells.....	92
4.2.9 Detection of Noggin in co-cultures and in osteoblast treated with PC3RFP-CM using western blot.....	93
4.3 Results.....	94
4.3.1 Analysis of TGF- β superfamily expression.....	94
4.3.1.1 Comparison of PC3RFP/SaOS2 gene expression in exponential and confluent phase.....	94
4.3.1.2 Comparison of PCRFP and SaOS2 cells grown alone in confluent phase.....	95
4.3.1.3 Comparison of PCRFP and MG63 cells grown alone in confluent phase.....	98
4.3.1.4 Comparison of SaOS2 gene expression grown alone and in co-culture with PC3RFP.....	100
4.3.1.5 Comparison of PC3RFP gene expression in these cells grown alone and in co-culture with SaOS2.....	102
4.3.1.6 Comparison of MG63 gene expression in these cells grown alone and in co-culture with PC3RFP.....	102
4.3.1.7 Comparison of PC3RFP gene expression in these cells grown alone and in co-culture with MG63.....	104
4.3.1.8 Comparison of SaOS2 gene expression in these cells grown in standard control medium and in SaOS2 treated with PC3RFP-CM.....	106
4.3.1.9 Comparison of MG63 gene expression in these cells grown in standard control medium and in MG63 treated with PC3RFP-CM.....	107
4.3.2 Detection of Noggin protein in PC3RFP condition media by ELISA.....	109
4.3.3 Effect of PC3RFP-CM and co-culture on Noggin expression in osteosarcoma cells using QRT-PCR.....	109

4.3.4 Immunofluorescence detection of Noggin in co-culture and in osteoblast grown in 50% PC3RFP-CM.....	110
4.3.5 Detection of Noggin protein in co-cultured SaOS2 and in SaOS2 treated with PC3RFP-CM by using flow cytometry.....	111
4.3.6 Detection of Noggin protein in co-cultured osteoblasts and in osteoblasts treated with PC3RFP-CM by using western blot.....	114
4.4 Discussion.....	116
4.4.1 The expression of the TGF- β superfamily in individual prostate cancer and osteoblastic cell populations and in cultures where these cells are in direct (i.e. via CM) or in direct contact in co-culture model.....	116
4.4.2 Effect of prostate cancer cells on Noggin expression by osteoblasts.....	117
Chapter 5 Noggin knockdown in PC3RFP and the effect of recombinant Noggin on osteoblast proliferation.....	122
5.1 Introduction	122
5.2 Material and method.....	125
5.2.1 Materials and disposable equipment.....	125
5.2.2 Knockdown Noggin in PC3RFP using Noggin short hairpin RNA (shRNA) Lentiviral	125
5.2.2.1 Polybrene killing curve.....	125
5.2.2.2 Puromycin killing curve.....	126
5.2.2.3 Lentiviral infection/transduction PC3RFP.....	126
5.2.3 Detection the presence of Noggin in PC3RFP-KD by QPCR.....	126
5.2.4 Detection the presence of Noggin protein in knockdown PC3RFP by western blot.....	127
5.2.5 Detection the presence of Noggin protein in conditioned media collected over knockdown PC3RFP by ELISA.....	127
5.2.6 Collecting conditioned media from PC3-KD and PC3-Mock cells.....	127

5.2.7 Analysing the effects of PC3-KD conditioned media on the proliferation of osteoblast cells (SaOS2) cells.....	127
5.2.8 Selecting Recombinant Noggin concentrations.....	127
5.2.9 Effect of recombinant Noggin on the proliferation of osteoblast (SaOS2) cells.....	128
5.3 Results.....	129
5.3.1 Polybrene and Puromycin killing curve.....	129
5.3.2 Validation of Noggin knockdown in PC3RFP cells by QPCR.....	129
5.3.3 Validation of Noggin knockdown in PC3RFP cells by ELISA.....	130
5.3.4 Validation of Noggin knockdown in PC3RFP cells by western blot.....	131
5.3.5 Validation of the stability of Noggin knockdown in PC3-KD clone 14 cells by QPCR and western blot.....	132
5.3.6 Effect of PC3-KD condition media on the proliferation of osteoblast (SaOS2) cells	133
5.3.7 Selecting recombinant Noggin concentration.....	134
5.3.8 Effect of recombinant Noggin on the proliferation of osteoblast (SaOS2) cells.....	135
5.4 Discussion.....	136
Chapter 6 Noggin in the interactions of prostate cancer with osteoblasts <i>in vivo</i>.....	139
6.1 Introduction.....	139
6.2 Material and method.....	141
6.2.1 Materials and disposable equipment.....	141
6.2.2 Cell line.....	141
6.2.3 Mice.....	141
6.2.4 <i>in vivo</i> imaging system (IVIS).....	141

6.2.5 PC3-mock and PC3-KD cells labelling with DiD solution.....	142
6.2.6 Intra-cardiac injection of PC3-mock and PC3-KD cells into immunosuppressed mice.....	142
6.2.7 Harvesting trabecular bone from mice.....	142
6.2.8 High-resolution micro-computed tomography (μ CT).....	143
6.2.9 Immunohistochemistry detection of Noggin in trabecular bone.....	143
6.3 Results.....	145
6.3.1 Effect of knockdown Noggin in prostate cancer cells on bone and their ability to form tumours.....	145
6.3.2 Noggin was expressed on the bone lining cells and bone surface <i>in vivo</i> in BALB/C nude male mice.....	149
6.4 Discussion.....	152
Chapter 7 General Discussion.....	155
7.1 General discussion.....	155
7.2 Future work.....	165
REFERENCE.....	167
APPENDIX A.....	199

List of Figures

Figure 1.1 The bone remodeling cycle.	6
Figure 1.2 Prostate Cancer Incidence	7
Figure 1.3 TGF- β structure.	9
Figure 1.4 BMP structure.	11
Figure 1.5 Structural relationships in the Smad family.	15
Figure 1.6 Smads domains.	16
Figure 1.7 Signaling specificity in the TGF- β superfamily.	17
Figure 1.8 TGF- β signaling pathways.	19
Figure 1.9 Possible multiple roles of TGF- β in tumour pathogenesis.	20
Figure 1.10 TGF- β stimulating apoptosis.	22
Figure 1.11 The vicious cycle of bone metastases.	28
Figure 1.12 Bone metastases in prostate cancer.	30
Figure 1.13 Role of TGF β in breast cancer metastasis	31
Figure 2.1 Plasmid map for the pDSRed-monomer-hyg-C1 used to produce PC3 RFP cells.	37
Figure 2.2 RNA integrity using RNA 6000 Nano Bioanalyzed kit.	42
Figure 2.3 Example of Protein assay standard curve.	46
Figure 2.4 Diagram illustrating the transfer apparatus for western blotting	49
Figure 3.1 Summarizes the design for the seeding of osteoblast cells in the 96 well plate for measuring ALP activity.	56
Figure 3.2 illustrate the DNA standard curve and the concentration that were used in the picoGreen assay.	58
Figure 3.3 Characterization of SaOS2 cell.	60
Figure 3.4 Characterization of MG63 cells.	61
Figure 3.5 Characterization of PC3RFP cell.	61
Figure 3.6 Assessment of the effect of different CM concentrations on the growth of SaOS2 cells during exponential growth.	62
Figure 3.7 Conditioned media (CM) increased the proliferation of SaOS2 cells.	63
Figure 3.8 Conditioned media (CM) did not affect the proliferation of MG63 cells. ...	63

Figure 3.9 Assessment of the effects of differentiating media on MG63.	64
Figure 3.10 Condition media had no effect on the proliferation of differentiated MG63 cells.....	65
Figure 3.11 Differentiation of SaOS2 cells were decreased by CM.....	67
Figure 3.12 Differentiation of MG63 cells was decreased by CM and co-culture at some time points.....	68
Figure 3.13 Differences in ALP activity in Osteoblastic cell lines evaluated over 12 days in the presence/absence of CM or co-culture with PC3RFP.....	69
Figure 3.14 Differences in ALP activity in PC3RFP cell lines evaluated over 12 days.	69
Figure 3.15 Mineralisation in SaOS2 cells was significantly increased in co-cultures with PC3-RFP but not by CM.....	70
Figure 3.16 Differences between SaOS2 and MG63 in Alizarin Red staining during 12 days.	71
Figure 3.17 Mineralization in MG63 was varyingly affected by CM and in co-cultures with PC3RFP.	72
Figure 3.18 Differences in Alizarin Red staining in Osteoblastic cell lines during 12 days.	73
Figure 3.19 Summary of the levels of expression of osteoblast markers; Runx2, COL1A2 and osterix in the SaOS2 cell line.	74
Figure 3.20 Summary of the levels of expression of osteoblast markers; Runx2, COL1A2 and osterix in the MG63 cell line.....	75
Figure 4.1 over view of Noggin antagonist affect on BMPs proteins during bone and cartilage formation.	82
Figure 4.2 Fluorescent images of PC3RFP colonies formed over SaOS2 cells.....	85
Figure 4.3 Fluorescent images of PC3RFP colonies formed over MG63 cells.....	86
Figure 4.4 Preparing serial standard dilutions from stock standard solution for ELISA.	88
Figure 4.5 Layout for 8 well chamber slides.	91
Figure 4.6 Scheme showing how samples were prepared for flow cytometry.....	93
Figure 4.7 Array Plate analysis in exponential SaOS2 compared to confluent SaOS2 in TGF- β superfamily genes.....	94
Figure 4.8 Array plate analysis in exponential PC3RFP compared to confluent PC3RFP in TGF- β superfamily genes.....	95

Figure 4.9 Array plate analysis of TGF- β superfamily genes in PC3RFP compared to SaOS2 during the confluent phase.....	96
Figure 4.10 Array plate analysis of the major differences between confluent PC3RFP and Confluent SaOS2 in TGF- β superfamily genes.	97
Figure 4.11 Array plate analysis of TGF- β superfamily genes in MG63 compared to PC3RFP during the confluent phase.....	98
Figure 4.12 Array plate analysis of the major differences between confluent PC3RFP and Confluent MG63 in TGF- β superfamily genes.	99
Figure 4.13 Array plate analysis of TGF- β superfamily genes in co-cultured SaOS2 compared to control SaOS2 during the confluent phase.....	100
Figure 4.14 Array plate analysis of the major differences between confluent SaOS2 and co-cultured SaOS2 in TGF- β superfamily genes.....	101
Figure 4.15 Array plate analysis of TGF- β superfamily genes in co-cultured PC3RFP/with SaOS2 compared to control PC3RFP during confluent phase.....	102
Figure 4.16 Array plate analysis of TGF- β superfamily genes in co-cultured MG63 compared to control MG63 during the confluent phase.....	103
Figure 4.17 Array plate analysis of the major differences between confluent MG63 and co-cultured MG63 in TGF- β superfamily genes.....	104
Figure 4.18 Array plate analysis of TGF- β superfamily genes in co-cultured PC3RFP/with MG63 compared to control PC3RFP during confluent phase.....	105
Figure 4.19 Array plate analysis of the major differences between co-cultured PC3RFP with MG63 compared to control PC3RFP cells in TGF- β superfamily genes.....	105
Figure 4.20 Array plate analysis of TGF- β superfamily genes in confluent SaOS2 compared to SaOS2 treated with PC3RFP-CM.....	106
Figure 4.21 Array plate analysis of the major differences between confluent SaOS2 and SaOS2 treated with PC3RFP-CM in TGF- β superfamily genes.	107
Figure 4.22 Array plate analysis of TGF- β superfamily genes in confluent MG63 compared to MG63 treated with PC3RFP-CM.....	108
Figure 4.23 Array plate analysis of the major differences between confluent MG63 and MG63 treated with PC3RFP-CM in TGF- β superfamily genes.....	108
Figure 4.24 Noggin Standard curve.....	109
Figure 4.25 Noggin mRNA expression was increased in osteoblast cells.....	110
Figure 4.26 The level of Noggin protein fluorescent was increased in co-culture and PC3RFP-CM groups.....	111
Figure 4.27 Noggin protein expression was significantly increased in SaOS2 cells treated with PC3RFP-CM and significantly decreased in co-cultured PC3RFP compared to control cells.....	112

Figure 4.28 A: Analysis of Noggin protein expression in SaOS2 treated with PC3RFP-CM compared to control cells using BD FACS Aria.	113
Figure 4.28 B: Analysis of Noggin protein expression in co-culture SaOS2 cells using FACS Aria.	114
Figure 4.29 Protein Noggin expression in PC3RFP, co-cultured PC3RFP, SaOS2 treated with PC3RFP-CM and co-cultured by western blot.	115
Figure 4.30 diagram summarizing gene expression pattern in prostate cancer cells and osteoblast cells during different experimental condition compared to control cells.	121
Figure 5.1 Polybrene and Puromycin killing curve.	129
Figure 5.2 Noggin expression in PC3RFP-KD and PC3RFP-Mock.	130
Figure 5.3 Noggin protein levels in PC3RFP-KD and PC3RFP-mock conditioned media.	131
Figure 5.4 Noggin protein production profile in PC3RFP-KD and PC3RFP-mock cells.	132
Figure 5.5 Noggin expressions in PC3-KD and PC3-mock cells.	133
Figure 5.6 Conditioned media from Noggin knockdown PC3-KD cells reduced the proliferation of SaOS2 cells.	134
Figure 5.7 The effect of various recombinant Noggin concentrations on the growth of SaOS2 cells.	135
Figure 5.8 Recombinant Noggin stimulates SaOS2 proliferation.	135
Figure 6.1 Experimental design of the in vivo study.	142
Figure 6.2 In vivo imaging of PC3 mock and PC3KD (Noggin) in cohorts of mice using bioluminescence detected using the IVIS system.	146
Figure 6.3 Effect of knockdown Noggin in prostate cancer cell line on bone disease in trabecular tibia bone using BALB/C nude male mice aged 12 weeks.	148
Figure 6.4 Immunohistochemistry optimization of Noggin protein in trabecular tibia bone.	150
Figure 6.5 Noggin was expressed on the bone lining cells and bone surface in vivo in BALB/C nude male mice.	151
Figure 7.1 Scheme showing the role of TGF- β , BMP7 and Noggin in cancer invasion and colonization.	164

List of Table

Table 4.1 illustrate the design of the TaqMan TGF- β Express plate that was used to quantified the RNA expression in all samples by real time PCR.	89
Table 6.1 summaries IVIS images of mice in all groups.	147
Table 1A Express plate gene expression in exponential SaOS2 and confluent SaOS2 cells.	199
Table 2A Express plate gene expression in exponential PC3RFP and confluent PC3RFP cells.	201
Table 3A Express plate gene expression in confluent PC3RFP and SaOS2 cells.	203
Table 4A Express plate gene expression in confluent PC3RFP and MG63 cells.	205
Table 5A TGF β superfamily gene expression in co-culture SaOS2 compared to control SaOS2 cells.	207
Table 6A TGF β superfamily gene expression in co-cultured PC3RFP with SaOS2 compared to control PC3RFP cells.	209
Table 7A TGF β superfamily gene expression in co-culture MG63 compared to control MG63 cells.	211
Table 8A TGF β superfamily gene expression in co-cultured PC3RFP with MG63 compared to control PC3RFP cells.	213
Table 9A Expressed plate gene expression in confluent SaOS2 compared to SaOS2 treated with PC3RFP-CM.	215
Table 10A Expressed plate gene expression in confluent MG63 compared to MG63 treated with PC3RFP-CM.	217

List of Abbreviation

ActR-II	Activin Receptor type II
ActR-IIB	Activin Receptor type IIB
ActRIB	Activin receptor type IB
ACVR1	Activin receptor 1
ACVR2A	Activin receptor type-2 A
Akt	Serine/threonine-specific protein kinase
ALK 4	Activin receptor-like kinase 4
ALP	Alkaline phosphatase
ANGPTL4	Angiopoietin-like 4
APS	Ammonium persulphate
BCA	Bicinchoninic acid
BMP	Bone morphogenetic protein
BMP10	Bone morphogenetic protein 10
BMP2	Bone morphogenetic protein 2
BMP3	Bone morphogenetic protein 3
BMP4	Bone morphogenetic protein 4
BMP5	Bone morphogenetic protein 5
BMP6	Bone morphogenetic protein 6
BMP7	Bone morphogenetic protein 7
BMP8A	Bone morphogenetic protein 8A
BMP8B	Bone morphogenetic protein 8B
BMPR-II	Bone morphogenetic protein receptor type II
BMPR1A	Bone morphogenetic protein receptor 1 A
BMPR1B	Bone morphogenetic protein receptor 1 B
BSA	Bovine serum albumin
CER1	Cerbeus 1
CHRD	Chordin
COL1A	Collagen type I alpha 1
CSF-1	Colony stimulating factor 1

CTGF	Connective tissue growth factor
CXCR4	Chemokine receptor 4
DAPK	Death-associated protein kinase
DiD	1,1'-dioctadecyl-3,3,3',3'- tetramethylindodicarbocyanine perchlorate
DKK-1	Dickkopf homologue 1
DMEM	Dulbecco's Modified Eagle Medium
DMSO	Dimethyl sulfoxide
dNTP	Deoxynucleoside triphosphates
EDTA	Ethylenediaminetetraacetic acid
EMT	Epithelial - mesenchymal transitions
ENG	Endoglin
EphB	Ephrin B
ET-1	Endothelin-1
FBS	Fetal Bovine Serum
FGF	Fibroblast growth factor
FGF2	Fibroblast growth factor
FST	Follistatin
GAPDH	Glyceraldehyde-3-phosphate dehydrogenase
GDF	Growth and differentiation factors
GDF1;LASS1	Growth differentiation Factor 1
GDF11	Growth differentiation Factor 11
GDF2	Growth differentiation Factor 2
GDF3	Growth differentiation Factor 3
GDF6	Growth differentiation Factor 6
GDF7	Growth differentiation Factor 7
GDF9	Growth differentiation Factor 9
GREM1	Gremlin 1
HRP	Horse Radish peroxidase
ID1	Inhibition of differentiation/DNA binding1
IFN γ	Interferon gamma
IGF-1	Insulin-like growth factor 1

IGF-2	Insulin-like growth factor 2
IL-1	Interleukin 1
IL-6	Interleukin 6
INH A	Inhibin alpha
INHBA	inhibin beta A
INHBB	Inhibin beta B
INHBC	Inhibin beta C
INHBE	Inhibin beta E
LAK	Lymphokine activated killer cells
LEFTY2	Lefty 2
LTBP1	Latent-transforming growth factor beta binding protein 1
MAPK	Mitogen-activated protein kinase
MET	Mesenchymal- Epithelial transitions
MH1	Mad homology 1
MH2	Mad homology 2
MMP-2,9	Matrix metalloproteinases 2,9
MSCs	Mesenchymal stem cells
NBF	Neutral buffered formalin
NBL1	Neuroblastoma 1
NFkB	Nuclear factor-kB
NK	Natural killer
NOG	Noggin
OPG	Osteoprotegerin
PAGE	Polyacrylamide gel electrophoresis
PAI-1	Plasminogen activator inhibitor 1
PAP	Prostatic acid phosphatase
PBS	Dulbecco's phosphate buffer saline
PDGF	Platelet derived growth factor
PGE2	Prostaglandin E2 receptor
PKA	Protein kinase A
pNPP	p-Nitrophenyl phosphate

PSA	Prostate specific antigen
PTH	Parathyroid hormone
PVDF	Polyvinylidene fluoride
RANKL	Receptor activator of NF- κ B ligand
RER	Rough endoplasmic reticula
RFP	Red fluorescent protein
RIPA	Radio-Immunoprecipitation Assay
RLT	RNeasy Lysis Buffer
RUNX2	Runt-related transcription factor 2
SDS	Sodium dodecyl sulfate
SHH	Sonic hedgehog
SOST	Sclerostin
TAK1	TGF- β activated kinase-1
TEMED	Tetramethylethylenediamine
TGF- β	Transforming growth factor beta
TGF- β 1	Transforming growth factor beta 1
TGF- β 2	Transforming growth factor beta 2
TGF- β 3	Transforming growth factor beta 3
TGFBR1	Transforming growth factor beta receptor 1
TGFBR2	Transforming growth factor beta receptor 2
TGFBR3	Transforming growth factor beta receptor 3
TIEG1	TGF- β -inducible early response gene 1
TNF α	Tumour necrosis factor alpha
TRAF	TNF receptor associated factor
uPA	Urinary plasminogen activator
VEGF	Vascular endothelial growth factor
Wnt	Wingless

Chapter1 Introduction and Background

1 Chapter1 Introduction and Background

1.1 General structure and function of bone

Bone is considered the major constituent of the skeleton. It is formed through two different ossification processes: intramembranous and endochondral. The difference between these two processes is that endochondral ossification is thought to be a complex multi-step process that requires the presence of a cartilaginous blastema as a template for axial and appendicular bone development (Prasanna Bukka *et al.* 2004). Intramembranous ossification gives rise to flat bones of the skull and parts of clavicle bones directly from mesenchymal cells, which then condense, and differentiate into osteoblasts. However, long bones are formed as a result of combined action between the two processes endochondral and membranous ossification (Taichman 2005)

Bones of adult human skeleton are composed of 80% cortical bone and 20% trabecular bone. This ratio varies according to different bones and skeletal sites within the bone itself (Eriksen *et al.* 1994). Cortical bone surrounds the marrow space and is characterized by a dense and solid appearance, a structure that generally gives mechanical strength, while trabecular bone is composed of a honeycomb like network of trabecular plates and rods scattered in the bone marrow compartment and is associated with higher metabolic capabilities (Eriksen *et al.* 1994).

Human skeleton aids different functions including providing a structural support and permitting body movement. It also protects the vital internal organs of the body. It plays an important role in maintaining mineral homeostasis and acid base balance. In addition it acts as a reservoir of several growth factors and cytokines and furthermore provides the environment for hematopoiesis in the marrow cavity (Taichman 2005).

1.1.1 Bone cells

Bone is composed from four types of cells: osteoblasts, osteocytes, bone-lining cells and osteoclasts (Marks and Popoff 1988). These cells may be classified according to their relationship to cells from which they originate: mesenchymal stem cells are the progenitors of osteoblasts, osteocytes and bone lining cells while, osteoclasts originate from hemopoietic cells. Another classification has been developed based on their function to bone forming (osteoblasts) and bone resorption (osteoclasts) cells. Osteoblasts, osteoclasts and osteocytes are located along the surface of the bone, whereas osteocytes are located in the interior of the bone (Marks and Odgren 1996; Ducky *et al.* 2000).

1.1.2 Osteoblasts

Active mature osteoblasts that are capable of synthesizing bone matrix are oval in shape with large nuclei located within the center of the cells. These cells contain large amounts of rough endoplasmic reticula (RER) and enlarged Golgi structure, as well as mitochondria, microtubules, lysosomes, glycogen and lipids. These cells secrete type I collagen and other matrix proteins. Osteoblasts cells are responsible for the production of the organic matrix of the bone that is composed from proteins and polysaccharides (Holtrop 1990). In addition, osteoblasts play a roll in the activation of osteoclasts through the release of certain mediators under the influence of parathyroid hormone and local cytokines. There are several mediators that regulate the differentiation and functions of osteoblasts including Bone morphogenetic protein BMP and wingless (Wnt) signaling pathways (Cao and Chen 2005; Day *et al.* 2005). BMP signaling controls the expression of Runt-related transcription factor 2 (RUNX2) which is essential for osteoblast differentiation via recruitment and activation of heterodimer Smad proteins (Ducy *et al.* 1997). Osteoblasts undergo one of three pathways: they either remain as active osteoblasts or become surrounded by matrix as osteocytes or they become inactive and form the bone-lining cells (Marks and Popoff 1988; Marks and Odgren 1996, Ducy *et al.* 2000).

1.1.3 Bone lining cells

In the mature skeleton, the bone surfaces are covered with thin, elongated cells called bone-lining cells. They are linked to each other or to osteocytes by cytoplasmic extensions or gap junctions. Since these cells are considered to be metabolically inactive they have fewer organelles and less cytoplasm than osteoblasts (Marks and Popoff 1988; Marks and Odgren 1996). These cells may regulate influx and efflux of mineral ions into and out of the bone extracellular fluid and thus function as a blood – bone barrier (Dobnig and Turner 1995). It is also suggested that bone-lining cells secrete enzymes that remove the surface of the bone in preparation for the removal of bone by osteoclasts cells. However, in the presence of parathyroid hormone they may differentiate into osteoblasts (Marks and Popoff 1988; Marks and Odgren 1996).

1.1.4 Osteocytes

In the adult skeleton, about 90% of bone cells are thought to be osteocytes. Initially, as they begin to be surrounded by bone matrix they are considered to be immature osteocytes and resemble osteoblasts in their structure with large amount of RER,

Golgi apparatus and mitochondria. As more bone matrix is accumulated over these cells, they move deeper into the bone tissue become more mature. Eventually they appear to lose cytoplasm around the nucleus, which appears more prominent (Marks and Popoff 1988; Holtrop 1990; Marks and POdgren 1996). Osteocytes lack the expression of alkaline phosphatase but express osteocalcin together with other matrix proteins important in supporting intercellular adhesion and regulate mineral exchange between bone fluids and the vascular supply (Plotkin *et al.* 2002).

1.1.5 Osteoclasts

Osteoclasts are much larger than other bone cells and are characterized by their multiple nuclei that can be seen as 3 to 20 oval dense shapes located at the center of the cell. Osteoclasts are located on the bone surface and are highly motile. They contain less RER compared to osteoblasts and large numbers of mitochondria. Their main function is bone resorption (Holtrop 1990; Sandberg 1991), which they achieve by close adherence to bone surfaces and the creation of a closed space between cell and matrix for the concentrated secretion of bone resorbing proteases and other factors.

1.1.6 Bone modeling and Remodeling

Bone modeling may be defined as the process that bone undergoes in order to change overall shape in response to either physiological or mechanical factors. This process occurs from birth to adulthood and results in an increase in skeletal mass. Bone formation and bone resorption are not usually coupled during this process which is less frequent in adult (Kobayashi *et al.* 2003). However, bone modeling may increase as results of some diseases such as hypoparathyroidism and renal osteodystrophy or as a result of treatment with certain anabolic agents (Ubara *et al.* 2003, Ubara *et al.* 2005; Lindsay *et al.* 2006).

Bone remodeling is the process by which the integrity of the skeleton and mineral homeostasis is maintained in equilibrium. This is achieved by continues removal of discrete packets of old bone by osteoclasts and replacing them with newly synthesized bone by osteoblasts thus preventing the accumulation of damaged bone. This process begins before birth and continues until death. This cycle is composed of four consequent phases: activation, resorption, reversal and formation Figure 1.1 (Burr 2002; Parfitt 2002). Activation phase starts by recruitment of mononuclear monocyte-macrophage osteoclast precursors via the action of colony stimulating factor 1 (CSF-1) and its activation through the release of receptor activator of NF- κ B

ligand (RANKL) and sRANKL from osteoblast and osteoblast precursors and its direct binding to membrane bound RANK molecules on osteoclast precursors (Roodman 1999; Boyle *et al.* 2003; Blair and Athanasou 2004). The activation of osteoclasts is regulated by another molecule produced from osteoblasts osteoprotegerin (OPG), which act as a decoy receptor preventing the binding of RANKL and sRANKL to RANK molecules on osteoclast precursor thus the ratio between RANKL and OPG controls the activation of osteoclasts (Eriksen 1986; Reddy 2004). There are other factors that regulate osteoclast formation, activation and resorption such as Interleucin-1 (IL-1), Interleucin-6 (IL-6), parathyroid hormone, 1,25-dihydroxyvitamin D and calcitonin (Boyle *et al.* 2003; Blair and Athanasou 2004). In the resorption phase, osteoclasts mobilize bone mineral by lowering its pH by secreting hydrogen ions via H⁺-ATPase proton pump and chloride channels in their cell membranes into the resorbing compartment. Osteoclasts also digest the organic matrix of the bone by secreting tartrate-resistant acid phosphatase, cathepsin K, matrix metalloproteinase 9 and gelatinase from their cytoplasmic lysosomes. At the end of this phase osteoclasts undergo apoptosis (Silver *et al.* 1988; Delaissé *et al.* 2003). Reversal phase is considered to be transitional phase between bone resorption and formation. After the completion of bone resorption, resorption cavities have several types of mononuclear cells including monocytes, osteocytes that are released from bone matrix and preosteoclasts preparing to begin bone formation. There are several proposed coupling signals that link the end of bone resorption with the beginning of bone formation, such as bone matrix derived factors, including transforming growth factor β (TGF- β), Insulin-like growth factor 1 (IGF-1), Insulin-like growth factor 2 (IGF-2), BMP, platelet derived growth factor (PDGF), or fibroblast growth factor (Hock *et al.* 1988; Bonewald and Mundy 1990; Locklin *et al.* 1999). In addition to these factors ephrin B (EphB) receptors and their ligands have been implicated in coupling signaling through bidirectional activating signaling: enhancing osteoblast differentiation and inhibiting osteoclast function (Matsuo 2010). The results of this bidirectional signaling results in switching off bone resorption and activating bone formation (Martin *et al.* 2010). Once bone formation starts it, takes around 4 to 6 months to be completed. Osteoblasts start synthesizing new collagenous organic matrix and release small membrane-bound matrix vesicles that help in concentrating calcium and phosphate in order to regulate matrix mineralization. Mineralization is also inhibited enzymatically by the actions of pyrophosphate or proteoglycans (Anderson 2003). By the end of bone formation

about 50 to 70% of osteoblasts undergo apoptosis, with the balance becoming osteocytes or bone lining cells (Dobnig and Turner 1995). Each bone remodeling cycle results in the production of a new osteon (Parfitt 1994). The principal recognizable function of bone remodeling is the preservation of bone mechanical strength by replacing old damaged bone with newer healthier bone and to maintain calcium and phosphate homeostasis (Clarke 2008).

Bone remodeling is controlled by either systemic mechanisms or by mechanical regulation. Systemic regulation is achieved by the action of four main hormones calcitonin, parathyroid hormone, vitamin D₃ and oestrogen (Zaidi *et al.* 2002). Mechanical force plays an important role in bone remodeling by influencing bone metabolism (Jacobs *et al.* 2010). Animal studies showed that different bone cells such as osteocytes and osteoblasts are able to sense and respond to mechanical forces (Bonewald and Johnson 2008).

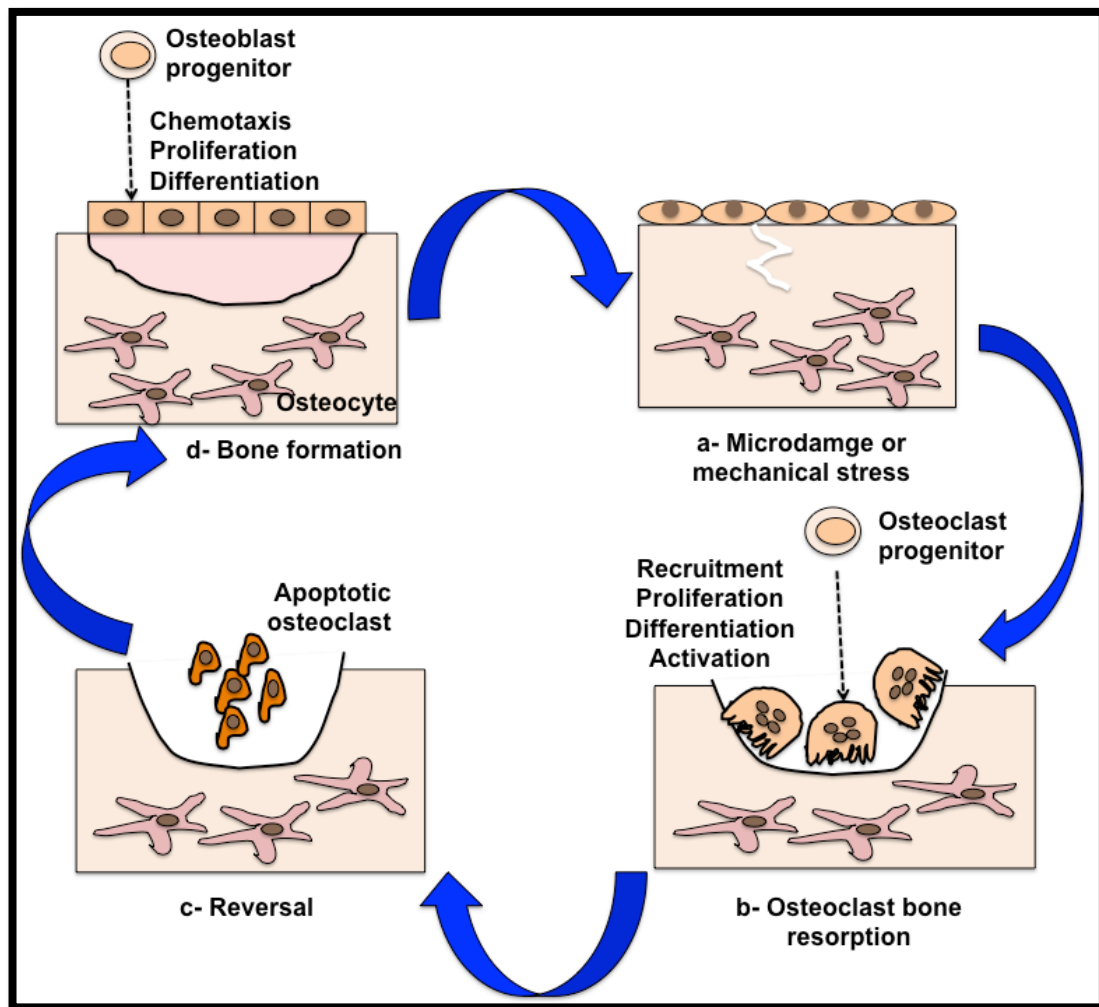


Figure 1.1 The bone remodeling cycle.

This Figure illustrate the four phases of bone remodeling cycle (a) Micro-damage or mechanical stress (b) This induce the recruitment, differentiation and activation of osteoclasts cell in order to resorb the damaged bone (c) osteoclast die by apoptosis (d) osteoblast migrate to the area of resorbed bone and replace it with un-mineralized osteoid witch then become mineralized. Adapted from (Crockett *et al.* 2011).

1.2 Epidemiology of prostate cancer

Prostate cancer is the second most common cancer in men. According to the World Health Organization (WHO) an estimated 1.1 million men worldwide were diagnosed with prostate cancer in 2012, accounting for 15% of the cancers being diagnosed (International Agency for Research on Cancer 2015). In the United Kingdom UK, prostate cancer accounts for approximately (25%) of the cancer burden in men. The incidence trends over the last decade in the UK vary according to the different types of cancer being increased in prostate cancer Figure 1.2 (Cancer Research UK 2011).

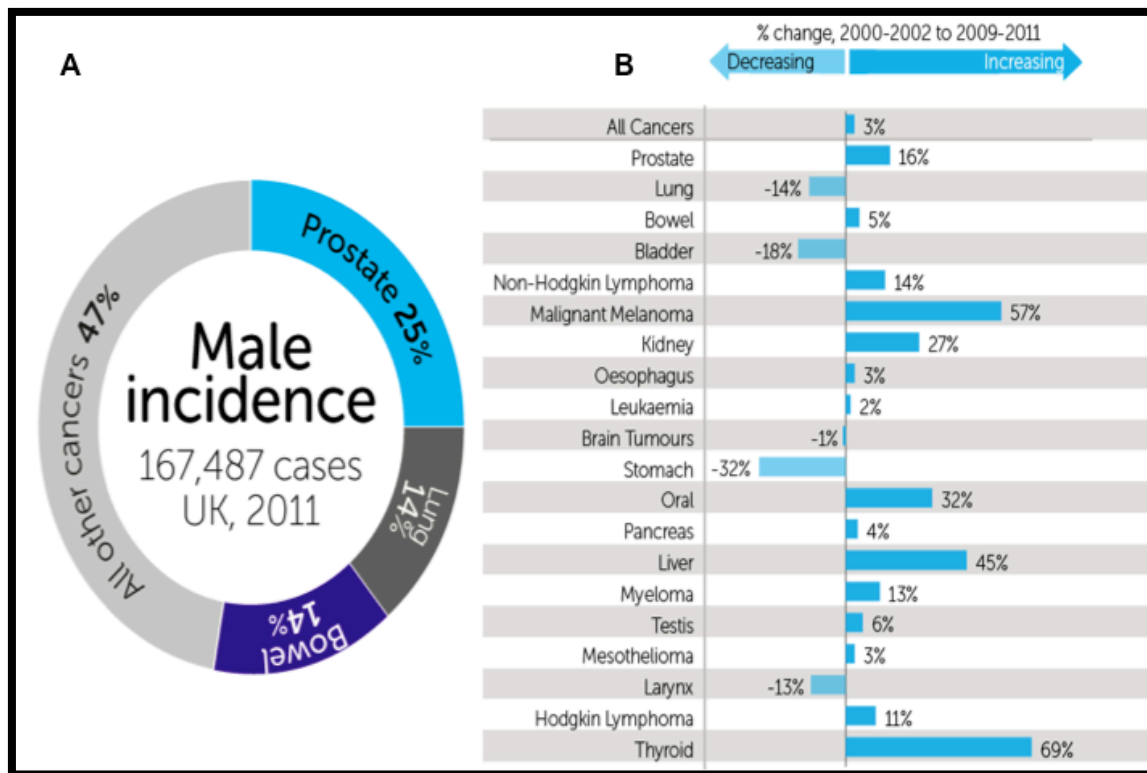


Figure 1.2 Prostate Cancer Incidence

(A) Represent the most Common Cancers in Males, Percentages of All Cancer Cases (C00-C97 excl. C44), UK, 2011. (B) Represent the 20 Most Common Cancers, Percentage Change in European Age-Standardized Three Year Average Incidence Rates, Males, UK, 2000-2002 and 2009-2011 (Cancer Research UK 2011).

Most patients who die from cancer, do so because of the spread of tumour cells to other sites away from the primary tumour (Wingo *et al.* 1995). About 90% of patients with advanced prostate cancer develop bone metastases (Larson *et al.* 2014).

1.2.1 Prostate cancer and Bone metastases

Advanced prostate cancer is most frequently associated with the development of bone metastasis (Keller and Brown 2004). Once the tumour reaches the bone it becomes incurable with current treatments (Coleman 2001). Bone metastasis is associated with several complications such as bone pain, impaired mobility, bone fracture, compression of the spinal cord and symptomatic hypercalcemia (Coleman 1997; Moul and Lipo 1999; Keller and Brown 2004). There are a number of factors that govern the special affinity that prostate cancer cells have to attach and survive in bone rather than other sites. These include vascular conditions such as elevated blood flow in the red marrow (Kahn *et al.* 1994) as well as the production of adhesion molecules by the tumour cells that allow them to bind to the bone marrow cells. The presence of the tumour results in an increase in the production of

angiogenic and bone resorbing factors that subsequently lead to the enhancement of the tumour growth in bone (Van Der Pluijm *et al.* 2001). Bone is also a repository for immobilized growth factors such as transforming growth factor beta (TGF β), Insulin like growth factor I and II (IGF I, IGF II), fibroblast growth factor (FGF), platelet-driven growth factor (PDGF), bone morphogenetic proteins (BMP) and calcium (Hauschka *et al.* 1986; Logothetis and Lin 2005). These factors are known to stimulate osteoblast function (bone formation) and proliferation (Logothetis and Lin 2005).

Prostate cancer is frequently associated with osteoblastic bone metastases (Charhon *et al.* 1983; Boyde *et al.* 1986). However, it seems that where prostate cancer bone metastases are present, while these lesions are predominantly osteoblastic, but there is some evidence that metastatic prostate cancer is also osteolytic, since the processes of bone resorption and bone formation are linked together (Charhon *et al.* 1983; Jung *et al.* 2004).

1.3 The transforming growth factor beta (TGF- β) superfamily and its signaling pathway

TGF- β family is a large group of structurally related ligands or cytokines that have an important role in regulating a variety of cellular processes, such as cell cycle progression, cell differentiation, motility, adhesion, bone morphogenesis, immune response as well as development in multi-organ systems. More than 30 factors have been discovered recently that belong to this superfamily (Chang *et al.* 2002; Derynck and Akhurst 2007).

The members of this superfamily can be divided into two subfamilies:

- 1- The first subfamily consists of TGF- β , activin, inhibin, Nodal, lefty and myostatin.
- 2- The second subfamily includes Bone morphogenetic protein (BMP), anti-mullerian hormone (AMH or MIS) as well as other growth and differentiation factors (GDFs) (Derynck and Akhurst 2007; Massagué 2008).

The TGF- β members are secreted as biologically inactive forms (Gentry *et al.* 1988). Usually, the activity of the mature domain of the TGF- β ligand is veiled by the propeptide, Latency associated peptide (LAP) which is cleaved from the mature domain by a furin-like endoprotease during secretion but remains associated with the mature domain by means of noncovalent interaction (Dubois *et al.* 1995). There

are several other mechanisms involved in the activation of the TGF- β superfamily including activation mediated by the extracellular matrix protein thrombospondin 1 (TSP-1) (Schultz-Cherry *et al.* 1994; Schultz-Cherry *et al.* 1994), integrin $\alpha_v\beta_6$ (Munger *et al.* 1999) and proteolysis (Schultz-Cherry *et al.* 1994; Munger *et al.* 1999).

1.3.1 TGF- β structure

The general structure of the monomeric TGF- β ligand which involves two pairs of antiparallel β -strands forming a flattened surface, projecting away from a long α -helix (Schlunegger and Grutter 1992).

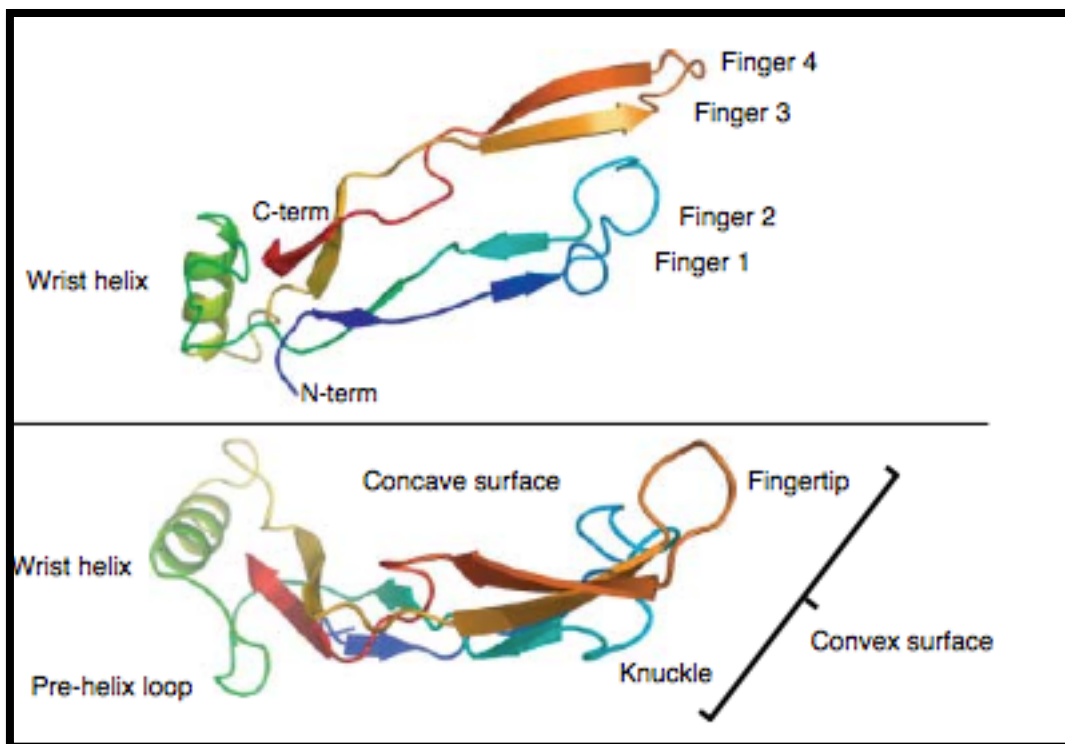


Figure 1.3 TGF- β structure.

The TGF- β monomeric structure involves a cysteine knot motif with two pairs of antiparallel β -strands (fingers) that extend from an α -helix. The β -strands are curved to form both a concave and convex surface for the interaction with the receptor. This picture is produced from (Lin *et al.* 2006).

A “cysteine knot” motif is formed at the core by one of the disulfide bonds that travel across a ring, which is formed, by two other disulfide bonds. This monomer has been described as a four-digit hand, each β -strand being compared to a finger. Finger 1 and 2 are antiparallel with finger 2 leading to a general helix ‘wrist’ at the N terminus, while finger 3 and 4 being antiparallel at the C terminus Figure 1.3 (Schlunegger and Grutter 1992; Lin *et al.* 2006).

There are three isoforms from the TGF- β : TGF β 1, TGF β 2 and TGF β 3 (Kingsley 1994). The TGF- β is synthesized as inactive precursors that require activation before they can bind to their receptors (Li and Flavell 2008). The active form of the TGF- β is a dimer which is stabilized by hydrophobic interactions, further strengthened inter-subunit disulfide bridge (Lin *et al.* 2006).

1.3.2 TGF- β function

Studies showed that mice that are mutant in some isoforms of the TGF- β show certain defects. For example more than 50% of mice lacking TGF- β 1 die during embryogenesis from yolk sac defect while those that survive develop inflammatory disorders and die within a month (Shull *et al.* 1992; Kulkarni *et al.* 1993; Dickson *et al.* 1995).

On the other hand, TGF- β 2 knockout mice are associated with various craniofacial, heart and renal defects. In addition this knockout is also associated with retinal hyperplasia, axial and appendicular skeletal abnormalities (Sanford *et al.* 1997). Both TGF- β 2 and TGF β 3 knockout mice are involved with perinatal mortality (Kaartinen *et al.* 1995; Proetzel *et al.* 1995). Studies involving TGF- β 3 knockout mice demonstrated that these mice have delayed lung development and platelet defect (Kaartinen *et al.* 1995; Proetzel *et al.* 1995).

1.3.3 Bone Morphogenetic proteins (BMP) structure

BMPs are another subfamily that are considered the largest branch of the transforming growth factor β superfamily, some of which are referred to as growth and differentiation factors (GDF) (Kawabata *et al.* 1998; Chang *et al.* 2002). They are dimeric proteins composed of two monomers joined together with a disulfide bond (Ducy and Karsenty 2000; Sebald *et al.* 2004). Additionally, the dimer contains a 'cysteine knot' which forms the core monomer consisting of seven highly conserved cysteines Figure 1.4 illustrate the structure of BMP7 as an example of BMP family (Griffith *et al.* 1996).

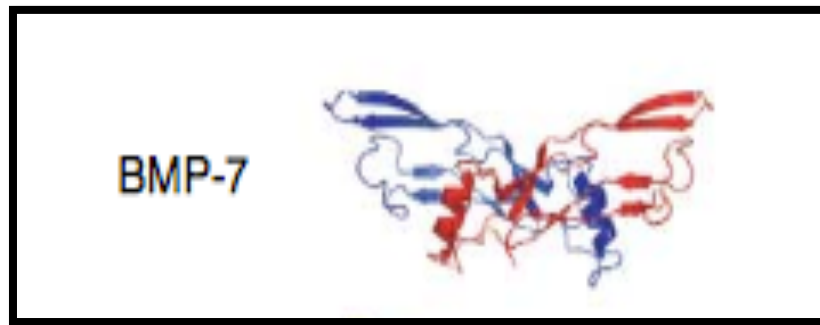


Figure 1.4 BMP structure.

This figure illustrates the structure for BMP7 as an example of the BMPs family: BMP7 exhibits extended symmetric arrangements. Monomers are coloured red and blue in the structure and aligned by a single monomer (blue). This picture is produced from (Lin *et al.* 2006).

In Humans, there are 21 members of the BMP family (BMP2, BMP7, BMP8A/B, BMP10, BMP15, GDF1-3, GDF5-7, GDF, myostatin, GDF9-11 and GDF15) (Schmierer and Hill 2007) which can be further divided into subgroups according to their amino acid sequences (Kawabata *et al.* 1998; Botchkarev 2003; Ye *et al.* 2007). BMPs exist as both homodimers and heterodimers. Although, the homodimers seem to be the major form of BMPs, the heterodimers are the most biologically active (Aono *et al.* 1995; Israel *et al.* 1996; Zhu *et al.* 2006). The BMPs are secreted as inactive propeptides that are then activated by proprotein convertase, for example the serine endoprotease furin (Uzel *et al.* 2001).

Even though, BMPs are synthesized mainly by skeletal cells, their synthesis is not limited to the bone. They are expressed by a variety of extraskelatal tissues where they play a central role in cell development and function (Pereira *et al.* 2000). BMP-1 through 6 are expressed by osteoblastic cell lines but the degree of the expression depends on the cell line/type studied (Pereira *et al.* 2000). BMP1 is unrelated to other BMPs and does not regulate the growth and differentiation of skeletal cells. It functions as a protease that cleaves procollagen fibrils as well as chordin that is a peptide that binds and antagonize the action of BMP2, 4 and furin (Uzel *et al.* 2001).

1.3.4 BMP function

BMPs have unique functions (Wozney and Rosen 1998). They initiate bone formation by stimulating the differentiation of mesenchymal cells into chondroblasts and osteoblasts (Wozney and Rosen 1998). This will lead to new bone formation during embryogenesis and bone repair in adult tissues (Reddi 1997; Wozney 2002).

Many studies in mouse models have described an association between some skeletal defects and mutation in TGF- β superfamily members, their receptors or their binding proteins (Wang *et al.* 1990; Ahrens *et al.* 1993; Asahina *et al.* 1993).

In addition, BMPs also regulate the primal stages of embryogenesis, formation of left-right asymmetry, neural patterning, tooth and eye development (Luo *et al.* 1995; Hogan 1996; Bei and Maas 1998; Zhao 2003). Many genetic studies indicate the role of TGF- β superfamily in heart development (Zhang and Bradley 1996), suggesting that BMP-2 is required for the initial formation of cardiac primordium. BMP2 null mice have either no heart or develop one that is malformed (Zhang and Bradley 1996).

There are different BMP antagonists that can bind to it and inhibit the effects of BMPs for example follistatin, Noggin and chordin (Iemura *et al.* 1998). Even though, both Noggin and chordin are not structurally related to the BMPs, they are capable of binding specifically to BMPs but not to activin or TGF- β . They act by blocking the interaction of BMPs with their receptors. Studies done on Noggin null mice showed that these mice had excess cartilage and failed to initiate joint formation (Brunet *et al.* 1998; McMahon *et al.* 1998).

1.3.5 BMP antagonist Noggin structure

Human Noggin protein is encoded by the NOG gene, that has 205 amino acids and is secreted as glycosylated covalently linked homodimer with a molecular mass of 64KDa (Smith and Harland 1992; Ogawa *et al.* 2002). Noggin primary structure contains of acidic amino-terminal and a cysteine-rich carboxyl-terminal, which contains nine cysteine residues. At the center of the Noggin protein structure there is a highly basic heparin-binding segment, which maintains the protein at the cell surface thus controlling its diffusion (Economides *et al.* 2000; Paine-Saunders *et al.* 2002). Noggin protein was first discovered in *Xenopus* produced by Spemann's organizer as a neural inducer (Smith and Harland 1992). The main physiological function of Noggin is to antagonize BMPs through preventing, their binding to both type I and type II serine-threonine kinase receptors and inhibiting their signals mediated by Smad1/5/8 (Zimmerman *et al.* 1996; Brunet *et al.* 1998; Groppe *et al.* 2002).

1.3.6 Noggin function

As the knowledge of BMPs and their role in different tissues has increased with time, so the understanding of Noggin's function has also increased. In Noggin null mice increased in BMP activity results in a series developmental abnormalities such as defects of the axial skeleton and joint lesions, impaired formation of the neural tube and hair follicle retardation (McMahon *et al.* 1998; Tylzanowski *et al.* 2006). Noggin contributes in somite differentiation (Marcelle *et al.* 1997; Tonegawa and Takahashi 1998). In addition, mice lacking Noggin demonstrate excessive cartilage formation, shorter extended limbs, and lack joint formation indicating the importance of Noggin in the regulation of chondrocyte proliferation and differentiation (Brunet *et al.* 1998).

Moreover, a new role of Noggin has been associated in osteolytic prostate cancer cell line where re-expression of Noggin in prostate cancer cells results in a reduction of their osteosclerotic capacity and balanced bone remodeling (Schwaninger *et al.* 2007).

1.3.7 The TGF- β superfamily signaling pathway

In general, this superfamily of proteins signals by stimulating the formation of specific heteromeric complexes of type I and type II serine/threonine kinase receptors. Type II receptors are encoded by five mammalian genes and binding to the ligand phosphorylates and activates the type I receptor. Type I receptors are encoded by seven mammalian genes (Whitman 1998; Patterson and Padgett 2000).

Type I receptors may have different names as a result of being cloned by independent groups. Such as Activin receptor-like kinase 4 (ALK 4) can also be called activin receptor type IB (ActRIB) since it could bind Activin and mediate certain Activin responses in cultured cells (Attisano *et al.* 1993; Yamashita *et al.* 1995; Attisano *et al.* 1996). These seven members of type I receptor are further divided into three groups according to their structure and function similarities (Kawabata *et al.* 1998). These three groups are as follows:

- 1- The BMPR-1 which include
 - BMPR-IA
 - BMPR-IB
- 2- The ALK-1
 - ALK-1
 - ALK-2

3- The TGF β R-I

ALK-4/ActR-IB

ALK-5/ TGF β R-I

ALK-7

On the other hand, there are three receptors that may serve as type II receptor: one of them is specific for the BMPs while the other two are shared by the other TGF- β family members including activin and myostatin respectively (BMPR-II, ActR-II and ActR-IIB) (Yu *et al.* 2005).

The only substrates for type I receptor kinase that is known to have a signalling function are Smads (Whitman 1998; Patterson and Padgett 2000). According to their function Smads fall into three subfamilies as described in the Figure 1.5: receptor-activated Smads (R-Smads): this group includes Smad1, Smad2, Smad3, Smad5 and Smad8, which are phosphorylated by the type I receptors. The second subfamily includes the common mediator Smads (Co-Smads) including Smad4 which is then oligomerised with the activated R-Smad. The third subfamily includes the inhibitory Smads (I-Smads) that includes (Smad6 and Smad7). The inhibitory Smads are induced by TGF- β family members and cause a negative feedback effect by competing with R-Smad for receptor interaction thus, marking it for degradation (Grishin 2001).

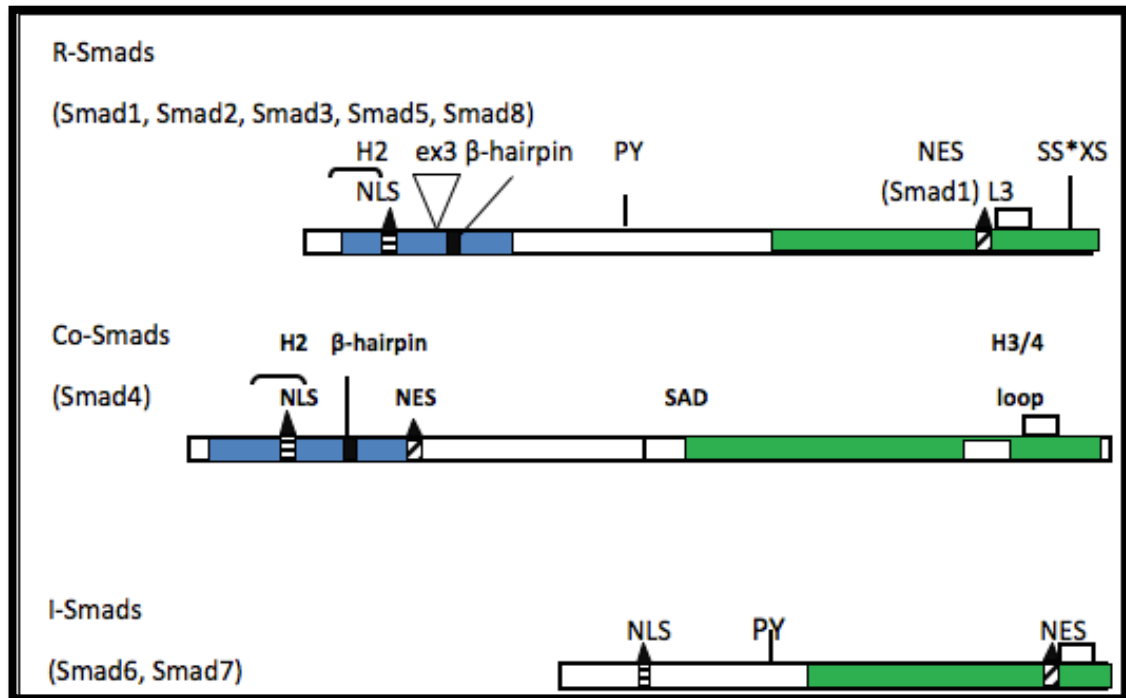


Figure 1.5 Structure relationships in the Smad family.

The figure illustrates the Smad proteins with the N-terminal Mad homology 1 (MH1) domains in blue and the C terminal Mad homology 2 (MH2) domains in green. Selected domains and sequence motifs are indicated as follow: α -helix H2, L3 and H3/4 loops, β -hairpin, the unique exon 3 of Smad2 (ex3), Nuclear localization sequence (NLS), Nuclear export signal (NES), the proline-tyrosin (PY) motif, Smad4 activating domain (SAD) and the SSXS motif of R-Smads with asterisks indicating the phosphorylated serine residues. This picture is adapted from (Moustakas *et al.* 2001).

The Smads have two domains, the N-terminal Mad homology 1 (MH1) and C-terminal Mad homology 2 (MH2) domains, which are joined with each other, by a linker region as shown in Figure1. 6 (Grishin 2001).

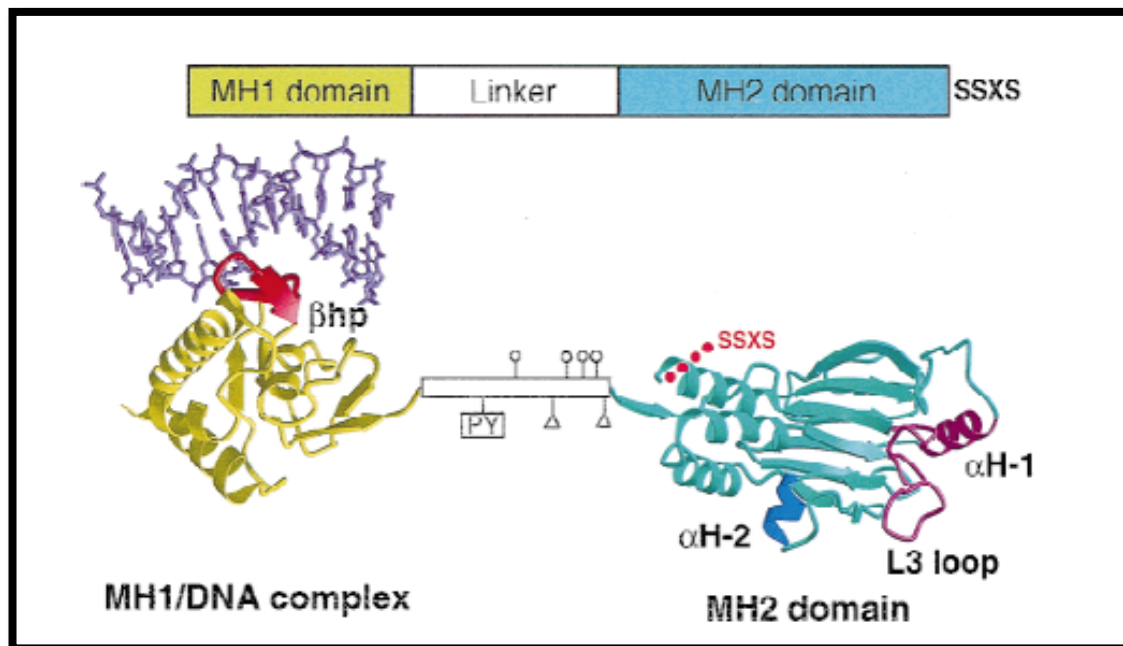


Figure 1.6 Smads domains.

This figure illustrates the three-dimensional structures of the Smad MH1 domain bound to the AGAC sequence, and the Smad MH2 domain. The principal interactions of these two domains are listed. The structures involved in these interactions are shown in different colors: the β -hairpin (β -hp) that mediated DNA binding, the L3 loop and α -helix 1 (α H-1) that specify Smad interactions with type I receptors, and the α -helix 2 (α H-2) that specifies Smad2 interaction with SSXS, receptor phosphorylation sites. This picture is produced from (Massagué and Chen 2000).

The MH 1 domain in R-Smads and Co-Smads is highly conserved and plays an important role in cytoplasmic anchoring, nuclear import, DNA binding and regulation of gene transcription. The MH 2 domain is highly conserved in all Smads (Grishin 2001; Shi and Massagué 2003). The MH 2 function is to regulate Smad oligomerisation reaction by type I receptors and interact with the cytoplasmic adaptors and other transcription factors (Shi 2001).

The first and crucial step in TGF- β signalling pathway is the phosphorylation of the R-Smads at the C-terminal SSXS motif by activated type I receptor (Abdollah *et al.* 1997; Shi and Massagué 2003). The L45 loop in the type I receptors and L3 loop in the R-Smad MH 2 domain both determine their binding to their specific substrates. Thus the Smad signalling cascade is classified into two groups TGF- β /Activin and nodal group which phosphorelayte Smad2 and Smad3 and the BMP group which phosphorylate Smad1, Smad5 and Smad8 as illustrated in Figure 1.7 (Chen *et al.* 1998).

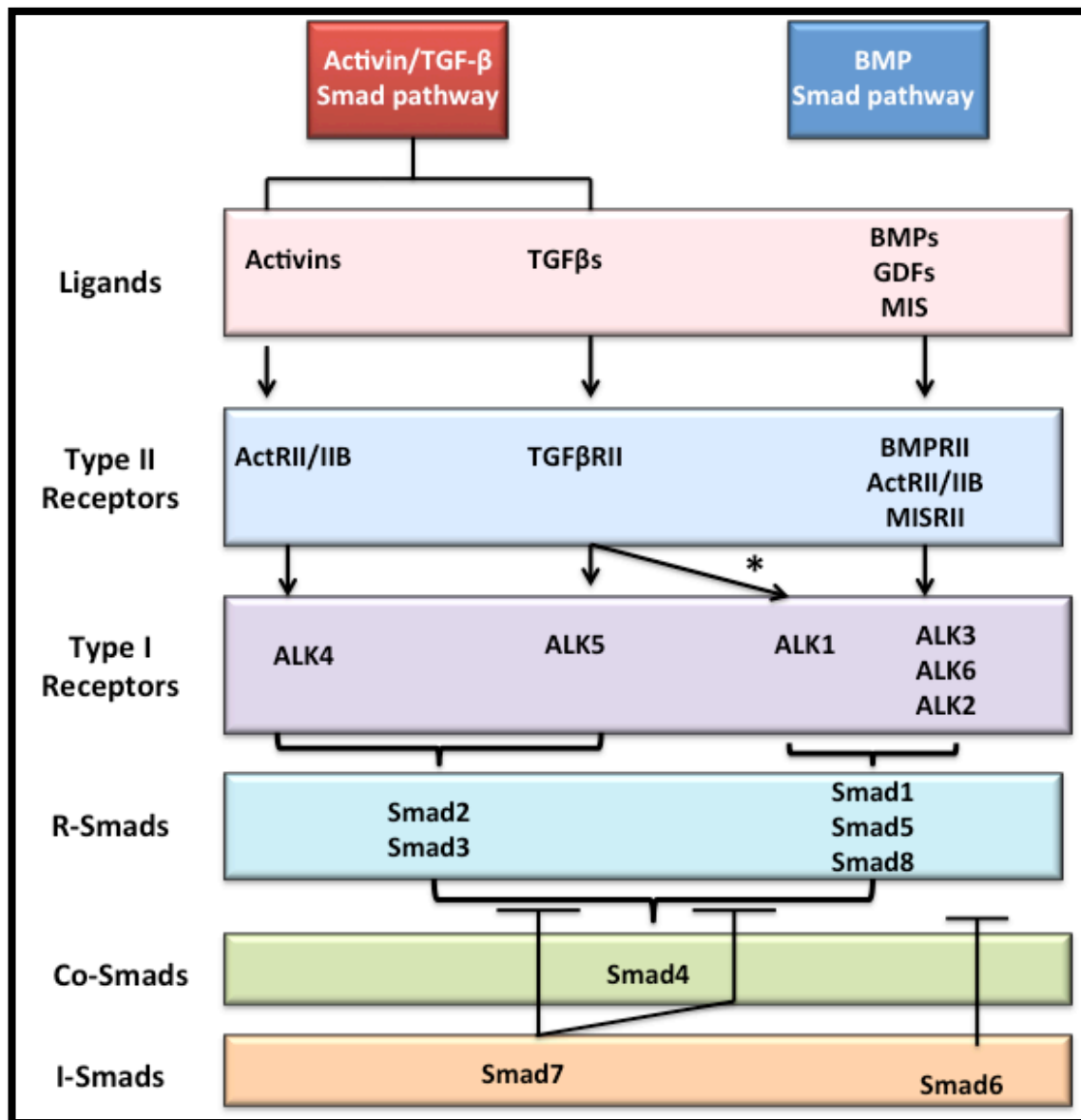


Figure 1.7 Signaling specificity in the TGF- β superfamily.

The mammalian Smad signaling cascades are classified into two important pathway Activin-TGF- β (red) and BMP (blue) each ligand binds to its specific type I and type II receptors as indicated in the diagram. Activin-TGF- β are phosphorylated by Smad2 and Smad3 (R-Smad) while BMP are phosphorylated by Smad1, 5 and 8. Both groups share the same Co-Smad. Smad7 acts as an inhibitor for Activin-TGF- β group and Smad6 as an inhibitor for the BMP group. Adapted from (ten Dijke *et al.* 2000; Moustakas *et al.* 2001).

After the activation, R-Smads form complexes with the Co-Smad (Smad4) which then enter the nucleus where they bind to DNA and regulate the transcription of target genes along with other different cofactors (Shi and Massagué 2003). This pathway is not only regulated with the I-Smads, which regulate the processes by feedback inhibition. Furthermore, the TGF- β signaling pathway is highly regulated at different levels (Kogawa *et al.* 1991; Shimonaka *et al.* 1991). For instance some extracellular proteins such as follistatin, Noggin and chordin, antagonize the effect of many TGF- β family members and alter their signaling processes (Shimonaka *et al.* 1991).

Follistatin can bind both activin and BMP7 and prevent their binding to their receptors (Iemura *et al.* 1998). On the other hand, Noggin and chordin bind to BMP-4 and antagonize its effect (Piccolo *et al.* 1996; Zimmerman *et al.* 1996). Additional mechanisms are involved in regulating the Smads pathway including, nucleocytoplasmic shuttling and ubiquitin-mediated proteasomal degradation (Shi and Massagué 2003). The TGF- β pathway can be activated in two ways Smad dependent and independent mechanism. The non Smad-mediated signaling pathway also has long been known to control other physiological processes (Massagué 2008). The nucleocapsid (N) protein can bind to Smad3, which interferes with complex formation between Smad3 and Smad4. As a result, a Smad3-p300 complex is formed in the nucleus (Zhao *et al.* 2008). In addition, TIF1 γ is found to be selectively associated with the phosphorylated Smad2/3 in hematopoietic, mesenchymal and epithelial cells in response to TGF- β and transduce the signal independently of Smad4 to promote erythropoiesis (He *et al.* 2006). Moreover, the ubiquitin E3 ligase TRAF6 has also been reported to interact with TGF β RI and this coupling is needed for TGF- β induced auto-ubiquitination of TRAF6 as well as subsequent activation of TAK1-p38 MAPK, leading to apoptosis (Sorrentino *et al.* 2008; Yamashita *et al.* 2008). Figure 1.8 illustrates the TGF- β signaling pathway both Smad dependent and independent mechanisms.

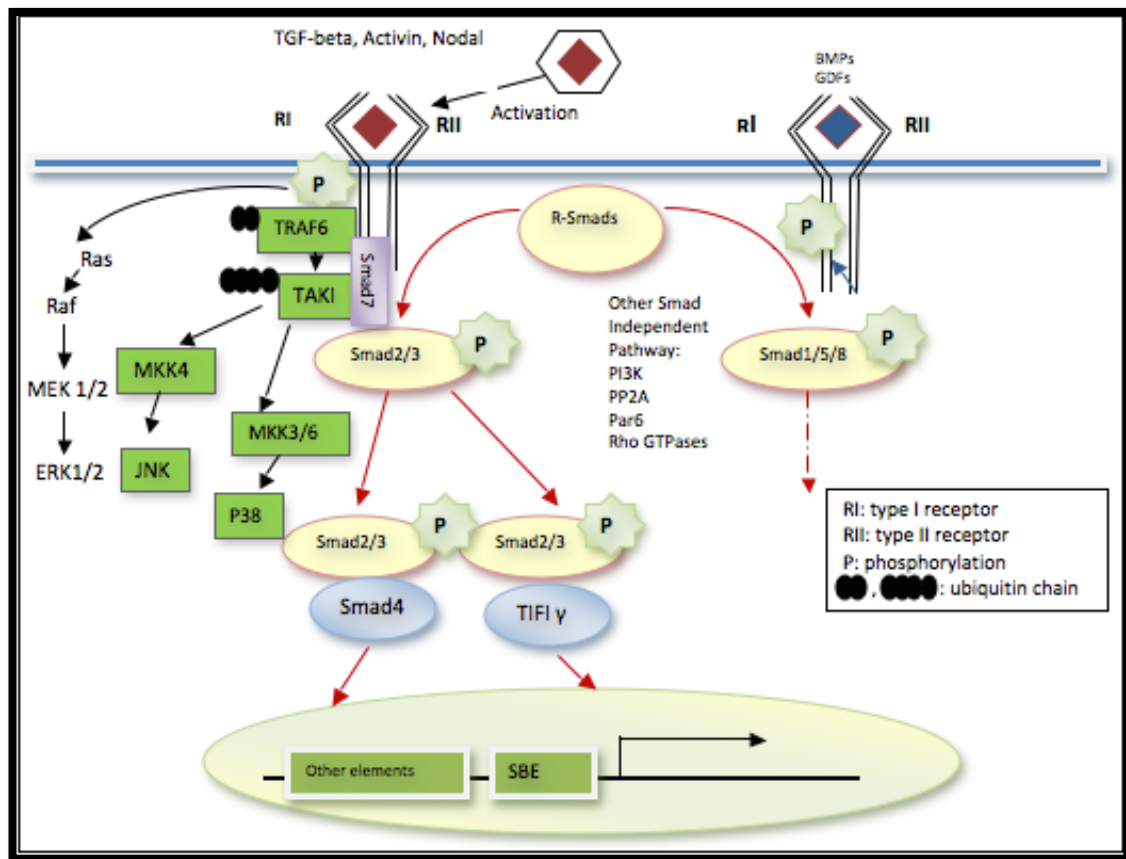


Figure 1.8 TGF- β signaling pathways.

After the activation of TGF- β it binds to two types of serine/threonine kinase receptors and transmits the signal through R-Smad phosphorylation, R-Smad binds to Co-Smad forming a complex that translocate to the nucleus and regulate the transcription of target genes. TGF- β can activate the signaling of MAPK in which Smad 7 act as a scaffold protein. TGF- β may activate other pathways including MAPK, PI3K, PP2A, Par6 and Rho GTPase independent of Smad signaling. Adapted from (Yan *et al.* 2009).

In normal physiological condition, TGF- β is known to inhibit the proliferation of cells by inducing apoptosis and inhibiting cell growth. As a consequence any deregulation of TGF- β expression or signaling has been associated with several diseases including cancer where, this inhibitory function is lost (Lindholm *et al.* 1992; Jennings and Pietenpol 1998) as shown in Figure 1.9.

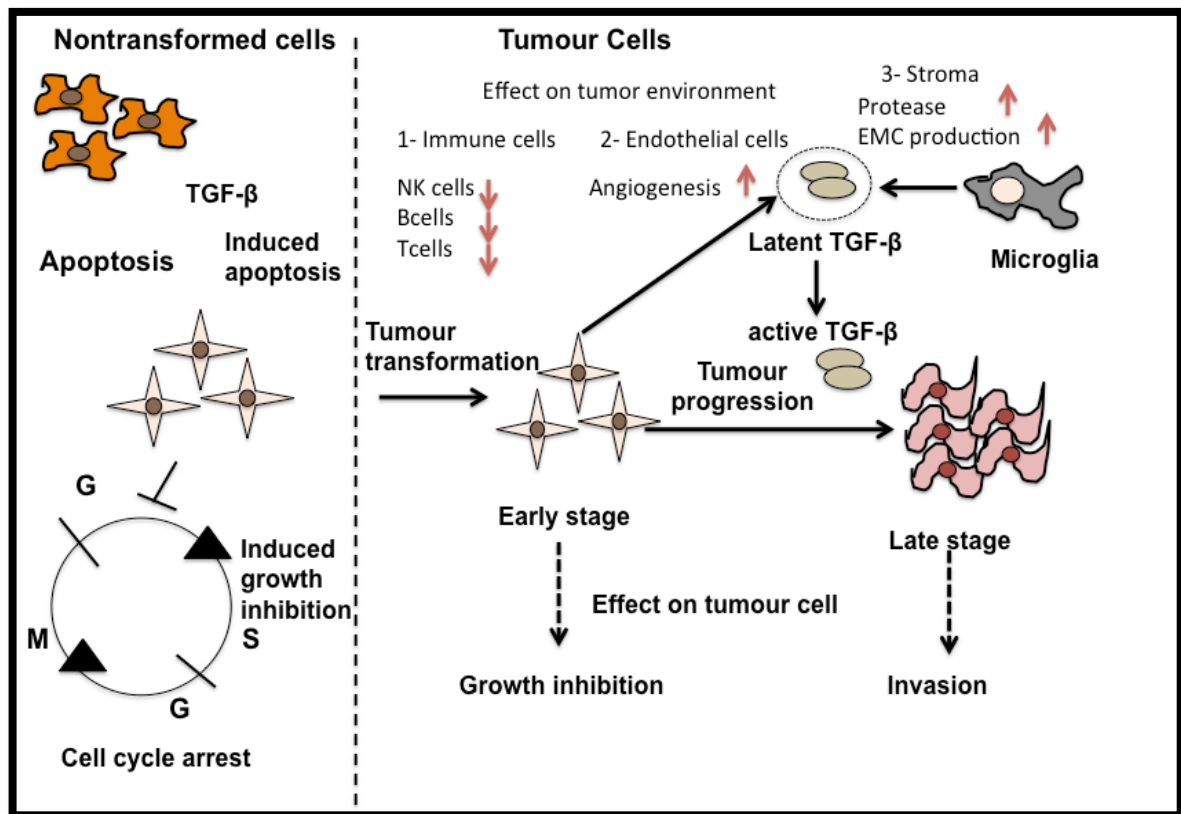


Figure 1.9 Possible multiple roles of TGF-β in tumour pathogenesis.

In non-transformed cells TGF-β can stimulate apoptosis or inhibit proliferation as cells progress to late stage they lose the growth inhibitory effect of TGF-β. During late stage of tumour development TGF-β are secreted by the tumour cells or stromal cells and contributes to the cell growth, invasion, metastases and decrease in the immune response of the host toward cancer cells. Adapted from (Kaminska *et al.* 2005).

1.4 The role TGF-β plays in different mechanisms

1.4.1 Apoptosis

A group of genes regulated by Smads is suggested to facilitate the pro-apoptotic effects of TGF-β. These genes include the ones that code for the phospholipid phosphatase SHIP, death-associated protein kinase (DAPK) and TGF-β-inducible early response gene 1 (TIEG1) (Ten Dijke *et al.* 2002; Siegel and Massague 2003). Moreover, by means of Smad3, TGF-β stimulates the expression and activates Fas receptors contributing to caspase-8 activation and apoptosis of gastric carcinoma cells (Kim *et al.* 2004).

However, as seen in Figure 1.10 there are clear participations of the mitogen-activated protein kinases MAPKs, such as p38 and Jun N-terminal Kinases (JNK) in the apoptotic mechanisms downstream of TGF-β ligands. Interaction between type II receptor for TGF-β and the proapoptotic adaptor protein Daxx, results in stimulation of JNK and it triggers apoptosis in both epithelial cells and hepatocytes (Perlman *et*

al. 2001). The Daxx-JNK pathway includes homeodomain interacting protein kinase 2 (HIPK2), that phosphorylates Daxx, regulating the MAPK kinases MKK4 and MKK7 activity which eventually results in JNK induced apoptosis as described in the Figure 1.10 below (Hofmann *et al.* 2003). There is another connection between receptor complexes and intracellular kinases. It involves the TGF- β -activated kinase 1 (TAK1), which can form a complex with the BMP receptors via its adhering partner TAB1 and the inhibitor of apoptotic caspases XIAP, an E3 ubiquitin ligase (Yamaguchi *et al.* 1999).

BMPs may also be responsible for apoptosis of diverse cell types through TAK1, p38, Smad6 and Smad7 as shown in Figure 1.10 (Yanagisawa *et al.* 2001).

TGF- β might further counteract pro-survival signals. The comparative levels of Smad3 and the pro-survival kinase Akt determine whether a cell transition to apoptosis in reaction to TGF- β (Conery *et al.* 2004; Remy *et al.* 2004). Nevertheless, TGF- β stimulates cell death of prostate carcinoma cells by boosting cooperation between Smad7 and TAK1-p38 signaling module (Edlund *et al.* 2003).

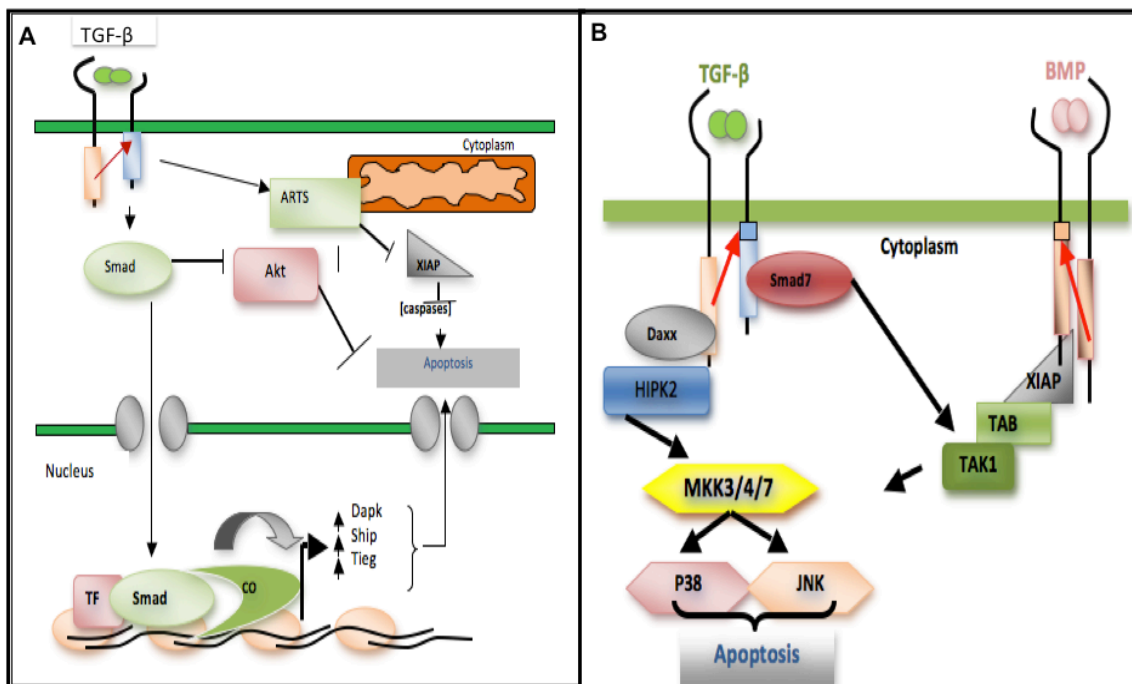


Figure 1.10 TGF-β stimulating apoptosis.

(A) illustrates the role of TGF-β in apoptosis through Smads. The expression of the pro-apoptotic genes including DAPK, Ship and Tieg is induced by the TGF-β via Smads. In addition Smads may promote apoptosis by binding and inactivating the survival kinase Akt. TGF-β stimulate apoptosis by mobilizing mitochondrial serpin ARTS to the nucleus, which blocks XIAPs the inhibitors of caspase. (B) illustrates the role of TGF-β in apoptosis through TAK1 pathway. The TGF-β typeI receptor binds Smad7 while typeII receptor binds the pro-apoptic protein Daxx. BMP receptors bind XIAP and its interacting partners TAB and TAK1. Both TGF-β and BMP receptors simulate the activation of MKK3, MKK4 and MKK7 thus leads to apoptosis via either activating JUK or p38. Adapted from (Moustakas and Heldin 2005).

1.4.2 Epithelial-mesenchymal transition and migratory responses

The TGF-β is crucial in modulating other important cellular responses including the cell migration and epithelial/endothelial- mesenchymal transitions (EMTs) which are essential at the time of embryogenesis and advanced cancer metastases (Tosh and Slack 2002; Condeelis and Segall 2003; Gotzmann *et al.* 2004).

Several studies have described the importance of Smads as mediators of actin cytoskeleton processing downstream of the TGF-β, since they promote a striking change in gene expression in the epithelial cells (Zavadil *et al.* 2001; Kowanetz *et al.* 2004; Vardouli *et al.* 2005). A work done by Valcourt *et al.* 2005 indicated that Smads particularly Smad3 and Smad4 are essential for initiating EMT response which is associated with the aggressive carcinoma spread in both *in vivo* and *in vitro*.

During EMT TGF-β receptor signaling acts synergistically with EGF signaling in the formation of tight junctions regulating the structural protein occludin, and interacting with the polarity protein Par6. In TGF-β signaling pathway, the type II receptor phosphorylates both the type I receptor and the type-I-receptor-tethered Par6

resulting in enlisting of the ubiquitin ligase Smurf1 and consequent ubiquitination and the breakdown of RhoA (Ozdamar *et al.* 2005). This results in local dismantling of the actin cytoskeleton and thus breakup of the strong binding, which is one of the characteristics of EMT (Thiery 2003). At the same time, stimulation of Smads by the type I receptor results in transcriptional initiation of genes that are involved in EMT including the ones encoding for Snail (Peinado *et al.* 2003), which is a transcriptional repressor of the gene encoding E-cadherin (Nieto 2002). A couple of reports directly connect the cytoplasmic protein kinase Limk1 to the long cytoplasmic tail of the BMP type II receptor (BMPRII) (Foletta *et al.* 2003; Lee *et al.* 2004). Limk1, a considerably studied kinase that signals downstream of Rho GTPases and modulates structural reordering of the actin cytoskeleton (Raftopoulou and Hall 2004), may be involved in the mechanism by which BMPs regulate the actin cytoskeleton at neuronal dendrite morphogenesis (Foletta *et al.* 2003; Lee *et al.* 2004). Conversely, the TGF- β type I receptor can stimulate the related Limk2 through Rho and its downstream effector ROCK1 in an indirect manner (Vardouli *et al.* 2005).

1.4.3 Cell proliferation

The role that TGF- β s have in apoptosis and morphogenetic responses, also induces growth inhibitory pathways via Smads which modulate gene expression and regulate transition through the G1 phase of the cell cycle (Massague 2004). There are several cell cycle inhibitors including p15, p21 and p57 that could be induced by Smad signaling, while the proto-oncogene product Myc and the inhibitors of differentiation (Id1, Id2, and Id3) are inhibited by Smads. The P21 activity is rapidly stimulated by all receptor complexes of the TGF- β superfamily (Massague 2004). FoxO, p53 and Sp1 together with Smads forms large transcriptional complexes on the p21 promoter enhancer. Reports have suggested that Smads themselves may inhibit cell growth by binding to protein kinase A (PKA) and activate the enzyme this effect is linked to the transcriptional activation of p21 and further inhibition of cell growth (Datto *et al.* 1995; Cordenonsi *et al.* 2003; Seoane *et al.* 2004).

TGF- β may alternatively, control the cell growth by inhibiting p70 s6 kinase through dephosphorylation by protein phosphatase PP2A. This leads to cell cycle progression and arrest in early G1 phase (Bhowmick *et al.* 2003; Kamaraju and Roberts 2005).

1.4.4 Matrix regulation

Several important components of the extracellular matrix and its regulatory enzymes are encoded by different genes that are stimulated by the TGF- β (Siegel and Massague 2003; Schiller *et al.* 2004), such as plasminogen activator inhibitor 1 (PAI-1), collagenase I and the collagens (Qing *et al.* 2000; Javelaud *et al.* 2003). Smads work together with transcription factors for instance, Sp1 and TFE3 in order to regulate the expression of PAI-1. However, signals from ERK and Rac1 are also required (Datta *et al.* 2000; Kutz *et al.* 2001).

In addition, exogenous TGF- β enhances the motion of glioma cells by increasing the expression of collagen and subunit of $\alpha_{2,5} \beta_3$ integrin and increasingly adjusting the activity of matrix metalloproteinases MMP-2,9 at the cell surface of glioma cells (Wick *et al.* 2001). This interaction between the cell surface receptor and its extracellular matrix components is important for tumour metastases and angiogenesis (Verrecchia and Mauviel 2002). Thus, the TGF- β regulated enzymatic degradation of extracellular matrix proteins may lead to an increase tumour spread (Platten *et al.* 2001).

1.4.5 Cell differentiation

Cell differentiation and the regulation of gene expression are linked together by TGF- β superfamily members (Miyazono *et al.* 2004). For instance, in order for the osteoblasts to differentiate from pluripotent progenitor cells they require BMP inputs in addition to the contribution of other factors such as Smad, transcription factors of the Runx family and Id proteins (Miyazono *et al.* 2004). Moreover, the association of p38, ERK and JNK pathways are quantifiably evidenced in the process of osteoblast differentiation in response to BMP-2, BMP-4 or BMP-7 (Gallea *et al.* 2001; Lai and Cheng 2002; Xiao *et al.* 2002). In addition, the modulation of Runx2 expression by TGF- β and BMP require Smad and p38 stimulation as well (Lee *et al.* 2002). As with cell proliferation, apoptosis and cell migration/cell differentiation induced by TGF- β family members largely utilizes the MAPK pathways and infrequently alternative non-Smad effectors (Moustakas and Heldin 2003).

1.4.6 Tumour mediated immunosuppression

TGF- β has been shown to have an essential role in glioma evasion from host immunity by system by inhibiting Major histocompatibility complex (MHC) class II expression on glioma cells, macrophages and microglia (Zagzag *et al.* 2005). Although, TGF- β wields its immunosuppressive effect on all cells of the immune system, its main target of action are T lymphocytes, which can develop into either

effector (CD⁺CTL) or helper (CD⁺4 TH1 or TH2) cells. The TGF- β has been found to be a major inhibitor of the T cells maturation (Gorelik and Flavell 2001; Chen *et al.* 2005).

Some experimental studies have suggested that the inhibition of immunostimulatory cytokine expression, such as interferon gamma (IFN γ) and Tumour necrosis factor alpha (TNF α), or the reduction of IL-2-mediated proliferative signals, mediate the effects of TGF- β 1 in immunity (Ranges *et al.* 1987).

In addition, TGF- β 1 can eliminate T cell stimulation by a negative effect on antigen presenting cells, for example dendritic cells. Furthermore, TGF- β 1 is also able to suppress macrophages by suppression of TNF α , H₂O₂ and nitric oxide formation. More to the point, TGF- β 1 might enhance the formation of immunosuppressive IL-10 by macrophages (Maeda *et al.* 1995).

Furthermore, targets of TGF- β 1-mediated immunosuppression are natural killer (NK) and lymphokine activated killer cells (LAK), as well as neutrophils (Kuppner *et al.* 1988). Several studies have suggested that blocking the TGF- β 1 signaling in the immune system cells will enhance the anti-tumour response (Gorelik and Flavell 2001; Bollard *et al.* 2002).

1.5 TGF- β superfamily expression and activities in prostate cancer and survival

The main characteristics of carcinogenesis and tumour cell autonomy are autocrine secretion of growth factors and the absence/inactivation of proteins encoded by tumour suppressor genes (Goustin *et al.* 1986; Weinberg 1989). Both human and rat prostates produce many peptide growth factors. Moreover, the proliferation of prostate cancer *in vitro* can be altered by the introduction of exogenous growth factors (Ware 1993).

It has been suggested that TGF- β 1 has actions in the formation and advancement of prostate cancer (Wilding 1991). Even though, TGF- β has been involved in immune suppression and angiogenesis, it is a powerful growth inhibitor in most cells specially inhibiting epithelial cell proliferation (Wilding 1991; Kulkarni *et al.* 1993).

Most prostate cancer cell lines are characterized by increased levels of TGF- β 1 expression *in vivo*. TGF- β 1 stimulates tumourigenicity in many cell types including prostate (Chang *et al.* 1993; Thompson *et al.* 1993; Eastham *et al.* 1995). This is

interesting with respect to the demonstrated growth inhibitory activity observed epithelia *in vitro*.

In a study done to evaluate the activity of the TGF- β in cultures of stromal cells isolated from benign prostatic hyperplasia tissue, challenge using wide dose range of TGF- β 1 demonstrated that low dose of TGF- β 1 (0.01ng/ml) was associated with the increase in the population growth while with higher doses the population growth was suppressed. One suggested mechanism by which low doses of the TGF- β could increase cell population size is by stimulating production of known growth promoters including fibroblast growth factor (FGF2). In addition, it may also result from lower apoptosis/differentiation in the treated population. In higher doses, TGF- β decreases population sizes by growth inhibition but not by increasing apoptosis (Bretland *et al.* 2001).

Prostate cancer cells and other cell types may develop resistant to the growth inhibitory effect of the TGF- β 1 by a varied set of mechanisms:

- 1- Only few cells can activate the endogenously produced TGF- β from their latent form, limiting bioavailability of active forms (Wakefield *et al.* 1987).
- 2- Cells may fail to respond to TGF- β if they have a faulty ligand-binding receptor system to cell surfaces. The absence of binding has been associated with the expression of little, no TGF β RII mRNA or carry TGF β RII gene mutations (Inagaki *et al.* 1993; Markowitz *et al.* 1995; Wang *et al.* 1995).
- 3- Finally, since TGF β RI and TGF β RII are heteromeric complex that interact with different targets to activate various signaling pathways, it is likely that the expression of different type I receptor isoforms or splice variants of type I or type II receptors affect these interactions, thus allowing cells to retain sensitivity to some effects of TGF- β 1, while acquiring resistance to other effects (Xu *et al.* 1994).

Moreover, a study by Kim *et al.* 1996, demonstrated reduced levels of expression of TGF β RI and TGF β RII in certain human prostate cancer cell lines and showed an inverse relationship between the levels of expression of TGF β RI and TGF β RII and the grade of prostate cancer. Sensitivity deprivation of TGF- β through the loss of its receptors would be likely to induce prostate cancer cells to increase the level of expression of TGF- β and this elevated level of TGF- β could then provide survival

advantages to prostate cancer cells by stimulating angiogenesis and suppressing the immune response (Kim *et al.* 1996).

Another paper by Kim *et al.* 1996 showed a correlation between a structural alteration in the TGF β RI gene and insensitivity to the effects of TGF- β by comparing three different prostate cancer cell lines including PC3 (Kim *et al.* 1996).

BMPs may have a role in prostate carcinogenesis similar to TGF- β isoforms. These proteins also signal through the interaction with their receptors BMPRI and BMPRII as discussed earlier in this thesis (Ide *et al.* 1997; Autzen *et al.* 1998). *In vitro*, most members of the BMPs bind to BMPRII which then combines with BMPRIA or BMPRIB (Liu *et al.* 1995). Kim *et al.* 2000, demonstrated that the human prostate cancer epithelial cell line have decreased level of expression of BMPRIA, BMPRIB and BMPRII as well as an inverse correlation between the levels of BMPR expression and tumour grade (Kim *et al.* 2000).

1.6 Bone microenvironment in tumour growth: a“vicious cycle”

Osteoblasts, osteoclasts, the mineralized bone matrix and many other cell types make up the bone microenvironment (Kozlow and Guise 2005). A vicious cycle of tumour growth and disease is promoted by the negative implication of tumour cells and the microenvironment as shown in Figure 1.11 (Yoneda and Hiraga 2005).

As demonstrated above, tumour cells secrete factors that stimulate osteoclast-mediated bone destruction and as a result the release of numerous factors which were previously immobilized in the bony matrix. These can act on the cancer cells, promoting survival, growth, more aggressive phenotypes and potentiating cancer spread and further bone destruction (Hall *et al.* 2006).

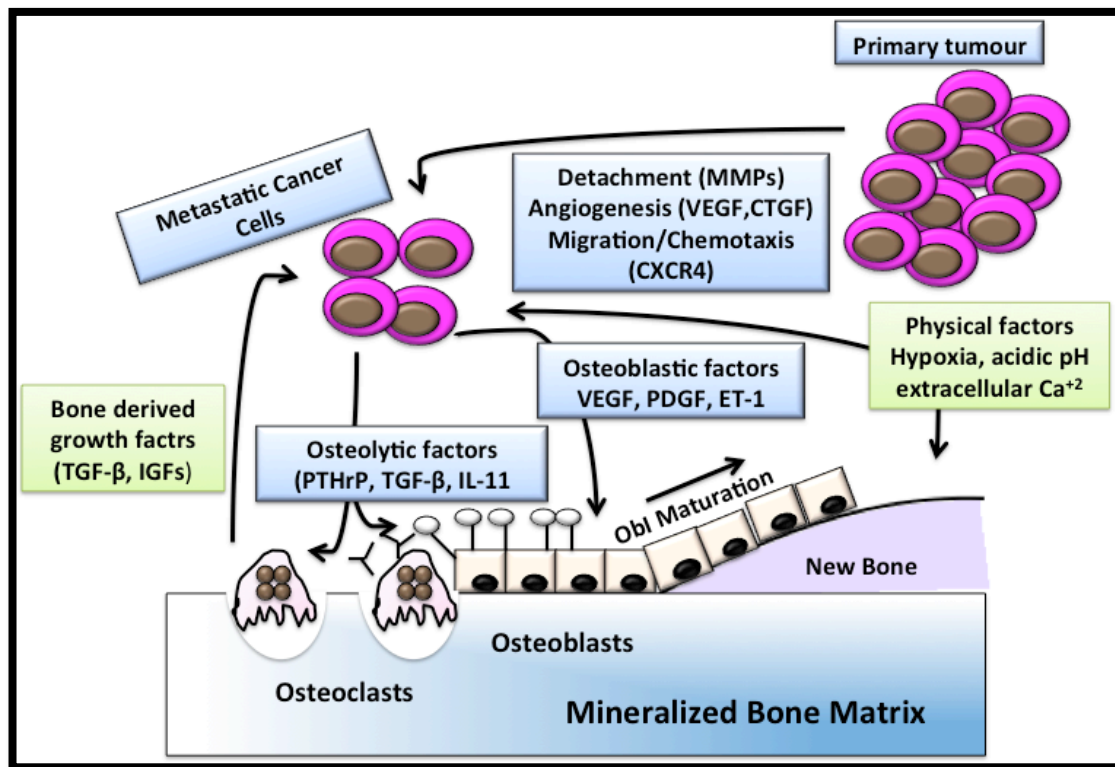


Figure 1.11 The vicious cycle of bone metastases.

There are several factors such as MMPs, chemokine receptor 4 CXCR4, vascular endothelial growth factor VEGF and connective tissue growth factor CTGF that are secreted from the primary tumour that target metastatic tumour cells to bone and enhance their survival within the bone microenvironment. Physical factors with the aid of bone derived growth factors including TGF-β and IGFs activate tumour cell to express osteoblast stimulatory factors and osteolytic stimulatory factors which in turn stimulate bone cells to release factors that promote tumour growth in the bone. Adapted from (Kingsley *et al.* 2007).

Additionally, the bone microenvironment contains physical factors, such as hypoxia, acidosis, and extracellular calcium plus growth factors like TGFβ that have been implicated in this vicious cycle (Kingsley *et al.* 2007).

1.7 Growth factors as mediators of the bone microenvironment

During the destruction of bone by osteoclasts calcium and many growth factors are released from the matrix including IGF, TGF-β, fibroblast growth factor (FGF), platelet-derived growth factor (PDGF) and bone morphogenetic proteins (Mohan and Baylink 1991). All of these factors have the potential to act on metastatic cells directly stimulation of cell proliferation or indirectly by promoting angiogenesis and increasing tumour production of osteolytic and osteoblastic factors that in turn remodel the skeleton to accommodate tumour growth (Derynck and Zhang 2003).

Although, TGF-β is not the most abundant growth factor in bone, it has an important role in osteolytic metastases (Derynck and Zhang 2003). Many studies indicate that TGF-β may stimulate bone metastases by inducing the proosteolytic gene expression

in association with PTHrP in both breast cancer cell line and prostate cancer cell lines such as PC3 (Guise *et al.* 1996; Yin *et al.* 1999). TGF- β induced PTHrP in turn increases Osteoblastic production of RANK ligand therefore, stimulate osteoclast formation and activity this consequent increase in bone resorption releasing more bone matrix factors to act on cancer cells thus sustaining a vicious cycle (Pollock *et al.* 1996; Kitazawa and Kitazawa 2002).

1.8 The role of TGF- β in the initiation of bone metastases

From the previous sections it is clear that the activity of the TGF β family in the context of tumour growth and metastasis is complex. On the one hand, these factors are potential growth inhibitors for the tumour population but on the other, they provide modification of the tumour phenotype and associated environment in bone that favours metastasis. As stated earlier, osteoblastic lesions are frequently produced by prostate cancer that metastasizes to the bone. The mechanism by which prostate cancer promote bone remodeling/mineralization is not well understood: prostate cancer cells produce different factors with, osteogenic properties (Boyce *et al.* 1999; Deftos 2000). These factors could be grouped into those that have direct effects on osteoblast function; BMPs, TGF β 1, TGF β 2, IGF1, IGF2, FGF, PDGF, WNT (Mundy 2002) and endothelin-1 (ET-1) (Kimura *et al.* 1992). ET-1 also has indirect effects: it stimulates the WNT signaling pathway by causing a reduction in the production of the WNT antagonist dickkopf homologue 1 (DKK-1) (Clines and Guise 2008). WNT signaling is a major osteoblast regulatory pathway, controlling normal osteoblast differentiation and function (Hall *et al.* 2005). A second category includes factors that have entirely indirect effects on osteoblast function such as vascular endothelial growth factor (VEGF) (Ducy *et al.* 1997) by modifying the bone microenvironment,

Several other proteins also work indirectly to stimulate bone formation, for example the serine proteases, prostate specific antigen (PSA), and urinary plasminogen activator urokinase (uPA). These proteases could enhance the activation of growth factors such as TGF β (Killian *et al.* 1993) and parathyroid hormone-related protein (PTHrP). How PSA facilitates the tumour growth has not been established but there is a possibility that it may also activate osteoblast stimulating factors such as TGF β and IGF by cleaving them from their inactivating peptides (Cramer *et al.* 1996; Iwamura *et al.* 1996). Figure 1.12 describes the bone formation in prostate cancer osteoblastic metastases.

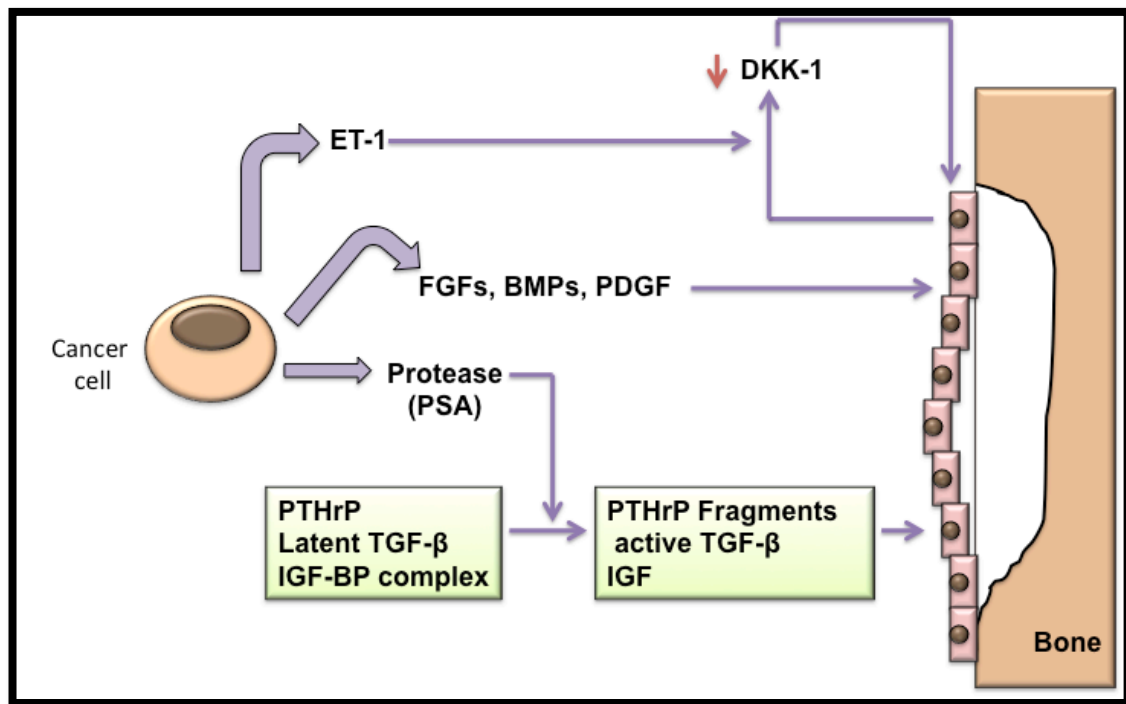


Figure 1.12 Bone metastases in prostate cancer.

Prostate cancer cells stimulate osteoblast proliferation and new bone formation via the secretion of many factors into the bone microenvironment such as endothelin-1 (ET-1), FGFs, BMPs and PDGF. ET-1 decreases the secretion of DKK-1, which is a Wnt pathway inhibitor that in turn results in the stimulation of osteoblast activity. Proteases, mostly prostate-specific antigen (PSA) produced from the tumour cell, cleave PTHrP, TGF- β and IGF from their binding proteins, which results in the production of fragments of PTHrP and active TGF- β , thus stimulating osteoblast activity. Adapted from (Clines and Guise 2008).

In breast cancer, metastases have been shown to stimulate osteoclastic activity in the bone marrow and cause the release of TGF- β from the bone matrix, which acts on cancer cells to stimulate the formation of PTHrP and Interleukin-11. These two factors act on osteoblasts and cause the release of the RANK ligand and other factors involved in osteoclast mobilization and feed-forward into the osteolytic metastases cycle, as seen in Figure 1.13 (Kingsley *et al.* 2007). Metastatic breast cancer cells in the bone microenvironment use Smad-dependent transcription, as revealed by a noninvasive imaging reporter in mice (Kang *et al.* 2005). PTHrP is a mediator of TGF- β osteolytic action (Kingsley *et al.* 2007). Apparently, TGF- β stimulates PTHrP secretion without increasing PTHrP mRNA levels (Käkönen *et al.* 2002). In addition, PTHrP promotes the production of RANK ligand in osteoblasts, which results in promoting the differentiation of osteoclast precursors and bone resorption (Käkönen *et al.* 2002).

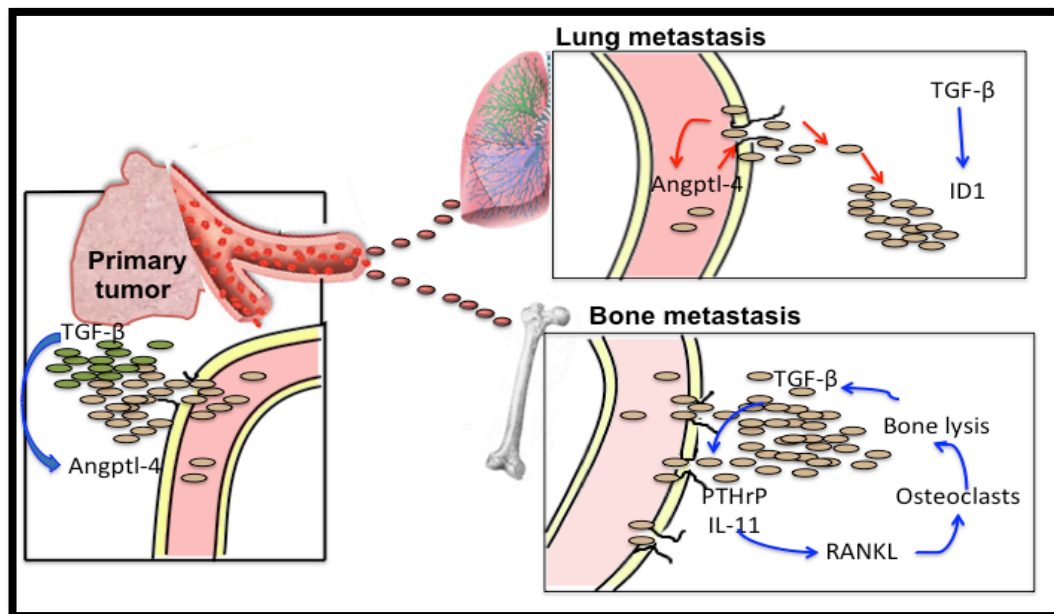


Figure 1.13 Role of TGF β in breast cancer metastasis

TGF- β derived from either infiltrating mesenchymal or myeloid precursor cells (green) or from the cancer cells themselves (brown) stimulates the expression of Angiopoietin-like 4 (ANGPTL4). Disseminated cancer cells then enter the circulation with increased ANGPTL4 have the advantage of seeding the lung this cytokines have the ability to disrupt vascular endothelial junctions. In the lung breast cancer cells respond to the local TGF- β thus results in an inhibition of differentiation/DNA binding1 (ID1). In addition circulating tumour cells enter the bone marrow where TGF- β being released from osteoblasts (blue) acts on the growing cancer cells and stimulate the production of parathyroid hormone-related protein (PTHrP) and interleukin-11. However these factors act on osteoblast cells and enhance the release of RANK ligand (RANKL) and other mediators of osteoclast mobilization initiating osteolytic metastases cycle. Adapted from (Massagué 2008).

Other mediators that modulate bone metastasis include interleukin-11 (IL-11) and connective tissue growth factor (CTGF), which are TGF β target genes (Kang *et al.* 2003; Kang *et al.* 2005). The induction of both IL-11 and CTGF expression by TGF β is mediated by Smad signaling (Kang *et al.* 2005).

In addition, Smad molecules can activate the transcription of downstream targets such as plasminogen activator inhibitor type I (PAI-1) (Tu *et al.* 2003). Reduction in the level of PAI-1 is associated with disruption of the TGF- β activity in prostate cancer, which in turn leads to inhibition of urokinase type plasminogen activator (uPA) mediated extracellular matrix proteolysis. This is suggested as another possible mechanism for modulating metastasis (Lyon *et al.* 1995; Soff *et al.* 1995). Blocking the effects of TGF- β may be essential to allow tumour growth but consequent restoration of the TGF- β pathway at the right time contributes to tumour cell motility, epithelial-to-mesenchymal transition and eventually metastasis (Derynck *et al.* 2001).

In addition to the above, TGF- β 1 was found to stimulate collagenase production and enhance tumour cell invasion and metastatic potential (Welch *et al.* 1990). Therefore autocrine production of TGF- β 1 may affect tumour cells directly by decreasing cell adhesion or enhancing degradation of extracellular matrix components (Morton and Barrack 1995).

Additionally, loss of BMPs is linked to advanced prostate cancer and bone metastasis (Soda *et al.* 1998). Prostate cancers maintaining high levels of BMP signaling may be unable to proliferate in such a microenvironment. However, prostate cancer cells that lack expression of BMPRs could be released from the growth inhibitory effect of BMPs and enabled to proliferate in the bone (Kim *et al.* 2000).

A work done by Hamdy *et al.* 1997 of the relation between the expression of BMP-6 in prostatic cancer tissue and skeletal metastases, suggested that BMP-6 might be partially the cause for the osteoblastic changes in metastatic lesions that occur in prostate cancer (Hamdy *et al.* 1997).

However, BMP-7 was found in another study done by Buijs *et al.* to provoke TGF- β signaling effect in human prostate cancer cells that are known to be metastatic to bone. This study suggested that BMP-7 may govern the epithelial homeostasis in human prostate gland by maintaining the epithelial phenotype. It has been suggested that BMP-7 could be used as a new therapeutic molecule for repressing the progress of prostate cancer (Buijs *et al.* 2007).

1.9 Modulation of the TGF- β signaling as a strategy to suppress the formation of the bone metastases

The accumulation of evidence of the various roles TGF- β in immunosuppression, regulation of tumour growth and metastasis, has given rise to an increased interest in TGF- β as a therapeutic target (Arteaga 2006; Bierie and Moses 2006; Wrzesinski *et al.* 2007).

A study done by (Muraoka *et al.* 2002) revealed that cutting off the action of TGF- β resulted in inhibiting mammary tumour cells viability, migration and metastases. Introduction of dominant negative TGF- β Type II receptors (T β RII) into mammary cells resulted in retarding the primary tumour and metastases formation and prevention of epithelial-to-mesenchymal transition (EMT) (Oft *et al.* 1998). Furthermore, in osteolytic bone metastases inhibiting TGF- β might result in

interruption in the osteoclastogenic cycle and the progression of tumour growth (Loeys *et al.* 2006).

In another study done by (Shah *et al.* 2002) retrovirus-mediated introduction of a dominant negative TGFRII to bone marrow cells resulted in production of leukocytes capable of potent anti-tumour response and suppression of metastasis in both melanoma and prostate cancer models. These mechanisms were based on the interaction between the cytokine and its receptors. Recently another effective therapy was introduced based on siRNA in order to repress TGF- β activity in malignant cells (Friese *et al.* 2004; Bholra *et al.* 2013). Blocking the cytokine expression by using siRNA against TGF- β was found to inhibit tumour cell migration, tumour invasion, and restore anti-tumour immune response in mouse model (Friese *et al.* 2004). Inhibitors target phosphorylation of Smad proteins have been used and result in the suppression of Smad nuclear translocation (DaCosta *et al.* 2004; Scott *et al.* 2004) and might be used to inhibit TGF- β action.

Aiming at the osteoblastic response to prostate cancer could also be promising. An endothelin A receptor (ETAR) antagonist is found to reduce the advancement of prostate cancer bone metastases (Clines and Guise 2008).

A new class of possible beneficial agents is recognized against a wide range of diseases this class includes Si/shRNA. On the other hand, the benefits of this approach depends mainly on the effective delivery of shRNAs to tumour cells. Transfection of shRNA with lentiviruses into cultured mammalian cells may be an encouraging method in specific, efficient and stable knockdown of various genes (An *et al.* 2003; Grimm *et al.* 2005).

However, these examples show the enormous potential of the pathway as a therapeutic target although there may be negative consequences: the inhibition of TGF- β might result in chronic inflammatory and autoimmune reactions. In addition, Inhibition of TGF- β receptor function could further result in the development of compensatory resistance mechanisms by other activators of the Smad pathway similar to those that occur in individuals with inactivating mutations in TGF β RI and TGF β RII (Loeys *et al.* 2006).

1.10 Aim of the study

Prostate cancer represents one of the most common cancers and the second most common cause of cancer deaths in men worldwide. More than 80% of patients with advanced prostate cancer develop bone metastases (Mundy 2002; Jemal *et al.* 2007). The human prostate cancer cell line PC3 preferentially colonizes vertebrae and the long bones of the hind limbs when injected into the circulation of immunosuppressed mice. The factors that regulate colonization of the skeleton and tumour growth in this model are not well understood. What is clear is that these cells produce lesions that are eventually osteolytic in appearance and that this is a result of tumour cells modifying the bone microenvironment during the formation of metastases. It is also apparent that PC3 cells produce significant levels of a number of cytokines that are osteoinductive such members of the TGF β family including TGF β 1, BMPs 2 and 3 and an antagonist in this system, Noggin. The relative contribution of these signaling molecules to the events of attachment of tumour cells to bone cells and early colony initiation is unknown, what is clear is that the effects of these cytokines are unlikely to be simply autocrine but also paracrine acting on tumour associated cell populations.

The aim of this study is to investigate the interaction between prostate cancer cells (PC3-RFP) and bone cells (SaOS-2 and MG63) and to determine which members of the TGF β superfamily contribute these interactions and potentially to the colonization of tumour cells to the skeleton. This study will test the hypothesis that tumour derived TGF β signaling regulates the growth and differentiation of osteoblastic lineage cells and contributes to the survival and growth of prostate cancer cells *in vivo*.

The hypothesis of my study was addressed through four objectives.

- 1- Determine the effect of Prostate cancer cells on the growth of osteoblastic cell lines and their differentiation (chapter 3).
- 2- Determine the expression of TGF- β superfamily genes in human prostate cancer cells grown alone and in direct contact with osteoblastic cells or when osteoblasts were exposed to products of prostate cancer cells present in conditioned medium. Levels of expression of these genes in these populations will be compared and important differences investigated further (chapter 4).
- 3- Determine the effect of Noggin on the growth of osteoblast SaOS2 cells. This will be achieved by evaluating the effect of conditioned media collected from PC3

knock down Noggin (PC3-KD) cells on the proliferation of osteoblast (SaOS2) cells compared to conditioned media collected from control PC3RFP-mock cells. In addition I will determine the effect of exogenous recombinant Noggin on the growth rate of osteoblast cells (chapter 5).

- 4- Determine whether tumour frequency and growth of PC3 prostate cancer cells (Noggin knockdown/ mock control) is affected by Noggin expression in the BALB/c nude mice (chapter 6)

Chapter 2: Material and Method

2 Chapter 2: Material and Method

2.1 Tissue culture Materials and Disposable Equipment:

Item	Supplier
Disposable pipettes (2,5,10 and 25ml)	Sterilin
Disposable Tips (200 and 1000µl)	Corning Incorporated
Centrifuge Tubes (15 and 50ml)	Sterilin
Flasks (T25 and T75)	IWAKI
Multi well plates (24 and 96 wells)	IWAKI
Cryovials 2ml	Corning Incorporated
Nalgene™ Cryo 1°C freezing container	NALGENE
Cell culture Materials	
DMEM without pyruvate	Gibco
Penicillin/streptomycin	Sigma
Sodium bicarbonate	sigma
Fetal Bovine Serum (FBS)	PAA-The cell culture Company
Trypsin/EDTA	Sigma
DMSO	Sigma
Ethanol	Sigma
Vi-CELL™ XR Quad Pak Reagent Kit	Beckman Coulter
Vi-Cell XR Cell Viability Analyzer	Beckman Coulter

2.2 Tissue culture techniques

2.2.1 Cell Lines

PC3 cell line was obtained from the American Type Cell Collection (ATCC), and was transfected with pDSRed-monomer-Hyg-C1 plasmid to become stable hygromycin resistance and to stably express RFP by Dr. Colby Eaton's group at Sheffield University.

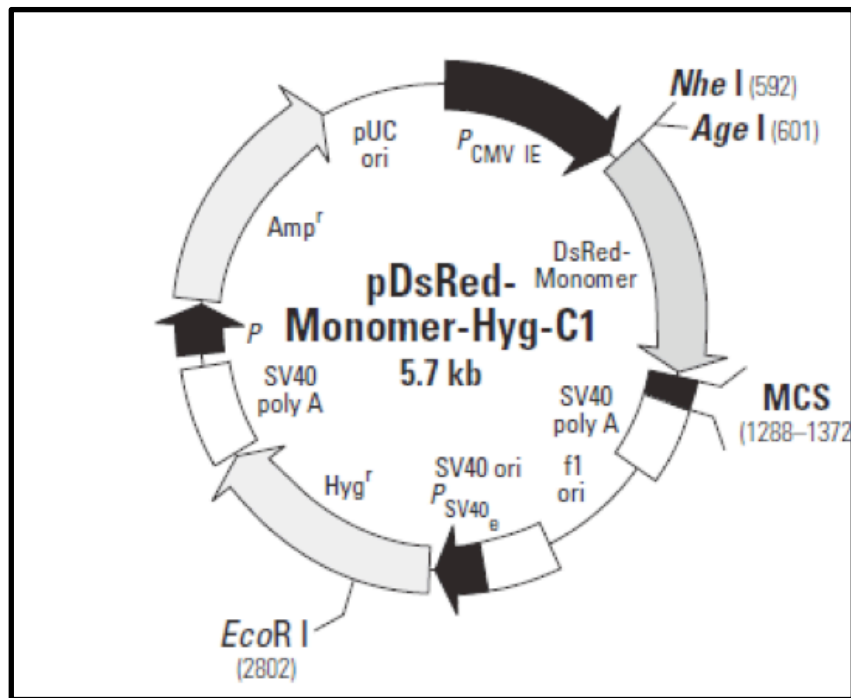


Figure 2.1 Plasmid map for the pDSRed-monomer-hyg-C1 used to produce PC3 RFP cells.

Illustrate that transfected cells acquire red fluorescent and hygromycin resistance.

The SaOS-2 cells are osteoblasts-like human cell lines derived from patient osteosarcoma (Rodan *et al.* 1987). They were acquired from the ATCC.

The MG63 cells were obtained from ATCC. They are human undifferentiated osteosarcoma cell line, which has both mature and immature osteoblastic characterization (Pautke *et al.* 2004).

All cell lines (PC3-RFP, SaOS-2 and MG63 cells) that have been used in these experiments were thankfully given by Dr. Colby Eaton at Sheffield University.

2.2.2 Maintaining and sub-culturing of cell lines

All cell lines were routinely maintained in sterile T75 flasks in humidified incubator at 37°C and 5% CO₂. PC3-RFP, MG63 and SaOS-2 cells were grown in a high glucose without Pyruvate formulation of Dulbecco's Modified Eagle Medium (DMEM) supplemented with 10% Fetal Bovine Serum (FBS) and 1% Penicillin/streptomycin (p/s). The confluence of the cultures was checked under an inverted microscope. When the cells were around 90% confluent the cells were harvested by trypsinisation and passaged in new T75 flasks and some of them were freeze down and stored in liquid nitrogen as a stock.

2.2.3 Cell harvesting by trypsinisation

Trypsinisation is a method that is used for harvesting the adherent cells to generate a cell suspension for either the purpose of sub-culture or for counting in order to re seed for a specific experiment.

For a T75 flask, the medium was removed, and the cells were washed with 10ml Dulbecco's phosphate buffer saline (PBS). 5ml of Trypsin-EDTA was added in order to detach the cells. The flasks were incubated in trypsin-EDTA at 37°C until all the cells detached. This was detected by using the inverted microscope. After cell dissociation, trypsin-EDTA was neutralized by adding 10ml of the standard medium with the correct percent of FBS designed for the experiment. The time for cells to dissociate differs according to the type of cell (5-10min for the PC3-RFP and MG63, 10-15min for the SaOS-2 cells) and the time it had been cultured.

2.2.4 Thawing and freezing of the Cells

Cell lines were regularly frozen for long-term storage. All experiments were done within 5 passages for PC3RFP and up to 20 passages for SaOS2 and MG63 cells.

2.2.4.1 Freezing cells

Cell lines were harvested near the confluent phase by trypsinisation. Cells were pelleted by centrifugation and re-suspended in 1ml of freezing medium (standard medium with 7.5% DMSO). The cell suspension was put in aliquots of 1ml in cryo-vials, placed in a Nalgene Cryo 1°C freezing container to allow slow freezing (-1°C/min) and frozen at -80°C overnight. After 24h, the cryo-vials were transferred to a liquid nitrogen storage tank for long term storage.

2.2.4.2 Thawing cells

The vials from liquid nitrogen were defrosted by partial immersion in water bath at 37°C. Then the cells were centrifuged (500xg, 5min). The pellets were re-suspended in standard medium and seeded in sterile flask.

2.2.5 Cell counting using Beckman Coulter Vi-cell^{XR} Cell Viability Analyzer

The Vi-cell Cell viability analyzer uses the same widely accepted trypan blue dye exclusion method to determine cellular viability.

In the Vi-CELL system a proprietary algorithm is utilized to determine which cells have absorbed the trypan blue dye and which have not.

In order to count the cells by using the Beckman coulter vi-cell cell viability analyzer the cells were harvested by trypsinisation method as described in 2.2.3. The cells

were centrifuged at (5000xg, 5min). The supernatant was removed and 10ml of the standard medium was added to the pellet. The cells were mixed well using 10ml syringe. 1ml from the solution was transferred to an empty cup designed for the Beckman coulter vi-cell cell viability analyzer. The results obtained will be in the form of Total cell/ml and viable cell/ml.

2.3 Molecular Techniques

2.3.1 Materials and Disposable Equipment used for RNA Extraction

ITEM	SUPPLIER
QIAGEN® RNAeasy Mini Kit	QIAGEN®
QIAGEN® DNase treatment	QIAGEN
Ethanol(for molecular biology)	Sigma-Aldrich
Nuclease Free PCR tubes 1.5ml	Fisher scientific
10cc Syringe	Hwajin medical company
NanoDrop-1000 spectrophotometer	Thermo-Fisher
RNA 6000 Nano Kit	Agilent
Agilent 2100 Bioanalyzer	Agilent
Chip Priming Station	Agilent
IKA vortex mixer	IKA
RNaseZAP	Ambion
RNase free Water	Ambion
Microcentrifuge	Agilent
Heating Block	Agilent
Reverse Transcription	
dNTP	Bioline
Oligo dt	Promega
Random (N) ₆ primer	Promega
DEPC- treated water	Ambion
Buffer	Invitrogen
0.1 dtt	Invitrogen
RNase inhibitor	Promega
Superscript III reverse transcriptase	Invitrogen
Quantitative real time PCR	
TaqMan Universal master Mix	Applied Biosystem
Human GAPDH(20X)	Applied Biosystem
COL1A	Applied Biosystem
TaqMan gene expression assay Noggin	Applied Biosystem
Runx2	Applied Biosystem
Osterix	Applied Biosystem
MicroAmp optical 96-wellreaction plate (0.1ml)	Applied Biosystem
StepOne Plus Real time PCR	Applied Biosystem

2.3.2 RNA Extraction from cells using Qiagen RNAeasy Mini Kit

Preparation of the RNeasy Lysis (RLT) Buffer:

Six microliter of β -mercaptoethanol was added to each 600 μ l of the RLT Buffer.

The amount of RLT buffer added to different sizes of Tissue culture flasks:

Tissue culture Flask	Amount of RLT buffer added	Amount of β -Mercaptoethanol
T25 flask	600 μ l	6 μ l
T75 flask	1200 μ l	12 μ l

First Step:

After preparing the RLT buffer, the medium was removed from the flask and cell were washed with 3ml cold PBS. RLT buffer was added to the flask and cells were removed completely from the flask in to RNase free PCR tube by using 10ml Syringe. The cells were mixed by vortex; at this point cells were stored at -80°C .

Second Step:

Samples were thawed out completely, and an equal amount of 70% ethanol was added to each sample (i.e. 1200 μ l Ethanol). The samples were mixed thoroughly by vortex for 1 min.

700 μ l of each sample were transferred to an RNAeasy Mini spin column placed in a 2ml collecting tube. The lid was closed carefully and centrifuged for 30 s at maximum speed (8000xg). The flow through was discarded and another 700 μ l of each of the samples were transferred to the same RNAeasy Mini spin column and steps were repeated again until all the samples were finished. 350 μ l of RW1 (washing Buffer lysate/ethanol) were added to each column of samples and centrifuged for 30 s at the maximum speed (8000xg) and again the flow was discarded.

DNA digestion step:

Preparation of the RNase-free DNase I Enzyme for the first time:

560 μ l RNase free water was injected into the enzyme vial and was gently mixed by inverting the vial. The enzyme should be divided into single use aliquots and store at -20°C .

70µl of RDD buffer were added to each 10µl of Enzyme for each sample. 80µl of the above mixture (enzyme+ buffer) were added to each sample and were kept at room temperature for 15min. 350µl of the RW1 were added to all samples and centrifuged at the maximum speed for 30 s. The flow was discarded and 500µl of the second washing buffer RW2 was added on all samples. The samples were centrifuged again for 30 s and the flow was discarded. Another 500µl of the RW2 were added and same previous step was repeated. The collecting tubes were changed and the samples were centrifuged for 1 min. The spin columns were placed on a new 1.5 collecting tube and a 30µl of RNase free water were added directly to the membrane of the column in order to dissolve the RNA. The lids were closed and the samples were centrifuged for 1 min, this is called the first elution. The spin columns were placed on another new 1.5 collecting tube and a 30µl of RNase free water were added directly to the membrane of the column in order to dissolve the RNA. The lids were closed and the samples were centrifuged for 1 min and this is called the second elution.

2.3.3 Quantification of RNA

The quality and the quantity of the RNA produced were assessed by using the Nandrop spectrophotometer. One microliter of each sample was loaded on the Nandrop spectrophotometer. The concentration of the RNA was measured at a wavelength of 260nm while the ratio between the two wavelengths A_{260} and A_{280} indicate its purity. In all experiments the concentration of the RNA extracted from cells ranges between 50-1000ng/µL. the A_{260}/A_{280} ratio in all experiments were above 1.8 which indicate that the RNA obtained were free from protein contamination.

2.3.4 Analyzing the RNA integrity by using the RNA 6000 Nano Bioanalyzer Kit

The integrity of the RNA was assessed by using RNA 6000 Nano Bioanalyzed kit, which resemble RNA agarose gel electrophoresis. A good quality undegraded RNA characteristic was indicated by the presence of 2 horizontal bands representing the 28S and the 18S ribosomal RNA as shown in Figure (2.2).

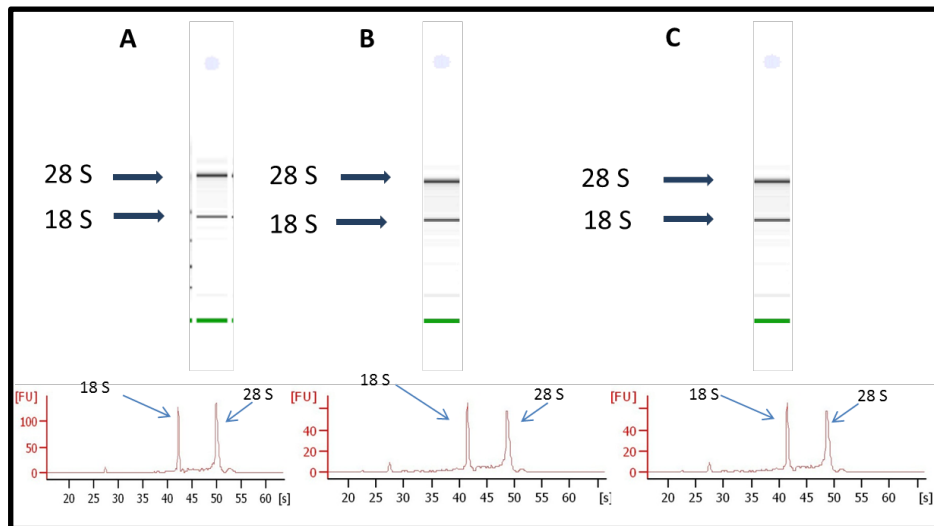


Figure 2.2 RNA integrity using RNA 6000 Nano Bioanalyzed kit.

clear 28S and 18S bands represent an intact RNA (A) illustrate RNA integrity in PC3RFP (B) illustrate RNA integrity in SaOS2 (C) illustrate RNA integrity in MG63

Preparing the RNA ladder:

The ladder was transferred to an RNase free vial and denatured for 2 min at 70°C then; the vial was immediately cooled down on ice. Aliquots were prepared in RNase free vials and stored at -80 °C. The ladder aliquot that will be used was thawed and was kept on ice.

Preparing the Gel:

All reagents were allowed to equilibrate to room temperature for 30 min. Five hundred fifty microliter of Agilent RNA 6000 Nano gel matrix (red) were added into the top receptacle of a spin filter. The spin filter was placed in a microcentrifuge and centrifuged for 10 min at 1500xg. The filtered gel was divided into aliquots containing 65µl in each 0.5ml RNase free microfuge tubes.

Preparing the Gel-Dye Mix:

All reagents were allowed to equilibrate to room temperature for 30 min. Note: the dye concentrate should be protected from light while keeping at room temperature. The RNA 6000 Nano dye concentrate was mixed buy vortex for 10 s and spun down. One microliter of the RNA 6000 Nano day concentrate was added to the 65µl aliquot of filtered gel was prepared previously. The tube was closed and mixed thoroughly. The tube was spun down for 10 min at room temperature at 13000xg.

Loading the gel-Dye mix:

The gel dye mix was allowed to equilibrate to room temperature for 30 min. A new RNA Nano chip was taken out of its sealed bag. The chip was placed on the chip priming station. 9µl of the gel dye mix was pipetted at the bottom of the well-marked **G**. The timer was set to 30 s and the plunger was positioned at 1ml. Then the chip priming station was closed. The plunger of the syringe was pressed down until it was held by the clip. The syringe was released after 30 s. The plunger was pulled back slowly to the position 1ml again. The chip priming station was opened. 9µl of the gel dye mix was pipetted to each of the wells.

Loading the RNA 6000 Nano Marker:

Five microliters of the RNA 6000 Nano marker were pipetted into each of the 12 sample wells and the ladder well.

Loading the ladder and the samples:

The ladder aliquots were thawed and kept on ice. The samples were heat denatured at 70°C for 2 min in order to minimize secondary structure before loading the samples. One microliter of the RNA ladder was pipetted into the well-marked with the ladder symbol on the top of the chip. One microliter of each sample was pipetted into each of the sample wells. The chip was placed horizontally in the adapter of the IKA vortex mixer and was mixed by vortex for 60 s. The chip was inserted into the Agilent 2100 bioanalyzer and the run was started.

2.3.5 Reverse Transcription and cDNA production

The RNA samples were diluted to be about 500ng/µl. one microlitter of the samples were added to 1 µl of dNTP, 0.5 µl of oligo dT, 0.5 µl random (N)₆ primer and DEPC-treated water to a total of 10 µl of volume. The solution was incubated at 65°C for 5 min, and chilled in ice for 1 min. Four microliter of the buffer, 1 µl of dtt and 1 µl of RNase inhibitor were added to the negative sample only. Four microliter of the buffer, 1 µl of dtt, 1 µl of RNase inhibitor and 1 µl of Superscript III reverse transcriptase were added to the positive sample and the No RNA tube. Samples were incubated for 2h at 50°C, and the reaction was terminated by increasing the temperature to 70°C for 15 min. The cDNA produced from the reaction was stored at -20°C.

2.3.6 Quantitative real time PCR

Reverse transcription RT/PCR is the most sensitive technique to determine the expression of specific transcript in an mRNA population. QRT/PCR was performed on cDNA samples either to test the quality of the cDNA produced by checking the expression of the housekeeping gene Glyceraldehyde-3-phosphate dehydrogenase (GAPDH) or to determine the expression of specific genes in the study. Taqman universal master mix was used with primer of interest. Each 20 μ L of cDNA sample was diluted with 20 μ L of DNase/RNase free water. 2 μ L of each sample was loaded in fast optical 96 well reaction plate (0.1ml). The volume of reagents added per reaction is listed in Table below.

Reagent	Volume (μ L)
Taqman universal master mix	5 μ L
Primer of interest	0.5 μ L
DNase/RNase free water	2.5 μ L

Quantitative RT/PCR was performed using StepOne plus PCR with denaturation temperature of 95°C, annealing temperature 55-65°C and elongation temperature of 72°C these three steps makes one cycle which is repeated for 40 times (40 cycles). Runx2, COL1A, Ostrix, Noggin and GAPDH assays were used. Expression was then normalised with housekeeping gene GAPDH.

2.4 Western blot

Western blot is a technique used to detect the presence of specific proteins according to their capability to bind to precise antibodies against these proteins. Polyacrylamide gel electrophoresis (PAGE) is used to separate proteins within samples. Samples must be treated with strong reducing agent to remove secondary and tertiary structure of protein allowing the separation to occur according to the molecular weight of the protein. Sodium dodecyl sulfate (SDS) was added to both the polyacrylamide gel and to the running buffer in order to maintain the polypeptides in the denatured form and to impart a uniform negative charge to linearized proteins.

Materials, disposable equipment and chemicals used in western blot technique

Item	Supplier
Protein extraction and measurement	
RIPA buffer	Sigma-Aldrich
Protease inhibitor cocktails	Sigma-Aldrich
Bicinchoninic (BCA)	Sigma-Aldrich
Copper (II) sulphate solution	Sigma-Aldrich
Bovine serum albumin (BSA)	Sigma-Aldrich
Western blot	
Mini protein electrophoresis apparatus with mini trans blot electrophoretic transfer cell	Biorad
0.25M TRIS	Sigma-Aldrich
Glycine	Sigma-Aldrich
SDS	Sigma-Aldrich
Methanol	Sigma-Aldrich
Phosphate buffer saline Tablet	Oxoid
Tween 20	VWR international
1.5M Tris-HCl pH8.8	Sigma-Aldrich
0.5M Tris-HCl pH6.8	Sigma-Aldrich
30% Acrylamide	Geneflow
ammonium persulphate (APS)	Sigma-Aldrich
Tetramethylethylenediamine (TEMED)	Sigma-Aldrich
BIO-RAD molecular weight marker	Biorad
β - Mercapto Ehanol	Sigma-Aldrich
Glycerol	Fisher scientific
Bromophenol blue	Sigma-Aldrich
Anti-Noggin antibody	abcam
Anti-GAPDH	abcam
Anti- β - actin	abcam
anti-rabbit IgG, horseradish peroxidase-linked species-specific secondary antibody	GE Healthcare
Polyvinylidene fluoride (PVDF)	Immubilon transfer membranes, milipore
Filter paper	Sigma-Aldrich
Supersignal west dura chemiluminescent substrate	Thermo-scientific
Kodax biomax MS film	Sigma-Aldrich
Skimmed milk powder	Marvel
Developer	AGFA
Rapid Fixer	AGFA

2.4.1 Protein extraction using Radio-Immunoprecipitation Assay (RIPA) buffer

RIPA buffer and protease inhibitor cocktail in ratio of (1:100) was used to extract proteins from cells. 500 μ L of RIPA buffer and 5 μ L of protease inhibitor cocktail were added to confluent T75 flask of either osteoblast or PC3RFP cells. Protease inhibitor cocktail was added in order to stop protein degradation.

2.4.2 Bicinchoninic acid (BCA) protein assay

Total protein concentration was determined by BCA protein assay method (Smith et al., 1985). The copper sulphate(II) in the reagent is reduced to copper sulphate(I) by the presence of peptide bonds in the proteins. The amount of proteins in the sample is relative to the amount of copper sulphate(II) that being reduced. Standard curve was conducted using the following BSA concentration, 1000 μ g/ml, 800 μ g/ml, 600 μ g/ml, 400 μ g/ml, 200 μ g/ml, 100 μ g/ml and 0 μ g/ml. 10 μ l of each standard protein concentration and samples were added in duplicate into 96 well plates. BCA working reagent was prepared by adding 50 part of BCA reagent to 1 part of copper sulfate (II). 200 μ l of BCA working reagent was added into each well of standard and samples. Plates were incubated for 30minutes at 37°C and read on a plate reader (DYNEX technologies, MRX II) at 562nm.

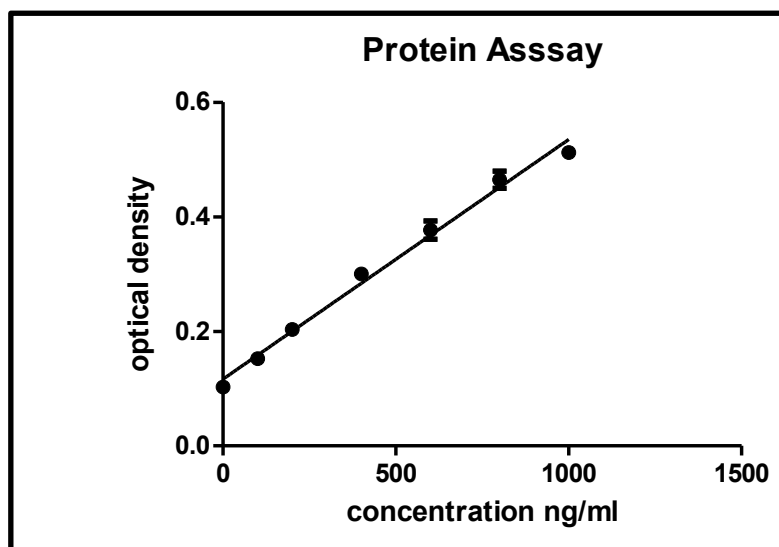


Figure 2.3 Example of Protein assay standard curve.

10 μ L of protein standards dilutions (BSA 1mg/ml) and of protein samples in duplicate were incubated with 200 μ L of BCA/copper sulfate solution for 30 min. It was measured using microplate reader at absorbance of 560nm. The concentration of the unknown protein samples was calculated from this protein standard curve.

Preparation of buffers used in Western Blot

10X Tris/Glycin (1L)		1X Transfer Buffer (2L)		5X Sample (Laemmli) buffer	
Tris 250mM MW 121.14g/mol	30.3g	10X Tris/Glycin	200ml	0.5M Tris-HCl pH 6.8	1.75ml
Glycin 1.92M MW 75.07	144.1g	Methanol 20%	400ml	Glycerol	4.5ml
1X Running Buffer (2L)		Washing Buffer (2L)		Washing Buffer (2L)	
10X Tris/Glycin	200ml	PBS	20 Tablet	SDS	0.5g
SDS 10%	20ml	Tween 20	1ml	Bromophenol blue 0.2%	0.5ml
Stripping Buffer (1L)				1X TBST	
Glycine		15g		10XTBS	100ml
SDS		1g		Tween 20	1ml
Tween 20		10ml		Complete the volume to 1L with ultra-pure water	
Adjust pH to 2.2 bring volume to 1L with ultra-pure water					

2.4.3 Sample preparation

All samples, whether the recombinant Noggin or cell lysate, were mixed with Laemmli Buffer X5, one part buffer with four parts sample. Protein sample and buffer solutions were mixed by inversion and denatured for 5 min at 95°C. Boiled samples were mixed by inversion and kept on ice until gel loading.

2.4.4 Sodium-Dodecyl-Sulphate Poly-Acrylamide Gel Electrophoresis (SDS-PAGE)

For each experiment two SDS 12%(w/v) resolving gel was prepared by a mixture of 8 ml of Acrylamide 30%, 5 ml of resolving gel buffer 1.5M Tris (pH8.8), 6.6 ml of water, 200 µl of 10% SDS, 200µl of 10% ammonium persulphate (APS) and 8µl of Tetramethylethylenediamine (TEMED). This was loaded between the spacer plates 1.5 mm apart and kept for 30 – 40 min to polymerise. To maintain an even gel level and stop gel dehydration, butan-2-ol was added covering approximately 0.5 cm of the

top of the gel. Once the separating gel had set, all traces of butan-2-ol was washed from the gel three times, using distilled water. 5%(w/v) stacking gel was prepared by mixing of 1.34ml of Acrylamide 30% (Total), 1ml of stacking gel buffer 0.5 M Tris, 5.4 ml of water, 80 μ l of 10% SDS, 80 μ l of 10% APS and 8 μ l of TEMED. These were loaded onto the resolving gel after it had polymerised. 10 or 15 plastic toothcombs were placed between the glasses in the separating gel to form wells for the samples. When the gel had set, the comb was removed and the glass plates were placed into an electrophoresis tank. The tank was filled with 1X running buffer. Horse Radish peroxidase (HRP) conjugated molecular marker (BIO-RAD) was added to the first lane of each gel and 40 μ g of protein in 30 μ l were then loaded into the gel slots for electrophoresis and run at 60 volts (constant voltage) for 40 min. Afterward, the volt was increased to 150 volts for another 40 min or until the sample buffer disappears from the gel.

2.4.5 Protein transfer

Following protein migration, the stacking gel was cut off from the remainder of the gel and discarded. The separating gel was dislodged from the glass pane. Polyvinylidene fluoride (PVDF) membrane was soaked in methanol prior to use. Within an open transfer cassette a sponge and one of the filter paper were placed followed by PVDF membrane then, the gel was placed on the PVDF membrane (marker facing top left of membrane) and sandwiched with another pieces of cellulose blotting paper and a sponge were made. The cassette was then closed and placed into an electrophoresis tank. The tank was filled with 1X transfer buffer, and ice pack and a magnetic stirrer to maintain temperature. Membranes were blotted at 70V for 55- 60 min at 4°C.

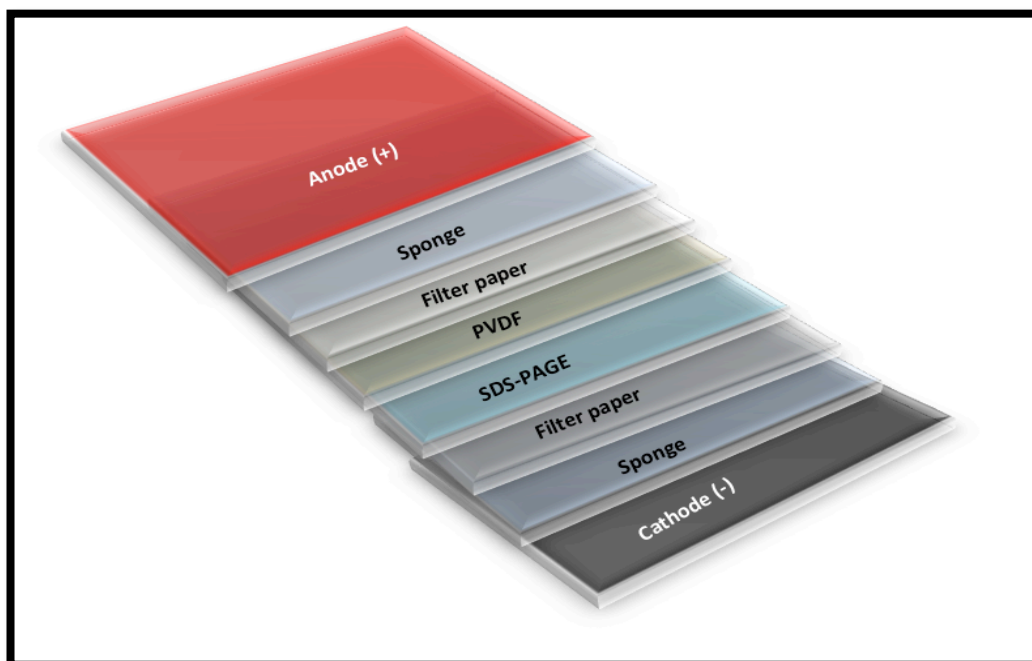


Figure 2.4 Diagram illustrating the transfer apparatus for western blotting

proteins, which are negative, charged with SDS travel to positive pole, when electric field is applied to the apparatus. The protein then was captured by PVDF membrane. Mini trans-blot electrophoretic transfer cell, Biorad is gathered in this order: cassette (red/anode, sponge, filter paper, PVDF, SDS-PAGE, filter paper, sponge and black/cathode side of the cassette).

2.4.6 Immuno-detection of Noggin on western blots

After the transfer, the membrane was blocked using 3% BSA in PBS /Tween for 1h at room temperature. After the blocking, the membrane was incubated on a rotary shaker overnight at 4°C with 10µL of anti-Noggin antibody (1:500 dilution) in 5ml 3% BSA. Membranes were washed 3 times for 10 min in PBS tween on a rotary shaker and incubated with 2µL anti-rabbit IgG, horseradish peroxidase-linked species-specific at a (1:15000 dilution) in 30ml 5% milk solution for 1h on a rotary shaker at room temperature. Membranes were washed 3 times for 20 min in PBS tween on a rotary shaker. Membranes were dipped in enhanced chemiluminescent substrate for 5min for detecting horseradish peroxidase, in which horseradish peroxidase cleave the chemiluminescent and produces luminescence in proportion to amount of protein. Films (Hyperfilm™, Amersham) were developed using AGFA Curix 60 in the dark room.

2.4.7 Antibody stripping and membrane re-probing

After membranes were analyzed with Noggin antibody the membrane was 'stripped off' and re-probed with housekeeping antibody (GAPDH or β -actin). In order to strip the membrane of bound antibodies, the membrane was washed twice with TBS/T for 5min on shaker at room temperature. Then it was washed twice with PBS/T for 5min. The membrane was blocked using BSA 3% for 1h at room temperature. Primary antibody of the housekeeping protein (GAPDH or β -actin) was added in 1:10,000 dilution and was incubated for 1h at room temperature on shaker. Same secondary antibody was used as described previously and washed with PBS/T. Then the membrane was visualized using chemiluminescent substrate for 5min. Films (Kodak™, Amersham) were developed using AGFA Curix 60 in the dark room.

2.5 Cell Sorting using Flow cytometry BD FACS Aria

Flow cytometry was used to separate different cell populations from each other to form highly purified cells for further specific characterization. PC3RFP were seeded with either SaOS2 or MG63 in co-culture experiments until cells reached specific cell densities when cells were separated and sorted using BD FACS Aria. The separation was based on the presence of the red fluorescent dye for which PC3RFP cells were considered to be positive cells and osteoblasts (SaOS2, MG63) were considered to be negative. The purity of all cells that were used in further experiments after sorting was above 92%.

2.6 Statistical analysis

All data were analysed using an ANOVA test (1-way analysis of variance) for more than two group comparisons or with *t* test for two group comparisons data was first tested for normality distribution if the data was normally distributed ANOVA test was used and Bonferroni test was used as post-hoc analysis. When data not normally distributed, ANOVA test (non-parametric Kruskal-Wallis test) was used for more than two group comparisons or non-parametric Mann–Whitney test was used for two group comparisons. Dunns test was used as post-hoc analysis when ANOVA test was used in not normally distributed data. Data were considered statistically significant when a p-value was equal to or less than 0.05. Results are expressed as mean \pm values of standard error (SME).

Chapter 3: General characterization of cell lines and assessment of the effects of prostate cancer cells on osteoblastic cell proliferation and differentiation

3 Chapter 3: General characterization of cell lines and assessment of the effects of prostate cancer cells on osteoblastic cell proliferation and differentiation

3.1 Introduction

Ninety percent of patients with advanced prostate cancer develop bone metastases (Bubendorf *et al.* 2000). Bone metastases associated with prostate cancer differ from those derived from other types of cancer in that they are characterized by an osteoblastic appearance. This is due to an imbalance between bone resorption and bone formation where the latter is favoured in prostate cancer metastases (Weilbaecher *et al.* 2011; Theriault and Theriault 2012). Bone is the most frequent single site for prostatic cancer metastasis, which suggests that prostate cancer cells have a specific affinity for bone both in terms of attachment and as a site for survival/growth outside the prostate. This interaction between cancer cells and bone microenvironment is thought to be mediated by survival/growth factors secreted by bone and cancer cells, as well as angiogenic factors and bone resorption regulators that promote the growth of cancer cells themselves inside a modified bone microenvironment (Mundy 2002; Roodman 2004). In addition, bone cells secrete other growth factors such as TGF- β and BMPs which enhance the survival of prostate cancer cells in the bone (Miyazono *et al.* 2010). A so called 'vicious cycle' of tumour growth leading to disrupted bone turnover and release of more tumour promoting factors has been suggested (Yoneda and Hiraga 2005).

The exact mechanisms by which prostate cancer stimulate bone growth are still unknown. For this reason many studies have focused on soluble protein that is secreted from the tumour cells which stimulate bone growth within the bone tumour microenvironment (Larson *et al.* 2014). Several studies have shown that condition media collected over the human prostate cancer cell line PC3 stimulated proliferation of osteoblast-like cells (Martínez *et al.* 1996; Larson *et al.* 2014). Nishimori *et al.* 2012 showed in his study that prostate cancer cells facilitate the differentiation of osteoblastic cells when co-culturing prostate cancer cell line LNCaP with mouse osteoblast MC3T3 (Nishimori *et al.* 2012).

Cell lines that were used in my study were a strain of human prostate cancer cell line PC3 (PC3RFP) and human osteosarcoma cell lines SaOS2 and MG63. Growth curves were conducted to all of these cell lines to determine their rate of growth during the log phase and exponential phase. Serum titration curve was established to determine the maximum and 1/2 maximal growth rates during the log phase which will be used in further experiments.

Aim

The aim of this study is to determine the effect of prostate cancer cells on the proliferation and differentiation of osteoblastic cells (SaOS2 and MG63).

Hypotheses

Prostate cancer cells stimulate the growth of osteoblastic cell lines and decrease their differentiation.

Objectives

- 1- To determine basic cell growth and differentiation characteristics of prostate cancer and osteoblast cell lines.
- 2- To evaluate the effect of prostatic cancer cell (PC3RFP) conditioned media (CM) on the growth of both SaOS2 and MG63.
- 3- To determine the effect of PC3RFP-CM and co-culture on the differentiation of osteoblastic cell lines by measuring ALP activity, Alizarin red and the expression of some of the structural protein genes associated with osteoblast differentiation such as Runx2, Col1A and Ostrix (SP7).

3.2 Materials and Methods

3.2.1 Materials and Disposable Equipment

Item	Supplier
Triton	Sigma-Aldrich
Fast p-nitrophenyl phosphate Tablets to prepare 20ml contains 1mg/mlPNPP and 0.2M tris buffer.	Sigma-Aldrich
Quant-iT PicoGreen dsDNA assay kit, 10×100µL enough for 2000 assays.	Invitrogen
Alizarin Red S	Sigma-Aldrich
DNase and RNase free water	Invitrogen
COL1A Taqman assay	Applied Biosystem
Runx2 Taqman assay	Applied Biosystem
Osterix Taqman assay	Applied Biosystem
Human GAPDH Taqman assay	Applied Biosystem
TaqMan Universal master Mix	Applied Biosystem

3.2.2 Generating Growth Curves

The cells were harvested by trypsinisation and counted by using the Beckman Coulter Vi-Cell counter as described in chapter 2 section (2.2.3 and 2.2.5). The PC3-RFP cells were seeded at a density of 5000cell/well in a 24 well plate for growth curve experiments. For the SaOS-2 and MG63 growth curves, the cells were seeded at a density of 15,000cell/well in a 24 well plate.

Cells were counted every 48h 12 days and each 48h time point was done in quadruplicate. The average (mean) cell numbers present were calculated for each day. The media was changed every 4 days during the growth curve and finally, a growth curve was generated for the number of cells present on each day in culture. In initial experiments, growth curves were done in medium containing 10% FBS to establish the start and duration of exponential growth and this information used in subsequent experiments to ensure cells were challenged during this growth phase.

3.2.3 Generating Serum titration curves

The cells were harvested by trypsinisation and counted by using the Beckman coulter counter and seeded in the same density as used in the growth curve experiments for both PC3-RFP and SaOS-2 cell lines using the standard medium of 10% FBS.

After 48h, cells were first washed with serum free media and then challenged with different FBS concentration starting from (0%, 1%, 2%, 4%, 5%, 6%, 8%, 10%, 12%, 14%, 15%, and 20%).

All cells were harvested and counted on day 6, which was estimated as mid exponential growth from 3.2.2.

3.2.4 Generating Condition media from PC3RFP cells

Ten T75 flasks were made with a density equivalent to the density that was used in the growth curves. Seven flasks were for the collection of conditioned medium (CM) and an additional three flasks were made for counting to monitor the growth of the cells. The cells were seeded in standard medium with 10% FBS.

After 48h the cells were washed with PBS and transferred to DMEM containing either 2% or 4% FBS. One flask was counted on the same day. Another two flasks were counted on day 4 and day 6. On day 6, the cells were found to be at the beginning of the confluent phase so the medium was changed in all flasks. On day 7, the medium was collected from the remaining flasks, transferred to a 50ml tube and centrifuged at room temperature at 1000xg for 10 min to pellet all cell debris and dead cells. The medium was filtered through 0.22 micrometre filter. Medium was divided into aliquots of 5ml each and stored in -80°C. The cells in each of the seven flasks were counted in order to know the exact number of cells present in each flask.

3.2.5 Challenging the SaOS-2 cell with the conditioned medium (CM)

The SaOS-2 cells were seeded in 24 well plates in the same density used for the growth curve using standard medium of DMEM with 10% FBS. After 48h, the cells were washed with PBS and the conditioned medium was added at different concentrations to quadruplicate cultures for each specific concentration (2%, 5%, 10%, 25%, 50%, 100% conditioned medium). The cells were counted on day 6 in the middle of the exponential growth and on day 10 at the end of the exponential growth. The same experiment was repeated but by using the concentration that was associated with the maximum observed growth.

3.2.6 Analysis of the effect of condition media (CM) on the proliferation of Osteoblastic cell lines

The cells were harvested by trypsinisation and counted as described in chapter 2 sections (2.2.3 and 2.2.5). The same seeding density was used in SaOS2 and MG63 that were used in growth curves in the 24 well plate using 50%CM containing either

2% (Saos2) or 4% (MG63) FBS. This was compared to controls for each type of cells grown in half maximum FBS concentration in standard DMEM media, which were 2%FBS for the SaOS2 cells and 4% with MG63 cells.

Cells were counted every 48h until day 12 and each 48h was done in quadruplicate and the mean cell numbers calculated for each day. The media was changed every 4 days during the growth curve in all groups.

3.2.7 Differentiating MG63 by using differentiation media

MG63 are considered to be an undifferentiated osteoblast cell line. These cells were differentiated by differentiation media. Differentiation media was prepared by adding 10mM β - glycerophosphate and 50 μ g/ml of Ascorbic acid in the standard DMEM with 4% FBS. The differentiation of MG63 was detected by measuring alkaline phosphatase (ALP) and alizarin red over 4 weeks. MG63 was seeded in nine 96 well plates (3000cells/well) for measuring ALP activity and in nine 24 well plates (15,000 cells/well) for measuring alizarin red in standard DMEM with 4%FBS. After 24 hours ALP activity and alizarin red were measured in the first 96 well plate and 24 well plate respectively. The media was changed to the differentiation media in the rest plates and ALP activity and alizarin red was measured on the days 2, 4, 7, 10, 14, 21 and 28. Media was changed regularly every 4 days.

3.2.8 Analysing the effects of condition media on the proliferation of differentiated MG63

After differentiation, MG63 cells were used to generate growth curves using 50% CM and DMEM 4% FBS as control. The same seeding density was used in previous growth curves in the 24 well plate.

Cells were counted in quadruplicate cultures every 48h until day 12 and the mean cell number was calculated for each day. The media was changed every 4 days during the growth curve in all groups.

3.2.9 Analysis of the effects of condition media and co-culture on the differentiation of Osteoblastic cell lines

The effects of challenging osteoblast cell lines with condition media collected over PC3RFP cells and of growing PC3RFP together with the osteoblasts in co-culture, on the differentiation of osteoblastic cell lines SaOS2 and MG63 were determined by measuring alkaline phosphatase (ALP) activity, alizarin red and the expression of differentiation genes such as COL1A, Osterix and Runx2. These assays were first

done 24h after seeding the cells as base line and then after every 48h until day 12. For both SaOS2 and MG63, ~ 3000cells/well were seeded in 96 well plates for ALP activity assay. ~ 15,000 cells/well in the 24 well plates and ~ 66,000 cells/75cm² in the T75 flasks for molecular biology assays. For the PC3RFP cells, which were used in the co-culture experiments, the cells density was 5000cells/well in 24 well plates, ~ 940 cells/well in 96well plate and ~ 220,000 cells/75cm² in T75 flasks. Figure 3.1 describes the seeding of cells in the 96 well plate.

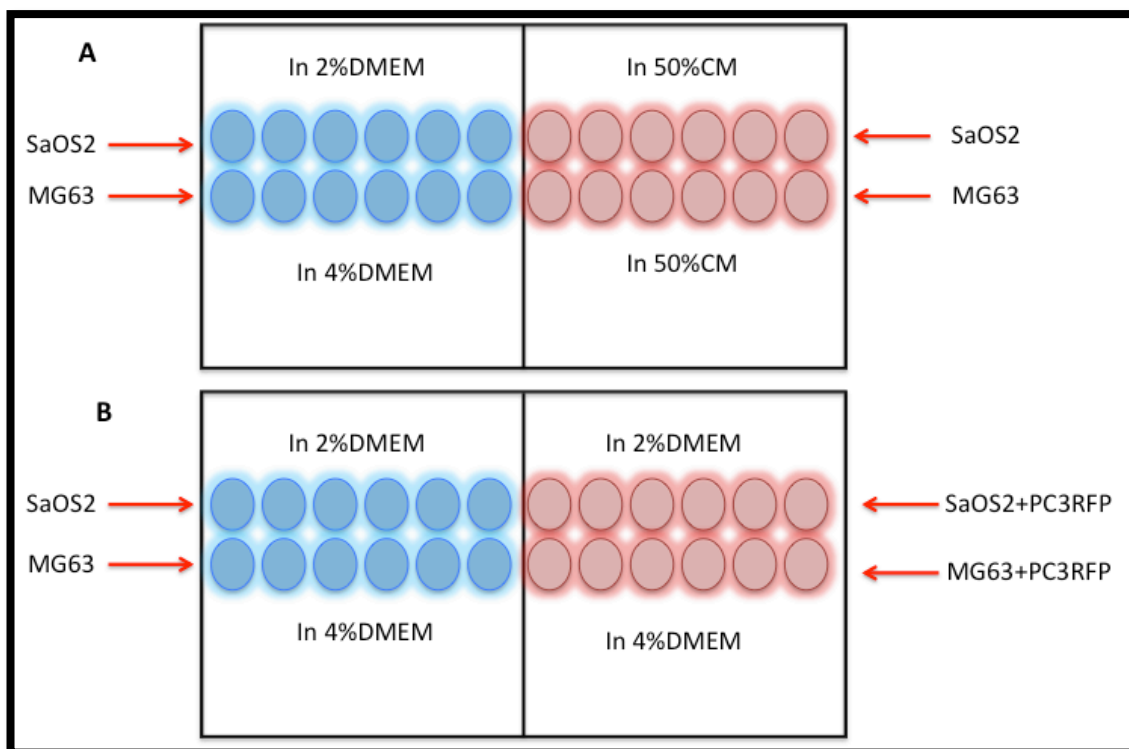


Figure 3.1 Summarizes the design for the seeding of osteoblast cells in the 96 well plate for measuring ALP activity.

A: represents the control osteoblasts seeded in medium containing their respective half maximum FBS concentration compared to osteoblasts grown in CM containing the same, respective FBS concentrations. B: represent the control osteoblast seeded in half maximum FBS compared to osteoblast in co-culture.

3.2.9.1 Alkaline phosphatase activity assay

Osteoblasts show alkaline phosphatase activity, which is increased during differentiation. ALP was also analysed in PC3RFP cultures over time courses. Alkaline phosphatase can easily be measured by using p-Nitrophenyl phosphate (pNPP) as a soluble substrate that gives a yellow color when it reacts with ALP. The intensity of color can be measured by spectrophotometer at wavelength of 405 nm (Xiao *et al.* 2006). Cells were washed twice with ice cold phosphate buffer saline (PBS) and permeabilised with 20µl of 0.1% Triton and were incubated on a shaker

for 20 min at room temperature. One pNPP Tablet and one tris buffer Tablet were dissolved in 20ml of water and 200 μ l of this solution were added carefully to the cells. ALP activity was measured by reading the absorbance at 405nm every 5min for 90 min. The following formula was used to calculate ALP activity

$$ALP\ activity = \frac{(OD(t_1) - OD(t_0)) \times 1000 \times Total\ volume}{Time \times \epsilon(18.75) \times Pathlength(0.0639) \times sample\ volume}$$

Where $OD_{(t_1)}$ is the last optical density, $OD_{(t_0)}$ is the start optical density, ϵ is constant and path length is the length of 200 volume of sample in 96 well plate. The value of ALP activity is expressed as U/ml/min/ μ g DNA.

3.2.9.2 PicoGreen assay

Alkaline phosphatase activity was normalized with osteoblast DNA concentration using the picogreen assay. PicoGreen double-strand DNA (dsDNA) quantitation reagent is a fluorescent nucleic acid stain used to quantify dsDNA (Xiao *et al.* 2006). 1X of TE buffer was prepared from 20X stock solution by adding 1ml of the 20X to 19ml of DNase free water. DNA standard with 2 μ g/ml concentration was prepared by adding 8 μ l of 100 μ g/ml DNA standard stock to 392 μ l of 1X TE buffer. A typical standard curve was prepared according to Figure (3.2).

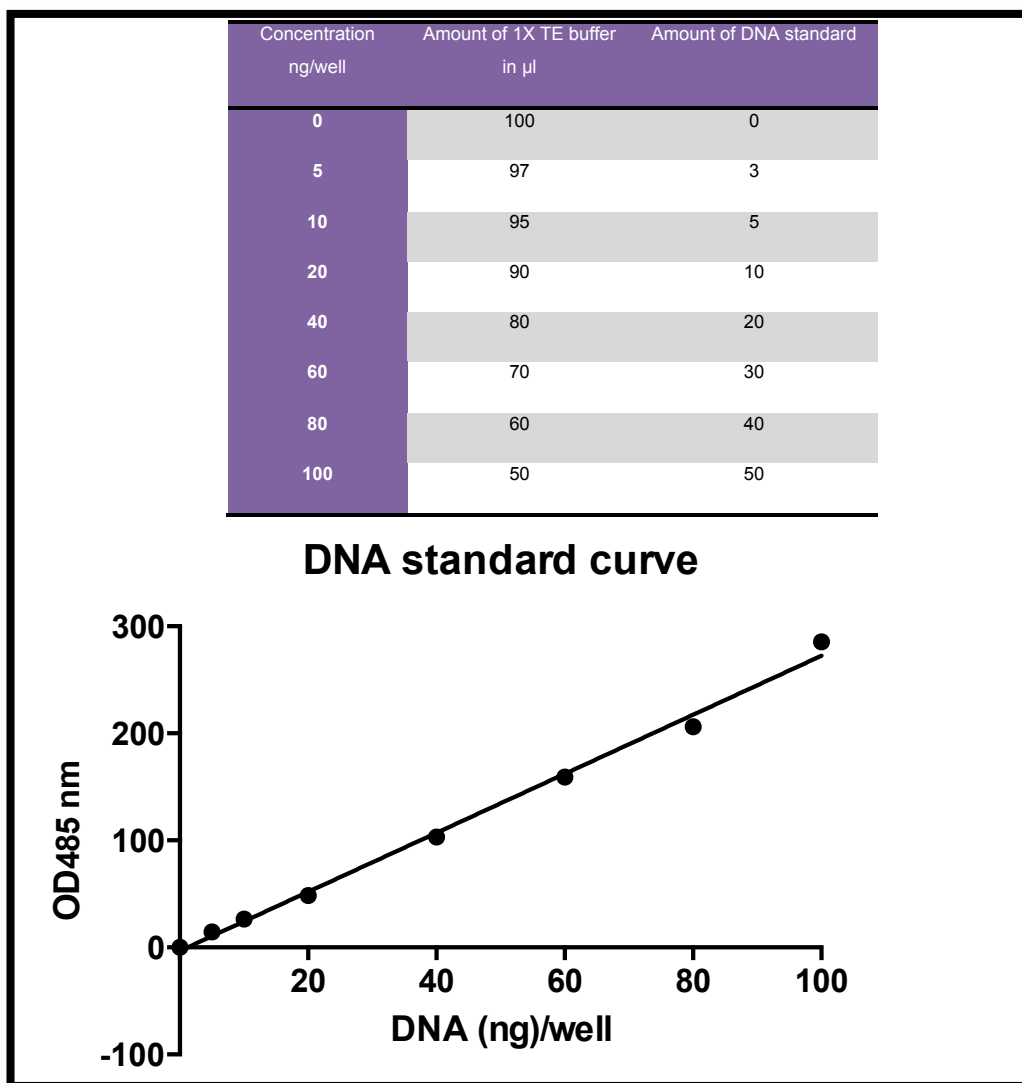


Figure 3.2 illustrate the DNA standard curve and the concentration that were used in the picoGreen assay.

Different DNA standard concentration was prepared from 2 μ g/ml DNA stock solution to form the following concentrations (5, 10, 20, 40, 60, 80 and 100) ng/well. 100 μ l of 1X TE buffer was added to DNA standard and unknown. 100 μ l of 1:200 dilution of picoGreen reagent was added to each unknown and standard samples. The DNA was then measured by exciting samples at 485nm and detecting fluorescence emission intensity at 530nm.

100 μ l of 1X TE buffer was added to standard and unknown DNA concentration of the osteoblast in a 96 well plate. 100 μ l of 1:200 dilution of picoGreen reagent was added to each unknown and standard samples, and incubated in the dark at room temperature on a shaker for 5min. The DNA was then measured by exciting samples at 485nm and detecting fluorescence emission intensity at 530nm.

3.2.9.3 Alizarin red staining

When osteoblasts become fully differentiated they start to deposit calcium in the matrix. Calcium can be specifically stained bright orange-red using Alizarin red. Cells were washed twice with cold PBS and fixed with 1ml of ice cold 100% ethanol for 1h

at 4°C. Cells then were rehydrated with water for 5min. 1ml of 1% alizarin red (pH 4.2) was added to each well and incubated for 10min at room temperature. The stain was removed from the plate and the cells were washed several times to remove excess stain. The plates were allowed to dry overnight at 25°C. ImageJ software was used to quantify the red colour of alizarin orange/red staining.

3.2.9.4 Differentiation gene expression (Runx2, Osterix and COL1A)

Cells were seeded in seven T75 flasks for generating RNA to assess the expression of genes involved in osteoblast differentiation, 24 hour after seeding and every 48 h until day 12. Cells were washed twice with PBS, total RNA was extracted from primary osteoblasts, and cDNA was synthesized as described in Chapter 2 section (2.3.5). Runx2 mRNA, COL1A2 mRNA and Osterix mRNA primers (see Table 3.1 in materials and methods) were used to quantify the expression of these genes during osteoblast differentiation using TaqMan Universal Master Mix (Applied biosystems, UK). Specific gene of interest expression levels were normalized by using GADH as housekeeping gene Chapter 2 section (2.3.6). In co-culture experiments, populations were sorted using FACS Aria and the PC3-RFP separated from Saos2/MG63 on the basis of red fluorescence. The purity of all cells that were used in all further experiments after sorting was above 92%. RNA was then extracted from separate populations as above.

3.3 Results

3.3.1 Characterization of Osteoblastic cell lines

In order to study the basic growth and differentiation characteristics of osteoblastic cell lines (SaOS2 and MG63), growth curves were done followed by serum titration curve. Growth curves were initially conducted using standard media DMEM with 10% FBS. Both cell lines had an exponential growing phase that started when cells reached ~10,000 cells on day 2 in a 24 well plate and finishes around day 8. However, SaOS2 cells tended to grow at a slower rate in Figure (3.3) (A) and Figure (3.4) (A) respectively.

FBS concentrations significantly modulated the growth of both cell lines SaOS2 and MG63 in a concentration dependent manner (1 way ANOVA, Bonferroni). Within the range 0-20% FBS DMEM both cell lines had their maximum growth at a concentration of 10% FBS DMEM and had a half maximum cell growth at concentrations of 2% and 4% respectively at day 6 Figure (3.3) (B) and Figure (3.4) (B). Growth curves were also conducted at the half maximum serum concentration to define the growth characteristics of both cell lines Figure (3.3) (A) and Figure (3.4) (A) respectively.

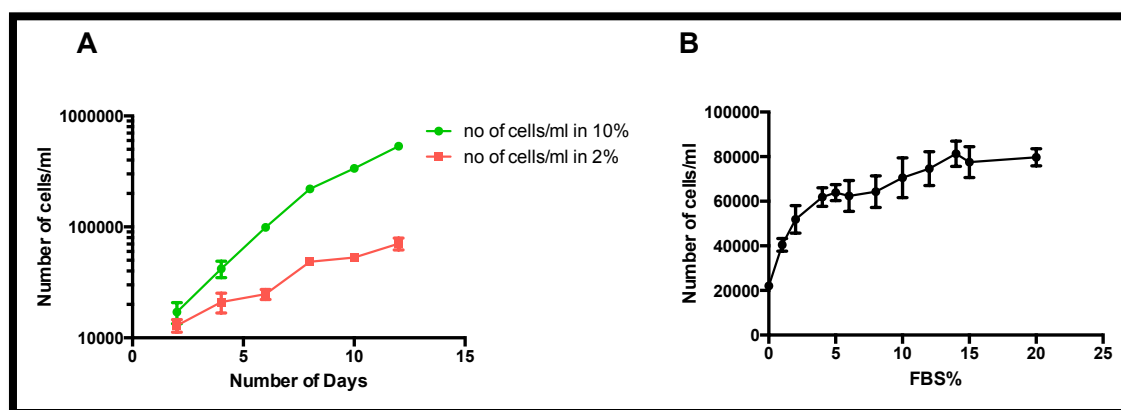


Figure 3.3 Characterization of SaOS2 cell.

(A) Representative growth curves in both concentration maximum and half maximum Showing the beginning of the exponential phase around day 2 and ending around day 8. (B). Serum titration curve of the SaOS2 cells showing maximum growth at 10% with half maximum at 2% $P=0.001$ (1 way ANOVA, Bonferroni). All data are displayed with mean \pm SEM of 3 independent experiments.

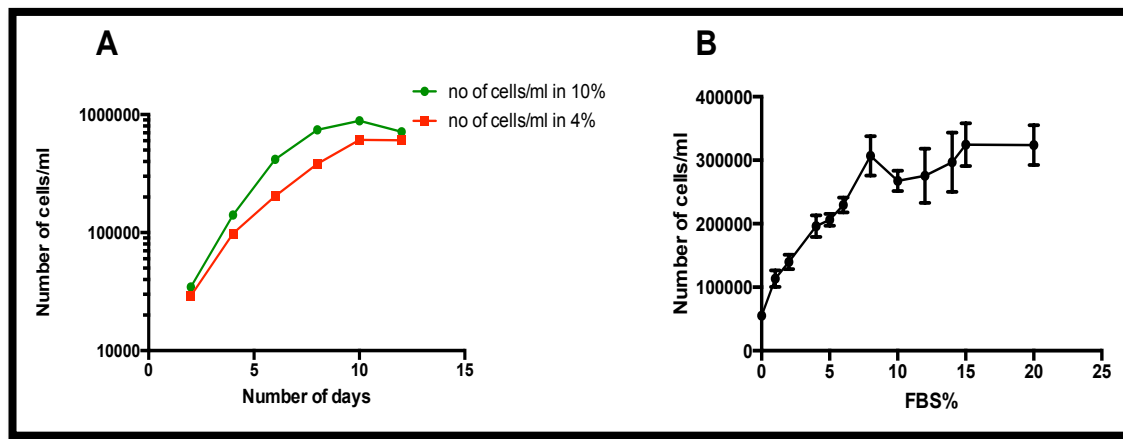


Figure 3.4 Characterization of MG63 cells.

(A) Illustrating growth curve in both concentration maximum and half maximum (B). Illustrate Serum titration curve of the MG63 cells showing maximum growth at 10% with half maximum at 4%. All data are displayed with mean \pm SEM of 3 independent experiments.

3.3.2 Characterization of the PC3-RFP prostate cancer cell line

Growth curves were initially conducted for PC3RFP using the standard DMEM 10%FBS to define the onset and duration of exponential growth. PC3RFP had an exponential growing phase that started when cells reach \sim 10,000 cells on day 2 in a 24 well plate and finished around day 8 Figure (3.5) (A). FBS concentrations significantly modulate the growth of the PC3RFP cell line in a concentration dependent manner (1 way ANOVA, Bonferroni). Within the range 0-20% FBS DMEM cells had their maximum growth at a concentration of 10% FBS DMEM and had a half maximum cell growth at a concentration of 2% at day 6 Fig (3.5) (B). Another growth curve was done using the half maximum FBS concentration Figure (3.5) (A).

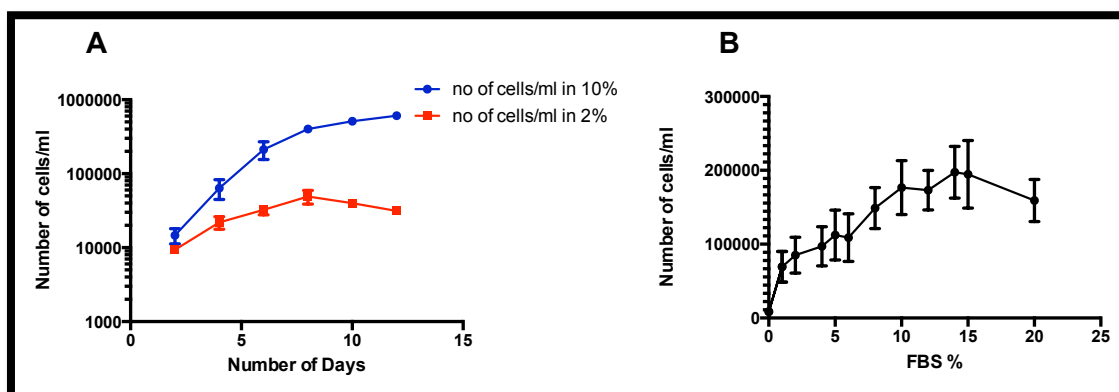


Figure 3.5 Characterization of PC3RFP cell.

(A) Growth curves in both concentration maximum and half maximum (B) Serum titration curve of the PC3RFP cells showing maximum growth at 10% with half maximum at 2% with $P=0.002$ (1 way ANOVA, Bonferroni). All data expressed as mean \pm SEM of 3 independent experiments.

3.3.3 Studies of the effect of various conditioned media concentrations on the growth of osteoblastic cell lines.

Osteoblastic cells were challenged with different conditioned media concentrations, collected over PC3RFP, in order to select the best concentration to use in further experiments. The concentrations tested were: 0, 5, 10, 25, 50 and 100%. SaOS2 were counted in two time point day6 and day10 Figure (3.6) (A) and Figure (3.6) (B) respectively. Maximum cell number was found to be associated with 50% on day10.

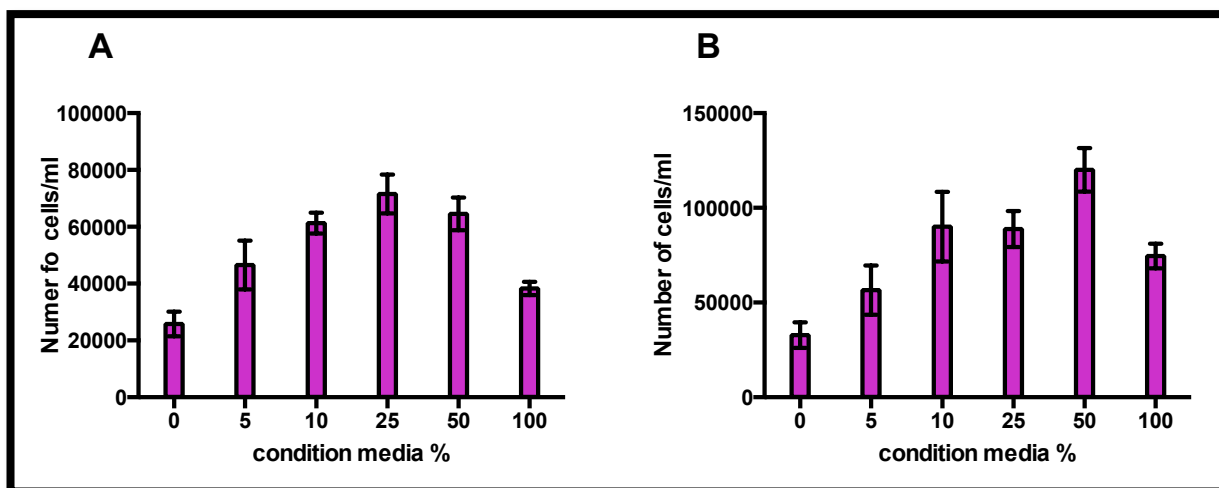


Figure 3.6 Assessment of the effect of different CM concentrations on the growth of SaOS2 cells during exponential growth.

(A) Illustrates the number of SaOS2 counted on day 6 (B) Illustrates the number of SaOS2 counted on day10. All data expressed as mean \pm SEM of 3 independent experiments.

3.3.4 Studies of the effects of conditioned media on the proliferation of Osteoblastic cell lines

Growth curves were done with both SaOS2 and MG63 cells using 50% conditioned media (CM) to test the effects on the proliferation of osteoblastic cell lines SaOS2 and MG63. Conditioned media significantly stimulated the growth of SaOS2 ($p < 0.05$, 1way ANOVA, Bonferroni) Figure (3.7) but it did not have a significant effect on MG63 cells Figure (3.8).

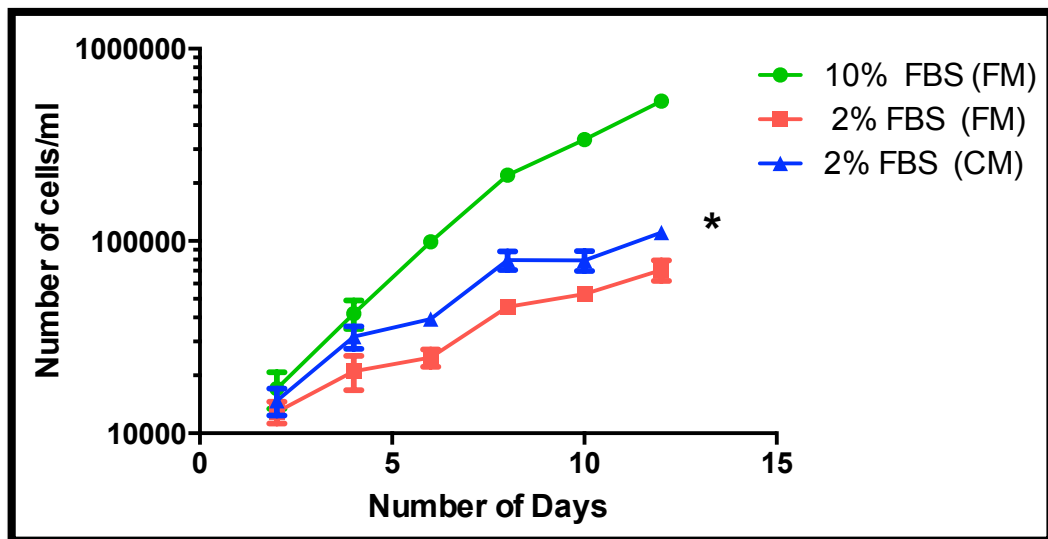


Figure 3.7 Conditioned media (CM) increased the proliferation of SaOS2 cells.

Growth curves showing the effect of 50% conditioned media (2% FBS) on the growth of SaOS2 cells compared to their growth in standard, unconditioned medium containing 10%FBS of fresh media (FM) or half maximum 2%FBS (FM). Conditioned media (CM) stimulated the growth of SaOS2 cell $p < 0.05$ (1way ANOVA, Bonferroni). All data expressed as mean \pm SEM of 3 independent experiments.

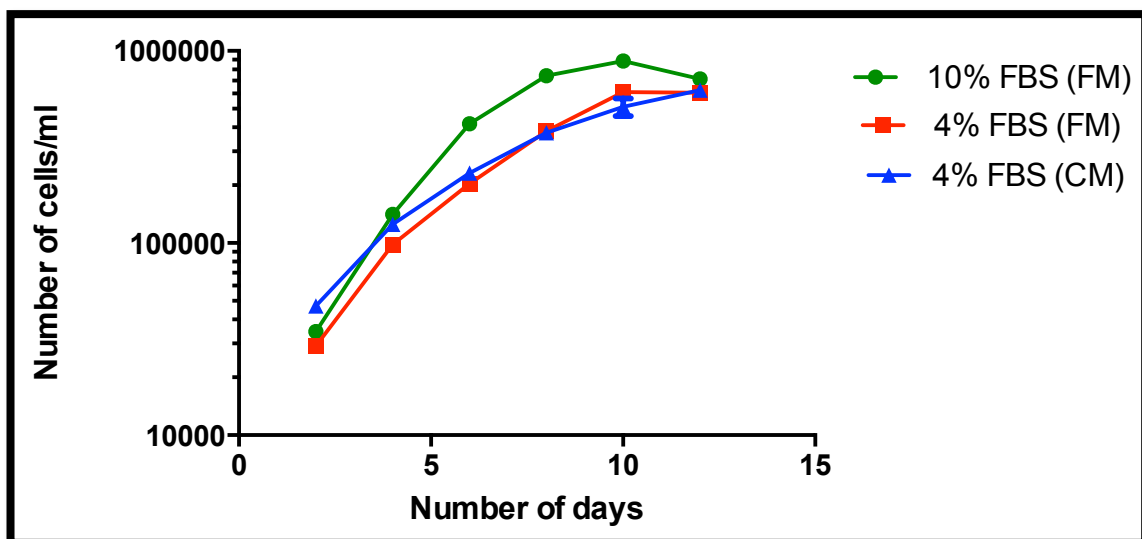


Figure 3.8 Conditioned media (CM) did not affect the proliferation of MG63 cells.

Growth curves showing the effect of 50% conditioned media (4% FBS) on the growth of MG63 cells compared to their growth in standard, unconditioned medium containing 10%FBS fresh media (FM) and half maximum 4%FBS (FM). All data expressed as mean \pm SEM of 3 independent experiments.

3.3.5 Differentiating MG63 cells by using differentiation media

ALP activity and Alizarin red were measured in MG63 cells grown in differentiation media for 4 weeks. The activity of ALP enzyme was measured initially on day 1 before the addition of the differentiation media and then on days 2, 4, 7, 10, 14, 21 and 28. ALP activity increased at the beginning of the experiment showing maximum level during day 4 Figure (3.9) (A). The density of alizarin red was measured in MG63 cells on the same days as ALP activity was measured. The density of stain colour increased with time until day 21, indicating an increase in the calcification of MG63 Figure (3.9) (B).

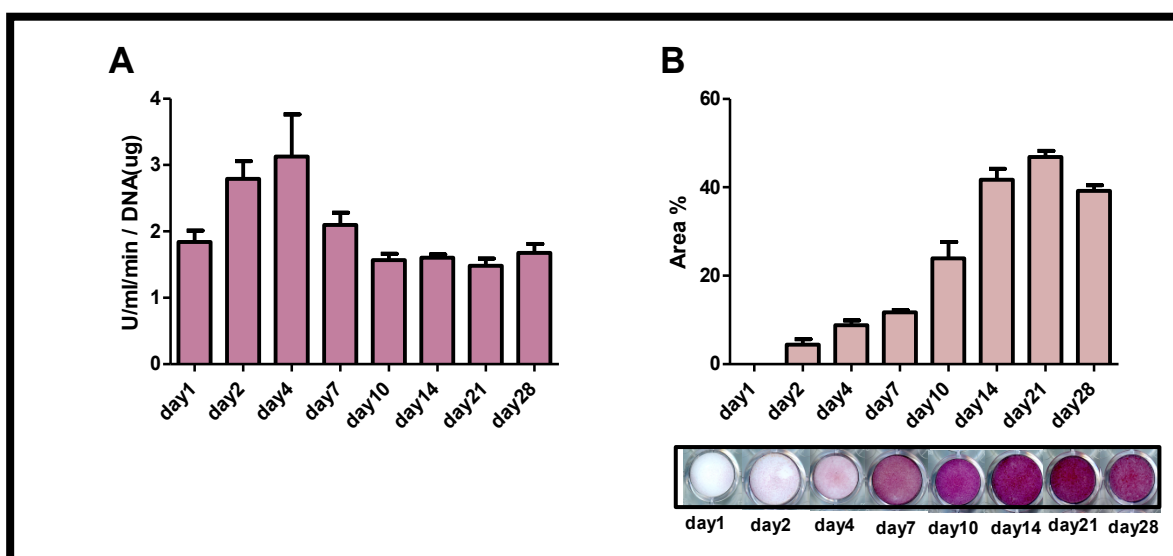


Figure 3.9 Assessment of the effects of differentiating media on MG63.

(A) illustrates the level of ALP activity in MG63 cells during 4 weeks under the influence of differentiating media containing 10mM β - glycerophosphate and 50 μ L ascorbic acid. ALP activity was measured at day 0 before the addition of the differentiation media and continue to be measured afterward during (2, 4, 7, 10, 14, 21, 28) days, Showing maximum level on day 4. (B) illustrates the density of alizarin red stain in MG63 cells during 4 weeks under the same conditions.

3.3.6 Assessment of the effects of conditioned media on the proliferation of differentiated MG63

MG63 were differentiated for 4 days using differentiation media. Growth curves were then done using differentiated MG63 grown in standard 4% media and in 50% CM (4% FBS). Growth in these cultures was compared with that of undifferentiated cells. Both differentiated and undifferentiated MG63 were not affected by CM (Figure 3.10). Since there were no difference between differentiated and undifferentiated MG63 the undifferentiated MG63 were used in all other experiments.

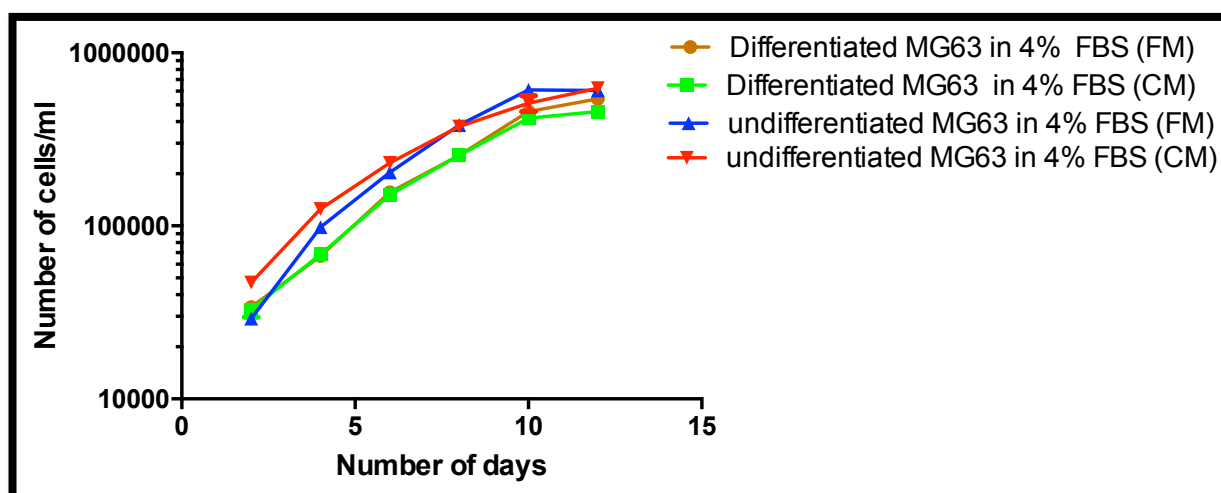


Figure 3.10 Condition media had no effect on the proliferation of differentiated MG63 cells.

Growth curves show the effect of 50% condition media on the growth of differentiated MG63 cells grown in standard 4% media and in 50% CM compared to the growth of undifferentiated MG63 grown in 4% media and in 50% CM. There was no difference between differentiated and undifferentiated cells grown in 50% CM and CM had no effect on the growth of either differentiated or non-differentiated cells. All data is expressed as mean \pm SEM of 3 independent experiments.

3.3.7 Assessment of the effect of CM and co-culture on the differentiation of osteoblastic cell lines

3.3.7.1 Analysis of alkaline phosphatase activity in osteoblasts

Alkaline phosphatase activity was measured as an early indicator of osteoblast differentiation in both osteoblast cell lines, SaOS2 and MG63, grown individually in their respective standard medium containing half maximum FBS concentrations (2% and 4% respectively) compared to 50% CM containing the same respective serum concentrations and growing in co-culture together with PC3RFP. Co-culture experiments were also done in the respective half maximal serum concentration for each osteoblast cell line. Conditioned media significantly decreased the differentiation of the SaOS2 cells on days 1, 2, 6, 8, 10 and 12 (1 way ANOVA, Bonferroni's $n=3$, $p<0.0019$, $p<0.0036$, $p<0.0036$, $p<0.0001$, $p<0.0057$ and $p<0.0003$ respectively, Figure 3.11). In addition, growing the SaOS2 cells in direct contact with PC3RFP had a similar effect on their differentiation during day 1, 2, 4, 6, 10 and 12 (1 way ANOVA, Bonferroni's $n=3$, $p<0.0019$, $p<0.0019$, $p<0.0001$, $p<0.019$, $p<0.0057$ and $p<0.0001$ respectively) Figure (3.11). Conditioned media showed the same effect of decreasing the differentiation of MG63 cells on day 1, 2, 6, and 10 (1 way ANOVA, Bonferroni's $n=3$, $p<0.0001$, $p<0.0001$, $p<0.019$ and $p<0.0057$ respectively) as seen in Figure (3.12). Growing MG63 together with PC3RFP inhibited MG63 differentiation only at the beginning of the experiment until day 4 (1 way ANOVA, Bonferroni's $n=3$, $p<0.0057$, $p<0.0001$ and $p<0.0001$) but stimulated their differentiation on day 6 and

10 only (1 way ANOVA, Bonferroni's $n=3$, $p<0.003$ and $p<0.0001$) Figure (3.12). All data for the effects of CM and co-culture in both cell lines presented in Figures 3.11 and 3.12 are compared in Figure 3.13. ALP was measured in cultures of PC3RFP cells grown alone, on day 1,2,4,6,8,10 and 12 Figure 3.14. ALP levels were around 1U/ml/min/ug DNA on day 1 and 2 but then declined <0.5 U/ml/min/ug DNA at all other time points. This suggests that PC3RFP derived ALP did not significantly contribute to levels measured in co-culture with SaOS2 (levels >400 U/ml/min/ug DNA in all cultures) but may have a small contribution to the levels present in MG63 co-cultures where ALP levels were lower.

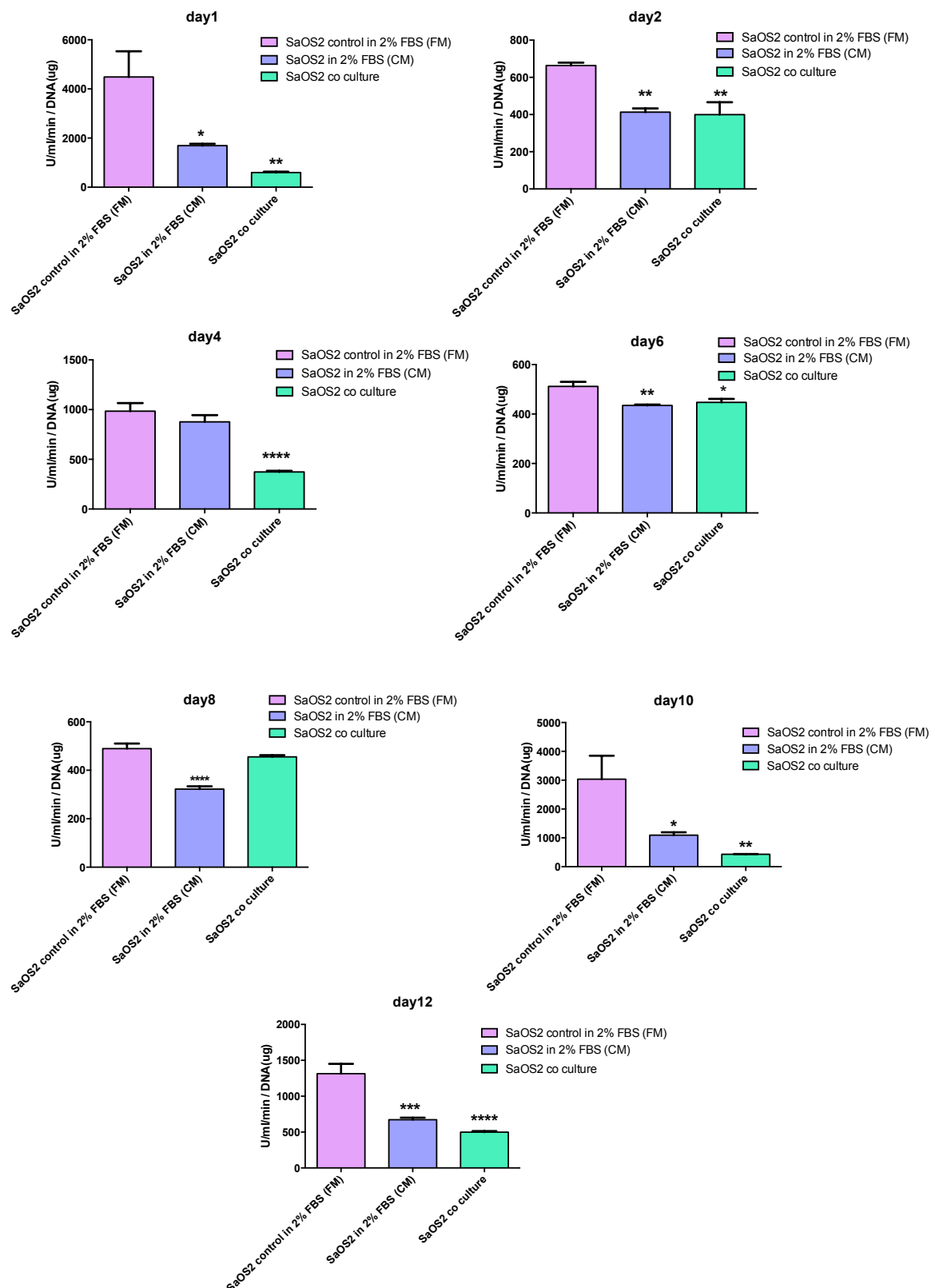


Figure 3.11 Differentiation of SaOS2 cells were decreased by CM.

The graphs illustrate ALP activity in SaOS2 cells grown individually in standard medium (2% FBS) compared to 50%CM and in co-culture with PC3RFP over 12 days. Conditioned media significantly decreased differentiation of SaOS2 on days, 6, 8, 10 and 12 $p < 0.0019$, $p < 0.0036$, $p < 0.0001$, $p < 0.0057$ and $p < 0.0003$ respectively. The co-culture group showed significant increase during day1, 2, 4, 6, 10 and 12 $p < 0.0019$, $p < 0.0019$, $p < 0.0001$, $p < 0.019$, $p < 0.0057$ and $p < 0.0001$ respectively (1 way ANOVA, Bonferronis). All data is expressed as mean \pm SEM of 3 independent experiments.

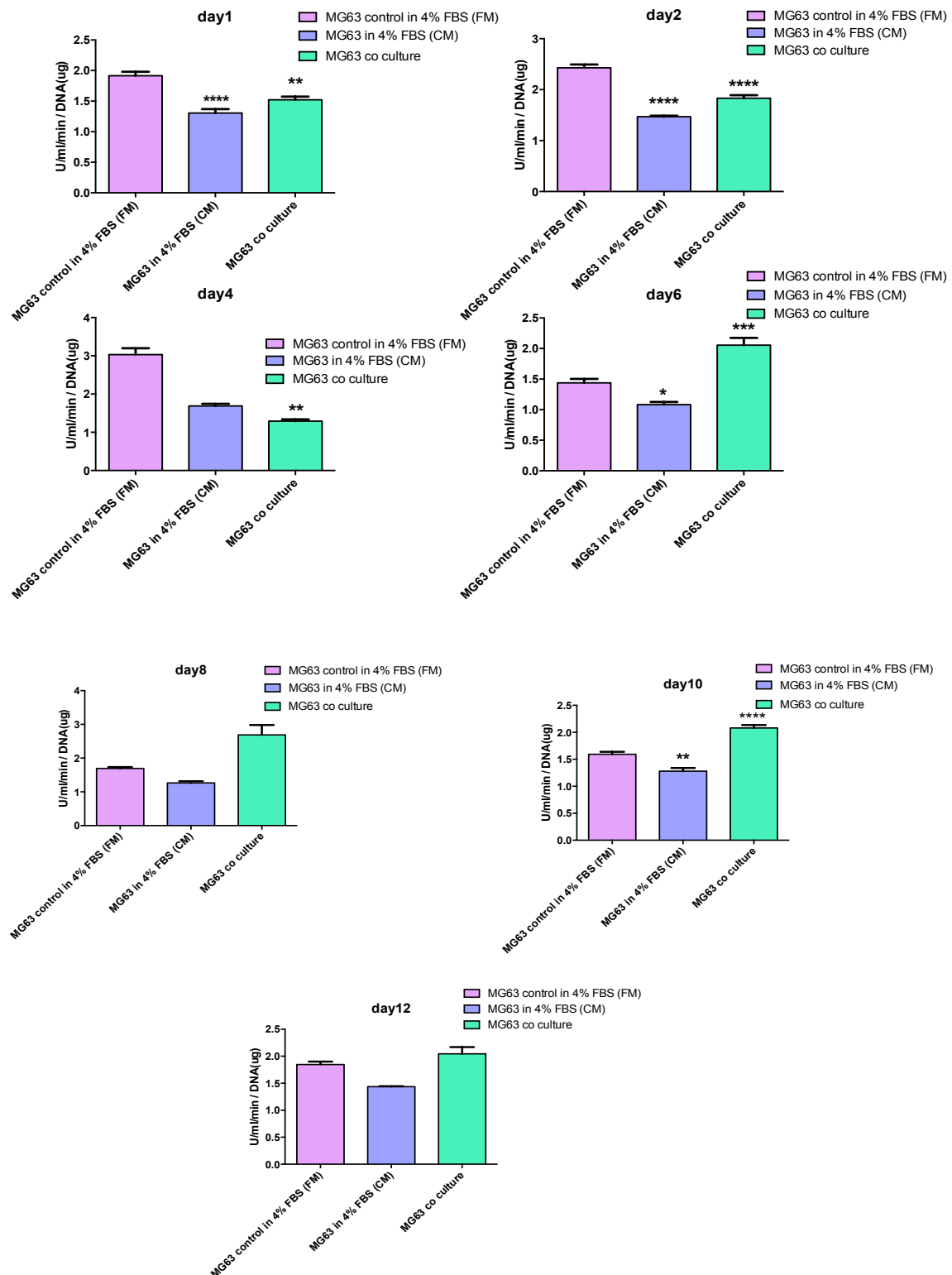


Figure 3.12 Differentiation of MG63 cells was decreased by CM and co-culture at some time points.

The graphs show ALP activity in MG63 cells grown individually in standard medium (4% FBS) compared to 50% conditioned media and in co-culture with PC3RFP during 12 days. Conditioned media decreased differentiation of MG63 with statistically significance on days 1, 2, 6 and 10 ($p < 0.0001$, $p < 0.0001$, $p < 0.019$ and $p < 0.0057$ respectively). Co-culture significant decreased differentiation in MG63 only on days 1, 2 and 4 ($p < 0.0057$, $p < 0.0001$ and $p < 0.0001$ respectively). Differentiation increased in the co-culture group starting from day6 until day12 but showing significance only at day6 and 10 $p < 0.003$ and $p < 0.0001$ respectively (1 way ANOVA, Bonferronis). All data is expressed as mean \pm SEM of 3 independent experiments.

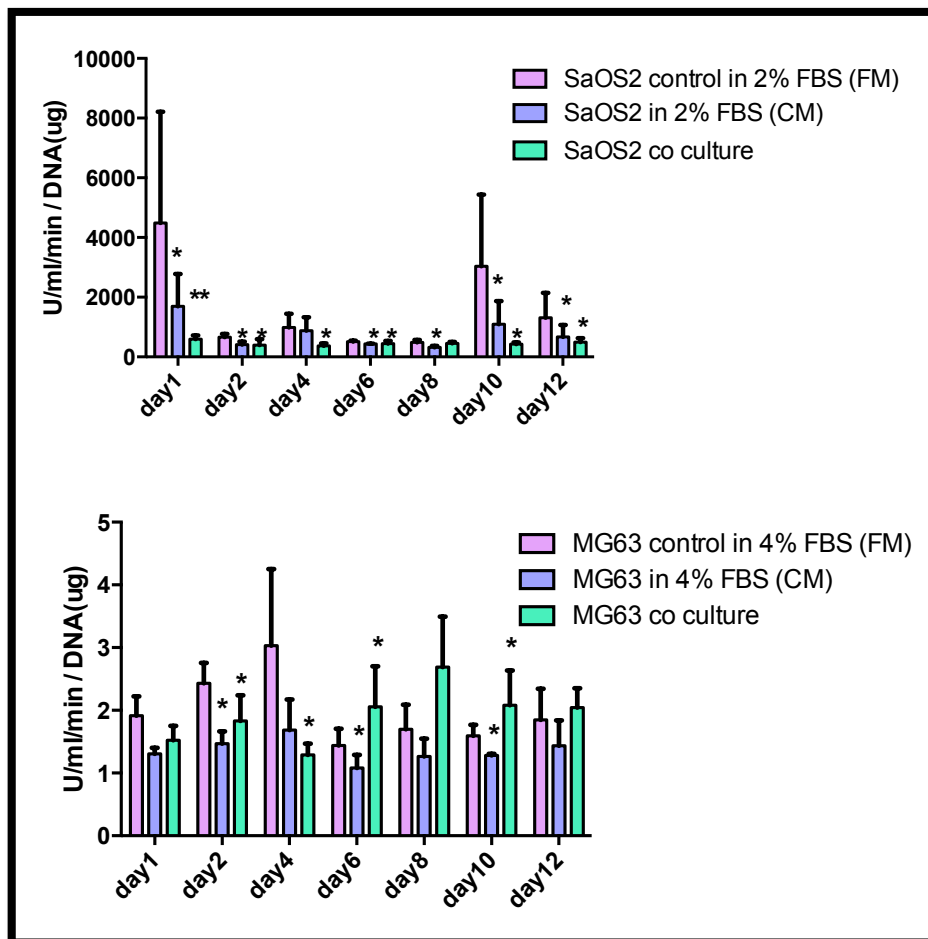


Figure 3.13 Differences in ALP activity in Osteoblastic cell lines evaluated over 12 days in the presence/absence of CM or co-culture with PC3RFP.

(A) ALP activity in SaOS2 cells (B) ALP activity in MG63 cells.

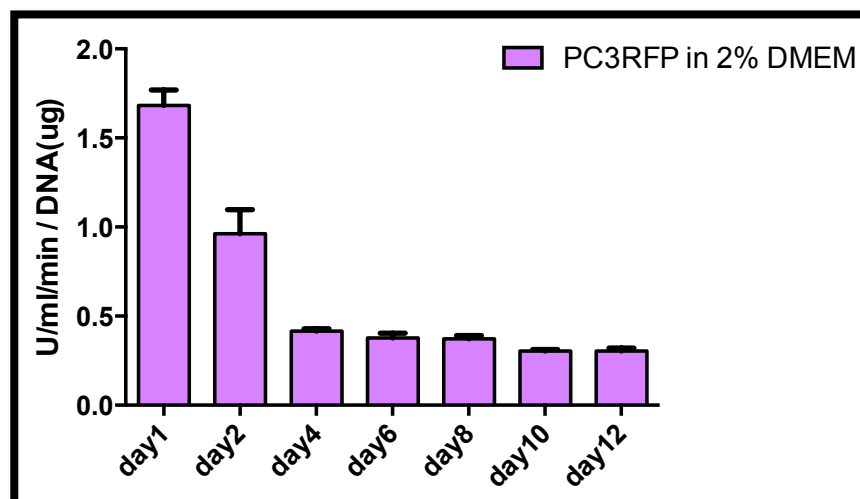


Figure 3.14 Differences in ALP activity in PC3RFP cell lines evaluated over 12 days.

ALP was measured in cultures of PC3RFP cells grown alone, on day 1,2,4,6,8,10 and 12. On day 1 and 2 ALP levels were around 1U/ml/min/ug DNA but then declined <0.5 U/ml/min/ug DNA at all other time points.

3.3.7.2 Analysis of mineralisation measured by alizarin Red staining in osteoblastic cell lines

Alizarin red was used to assess mineralization in osteoblastic cells. The SaOS2 cells started to mineralize from day 6. In the SaOS2 co-culture group mineralization increased significantly on days 8, 10 and 12 (1 way ANOVA $n=3$, $p<0.0073$, $p<0.0097$ and $p<0.018$ respectively) as seen in Figure (3.15). In MG63 mineralization started by day 2, earlier than in cultures of SaOS2 cells Figure (3.16). Conditioned media significantly increased the mineralization only at day 4 while, mineralization in MG63 co-culture group was significantly induced at day 8 compared to control (1way ANOVA, Bonferroni) $n=3$, $p<0.019$ and $p<0.019$ respectively) Figure (3.17). The mineralization increased over time in all groups in all osteoblastic cell lines Figure (3.18).

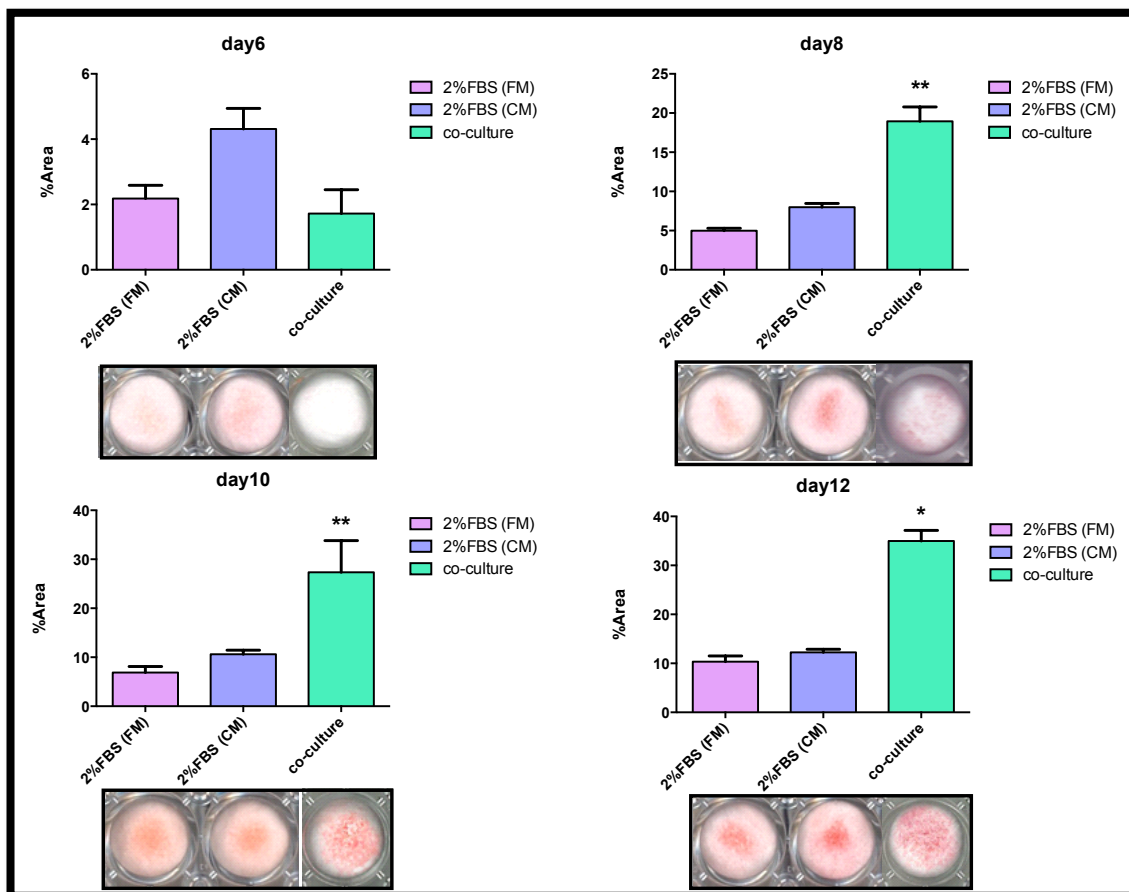


Figure 3.15 Mineralisation in SaOS2 cells was significantly increased in co-cultures with PC3-RFP but not by CM.

Graphs show mineralization (assessed by Alizarin Red staining) was increased significantly in co-culture group on days 8, 10, and 12 ($p<0.0073$, $p<0.0097$ and $p<0.018$ respectively) (1 way ANOVA, Bonferroni). All data expressed as mean \pm SEM of 3 independent experiments.

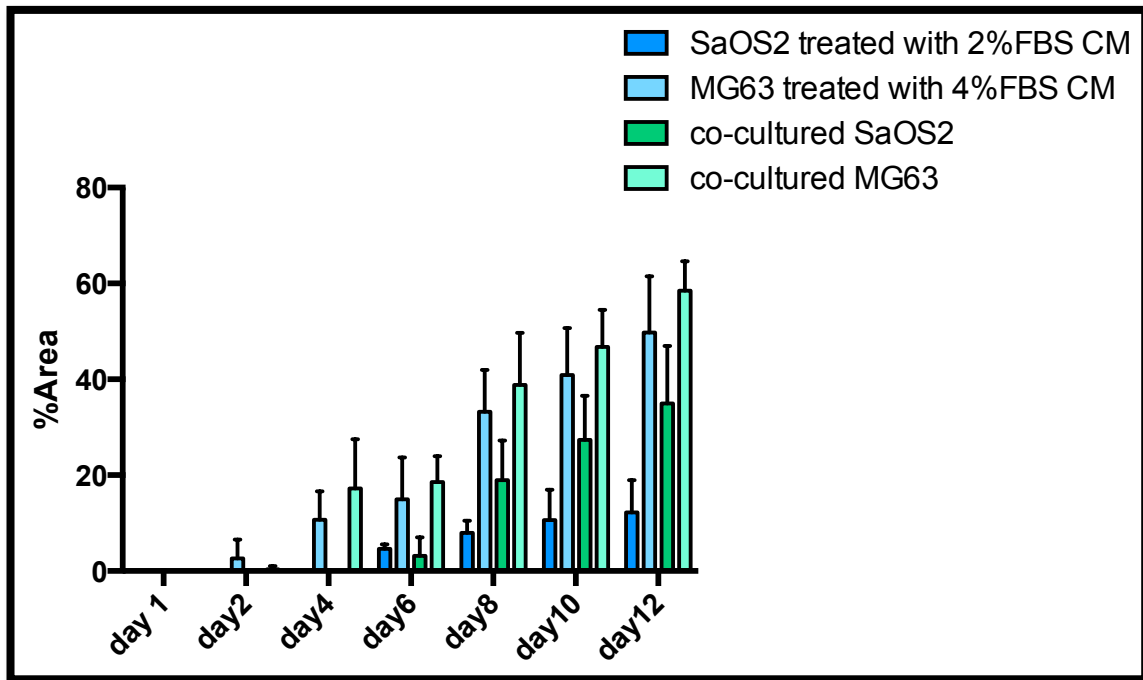


Figure 3.16 Differences between SaOS2 and MG63 in Alizarin Red staining during 12 days.

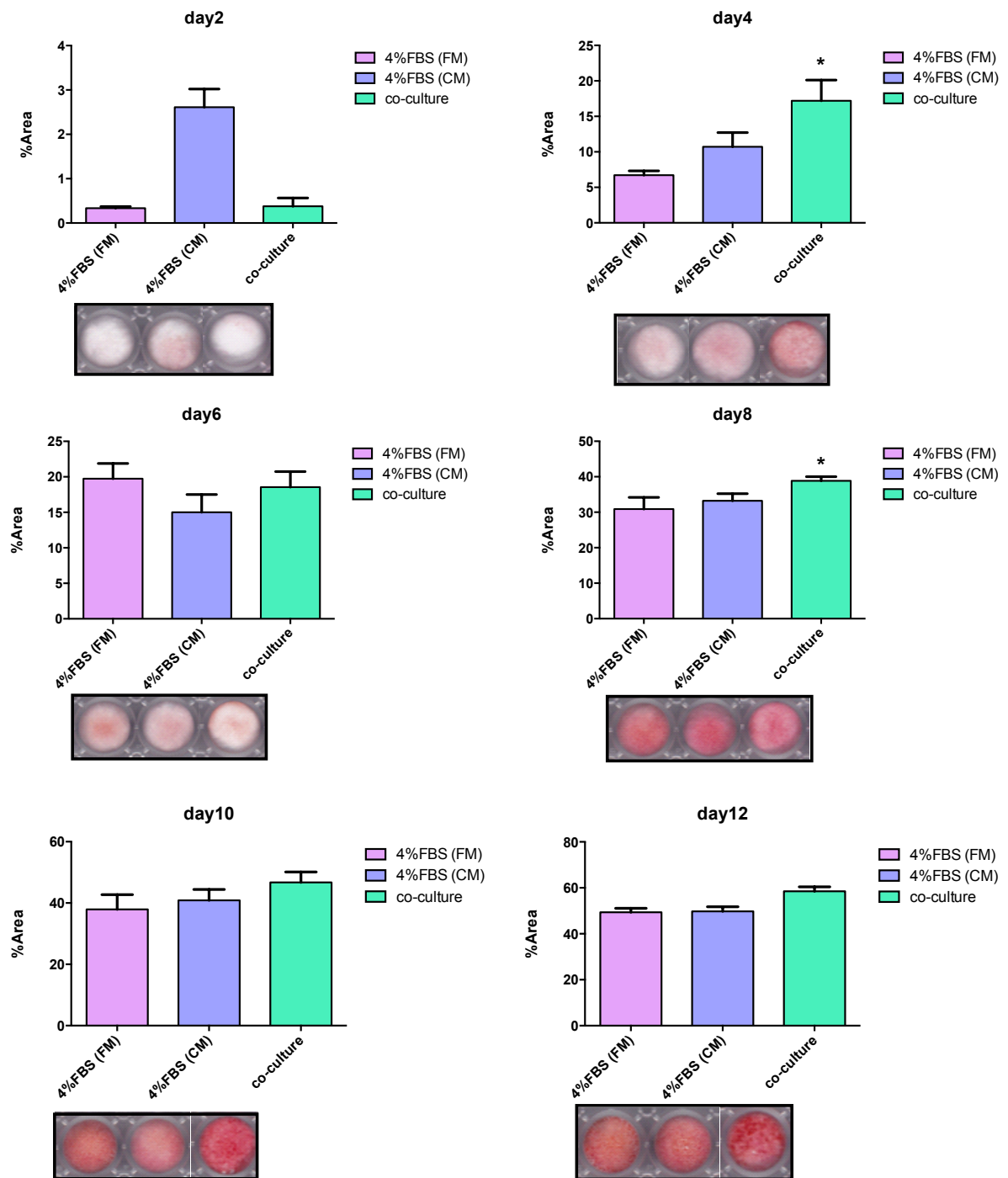


Figure 3.17 Mineralization in MG63 was varyingly affected by CM and in co-cultures with PC3RFP.

Graphs show that mineralization (assessed by Alizarin Red staining) increased significantly in condition media group at day 4 and on day 8 in the co-culture group ($p < 0.019$ and $p < 0.019$ respectively) (1 way ANOVA, Bonferroni). All data is expressed as mean \pm SEM of 3 independent experiments.

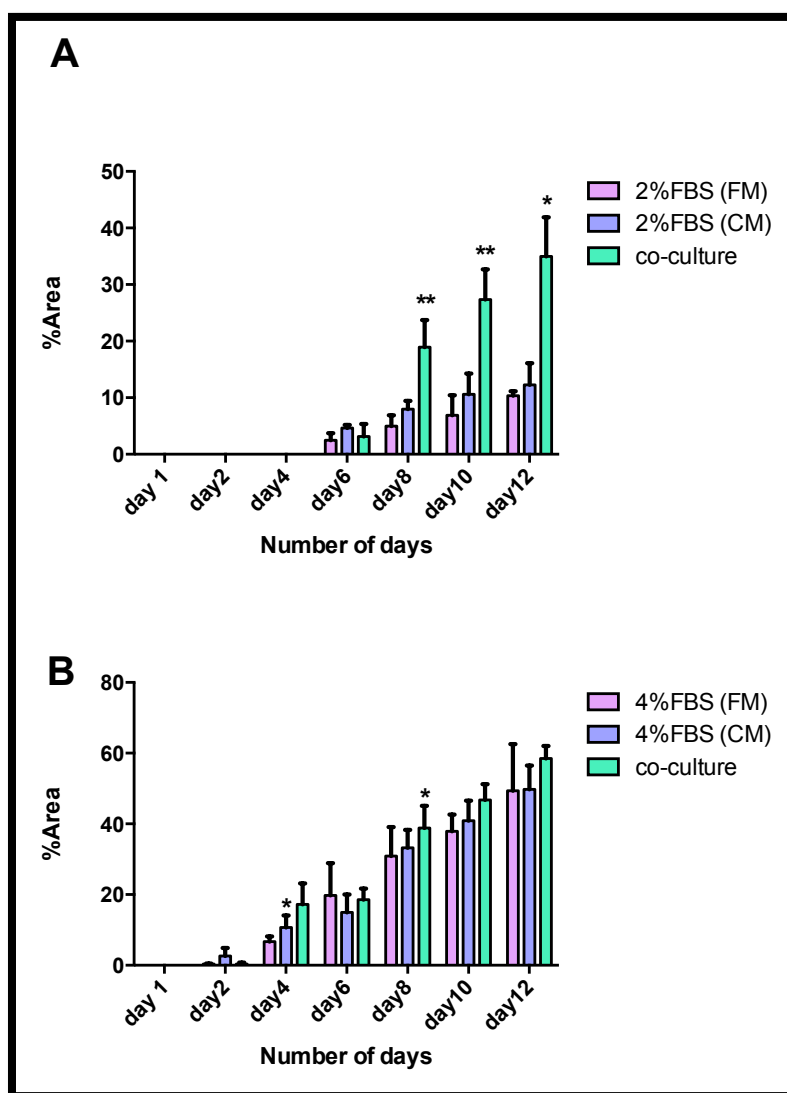


Figure 3.18 Differences in Alizarin Red staining in Osteoblastic cell lines during 12 days.

(A) alizarin red stain in SaOS2 cells (B) alizarin red stain in MG63 cells.

3.3.7.3 Expression of osteoblast differentiation genes COL1A, Osterix and Runx2 in osteoblastic cell lines.

The level of expression of osteoblast markers; Runx2, COL1A2 and osterix genes were analysed using TaqMan. Expression of these genes was normalised to the expression of a housekeeping gene, GAPDH. Figure (3.19) (A) shows the level of COL1A mRNA expression in SaOS2 in three groups (control SaOS2 in DMEM 2% FBS, SaOS2 in 50% CM and SaOS2 in co-culture, 2% FBS) (B) shows the level of osterix mRNA expression in SaOS2 in the same three groups (C) shows the level of RUNX2 mRNA expression in SaOS2 again in the three groups. There was no significant difference in the expression of all differentiation markers COL1A, osterix and RUNX2 between all groups except for osterix and RUNX2 which were significantly increased in SaOS2 treated with CM group at day 8 $P=0.03$ and $P=0.03$

respectively (1 way ANOVA, Bonferroni). Although the expression of these differentiation markers COL1A, osterix and RUNX2 was lower in the co-culture group during the three time point day (6, 8 and 10) but with no statistical significance. Figure (3.20) (A) shows the level of COL1A mRNA expression in MG63 in three groups (control MG63 in DMEM 4% FBS, MG63 in 50% CM and MG63 in co-culture) (B) shows the level of osterix mRNA expression in MG63 in the same three groups (C) shows the level of RUNX2 mRNA expression in MG63 again in the three groups. Moreover, there was no significant change in the expression of all differentiation markers COL1A, osterix and RUNX2 between all groups. Co-culture group expressed lower amount of these markers but with no statistical significance.

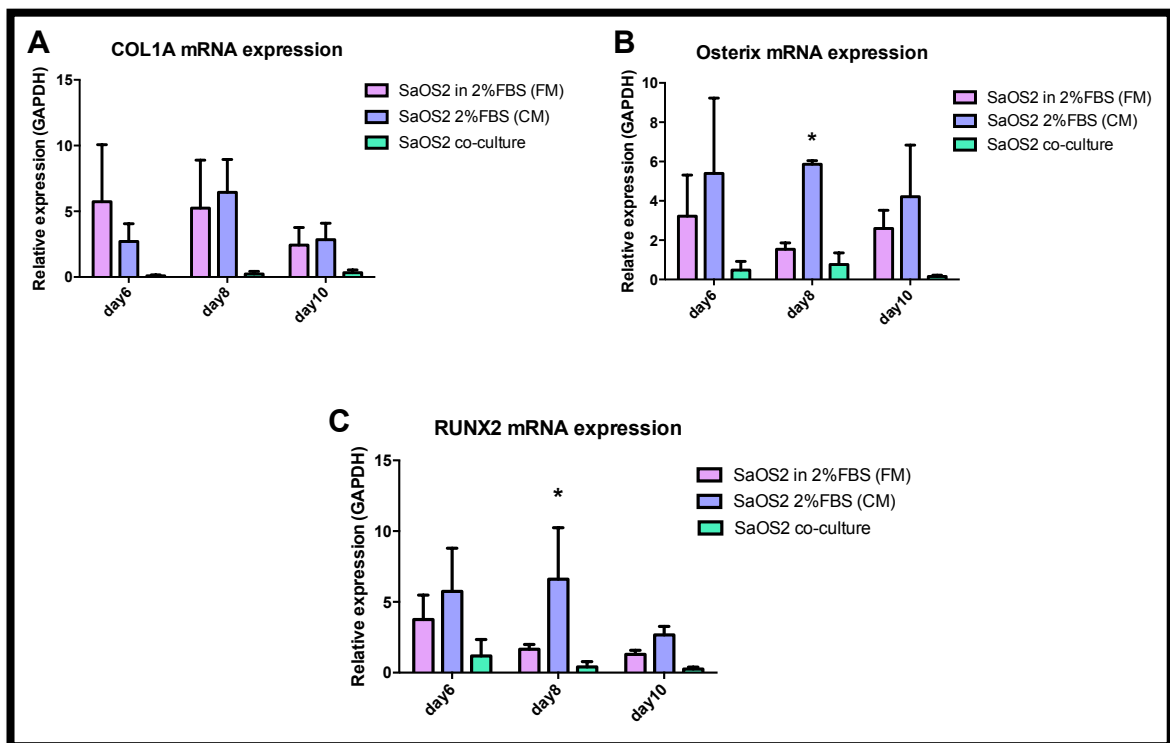


Figure 3.19 Summary of the levels of expression of osteoblast markers; Runx2, COL1A2 and osterix in the SaOS2 cell line.

(A) shows the level of COL1A mRNA expression in SaOS2 in three groups (control SaOS2 in DMEM 2% FBS, SaOS2 in 50% CM and SaOS2 in co-culture) (B) shows the level of osterix mRNA expression in SaOS2 in the same three groups (C) illustrates the level of RUNX2 mRNA expression in SaOS2 again in the three groups. There was no significant differences in the expression of all three markers in all groups during day 6 and 10 while, both Runx2 and Osterix showed significant increase during day 8 $P=0.03$ and $P=0.03$ respectively (1 way ANOVA, Bonferroni). All data is expressed as mean \pm SEM of 3 independent experiments.

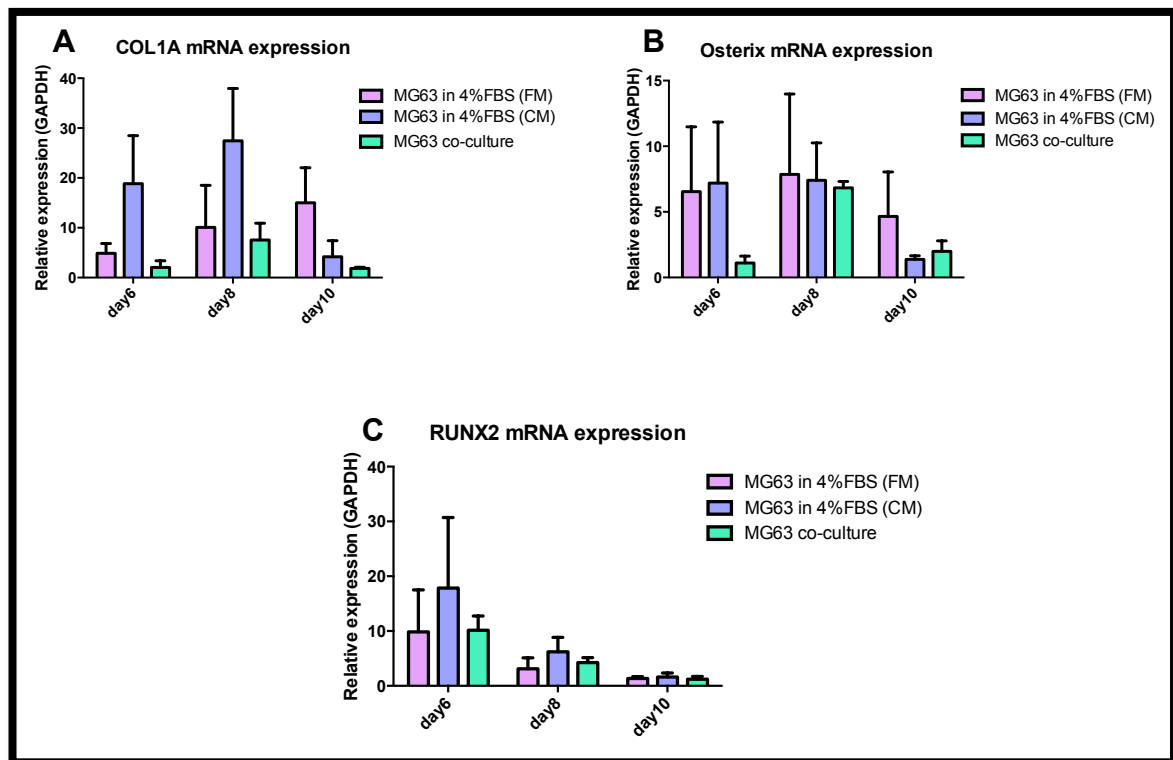


Figure 3.20 Summary of the levels of expression of osteoblast markers; Runx2, COL1A2 and osterix in the MG63 cell line.

(A) illustrates the level of COL1A mRNA expression in MG63 in three groups (control MG63 in DMEM 4%FBS, MG63 in 50% CM and MG63 in co-culture) (B) illustrates the level of osterix mRNA expression in MG63 in the same three groups (C) illustrates the level of RUNX2 mRNA expression in MG63 again in the three groups. There were no significant differences in the expression of all three markers in all groups. All data is expressed as mean \pm SEM of 3 independent experiments.

3.4 Discussion

3.4.1 Cells Growth Characteristics

Determination of the growth characteristics of cell lines is an essential prerequisite before undertaking experiments where effects of agents on growth of cells are to be considered. Understanding the standard behaviour of cells through generating growth curves is also important to ensure that cancer cell lines are behaving in a reproducible manner. Any deviation in the predicted trajectory of the curve serves as a warning that either the cells are changing, something is wrong in the culture environment or that contamination has occurred. Under regular growth conditions using the standard medium containing 10% FBS all cell lines (PC3-RFP, SaOS-2 and MG63) have relatively consistent growth rates, generating growth curves where they entered the exponential phase around day 2 after culture initiation and this phase ended around day 8 for all cell types.

The effect of FBS concentration was tested on the growth of prostate cancer cell line (PC3RFP) and osteosarcoma cell lines (SaOS-2 and MG63). The concentration that gave maximal growth rate in all cell lines was ~10%. 2% and 4% FBS concentrations were used in subsequent experiments for SaOS2 and MG63 respectively. These concentrations provided the population sizes of SaOS2 and MG63 that were half those observed when these cells were grown in 10% FBS at day 6 (i.e. in mid-exponential growth). The rationale for using 2% and 4% was that by using these concentrations it would be subsequently possible to test effects of treatments on final population sizes. However, with higher FBS concentration, the cells would have been growing maximally and it may not have been possible to rigorously test proliferative or inhibitory effects in this environment with cell proliferation proceeding as fast as was possible. Conversely, with lower FBS concentration cells would not grow, it would be impossible to test anti-proliferative effects and be certain that the lack of any induction of proliferation was a real observation or simply a result of cells not having sufficient basic nutrients to grow or survive.

3.4.2 The effect of prostatic cancer cells on the proliferation and differentiation of osteoblast cells

The experiments presented in this chapter were conducted to investigate the proliferative and differentiation response of cultured osteoblasts (SaOS2 and MG63) cells to conditioned media from prostatic PC3RFP cells. Prostate cancer cells produce many soluble factors that alter bone remodelling including RANKL, OPG and

TGF- β (Dai, Hall et al. 2008, Weilbaecher, Guise et al. 2011, Theriault and Theriault 2012). These factors which are secreted into the media stimulate the proliferation of osteoblast cells and may inhibit their differentiation (Koutsilieris *et al.* 1987; Martínez *et al.* 1996). In this study, PC3RFP conditioned media (PC3RFP-CM) was found to stimulate the growth of SaOS2 especially when cells become close to confluence but PC3RFP-CM did not have any effect on MG63. I initially thought that these differences could be due to differences in the native differentiation status of SaOS2 vs MG63 however, even when, MG63 were differentiated using osteogenic media for 4 days, PC3RFP-CM did not affect proliferation of the latter. Perkel *et al.*, Rabbani *et al.* and Martínez *et al.* reported the same finding with SaOS2 suggesting that PC3 conditioned media contains many components other than urokinase-like plasminogen activator (u-PA) contributing to these proliferative stimuli (Perkel *et al.* 1990; Rabbani *et al.* 1990; Martínez *et al.* 1996). Many studies have indicated that prostatic cancer produce and secrete into their media different growth factors including Fibroblast growth factor-2 (FGF-2) and platelet derived growth factor (PDGF) (Sitaras *et al.* 1988; Lawson 1990). A study done by (Hughes-Fulford and Li 2011) suggested that the rate of osteoblast proliferation was depending on the amount of FGF-2, TGF- β and PGE2 since FGF-2 was found to down regulate genes associated with mineralization while it increases genes associated with osteoblast proliferation.

Osteoblast differentiation is characterized by three stages: Cell proliferation, matrix secretion/maturation that is associated with increased level of ALP activity and finally matrix mineralization. Specific genes encoding structural proteins such as COL1A, osteocalcin, osterix and Runx2 are expressed at various times during differentiation to functional osteoblasts (Stein and Lian 1993; Kasperk *et al.* 1995). Once mineralization is completed calcium deposition can be visualized by Alizarin red staining. SaOS2 cells have a more mature osteoblastic phenotype, associated with intrinsically high ALP activity, compared to MG63 cultures which contain both mature and immature osteoblast phenotypes and a have generally very low ALP activity (Chichester *et al.* 1993; Voegele *et al.* 2000).

My results, showed that either growing the more differentiated osteoblast cells SaOS2 cells in PC3RFP conditioned media or in direct contact with the PC3RFP in co-culture both decreased the differentiation of these cells. These treatments had similar effects on MG63, but this was confined to the beginning of the experiment as the cells were starting to differentiate up to day 4. After this time point the

differentiation of MG63 were increased in co-culture group only. My findings contradict the results found in a study done by (Jung *et al.* 2004; Nishimori *et al.* 2012) showing an increase in ALP activity when the prostate cancer LNCaP cells came in contact with the bone stromal cell line MC3T3 cells, with the addition of exogenous BMP-2 to the CM. It was suggested that the addition of BMP2 into the media stimulated differentiation of mouse bone stromal cells by activating Sonic hedgehog (SHH) signalling through Smad dependent pathway. However these effects may also be due to secretion of endothelin 1, urokinase-type plasminogen activator and prostate specific antigen by prostate cancer cells, any/all of which could stimulate differentiation of osteoblasts. Other studies have shown that PC3-CM affects ALP activity only during proliferative phase suggesting that prostate cancer cell produce various stimuli for cell growth allowing osteoblasts to retain proliferative status and by inhibiting differentiation genes (Martínez *et al.* 1996). Many previous studies have confirmed the expression of BMP and its receptors in bone cells and that this signalling system promotes the differentiation of osteoblasts and plays an important role in bone remodelling. These signalling molecules also bind with high affinity to an antagonist, Noggin and this results in blocking their biological effects (Iwasaki *et al.* 1995; Zimmerman *et al.* 1996; Zehentner *et al.* 2002).

My results showed an increase in the mineralization of SaOS2 and on day 4 in MG63 when osteoblast cells were in direct contact with prostatic cancer cells in co-cultures. This was similar to studies reported previously (Larson *et al.* 2014) where prostate cancer cells promoted the mineralization in osteoblast MC3T3 and that these cells secrete high level of prostatic acid phosphatase (PAP). The divergences found in my results; the reduction of ALP activity and increased mineralization in co-culture and CM treated groups, would suggest that prostate cancer cells produce factors affecting different stages of osteoblast differentiation: the initial signals controlling matrix production and those regulating mineralization and its progression. Alkaline phosphatase is important only in the initiation stage of osteoblast differentiation but not in its progression since once mineralization is initiated this may proceed even in the absence of high phosphate level produced by ALP (Tenenbaum 1987). Another study done by Tenenbaum *et al* reported that in cultures of chick periosteal the induction of mineralization by β -glycerophosphate was associated with decreased alkaline phosphatase activity (Tenenbaum *et al.* 1989). The expression of COL1A was not affected in SaOS2 by the presence of PC3-CM. on the other hand; osterix and Runx2 were not affected in SaOS2 by the presence of PC3-CM during day 6 and

10 while, on day 8 both osterix and Runx2 were significantly increased in CM treated group. In a study done by Thomas et al reported that Runx2 were underexpressed in many osteosarcoma cell lines including SaOS2 cells compared to osteoblast-like reference cells he reported also in his study that SaOS2 cells express the osteoblast-specific MASN isoform of Runx2 which have the ability to stimulate osteocalcin the gene responsible for mineralization but not ALP (Harada *et al* 1999; Thomas *et al* 2004). In co-culture, the levels of expression of these genes were not reduced. This finding was similar in MG63 cells. Fan reported that down regulating Noggin enhanced the expression of Runx2, Col1A and ALP in adipose derived stem cells (Fan *et al.* 2013), which suggests that the presence of such inhibitors of BMP signalling would have the opposite effect. The potential production of regulators of TGF β superfamily members by tumour cells and osteoblasts will be investigated in the next chapter.

In conclusion the results presented in this chapter support the hypothesis that prostate cancer cells produce soluble factors in CM that can stimulate the growth and decrease the differentiation of one osteoblastic cell line, SaOS2. However this effect appears to be confined to the early stages of differentiation and mineralization was not significantly affected. Conversely co-culture of prostate cancer cells with SaOS2 significantly increased mineralization, suggesting that direct contact between cells had a separate effect to that produced by soluble factors derived from tumour cells. In the second cell line, MG63, growth was not affected by CM, but an early marker of differentiation was significantly suppressed at early stages of differentiation. This effect was reversed at later time points when these cultures became more strongly mineralised. The expression of known regulators of osteoblast differentiation in the osteoblast cell lines grown under the conditions used here will be examined in the next chapter.

Chapter 4: Comparative gene expression profiles for the TGF- β superfamily in human prostatic cancer and osteoblastic cell lines grown alone and in direct/indirect contact

4 Chapter 4: Comparative gene expression profiles for the TGF- β superfamily in human prostatic cancer and osteoblastic cell lines grown alone and in direct/indirect contact

4.1 Introduction

The TGF- β superfamily contributes in many cellular functions including embryonic development, angiogenesis, proliferation, differentiation and apoptosis (Bello-DeOcampo and Tindall 2003). In normal epithelium, TGF- β 1 inhibits their growth by arresting the cells in the G1 cell cycle thus stimulating them to undergo differentiation or apoptosis (Wikström *et al.* 2001). In contrast, deregulation of TGF- β 1 signalling has been associated with the pathogenesis of many diseases such as cancer (Moses and Barcellos-Hoff 2011). Cancer cells become resistance to the growth inhibitory effect of TGF- β 1 and continue to proliferate even with its presence (Steiner *et al.* 1994). In addition as the tumour progress TGF- β become a tumour enhancer by altering the tumour microenvironment, stimulating angiogenesis, migration and metastasis (Bello-DeOcampo and Tindall 2003). There are two suggested routes by which TGF- β signalling pathway contributes to tumour progression; first it may be caused by mutations in gene encoding TGF- β receptors such as TGF β R2 or by impaired TGF- β receptors availability at the cell surface. Second, due to disturbance in the TGF- β signalling pathway by epigenetic mechanisms such as activation of Ras pathway thus leading to a weakened growth inhibitory response drawing more attention towards activities that increases tumour progression (Knaus *et al.* 1996; Kim *et al.* 2000; Derynck *et al.* 2001).

One of the largest subgroup of TGF- β superfamily are bone morphogenetic proteins (BMPs) group of extracellular signalling molecules (Chang *et al.* 2002). Previously these proteins were known by their ability to induce bone formation at extra skeletal sites but are now known to play an important role in the regulation of many cellular functions such as proliferation, differentiation and motility mainly during development (Hogan 1996; Wozney *et al.* 1998; Wozney 2002). BMPs are additionally thought to be involved in cancer development, especially in tumours that form bone metastases such as prostate cancer. This may be due to their role in bone formation and turnover (Alarmo *et al.* 2006; Feeley *et al.* 2006). Metastatic prostate cancer may stimulate new bone formation by producing various factors, including BMPs, which directly stimulate osteogenic differentiation and activity (Goltzman *et al.* 1992; Koeneman *et al.* 1999). BMPs 2-4, 6 and 7 have been reported to be over expressed by prostate cancer and prostate cancer cell lines (Bentley *et al.* 1992; De Pinieux *et al.* 2001). Several studies showed that BMP6 was associated with cancer progression and may have direct osteoinductive role in facilitating prostate cancer metastasis to bone

(Hamdy *et al.* 1997; Autzen *et al.* 1998; Dai *et al.* 2005). On the other hand, BMP7 has been shown anti-proliferative effects on tumour growth of androgen –insensitive prostate carcinoma cells *in vivo* (Miyazaki *et al.* 2004).

Noggin is another protein that belongs to TGF- β , which is expressed in conjunction with BMPs during embryological development. This protein plays a key role in defining the final shape and size of BMP-derived structures such as bones and joints (Brunet *et al.* 1998). BMPs signalling are regulated extracellularly by this soluble inhibitor, which physically binds to BMPs preventing their receptor binding (Walsh *et al.* 2010). *In vitro* experiments have indicated that Noggin binds with different affinities to BMP-2, -4, -5, -6, -7, -13, -14 and variably inhibiting their action (Figure 4.1) (Zimmerman *et al.* 1996; Gamer *et al.* 2005; Song *et al.* 2010). Noggin expression in osteoblasts was found to be increased in the presence of BMP-2, -4, -5, -6, and -7 (Gazzerro *et al.* 1998; Song *et al.* 2010).

Aim

The aim of this study was to determine the expression of TGF- β superfamily genes in human prostate cancer cells grown alone and in direct contact or when osteoblasts were exposed to products of prostate cancer cells present in conditioned medium. Levels of expression of these genes in these populations will be compared and important differences investigated further.

Hypothesis

Interactions between osteoblast cells with prostate cancer cells either by direct contact or by indirect interaction studied by treating the osteoblasts with PC3RFP-CM, alter the expression of TGF- β family genes associated with the regulation of growth and differentiation in osteoblast lineage cells.

Objectives

- 1- To determine the expression of TGF- β superfamily in prostate cancer and osteoblast individually during the confluent phase using Taqman expressed plate.
- 2- To determine the differences in the expression of the TGF- β superfamily after co-culturing prostate cancer with osteoblast or when treating osteoblast with PC3RFP-CM (Taqman express plates).
- 3- To investigate the effect of the presence of PC3RFP cells or PC3RFP-CM on Noggin expression in osteoblast cells both in mRNA by QPCR or protein level by western blot and flow cytometry.
- 4- To illustrate the patterns of colonization that PC3RFP cells form when seeded over osteoblast cells.

4.2 Material and method

4.2.1 Materials and Disposable Equipment

Item	Supplier
TaqMan Universal master Mix	Applied Biosystem
Human GAPDH(20X)	Applied Biosystem
TaqMan Array 96-well fast plate TGF- β custom format 48 plus candidate endogenous control genes	Applied Biosystem
MicroAmp 96-wellreaction plate (0.1ml)	Applied Biosystem
Enzyme-linked immunosorbent assay (ELISA) kit for Noggin (NOG)	Uscn Life Science Inc.
Negative control Rabbit immunoglobulin fraction	Dako
BD phosflow perm/wash buffer I	BD Biosciences
TaqMan gene expression assay Noggin	Applied Biosystem
Normal donkey serum	abcam
Anti-Noggin antibody	abcam
Donkey anti-rabbit IgG H&L (Alexa Fluor488)	abcam
Formaldehyde	Simport
Bovine-serum Albumin	Sigma-Aldrich
DAPI nuclear stain	Invitrogen
Triton	Sigma-Aldrich

4.2.2 Identifying the ability of PC3RFP to form colonies when seeded over Osteoblast cell lines

In order to test the ability of PC3RFP to form colonies with/over osteoblasts (SaOS2, MG63) PC3RFP were seeded over 70% confluent osteoblast cells. Osteoblast cells either SaOS2 or MG63 were seeded in T75 flask using the same densities that were used previously. When osteoblastic cells became confluent, PC3RFP cells were added at the same cell density that was used in all other experiments. To assess the behaviour of colonized PC3RFP cells Images were acquired during day 2, 4, 6 and 9 after seeding PC3RFP cells using Leica fluorescent inverted microscope as seen in Figure 4.2 and Figure 4.3 respectively.

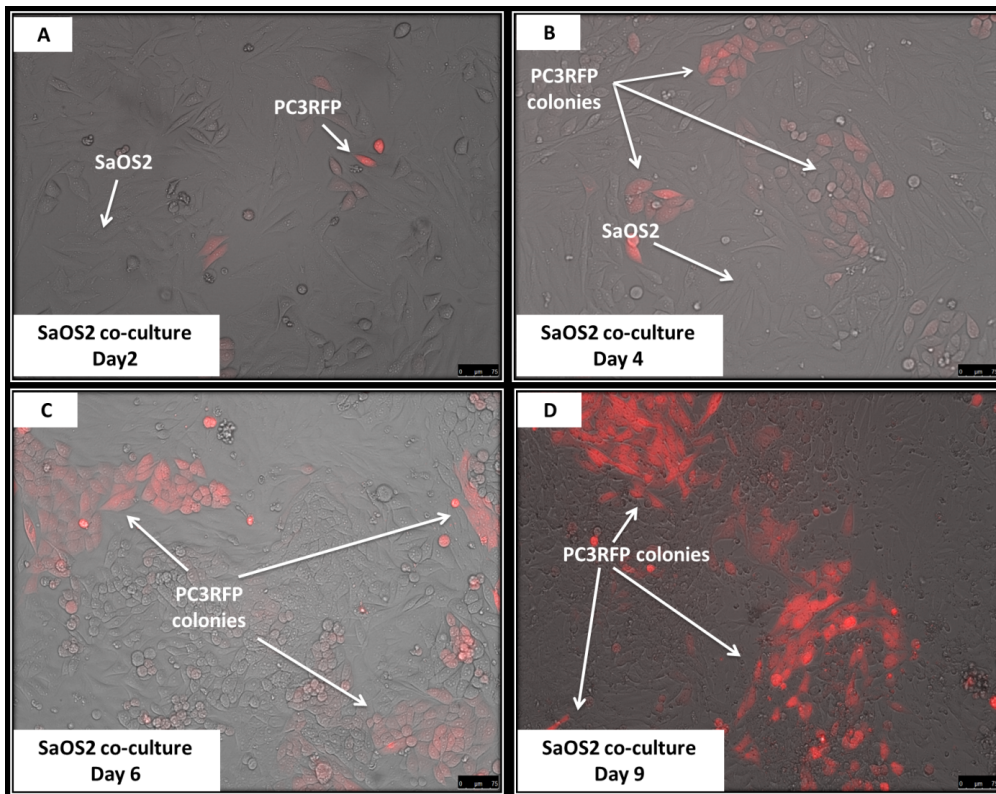


Figure 4.2 Fluorescent images of PC3RFP colonies formed over SaOS2 cells.

PC3RFP cells (red stain) were seeded over 70% confluent SaOS2 cells (A) illustrates PC3RFP seeded over SaOS2 cells after the first 2 days where few cells were observed. (B) illustrates colonies of PC3RFP formed by day 4. (C) illustrates colonies of PC3RFP during day 6. (D) illustrates colonies of PC3RFP by day 9. Images were obtained by Leica fluorescent microscope with 20X objective.

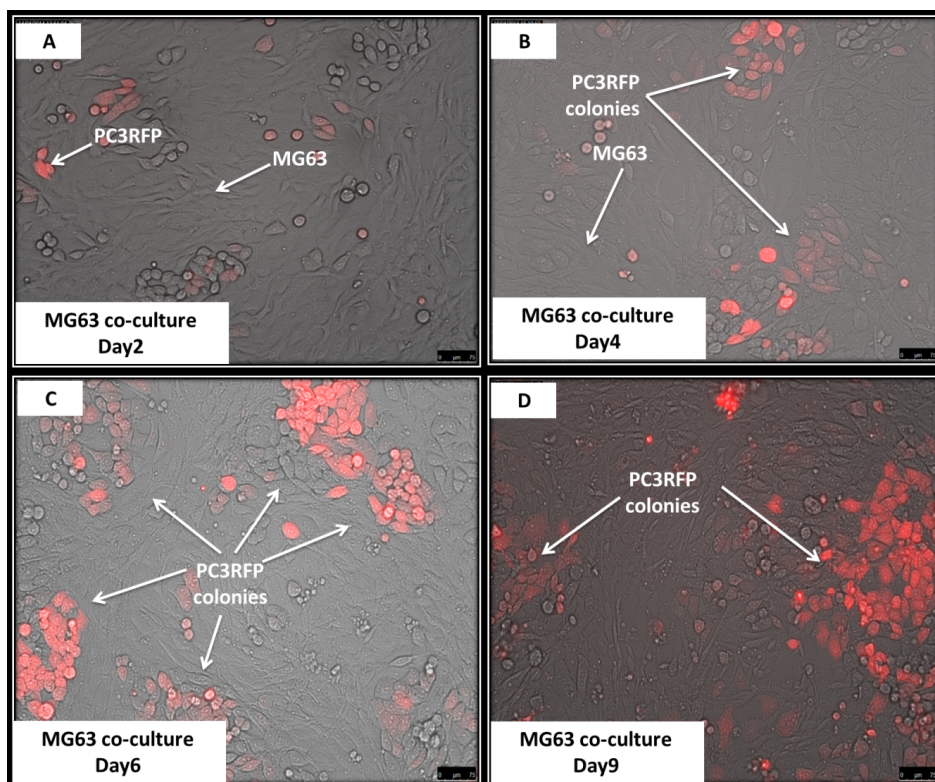


Figure 4.3 Fluorescent images of PC3RFP colonies formed over MG63 cells.

PC3RFP cells (red stain) were seeded over 70% confluent MG63 cells (A) illustrates PC3RFP seeded over MG63 cells after the first 2 days where few cells were observed. (B) illustrates colonies of PC3RFP formed by day 4. (C) illustrates colonies of PC3RFP by day 6. (D) illustrates colonies of PC3RFP by day 9. Images were obtained by Leica fluorescent microscope with 20X objective.

4.2.3 Real-time RT-PCR using TaqMan Express™ plates to evaluate TGF β superfamily gene expression in prostate cancer cell line and osteosarcoma cell lines

RNA was extracted from PC3RFP, SaOS2 and MG63 cell lines during exponential and confluent growth phases. The RNA was quantified by Nanodrop and its integrity was tested by Bioanalyzer as discussed in Chapter 2 section (2.3.3) and (2.3.4). This was followed by cDNA synthesis as described in chapter 2 section (2.3.5). The quality of the cDNA produced was tested by checking the expression of the housekeeping gene (GAPDH) in all samples by QRT-PCR as discussed in Chapter 2 section (2.3.6). Taqman Array 96-well plate custom format with TGF- β superfamily genes was used to quantify the RNA expression of all samples. Table (4.1) shows the design of the Express plate and list of gene analysed. The Taqman 96 well plate was centrifuged at 1000rpm for 1min. A reaction mix was made for each sample by adding 500 μ l of water, 40 μ l of cDNA and 540 μ l master mix. Twenty microliter of the samples were loaded into each well. After loading the two samples each to its designated position in the

plate, the plate was sealed properly and was centrifuged again at 1000rpm for 1min and was run on StepOne plus real time PCR as described in chapter 2 section (2.3.6).

4.2.4 Real-time RT-PCR using TaqMan Express™ plates to evaluate TGFβ superfamily gene expression in co-cultured cells.

PC3RFP cells were seeded with osteoblast cells in a T75 flask using the density equivalent to the density used in growth curves. ~ 220,000 cells of PC3RFP were seeded with ~660,000 cells of either SaOS2 or MG63 in T75 flask in standard 10%FBS media. After 48h, cells were washed with PBS and the media were changed with 2% for co-culture SaOS2 and 4% for co-culture MG63. When cultures were 80% confluent, around day 7, cells were harvested and sorted using FACS Aria. RNA was extracted from both cells PC3RFP, SaOS2 and PC3RFP, MG63 and cDNA were synthesized as described previously in chapter 2 section (2.3.5). Taqman Array 96-well plate Table (4.1) custom format with TGF-β superfamily genes was used to quantify the RNA expression of all samples as described earlier (4.2.3).

4.2.5 Analysis of Noggin protein concentrations in PC3RFP Condition media by ELISA

Enzyme-linked immunosorbent assay kit was used to detect the presence of Noggin protein in condition media collected over PC3RFP cells. All kit components and samples were brought to room temperature prior to use. Standard Noggin stock solution of a concentration 10ng/ml was prepared by adding 1ml of the standard diluent to lyophilized standard and was mixed gently without foaming. Different standard concentrations were made by serial dilution using the standard stock solution as seen in Figure (4.4). Both detection reagent A and B were spun down prior to use and both assays diluent A and B were prepared by adding 2ml of diluent A or B to 2ml deionized water. Detection reagent was then added to the prepared assay diluent in 1:100 dilution (40μL). 100μL of standard and condition media were then loaded in duplicate on the ELISA plate. The plate was covered with the plate sealer and was incubated for 2h at 37°C. The liquid were removed from all wells without washing the plate and 100μL of detection reagent A was added to each well without touching the sides of the wells, the plate was covered and incubated for 1h at 37°C. Wash solution was prepared by adding 20ml of washing solution to 580ml deionized water. After an incubation of 1h, the solution was aspirated from the wells and the wells were washed with 350μL of washing solution. This process was repeated three times. The remaining liquid was removed from the plate completely by inverting the plate on absorbent

paper. 100 μ L of detection reagent B were added to each well and the plate was recovered and incubated for 30min at 37°C. After this, the washing step was repeated as previously, 5 times. 90 μ L of substrate solution TMB were added to each well and the plate was covered and incubated for 15-25 min at 37°C in the dark. Finally, 50 μ L of stopping solution were added to each well. The colour in the wells changed from blue to yellow and the intensity of the colour was measured by using microplate reader at wavelength of 450nm. The concentrations of the unknowns were calculated from standard curves.

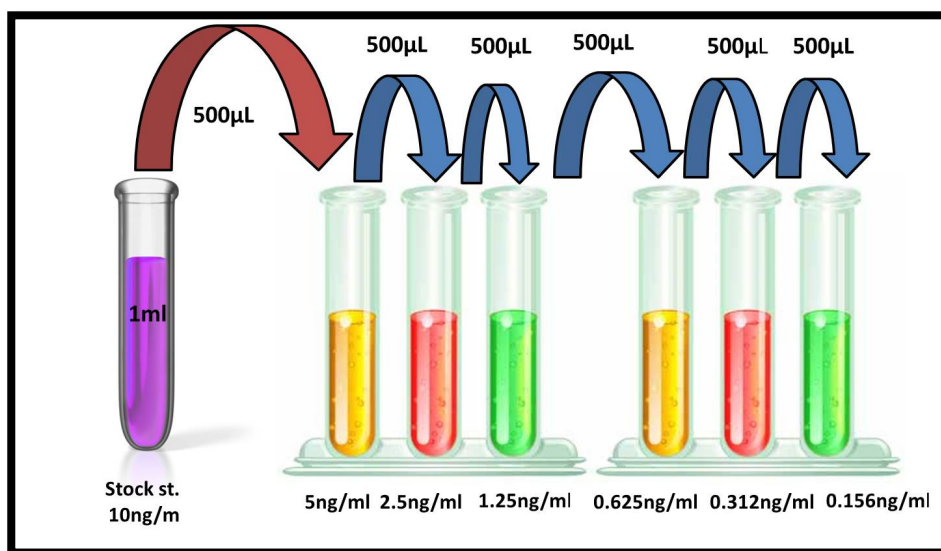


Figure 4.4 Preparing serial standard dilutions from stock standard solution for ELISA.

Standard stock solution of a concentration 10ng/ml was prepared by adding 1ml of the standard diluent to lyophilized standard and was mixed gently without foaming. 6 tubes were prepared by adding 500 μ L of standard diluent in each tube. 500 μ L from stock standard solution was added to the first tube mixed well and 500 μ L transferred to the next tube and so on making the following concentrations (5, 2.5, 1.25, 0.625, 0.312 and 0.156) ng/ml.

Table 4.1 illustrate the design of the TaqMan TGF-β Express plate that was used to quantified the RNA expression in all samples by real time PCR.

Gene Symbols	1	2	3	4	5	6	7	8	9	10	11	12
A	18S	GAPDH	HPRT1	GUSB	ACVR1	TGFBR1	18S	GAPDH	HPRT1	GUSB	ACVR1	TGFBR1
B	TGFBR2	TGFBR3	ENG	GDF1;LASS1	GDF3	GDF9	TGFBR2	TGFBR3	ENG	GDF1;LASS1	GDF3	GDF9
C	BMP4	BMP2	BMP7	BMP6	BMP3	CHRD	BMP4	BMP2	BMP7	BMP6	BMP3	CHRD
D	BMP5	BMP10	GDF7	GDF6	BMP8B;BMP8A	GDF2	BMP5	BMP10	GDF7	GDF6	BMP8B;BMP8A	GDF2
E	GDF11	BMPR1A	BMPR1B	BMPR2	SOST	GREM1	GDF11	BMPR1A	BMPR1B	BMPR2	SOST	GREM1
F	NOG	CER1	NBL1	FST	ACVR1B	ACVR2A	NOG	CER1	NBL1	FST	ACVR1B	ACVR2A
G	ACVR2A	ACVR2B	INHA	TGFB2	TGFB3	TGFB1	ACVR2A	ACVR2B	INHA	TGFB2	TGFB3	TGFB1
H	LEFTY2	LTBP1	INHBB	INHBA	INHBC	INHBE	LEFTY2	LTBP1	INHBB	INHBA	INHBC	INHBE

(18s,GAPDH,HPRT1 and GUSB were housekeeping genes) (the TGF-β superfamily include: Activin receptor 1 ACVR1, Transforming growth factor beta receptor 1 TGFBR1, Transforming growth factor beta receptor 2 TGFBR2 , Transforming growth factor beta receptor 3 TGFBR3, endoglin ENG, Growth differentiation Factor 1 GDF1;LASS1, Growth differentiation Factor 3 GDF3, Growth differentiation Factor 9 GDF9, Bone morphogenetic protein 4 BMP4, Bone morphogenetic protein 2 BMP2, Bone morphogenetic protein 7 BMP7, Bone morphogenetic protein 6 BMP6, Bone morphogenetic protein 3 BMP3, Chordin CHRD, Bone morphogenetic protein 5 BMP5, Bone morphogenetic protein 10 BMP10, Growth differentiation Factor 7GDF7, Growth differentiation Factor 6 GDF6, Bone morphogenetic protein 8B BMP8B, Bone morphogenetic protein 8A BMP8A, Growth differentiation Factor 2 GDF2, Growth differentiation Factor 11 GDF11, Bone morphogenetic protein receptor 1 A BMPR1A, Bone morphogenetic protein receptor 1 B BMPR1B, Bone morphogenetic protein receptor 2 BMPR2, Sclerostin SOST, Gremlin 1 GREM1, Noggin NOG, Cerbeus 1 CER1, Neuroblastoma 1 NBL1, Follistatin FST, Activin receptor type-1B ACVR1B, Activin receptor type-2 A ACVR2A, Activin receptor type-2 B ACVR2 B, inhibin alpha INHA, Transforming growth factor beta 2 TGF-β2, Transforming growth factor beta 3 TGF-β3, Transforming growth factor beta 1 TGF-β1, Lefty 2 LEFTY2, Latent-transforming growth factor beta binding protein 1 LTBP1, inhibin beta B INHBB, inhibin beta A INHBA, inhibin beta C INHBC, inhibin beta E INHBE)

4.2.6 Further analysis of the effects of PC3RFP-CM and co-culture on Noggin expression in osteoblast cell lines using QRT-PCR

The expressions of Noggin in mRNA of osteoblast cells were measured using Taqman single gene assay of Noggin. PC3RFP cells were seeded with osteoblast cells using the same cells density and procedure that were used earlier (4.2.3). Cells (SaOS2 and MG63) were seeded individually again in the same way but the media was changed with PC3RFP-CM after the first 48h. CM was generated over PC3-RFP cells as described in Chapter 3 section (3.2.4) using 2% and 4% FBS respectively. RNA was extracted from all cells groups co-culture and treated with PC3RFP-CM and cDNA were synthesized as described previously in Chapter 2 section (2.3.5). Noggin expression was measured with relative expression to housekeeping gene GAPDH as described earlier in Chapter 2 section (2.3.6).

4.2.7 Immunofluorescence detection of Noggin in co-culture and in osteoblast grown in PC3RFP-CM

Immunofluorescent microscopy was used to identify Noggin in cells using specific antibodies. Rabbit polyclonal anti-Noggin antibody (abcam, UK) and donkey anti-rabbit IgG H&L (Alexa Fluor 488) antibodies (abcam, UK) were used as primary and secondary antibodies. SaOS2 ~ 10,000 cells/cm² and PC3RFP 3000cells/ cm² were seeded in 8 chamber slides (BD, UK) and cultured in DMEM containing 10% FBS, 1% penicillin/ streptomycin as seen in Figure 4.2. After, 48hour the cells were washed with PBS, and the media were changed to the same formulation but with 2%FBS in the co-culture group and controls (SaOS2 and PC3RFP) or with PC3RFP-CM (Saos2 cells). After cultures had become 80% confluent they were washed twice with PBS and fixed with 200µl of 10% neutral buffered formalin for 10 min at room temperature. Cells were washed again twice with PBS, and permeabilised with 200µL 0.1% Triton in PBS for 10 min at room temperature on shaker. Cells were washed twice with PBS at room temperature blocked with 200µL 10% normal donkey serum in PBS for 30 min at room temperature.

In optimising antibody concentrations, cells were incubated overnight at 4°C with 200µl of anti-Noggin antibody (abcam, UK) in different dilutions in 10% Donkey serum (1:50), (1:100), and (1:200). The same dilutions of negative control rabbit immunoglobulin isotype (Dako,UK) were added to the negative controls chambers.

Cells were washed twice with 500µL PBS for 3 min on a shaker at room temperature. 100µL of the secondary donkey anti-rabbit IgG H&L (Alexa Fluor 488) antibody in 10%

donkey serum was added in (1:200) dilution to each well. The slides were incubated for 1h in the dark at room temperature. The washing step was repeated again and slides were mounted using ProLong Antifade Reagents mounting medium containing DAPI stain (Invitrogen, UK), DAPI stain was used to stain nuclei. Images were acquired using Leica fluorescent microscope. 1:100 dilutions of primary antibody with 1:200 secondary antibodies were identified as the optimum primary and secondary antibody concentrations respectively and were used. Subsequent experiments used the optimum antibody concentration.

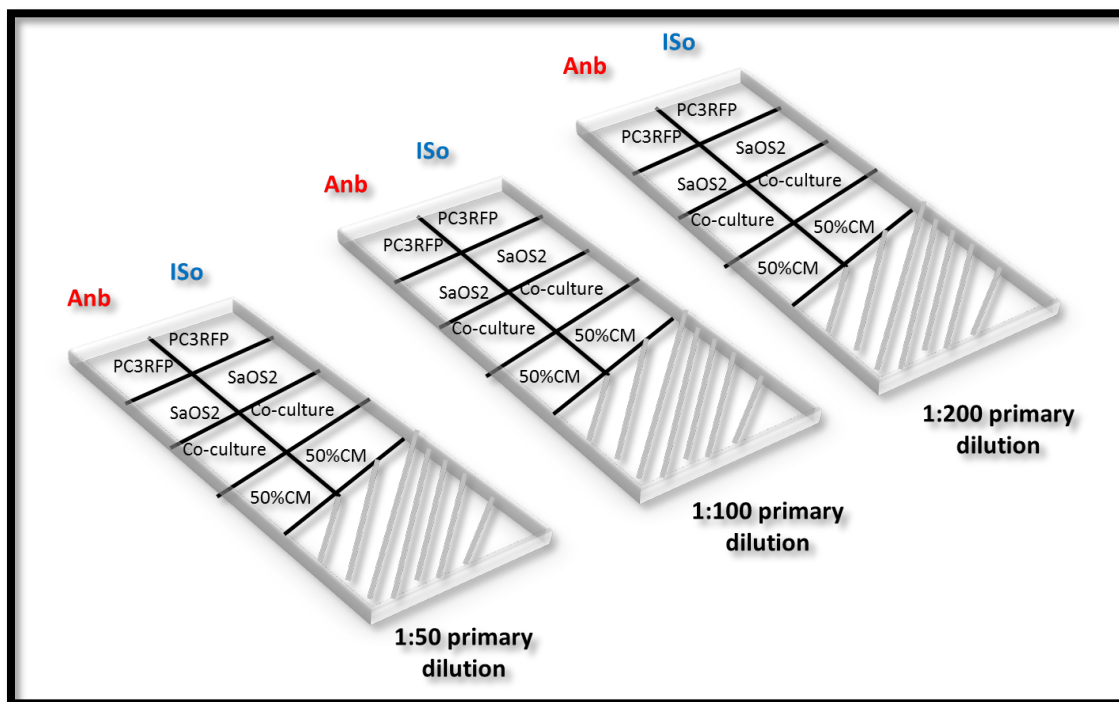


Figure 4.5 Layout for 8 well chamber slides.

The Figure illustrates the set-up for cell cultures in three 8 well chamber slides with different antibody concentrations (1/50, 1/100 and 1/200) on the left top well in each slide, PC3RFP was stained with anti-Noggin antibody (Anb) on the top right PC3RFP was stained with Isotype IgG (iso) as negative control. The rest of the wells were as labelled, with one side of the slide stained with Noggin antibody and the other with the isotype control.

4.2.8 Detection of Noggin protein in co-cultures and in osteoblasts treated with PC3RFP-CM by using flow cytometry

Flow cytometry is a useful technique for separating and measuring particles such as cells, cell surface antigen and intracellular proteins based on fluorescence detection. When cell passes through laser beam the flow cytometry records how the cells or particle distributes incident laser light and releases fluorescence. Noggin protein was detected in osteoblasts grown alone and staining was compared to that in co-cultured SaOS2 and in SaOS2 treated with PC3RFP-CM by using BD FACS Aria flow cytometry.

4.2.8.1 Preparation of cells

PC3RFP cells were seeded with SaOS2 cells using the density equivalent to the density used in growth curve. Around 220,000 cells of PC3RFP were seeded with ~660,000 cells of SaOS2 in T75 flask in standard DMEM 10%FBS media. ~660,000 cells of SaOS2 were seeded in an additional two T75 flasks, one of which was used as negative control. Around 220,000 cells of PC3RFP were seeded in a T75 and these were used as controls to set the gate on the flow cytometer. After 48h, cells were washed with PBS and the media were changed with PC3RFP-CM in one of the SaOS2 flask and with DMEM 2% FBS for co-culture, SaOS2 control and PC3RFP control flasks. When cultures were 80% confluent around day 7, cells were harvested with trypsin and counted as described in Chapter 2 section (2.2.3) and (2.2.5). From each flask three tubes were made (primary antibody, isotype and control) with $\sim 1 \times 10^6$ cells in each tube. These were transferred to 1.5ml eppendorf tubes and washed with 1ml PBS cells were centrifuged at 500 xg for 3 min. PBS was removed and the cells were fixed with 300 μ L of 4% formalin in PBS at room temperature on a rotator for 10 min. Cells were washed again with 1ml PBS and centrifuged at 500 xg for 3 min. Cell pellets were re-suspended in 0.1% triton in order to permeabilised cell membrane for 10 min. Cells were washed twice with PBS to remove all traces of fixative and detergent. Cells were blocked using 10% donkey serum diluted in 0.5% BSA solution for 30 min at room temperature. Cells were washed once more with PBS. Supernatant was removed thoroughly by inversion on an absorbent paper and 20 μ L of BD phosflow perm/wash buffer I 1X solution, which was made from 10X stock solution, and was added to cell pellet. BD phosflow perm/wash buffer was used to permeabilize the cells; it also acts as an antibody diluent and cell wash buffer at the same time. 100 μ L of 1/200 of rabbit anti-Noggin polyclonal antibody was added and cells incubated in the dark for 30 min. Cells were washed with PBS and centrifuged and the liquid was removed completely.

100µL of 1/2000 of secondary donkey anti-rabbit IgG H&L (Alexa Fluor 488) polyclonal antibody was added to the cells and incubated for 30 min in the dark. Cells were washed with PBS once and twice with 1X perm buffer. Finally, cells were re-suspended in 300µL of 1X perm buffer and cells were analysed by using BD FACS Aria flow cytometry.

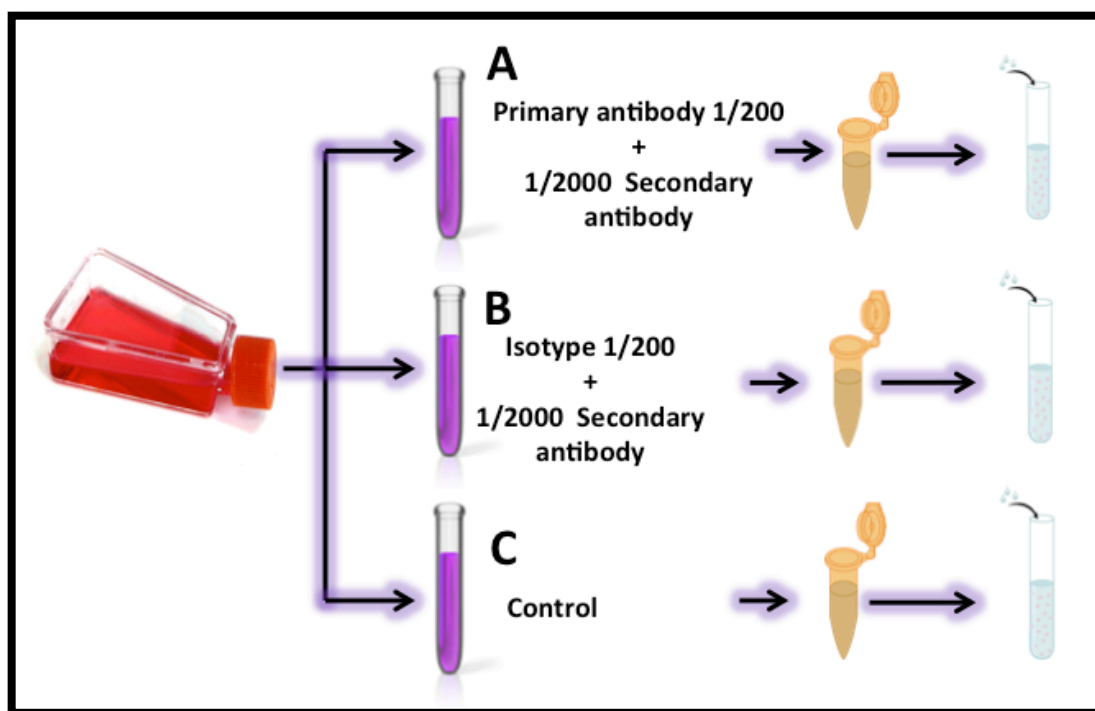


Figure 4.6 Scheme showing how samples were prepared for flow cytometry.

The Figure illustrates the distribution of cells from each flask in to three test tubes. Cells were counted from the T75 and around 1×10^6 cells were placed in each tube. Tube (A) primary antibody 1/200 dilution and 1/2000 secondary antibody (B) Isotype used as negative control 1/200 dilution isotype with secondary antibody 1/2000 (C) is a control without the addition of any antibodies.

4.2.9 Detection of Noggin protein in co-cultures and in osteoblast treated with PC3RFP-CM using western blot

PC3RFP cells were seeded with osteoblast cells using the same cell densities and procedure that were used earlier (4.2.3). SaOS2 was seeded individually again in the same way but the media was changed to either PC3RFP-CM or to 2% DMEM as a control after the first 48h. Protein was extracted from 80% confluent flasks for all cells, PC3RFP-CM and control and quantified as described in Chapter 2 section (2.4.1) and (2.4.2). 40 µg of protein samples were separated on 12% SDS-PAGE, blotted on PVDF membranes and probed with anti-Noggin and anti-β-actin and anti-GAPDH as housekeeping genes using the concentration as described in Chapter 2 sections (2.4.4), (2.4.5), (2.4.6) and (2.4.7).

4.3 Results

4.3.1 Analysis of TGF- β superfamily expression

The expressions of 43 genes of the TGF- β superfamily were quantified by real time PCR using Taqman custom format 48 (TGF- β) plate. The expression of each gene was firstly assessed as high (ct<25), moderate (ct=25-30), low (ct=31-35) or non expressed (ct>35). After adjustment for housekeeping gene expression (GAPDH), delta ct values were compared between cell lines/treatment groups.

4.3.1.1 Comparison of PC3-RFP/SaOS2 gene expression in exponential and confluent phase

There were no differences between SaOS2 cells or PC3-RFP cells grown in different growth phases Figure (4.7) and Figure (4.8) (for detailed information about the ct value and the calculated Δ dct value see Table 1A and Table 2A in the Appendix A). Since this was the case, all subsequent experiments were done with cells in confluent phase. This maximised RNA yields in these experiments.

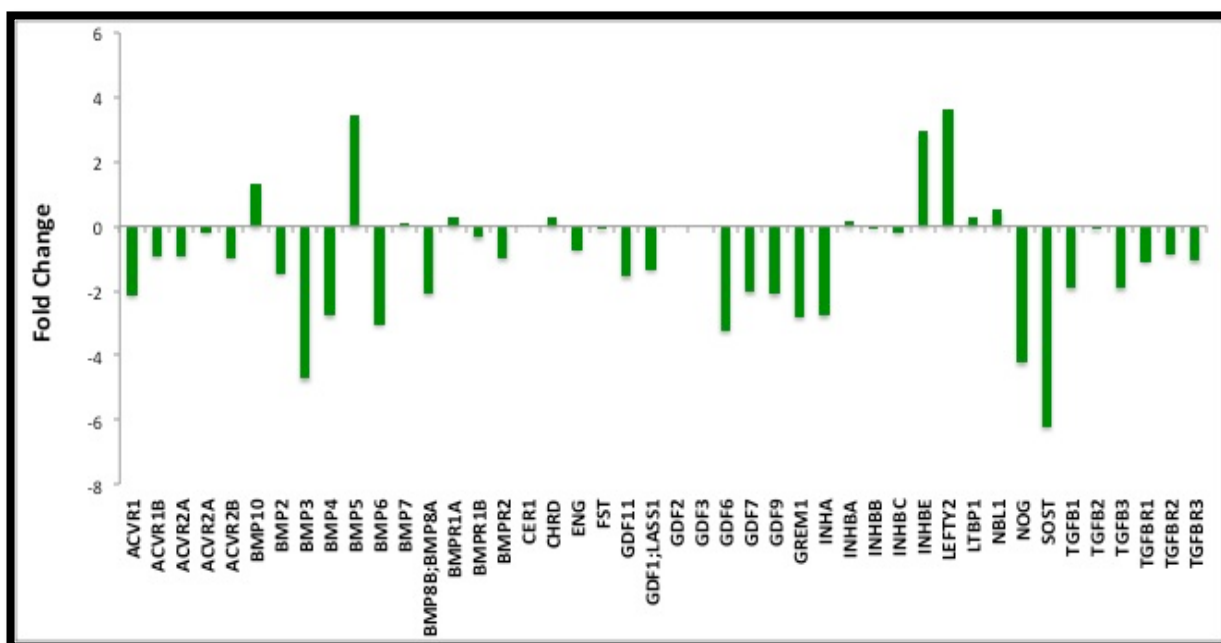


Figure 4.7 Array plate analysis in exponential SaOS2 compared to confluent SaOS2 in TGF- β superfamily genes

This Figure shows the differences between exponential SaOS2 and Confluent SaOS2 in terms of fold change after being adjusted to housekeeping gene (GAPDH). The Fold Change was calculated by using the equation $\frac{\Delta\text{dct}}{3.3} \times -10$. Data expressed as mean of 3 independent experiments.

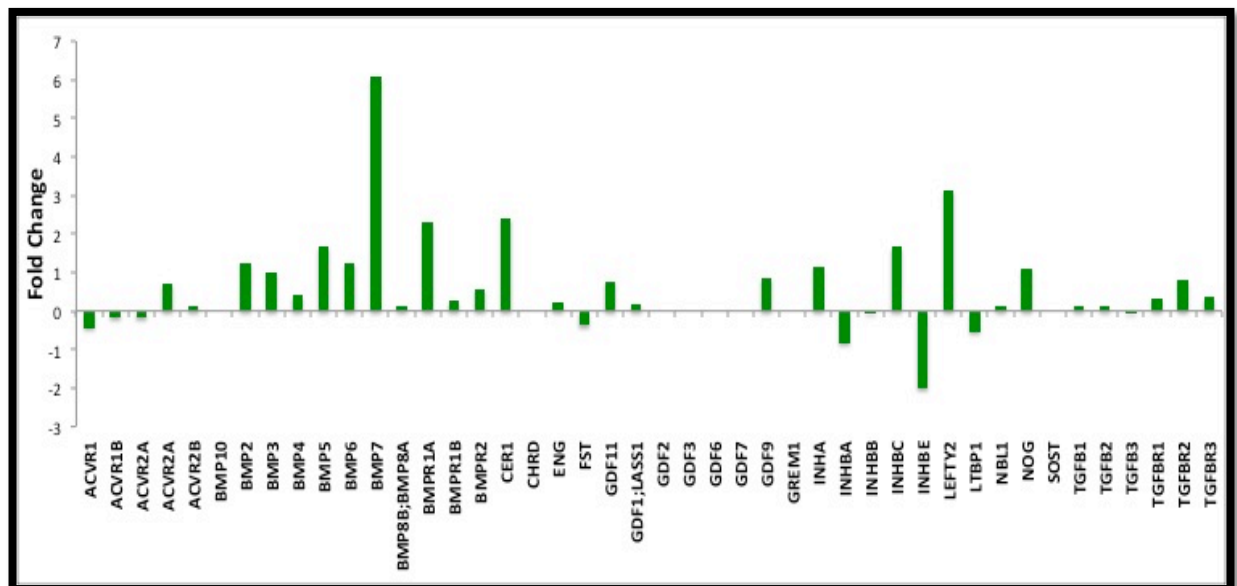


Figure 4.8 Array plate analysis in exponential PC3RFP compared to Confluent PC3RFP in TGF-β superfamily genes.

This Figure shows the differences between exponential PC3RFP and Confluent PC3RFP in terms of fold change after being adjusted to housekeeping gene (GAPDH). The Fold Change was calculated by using the equation $\frac{\Delta_{dct}}{3.3} \times -10$. Data expressed as mean of 3 independent experiments.

4.3.1.2 Comparison of PC3RFP and SaOS2 cells grown alone in confluent phase

As in 4.3.1.1, there were no genes in the TGF-β superfamily that were expressed at high levels in PC3RFP. As seen in Figure (4.9) the following genes were not expressed by PC3RFP: bone morphologic protein 5 (BMP5), bone morphologic protein 7 (BMP7), Cerebus (CER1), Endoglin (ENG), Growth differentiation Factor 1 (GDF1), Growth differentiation Factor 7 (GDF7), Inhibin beta B (INHBB), LEFTY 2. In SaOS2 cells only bone morphologic protein 4 (BMP4) and transforming growth factor beta 1 (TGFβ1) were highly expressed. The following genes were not expressed by SaOS2: bone morphologic protein 10 (BMP10), bone morphologic protein 5 (BMP5), bone morphologic protein3 (BMP3), Chordin (CHRD), Growth differentiation Factor 7 (GDF7), Growth differentiation Factor 9 (GDF9), Inhibin beta C (INHBC), LEFTY 2, Sclerostin (SOST). The rest of the TGF-β superfamily genes were expressed at either moderate or low levels in either cell line. There were clear differences in the levels of expression after adjustment for housekeeper expression shown as (Δdct) value (as seen highlighted in Table 3A in the Appendix A). The major differences presented as relative expression after adjusting with housekeeping gene (GAPDH) was shown in Figure 4.10.

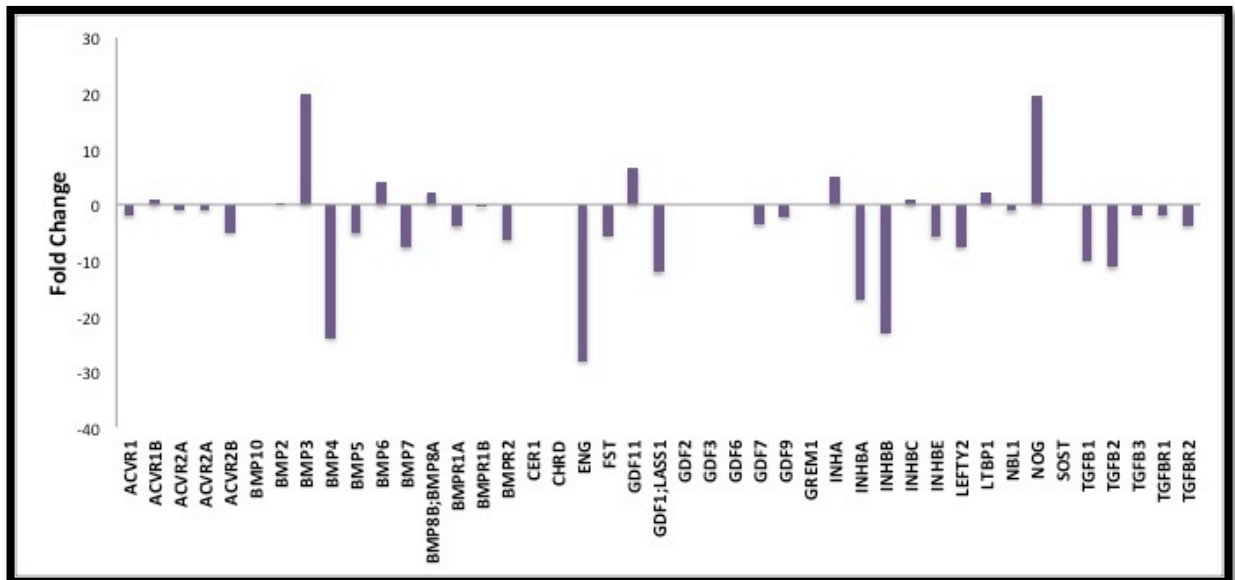


Figure 4.9 Array plate analysis of TGF-β superfamily genes in PC3RFP compared to SaOS2 during the Confluent Phase.

This Figure shows the differences between PC3FP and SaOS2 in terms of fold change after being adjusted to housekeeping gene (GAPDH). The Fold Change was calculated by using the equation $\frac{\Delta d_{ct}}{3.3} \times -10$. Data expressed as mean of 3 independent experiments.

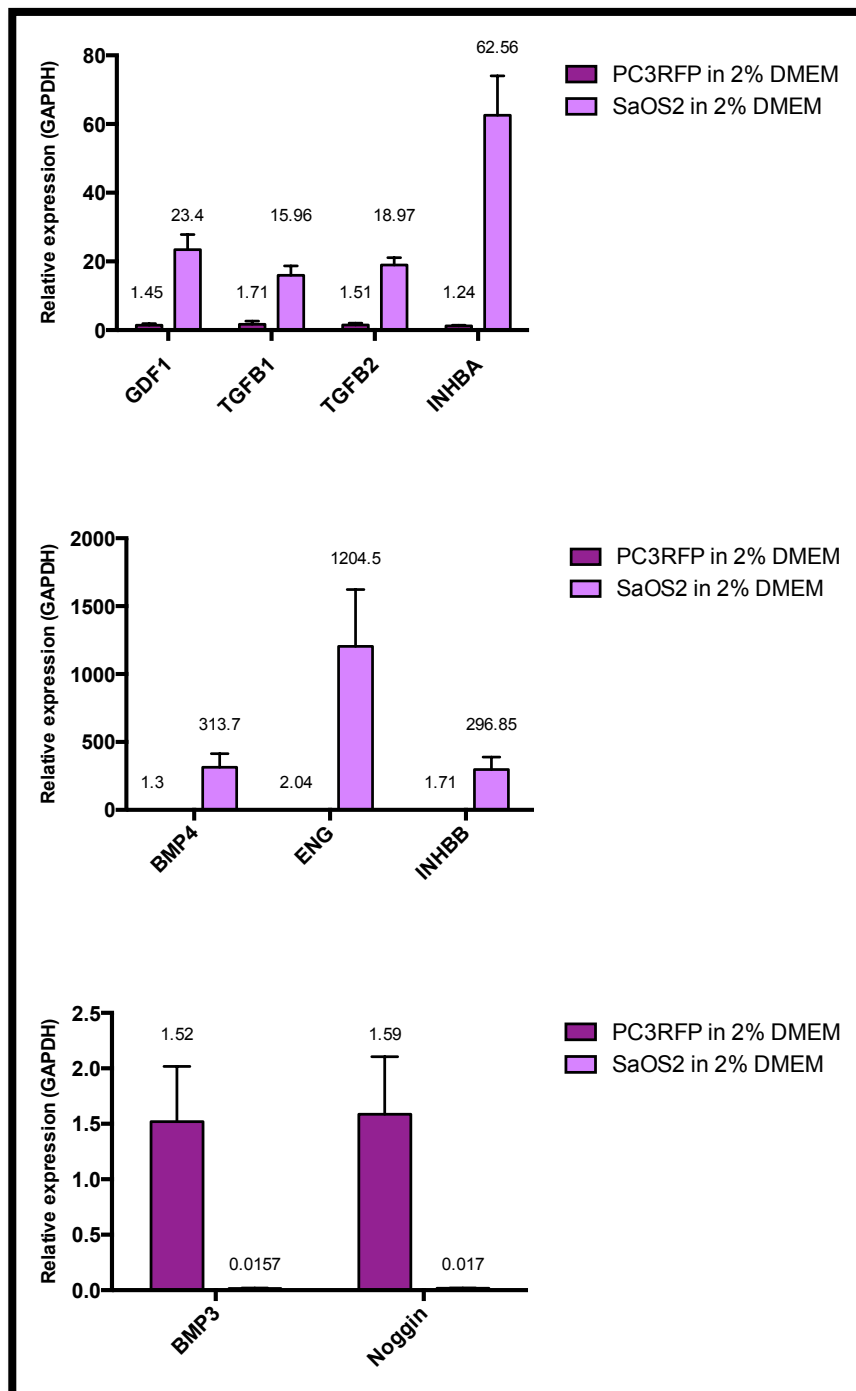


Figure 4.10 Array plate analysis of the major differences between confluent PC3RFP and Confluent SaOS2 in TGF- β superfamily genes.

This Figure shows the differences between confluent PC3RFP and Confluent SaOS2 in terms of relative expression after being adjusted to housekeeping gene (GAPDH). The following genes were expressed at a higher level in SaOS2 cells: GDF1, TGF- β 1, TGF- β 2, INHBA, INHBB, BMP4 and ENG. While, PC3RFP showed an increase in BMP3 and Noggin expression compared with these genes in SaOS2 cells. Relative expression was calculated after calculating dct and Δdc then Δdc was raised to the square root. Data expressed as mean of 3 independent experiments.

4.3.1.3 Comparison of PC3RFP and MG63 cells grown alone in confluent phase

As in 4.3.1.1, there were no genes in the TGF- β superfamily that were expressed at high levels in PC3RFP while, only (ENG) was expressed at high levels in MG63. As seen in Figure (4.11) the following genes were not expressed by MG63: BMP3, BMP6, CER1, GDF3, INHBB, INHBC and LEFTY2. The rest of the genes were expressed at either moderate or low levels in either cell line. There were clear differences in the levels of expression after adjustment for housekeeper expression shown as (Δ dct) value (as seen highlighted in Table 4A in the Appendix A). The major differences presented as relative expression after adjusting with housekeeping gene (GAPDH) was shown in Figure 4.12

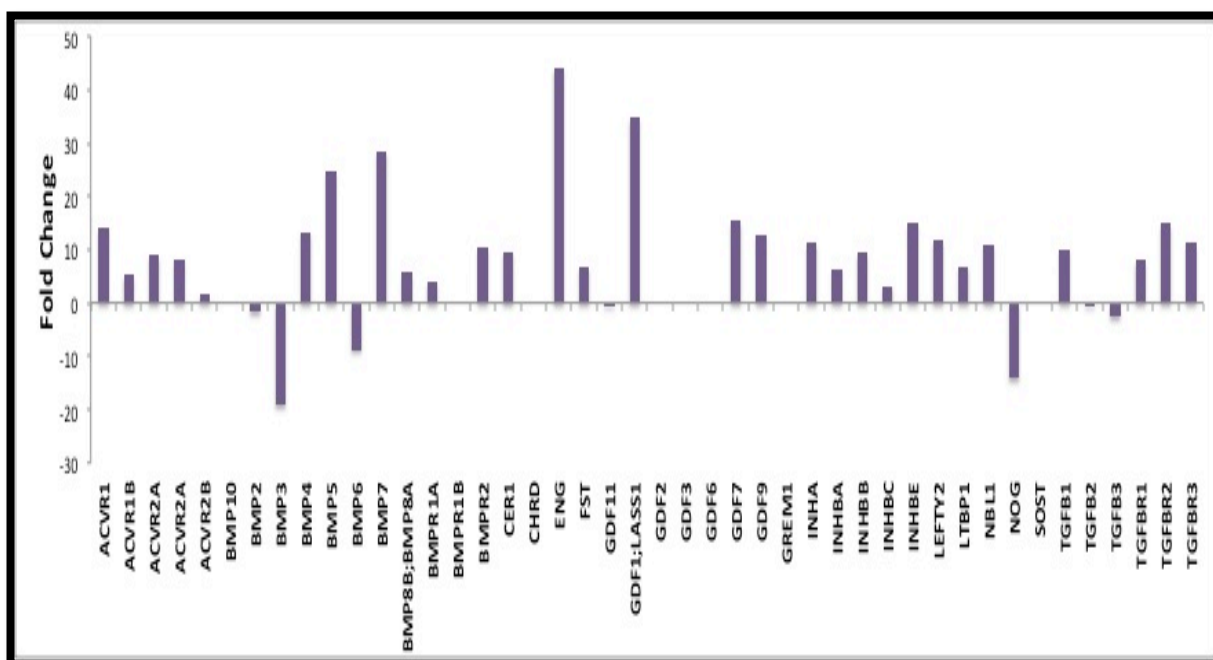


Figure 4.11 Array plate analysis of TGF- β superfamily genes in MG63 compared to PC3RFP during the Confluent Phase.

This Figure shows the differences between MG63 and PC3RFP in terms of fold change after being adjusted to housekeeping gene (GAPDH). The Fold Change was calculated by using the equation $\frac{\Delta\text{dct}}{3.3} \times -10$. Data expressed as mean of 3 independent experiments.

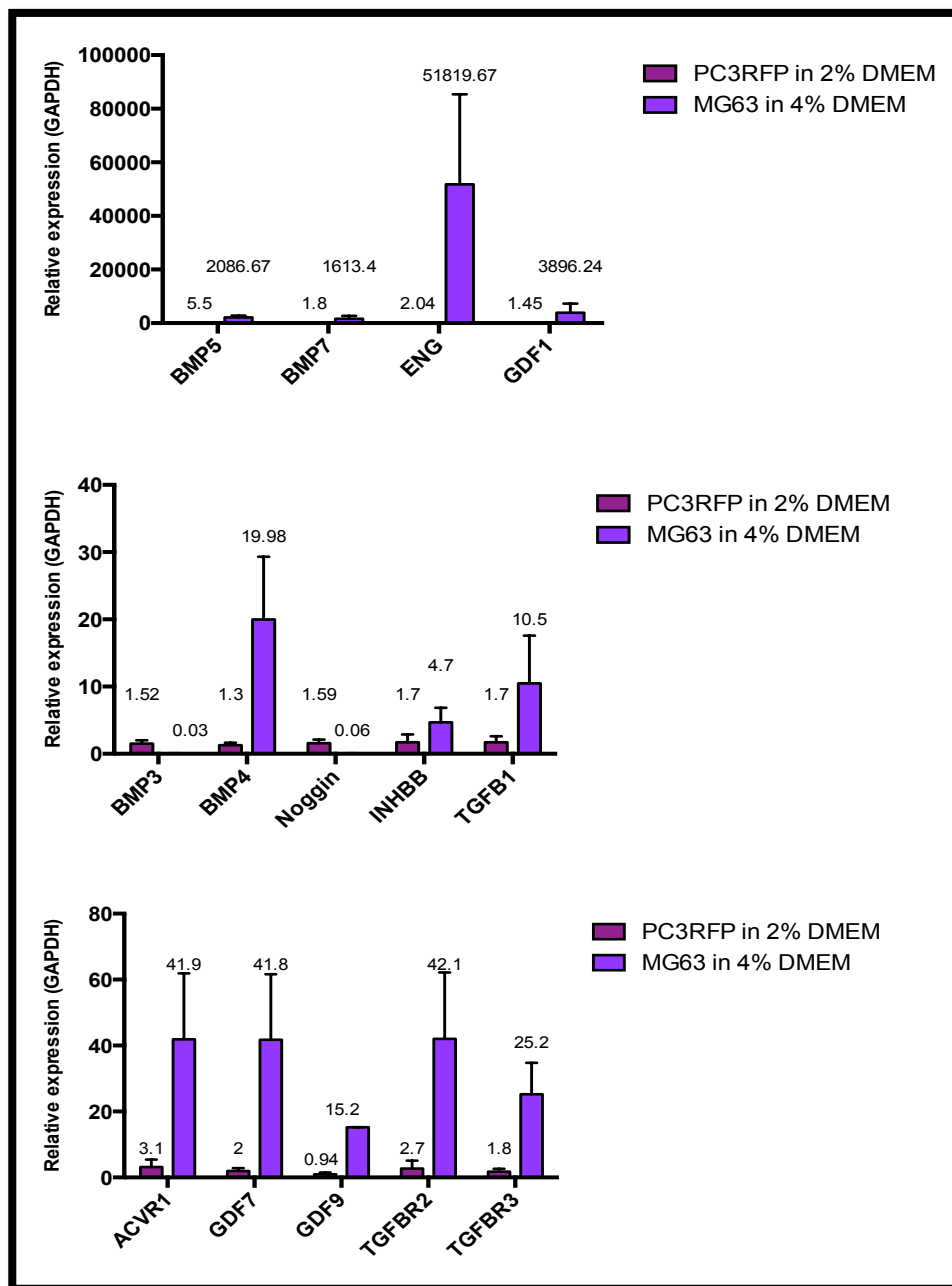


Figure 4.12 Array plate analysis of the major differences between confluent PC3RFP and Confluent MG63 in TGF-β superfamily genes.

This Figure shows the differences between confluent PC3RFP and Confluent MG63 in terms of relative expression after being adjusted to housekeeping gene (GAPDH). The following genes were expressed at a higher level in MG63 cells: GDF1, TGF-β1, INHBB, BMP5, BMP7, BMP4, Activin receptor 1 (ACVR1), GDF7, GDF9, Transforming growth factor beta receptor 2 (TGFB2), Transforming growth factor beta receptor 3 (TGFB3) and ENG. While, PC3RFP showed an increase in BMP3 and Noggin expression compared with these genes in SaOS2 cells. Relative expression was calculated after calculating dct and Δdc then Δdc was raised to the square root. Data expressed as mean of 3 independent experiments.

4.3.1.4 Comparison of SaOS2 gene expression grown alone and in co-culture with PC3RFP

Osteoblast cells (SaOS2) were seeded together with PC3RFP cells in co-culture and they were incubated together for 7 days until they become confluent. The cells were sorted using BD FACS Aria. The expression of the same 43 genes of the TGF- β superfamily were quantified by real time PCR using the same Taqman custom format 48 (TGF- β) Expresstm plate that was used with confluent cells. As in 4.3.1.1, both BMP4 and TGF- β 1 were expressed at high level in both confluent SaOS2 and co-cultured SaOS2. As seen in Figure (4.13) the following genes continued not to be expressed by co-cultured SaOS2: BMP10, BMP5, CHR1, GDF7, GDF9, Inhibin beta C INHBC, LEFTY2 and SOST. The rest of the genes were expressed at either moderate or low levels in either cell line. There were no differences in most of the genes between confluent SaOS2 and co-cultured SaOS2 the only clear differences in the levels of expression after adjustment for housekeeper expression shown as (Δ dct) value were found in BMP3, BMP6, GREM1 and Noggin being expressed more in SaOS2 after being co-cultured with PC3RFP (as seen highlighted in Table 5A in the Appendix A). The major differences presented as relative expression after adjusting with housekeeping gene (GAPDH) was shown in Figure (4.14).

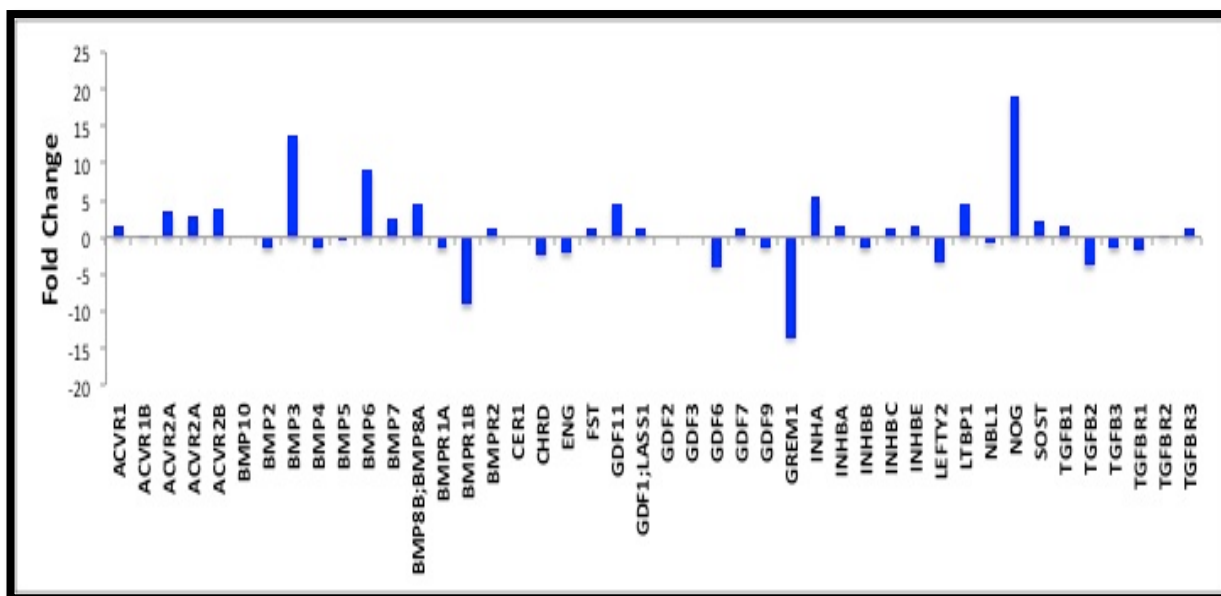


Figure 4.13 Array plate analysis of TGF- β superfamily genes in co-cultured SaOS2 compared to control SaOS2 during the Confluent Phase.

This Figure shows the differences between co-cultured SaOS2 and control SaOS2 in terms of fold change after being adjusted to housekeeping gene (GAPDH). The Fold Change was calculated by using the equation $\frac{\Delta\text{dct}}{3.3} \times -10$. Data expressed as mean of 3 independent experiments.

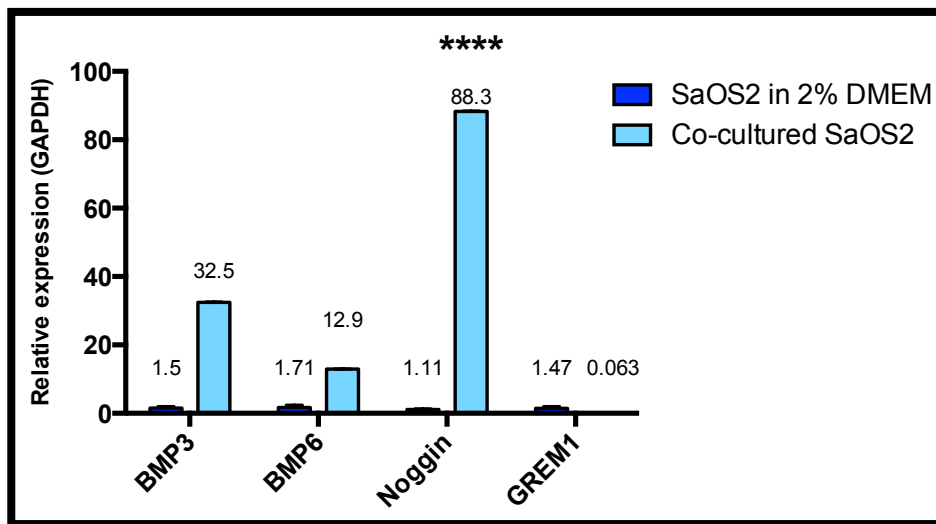


Figure 4.14 Array plate analysis of the major differences between confluent SaOS2 and co-cultured SaOS2 in TGF- β superfamily genes.

SaOS2 cells were cultured together with PC3RFP for 7 days. The cells were then sorted using BD FACS Aria. RNA was collected and cDNA was run on the same Taqman expressed plate. This Figure shows the differences between confluent SaOS2 and co-cultured SaOS2 in terms of relative expression after being adjusted to housekeeping gene (GAPDH). The following genes were expressed at a higher level in co-cultured SaOS2: BMP3, BMP6, Noggin and GREM1. Noggin was significantly increased ($P=0.0001$) unpaired t test. Relative expression was calculated after calculating dct and Δdc then Δdc was raised to the square root. Data expressed as mean of 3 independent experiments.

4.3.1.5 Comparison of PC3RFP gene expression in these cells grown alone and in co-culture with SaOS2

There were no differences in relative gene expression between confluent PC3RFP cells and PC3RFP being co-cultured with SaOS2 cells as seen in Figure (4.15) (for detailed information about the ct value and the calculated Δdct value see Table 6A in the Appendix A).

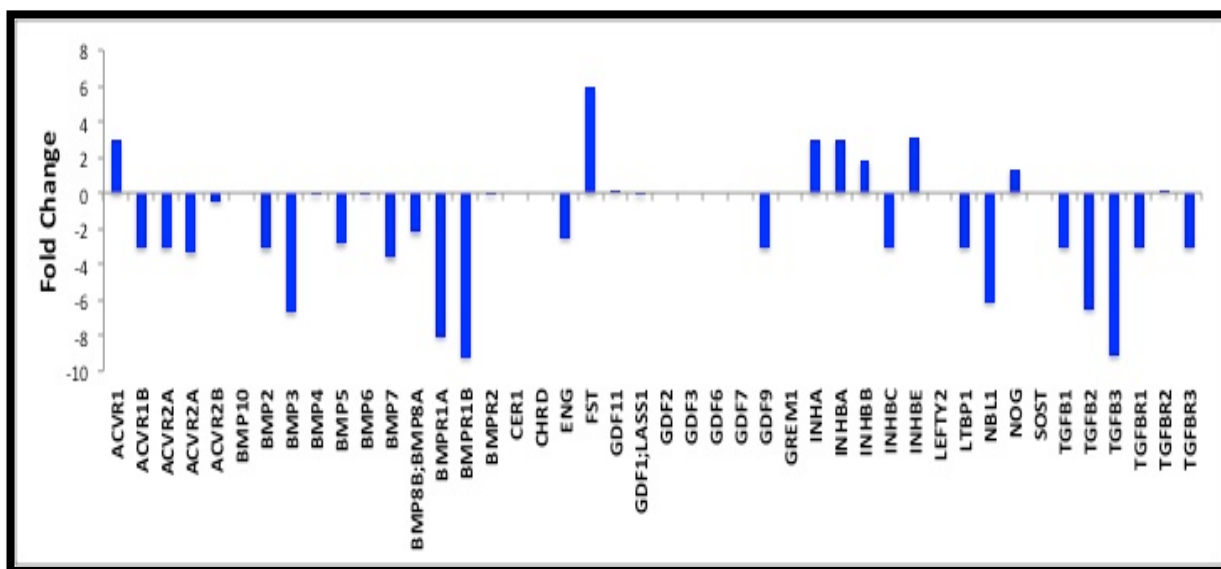


Figure 4.15 Array plate analysis of TGF- β superfamily genes in co-cultured PC3RFP/with SaOS2 compared to control PC3RFP during the Confluent Phase.

This Figure shows the differences between co-cultured PC3RFP/with SaOS2 and control PC3RFP in terms of fold change after being adjusted to housekeeping gene (GAPDH). The Fold Change was calculated by using the equation $\frac{\Delta\text{dct}}{3.3} \times -10$. Data expressed as mean of 3 independent experiments.

4.3.1.6 Comparison of MG63 gene expression in these cells grown alone and in co-culture with PC3RFP

Osteoblast cells (MG63) were seeded together with PC3RFP cells in co-culture and they were incubated together for 7 days until they become confluent. The cells were sorted using BD FACS Aria. The expressions of the same 43 genes of the TGF- β superfamily were quantified by real time PCR using the same Taqman custom format 48 (TGF- β) Expresstm plate that was used with confluent cells. There were no genes in the TGF- β superfamily that were expressed at high level except for ENG which was expressed at high level in both MG63 confluent and in MG63 co-cultured with PC3RFP. The same genes that were not expressed in confluent MG63 were also not expressed when cells were cultured with PC3RFP as seen in Figure (4.16). The clear differences in the relative gene expression after adjusting with housekeeping gene GAPDH was seen in Noggin, CHR1 and Active receptor 2 B (ACVR2B) being expressed more in co-culture group. While, Active receptor 2 A (ACVR2A) was found

to be expressed more in confluent MG63 (as seen highlighted in Table 7A in the Appendix A). These differences were presented as relative gene expression in Figure 4.17.

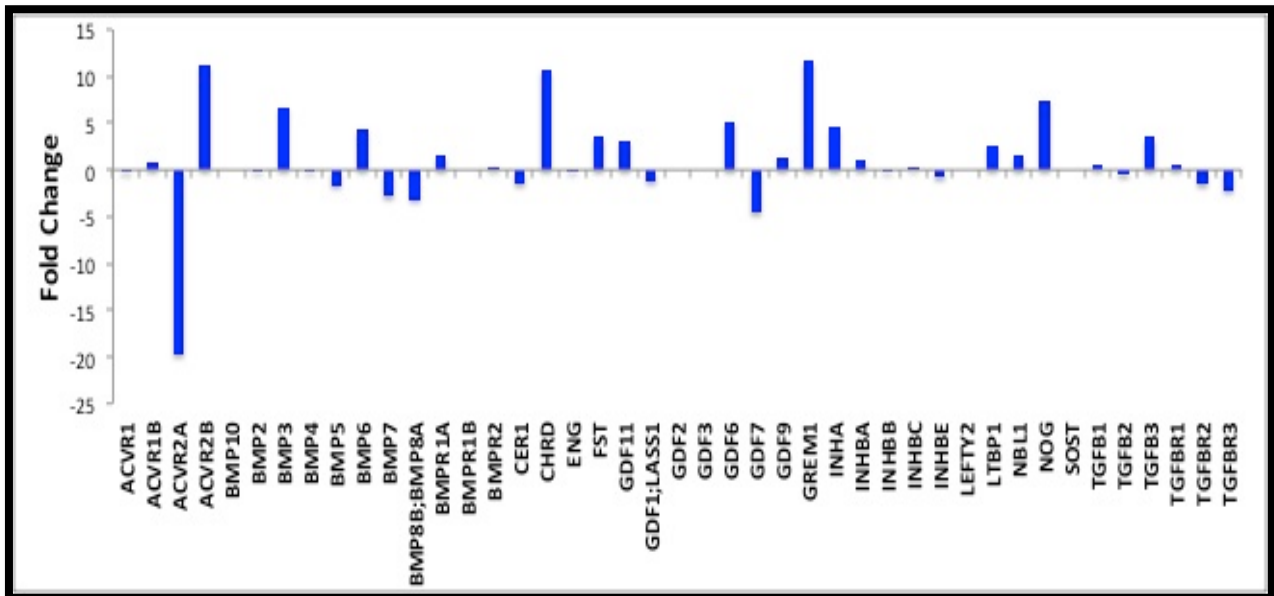


Figure 4.16 Array plate analysis of TGF- β superfamily genes in co-cultured MG63 compared to control MG63 during the Confluent Phase.

This Figure shows the differences between co-cultured MG63 and control MG63 in terms of fold change after being adjusted to housekeeping gene (GAPDH). The Fold Change was calculated by using the equation $\frac{\Delta_{ct}}{3.3} \times -10$. Data expressed as mean of 3 independent experiments.

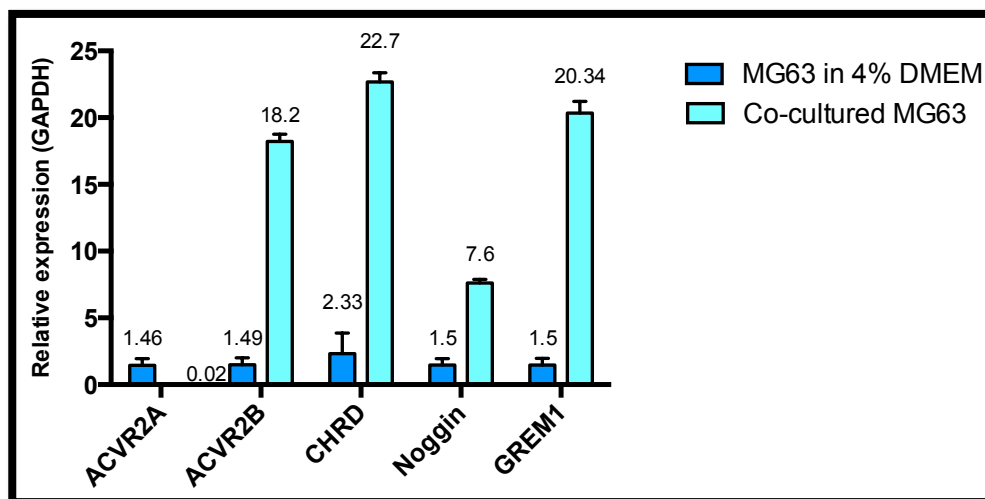


Figure 4.17 Array plate analysis of the major differences between confluent MG63 and co-cultured MG63 in TGF- β superfamily genes.

MG63 cells were cultured together with PC3RFP for 7 days. The cells were then sorted using BD FACS Aria. RNA was collected and cDNA was run on the same Taqman expressed plate. This Figure shows the differences between confluent MG63 and co-cultured MG63 in terms of relative expression after being adjusted to housekeeping gene (GAPDH). The following genes were expressed at a higher level in co-cultured MG63: ACVR2B, CHR1, Noggin and GREM1. Confluent MG63 express more ACVR2A compared to MG63 co-cultured with PC3RFP. Relative expression was calculated after calculating dct and Δdc then Δdc was raised to the square root. Data expressed as mean of 3 independent experiments.

4.3.1.7 Comparison of PC3RFP gene expression in these cells grown alone and in co-culture with MG63

As in 4.3.1.1, there were no genes in the TGF- β superfamily that were expressed at high level in PC3RFP co-cultured with MG63. Most of the genes that were not expressed in confluent PC3RFP remained unexpressed even after being co-cultured with MG63 cells. The rest of the TGF- β superfamily genes were expressed at either moderate or low levels in PC3RFP co-cultured with MG63 cells as seen in Figure (4.18). There were clear differences in the relative gene expression between the two groups in ENG, INHBE and GDF1 (as seen in Table 8A in the Appendix). The major differences presented as relative expression after adjusting with housekeeping gene (GAPDH) was shown in Figure (4.19).

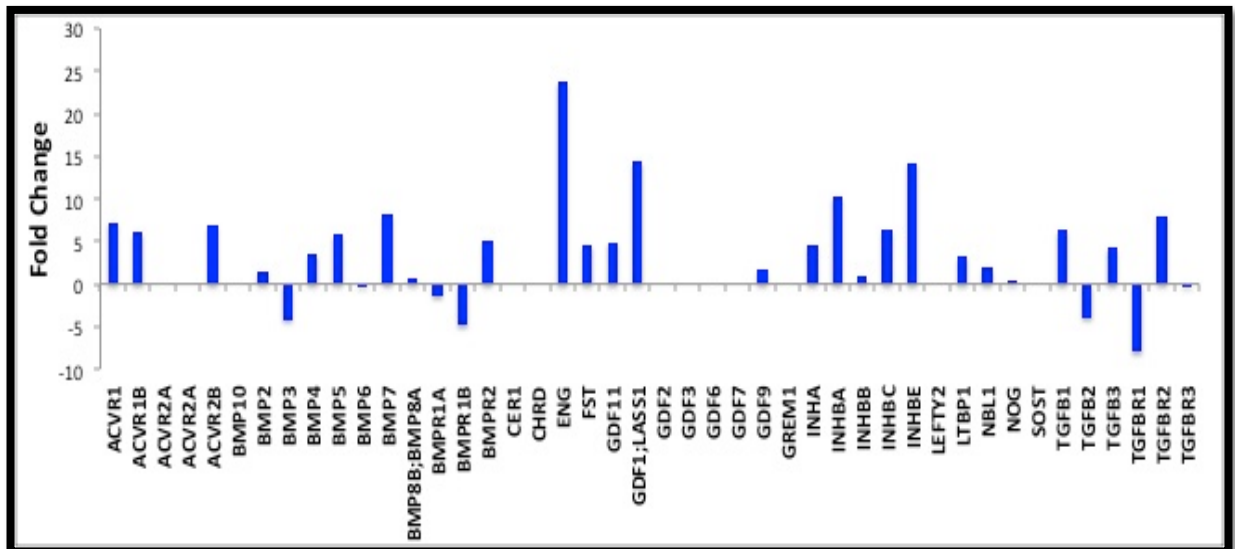


Figure 4.18 Array plate analysis of TGF- β superfamily genes in co-cultured PC3RFP/with MG63 compared to control PC3RFP during the Confluent Phase.

This Figure shows the differences between co-cultured PC3RFP/with MG63 and control PC3RFP in terms of fold change after being adjusted to housekeeping gene (GAPDH). The Fold Change was calculated by using the equation $\frac{\Delta_{dct}}{3.3} \times -10$. Data expressed as mean of 3 independent experiments.

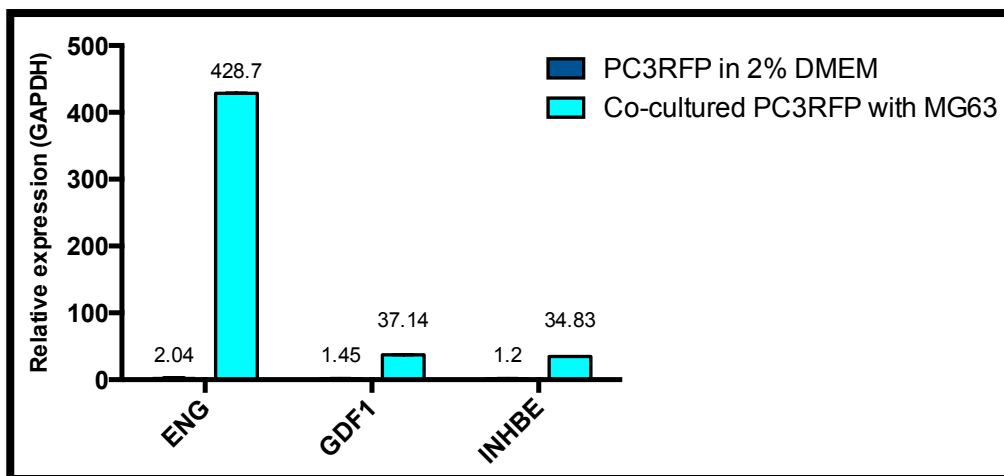


Figure 4.19 Array plate analysis of the major differences between co-cultured PC3RFP with MG63 compared to control PC3RFP cells in TGF- β superfamily genes

MG63 cells were cultured together with PC3RFP for 7 days. The cells were then sorted using BD FACS Aria. RNA was collected and cDNA was run on the same Taqman expressed plate. This Figure shows the differences between confluent PC3RFP and PC3RFP co-cultured with MG63 in terms of relative expression after being adjusted to housekeeping gene (GAPDH). The following genes were expressed at a higher level in co-cultured PC3RFP: ENG, GDF1 and INHBE. Relative expression was calculated after calculating dct and Δ_{dc} then Δ_{dc} was raised to the square root. Data expressed as mean of 3 independent experiments.

4.3.1.8 Comparison of SaOS2 gene expression in these cells grown in standard control medium and in SaOS2 treated with PC3RFP-CM

Osteoblast cells (SaOS2) were treated with PC3RFP-CM. The expressions of the same 43 genes of the TGF- β superfamily were quantified by real time PCR using the same Taqman custom format 48 (TGF- β) Expresstm plate and was compared to the gene expression profile of confluent SaOS2 cells. As in 4.3.1.1, there were no genes of the TGF- β superfamily that were expressed at high level in SaOS2 treated with PC3RFP conditioned media. As seen in Figure (4.20) the following genes continued not to be expressed by SaOS2 treated with PC3RFP conditioned media: bone morphologic protein 10 (BMP10), BMP5, Chordin (CHRD), GDF7, Growth differentiation Factor 9 (GDF9), Inhibin beta C (INHBC), GDF2, LEFTY, Sclerostin (SOST), (CER) with the addition of other gene BMPR1B. The rest of the genes were expressed at either moderate or low levels in either cell line. There were no differences in most of the genes between confluent SaOS2 and SaOS2 treated with PC3RFP-CM the only clear differences in the levels of expression after adjustment for housekeeper expression shown as (Δ dct) value were found is in Noggin being significantly expressed more in SaOS2 after being treated with C3RFP-CM with $p=0.008$ by using unpaired t test as seen in Figure 4.21 (for detailed information about the ct value and the calculated Δ dct value see Table 9A in the Appendix A)

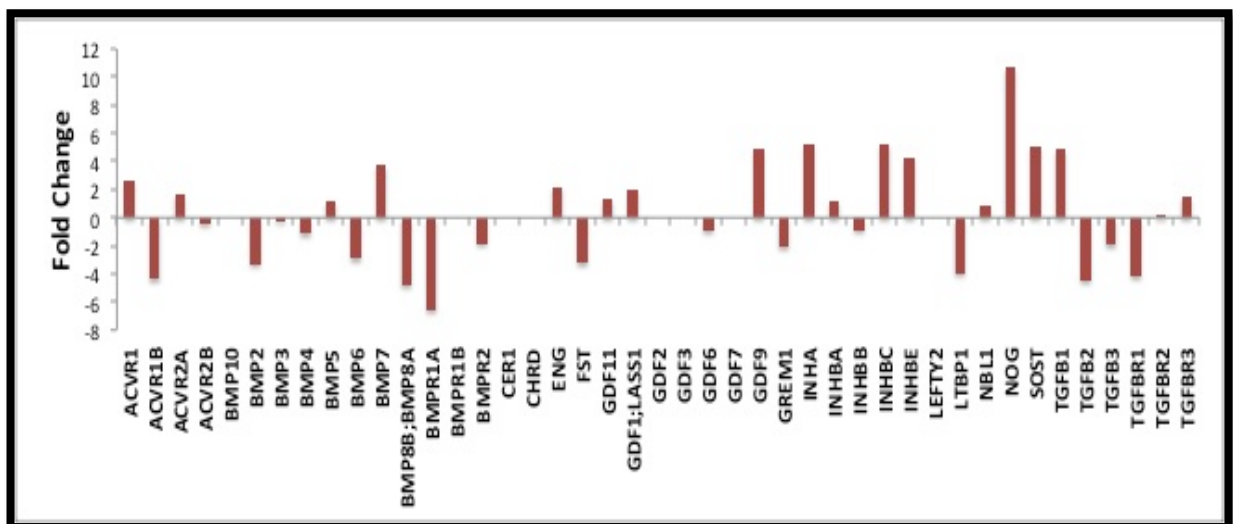


Figure 4.20 Array plate analysis of TGF- β superfamily genes in Confluent SaOS2 compared to SaOS2 treated with PC3RFP-CM.

This Figure shows the differences between confluent SaOS2 and SaOS2 treated with PC3RFP-CM in terms of fold change after being adjusted to housekeeping gene (GAPDH). The Fold Change was calculated by using the equation $\frac{\Delta\text{dct}}{3.3} \times -10$. Data expressed as mean of 3 independent experiments.

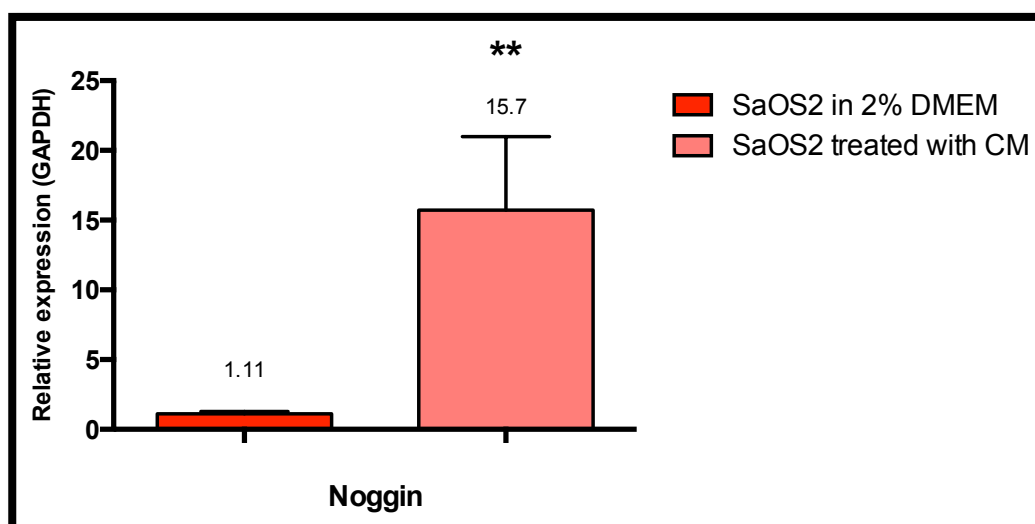


Figure 4.21 Array plate analysis of the major differences between confluent SaOS2 and SaOS2 treated with PC3RFP-CM in TGF- β superfamily genes.

This Figure shows the differences between confluent SaOS2 and SaOS2 treated with PC3RFP-CM in terms of relative expression after being adjusted to housekeeping gene (GAPDH). Noggin gene was found to be expressed more in the SaOS2 treated group ($p=0.008$) unpaired t test. Relative expression was calculated after calculating dct and Δdc then Δdc was raised to the square root. Data expressed as mean of 3 independent experiments.

4.3.1.9 Comparison of MG63 gene expression grown alone and in MG63 treated with PC3RFP-CM

There were no genes of the TGF- β superfamily that were expressed at high level in MG63 treated with PC3RFP conditioned media. The same genes that were not expressed in confluent MG63 contained to be unexpressed when cells were treated with PC3RFP-CM as seen in Figure (4.22). The clear differences in the relative gene expression after adjusting with housekeeping gene GAPDH was seen in BMP5, ENG, GDF11, TGFBR1, TGFBR2 and TGFBR3 being expressed less in the treated group (as seen highlighted in Table A10 in the Appendix) and were presented as relative gene expression in Figure (4.23).

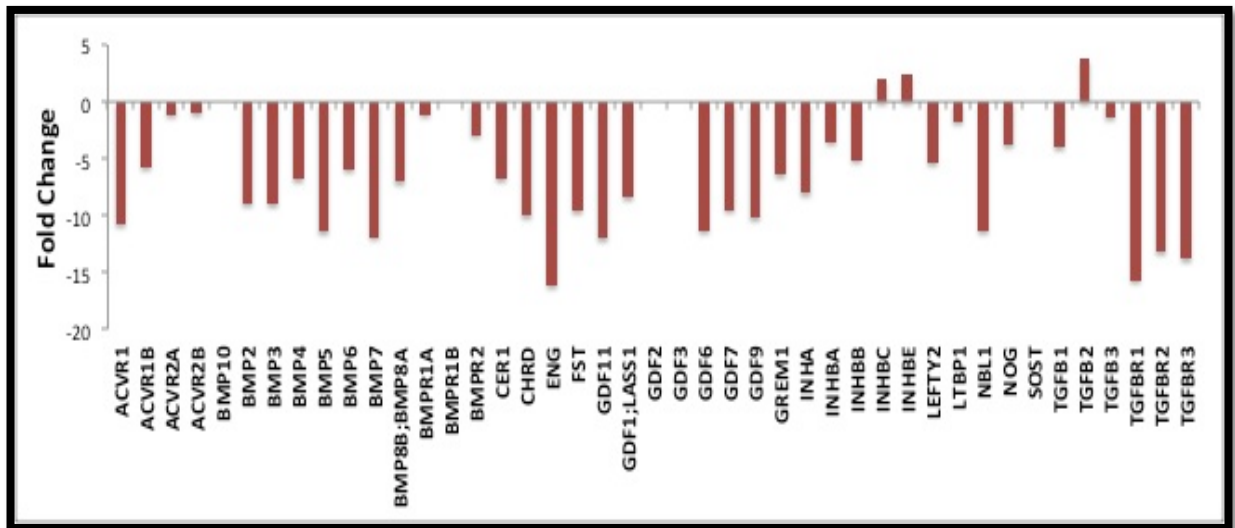


Figure 4.22 Array plate analysis of TGF- β superfamily genes in Confluent MG63 compared to Mg63 treated with PC3RFP-CM.

This Figure shows the differences between confluent MG63 and MG63 treated with PC3RFP-CM in terms of fold change after being adjusted to housekeeping gene (GAPDH). The Fold Change was calculated by using the equation $\frac{\Delta_{dct}}{3.3} \times -10$. Data expressed as mean of 3 independent experiments.

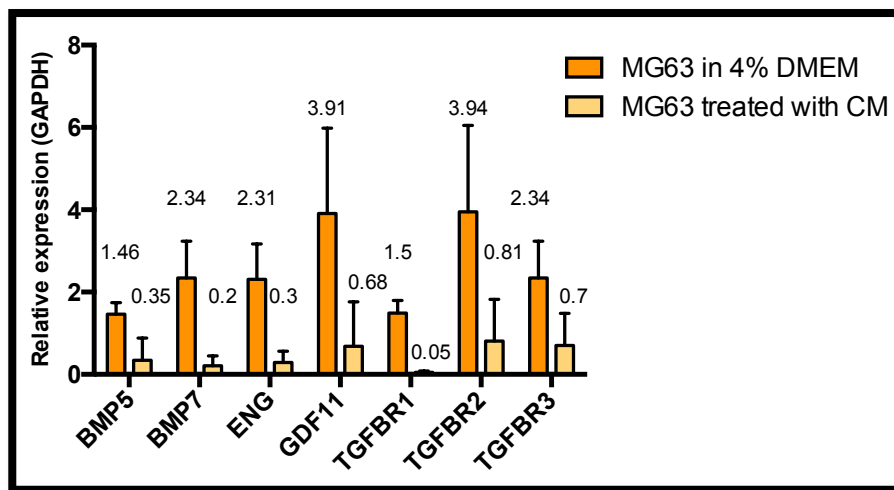


Figure 4.23 Array plate analysis of the major differences between confluent MG63 and MG63 treated with PC3RFP-CM in TGF- β superfamily genes.

This Figure shows the differences between confluent MG63 and MG63 treated with PC3RFP-CM in terms of relative expression after being adjusted to housekeeping gene (GAPDH). The following genes were expressed more in confluent MG63 that MG63 treated with PC3RFP-CM: BMP5, BMP7, ENG, GDF11, TGFB1, TGFB2 and TGFB3. Relative expression was calculated after calculating dct and Δ_{dc} then Δ_{dc} was raised to the square root. Data expressed as mean of 3 independent experiments.

4.3.2 Detection of Noggin protein in PC3RFP Condition media by ELISA

Condition media collected over PC3RFP was tested for the presence of Noggin protein by ELISA. Noggin protein was detected in Condition media collected from different flasks. The concentration of Noggin was measured from three independent batches of CM and was calculated using standard curve Figure 4.24. The concentration of Noggin present in PC3RFP conditioned media was found to be 0.293 ± 0.0046 ng/mL.

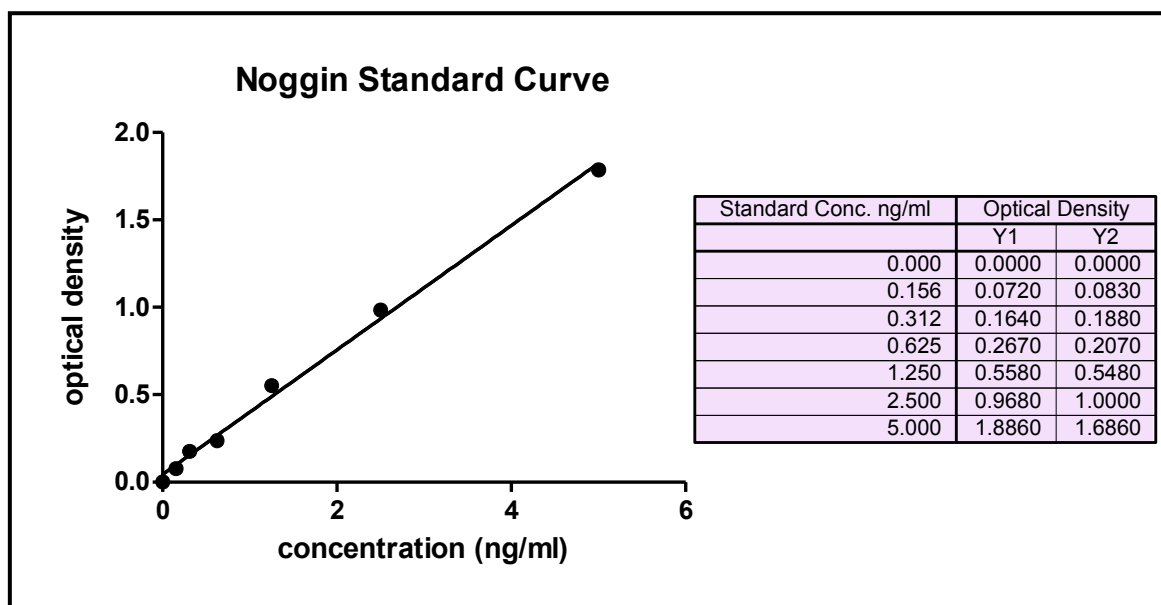


Figure 4.24 Noggin Standard curve.

This Figure represent Noggin standard curve with standard value of (0.156, 0.312, 0.625, 1.250, 2.5 and 5) ng/ml. Samples of conditioned media from 3 different flasks and standards were measured in duplicate. This curve was used to calculate the concentration of Noggin present in PC3RFP conditioned media. All data expressed as mean \pm SEM of 3 independent experiments.

4.3.3 Effect of PC3RFP-CM and co-culture on Noggin expression in osteosarcoma cells using QRT-PCR

The result obtained from the express plate was tested by measuring mRNA Noggin expression as a single gene assay, using QRT-PCR. Treating SaOS2 cells with PC3RFP-CM or growing them in direct contact with PC3RFP cells in co-culture both increased the mRNA Noggin expression significantly ($p=0.0002$) by using (1 way ANOVA, Bonferroni) Figure (4.25). On the other hand, treating MG63 cells with PC3RFP-CM or growing the cells together with PC3RFP both increased Noggin mRNA expression but this did not reach significance. These results confirmed the expressed plate data presented previously in this chapter.

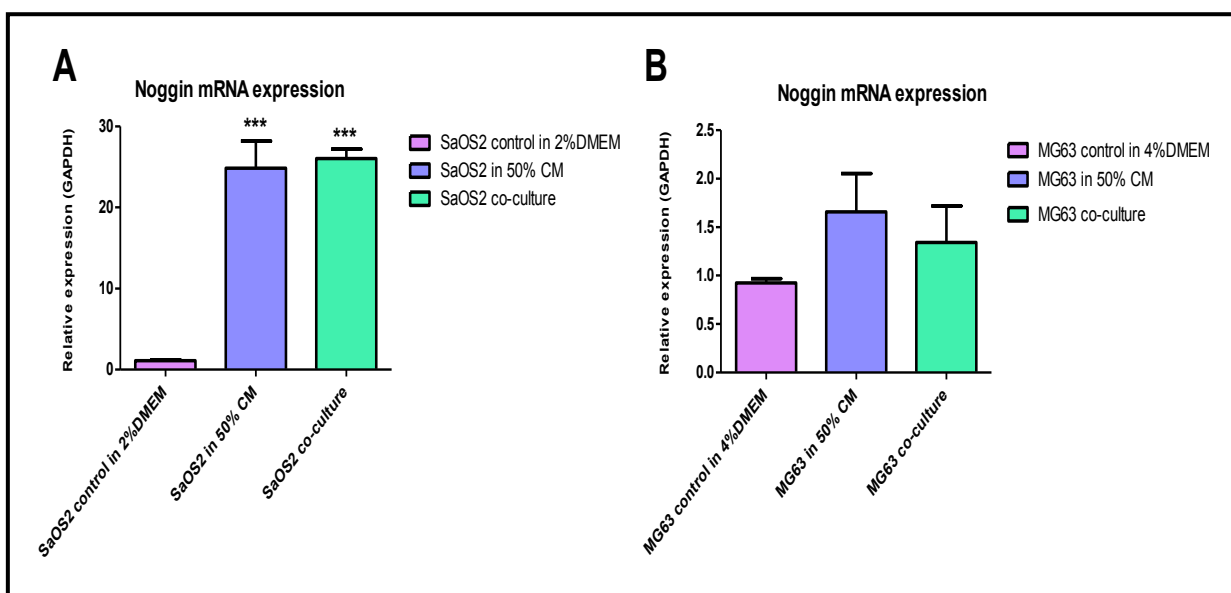


Figure 4.25 Noggin mRNA expression was increased in osteoblast cells.

(A) illustrates mRNA Noggin expression in SaOS2 cells in standard DMEM 2% media compared to treated SaOS2 cell with PC3RFP-CM and co-cultured SaOS2. Both PC3RFP-CM treated cells and co-cultured cells showed significant increase in the expression of Noggin mRNA with $p=0.0002$ (1 way ANOVA, Banferroni). (B) illustrate mRNA Noggin expression in MG63 cells in standard DMEM 4% media compared to treated MG63 cell with PC3RFP-CM and co-cultured MG63. There were no significant change in the expression of Noggin mRNA in either co-culture or CM treated compared to controls although there was an increase in Noggin expression in both groups. Relative expression was calculated after calculating dct and Δdc then Δdc was raised to the square root. All data expressed as mean \pm SEM of 3 independent experiments.

4.3.4 Immunofluorescence detection of Noggin in co-culture and in osteoblast grown in 50%PC3RFP-CM

SaOS2 cells were seeded in 8 well chamber slides either treated with PC3RFP-CM or were grown in direct contact with PC3RFP in co-culture. These cells were then labeled with Rabbit polyclonal anti-Noggin antibody (abcam, UK) and donkey anti-rabbit IgG H&L (Alexa Fluor 488) antibodies (abcam, UK) as primary and secondary antibodies. Images were acquired using a Leica fluorescent microscope. The level of Noggin protein, detected as green stain was increased in SaOS2 cells treated with PC3RFP-CM and in co-culture group compared to control SaOS2 in standard media as seen in Figure (4.26).

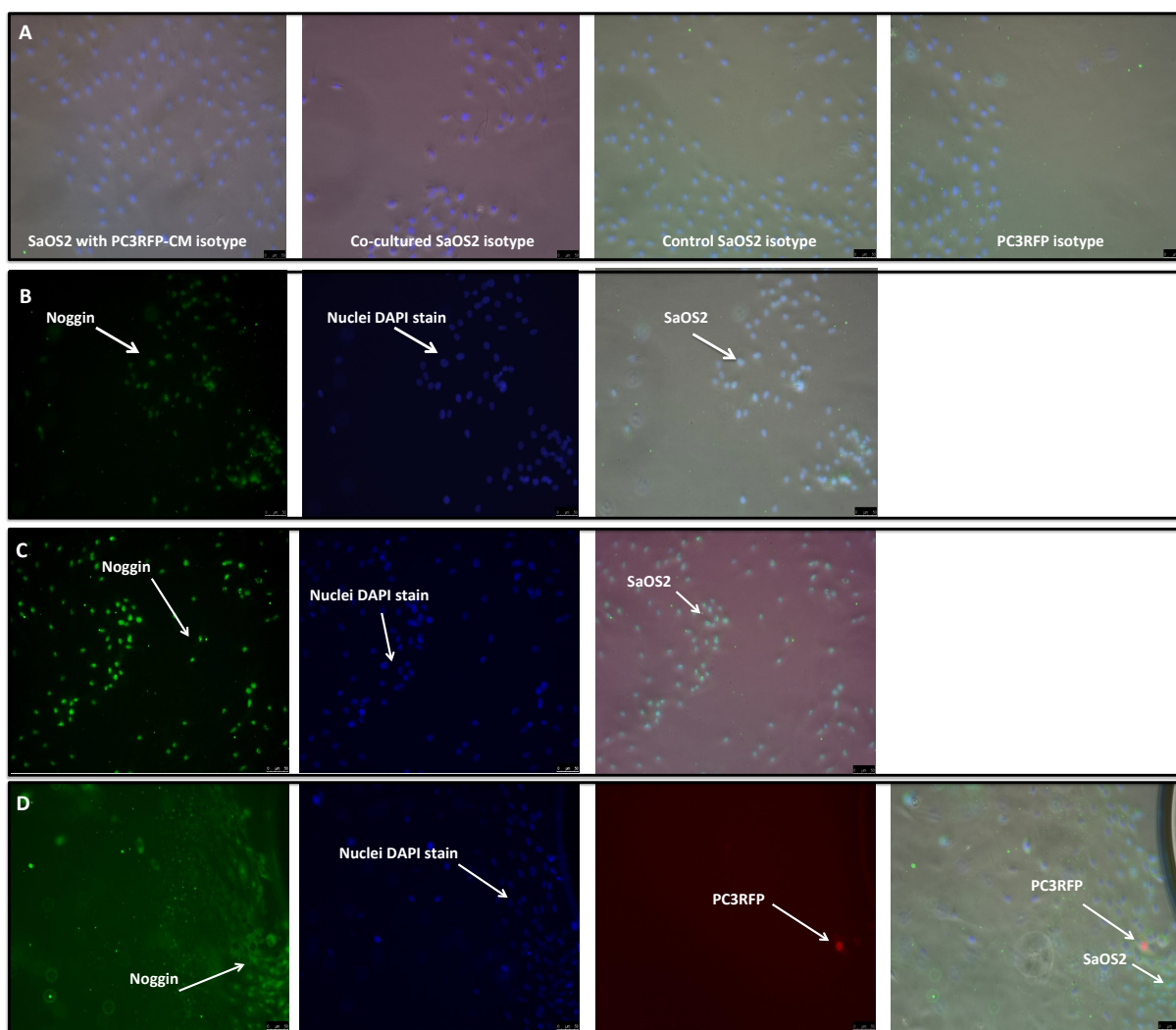


Figure 4.26 The level of Noggin protein fluorescent was increased in co-culture and PC3RFP-CM groups.

Fixed and permeabilised cells were stained with rabbit polyclonal primary anti-Noggin antibody or isotype control normal rabbit IgG antibody. Nuclei were stained with DAPI (blue fluorescence). Images were obtained by Leica fluorescent microscope with 20X objective. **(A)** Shows Isotype 1/100 with no staining in SaOS2 treated with CM, co-cultured SaOS2, SaOS2 control in standard media and PC3RFP control in standard media. **(B)** Shows SaOS2 grown alone labelled with Noggin (green fluorescent) Antibody 1/100 dilution. **(C)** Illustrates SaOS2 cells treated with PC3RFP-CM labelled with Noggin (green fluorescent) Antibody 1/100 dilution. **(D)** Illustrate co-cultured SaOS2 cells labelled with Noggin (green fluorescent) Antibody 1/100 dilution.

4.3.5 Detection of Noggin protein in co-cultured SaOS2 and in SaOS2 treated with PC3RFP-CM by using flow cytometry

Flow cytometry was used to detect the presence of Noggin protein in SaOS2 osteoblast cells and to compare the amount of Noggin protein present in control SaOS2 in standard media with both co-cultured SaOS2 and SaOS2 treated with PC3RFP-CM. Rabbit polyclonal anti-Noggin antibody 1/200 dilution (abcam, UK) and donkey anti-rabbit IgG H&L (Alexa Fluor 488) antibody 1/2000 (abcam, UK) were used as primary and secondary antibodies respectively. Normal rabbit IgG antibody was used as Isotype control. Cells were analysed using BD FACS Aria as seen in Figure

4.28 A and B. Noggin protein expression increased significantly $p=0.0001$ (1 way ANOVA, Banferroni) in the SaOS2 treated with PC3RFP-CM group but not in the co-cultured group. While, the expression of Noggin protein was found to be decreased significantly in the PC3RFP co-culture group $p=0.0001$ (1 way ANOVA, Banferroni) compared to PC3RFP as control as seen in Figure (4.27).

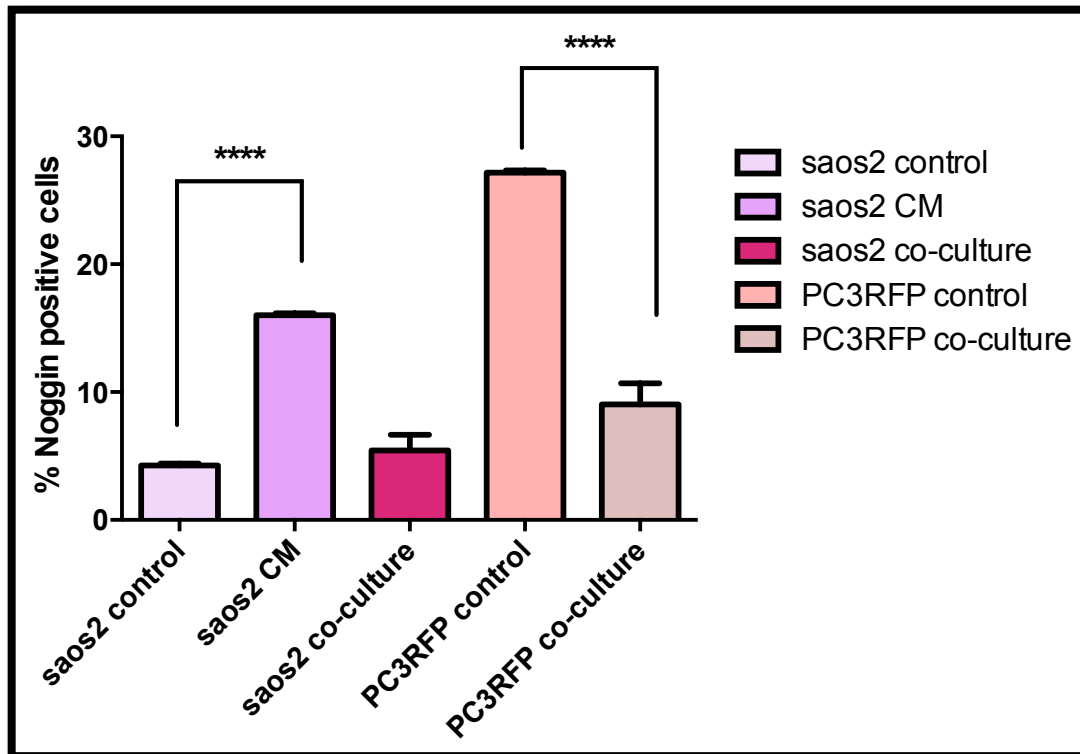


Figure 4.27 Noggin protein expression was significantly increased in SaOS2 cells treated with PC3RFP-CM and significantly decreased in co-cultured PC3RFP compared to control cells.

Fixed and permeabilized cells were stained with rabbit polyclonal primary anti-Noggin primary antibody 1/200 dilution or isotype control normal rabbit IgG antibody. Donkey anti-rabbit IgG H&L (Alexa Fluor 488) was used as secondary antibody 1/2000 dilution. Cells were analyzed using BD FACS Aria. This Figure illustrates significantly increased Noggin protein expression in SaOS2 cells treated with CM ($p=0.0001$) (1 way ANOVA, Bonferroni) but not in the co-cultured group. Noggin expression was significantly decreased in the co-cultured PC3RFP with ($p=0.0001$). The % of Noggin positive cells from each group of cells was subtracted from its isotype to give the real % value. All data expressed as mean \pm SEM of 3 independent experiments.

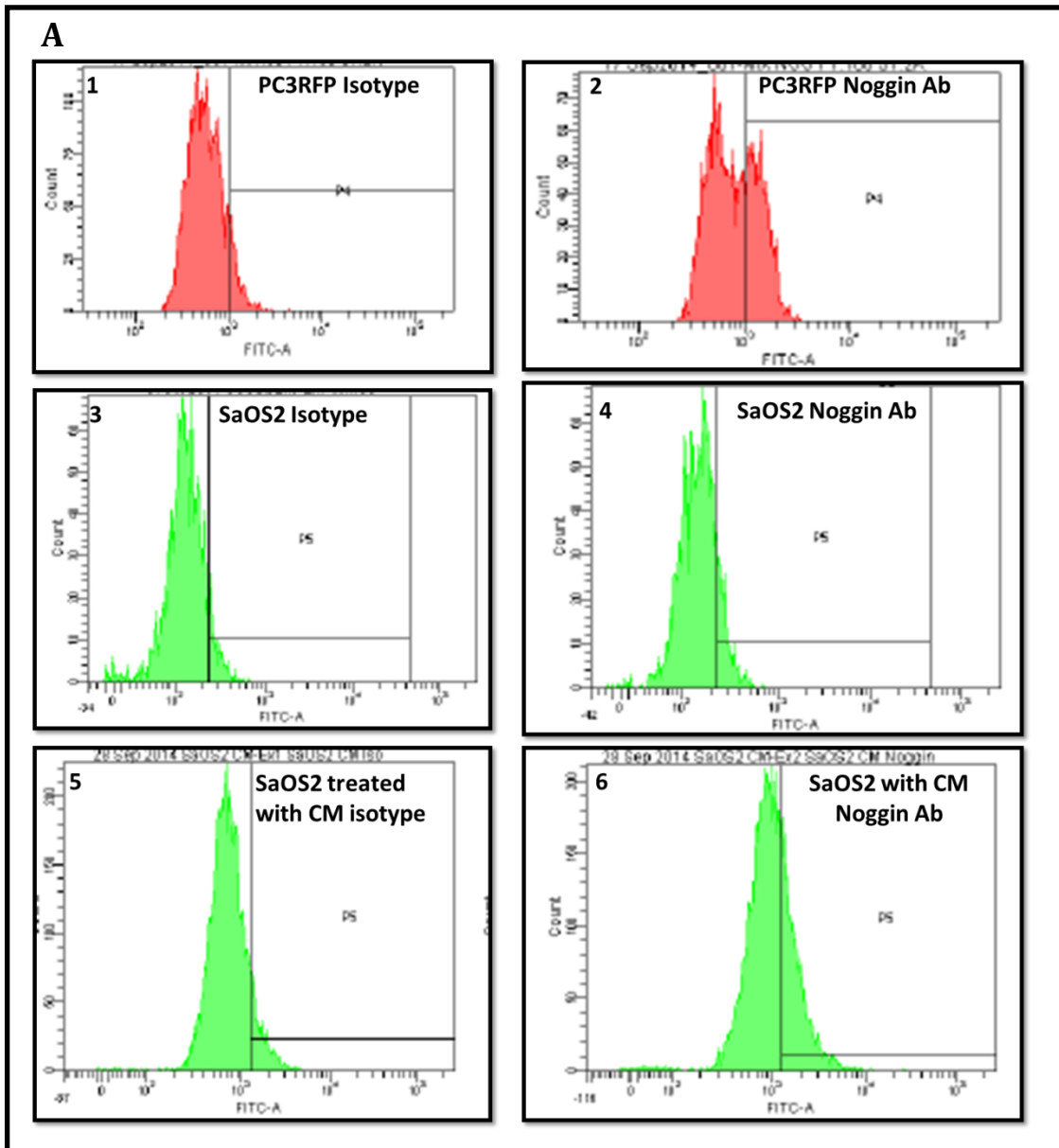


Figure 4.28 A: Analysis of Noggin protein expression in SaOS2 treated with PC3RFP-CM compared to control cells using BD FACS Aria.

Fixed and permeabilized cells were stained with rabbit polyclonal primary anti-Noggin primary antibody 1/200 dilution or isotype control normal rabbit IgG antibody. Donkey anti-rabbit IgG H&L (Alexa Fluor 488) was used as secondary antibody 1/2000 dilution. Cells were analyzed using BD FACS Aria. Panels (1, 3 and 5) show control normal rabbit IgG antibody Isotype 1/200 dilution in control PC3RFP, control SaOS2 and control SaOS2 treated with PC3RFP-CM. Panels (2, 4 and 6) shows Noggin protein expression in control PC3RFP, control SaOS2 and control SaOS2 treated with PC3RFP-CM. All data expressed as mean \pm SEM of 3 independent experiments.

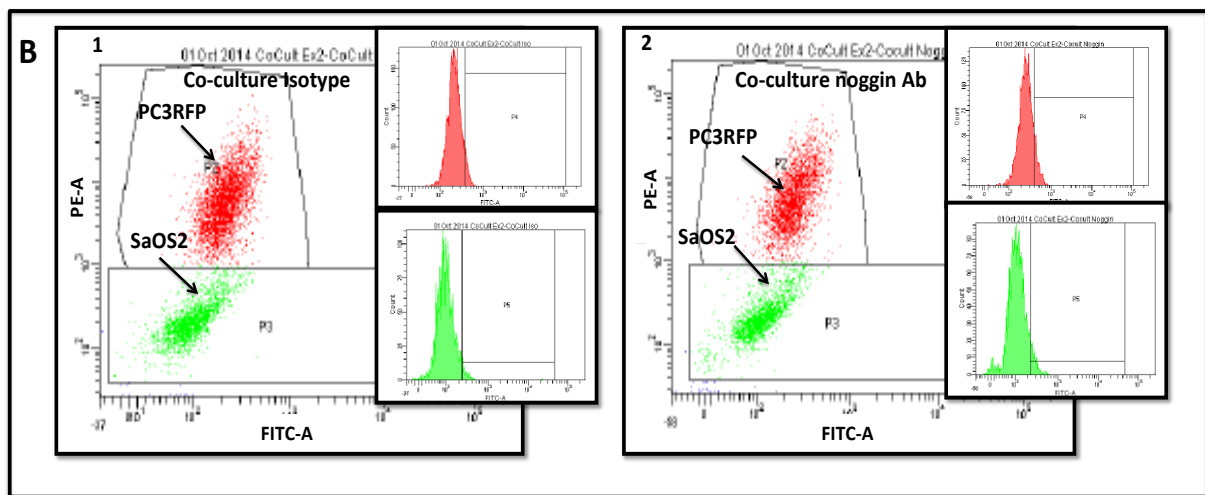


Figure 4.28 B: Analysis of Noggin protein expression in co-culture SaOS2 cells using FACS Aria.

Fixed and permeabilized cells were stained with rabbit polyclonal primary anti-Noggin primary antibody 1/200 dilution or isotype control normal rabbit IgG antibody. Donkey anti-rabbit IgG H&L (Alexa Fluor 488) was used as secondary antibody 1/2000 dilution. Cells were analyzed using BD FACS Aria. Panel (1) represents control normal rabbit IgG antibody Isotype 1/200 dilution in co-cultured cells (SaOS2 and PC3RFP). Panel (2) represents Noggin protein expression in in co-cultured cells (SaOS2 and PC3RFP). All data expressed as mean \pm SEM of 3 independent experiments.

4.3.6 Detection of Noggin protein in osteoblasts in co-culture and in osteoblasts treated with PC3RFP-CM by using western blot

Polyclonal rabbit anti-Noggin was used as primary antibody and donkey anti-rabbit IgG as secondary antibody to detect Noggin in co-cultured SaOS2, SaOS2 treated with PC3RFP-CM, in SaOS2 cells as control in standard media, co-cultured PC3RFP and in control PC3RFP by using western blot. Protein was collected from cells grown individually and from co-cultured cells after sorting the cells with BD FACS Aria. Recombinant Noggin was used as positive control. SaOS2 cells treated with PC3RFP-CM were found to produce more Noggin protein than control cells or cells in co-culture. On the other hand, PC3RFP cells produced less Noggin protein after being co-cultured with SaOS2 cells as seen in Figure (4.29), which shows Noggin expression in SaOS2 control, SaOS2 treated with PC3RFP-CM, co-cultured SaOS2, co-cultured PC3RFP, and control PC3RFP as indicated. The second line shows the expression of β -actin house keeping protein production in all of these cells is also shown as a loading control.

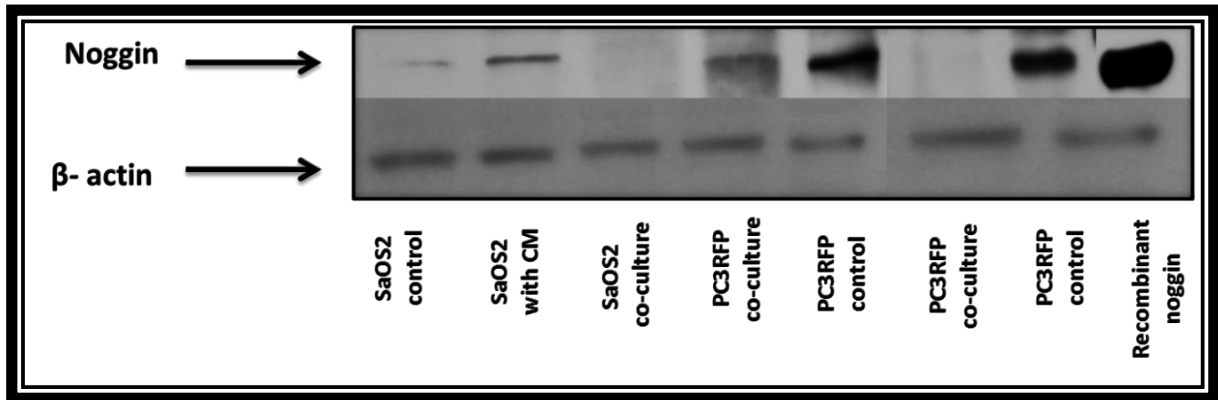


Figure 4.29 Protein Noggin expression in PC3RFP, co-cultured PC3RFP, SaOS2 treated with PC3RFP-CM and co-cultured by western blot.

This Figure illustrates the differences in Noggin protein levels in SaOS2 and PC3RFP cells seeded in standard media as control compared to levels after being in co-culture and in SaOS2 cells treated with PC3RFP-CM. These were compared to recombinant Noggin as positive control. Loading of protein was confirmed by using β -actin expression. Mwt of Noggin is 26KD and Mwt of β -actin is 42KD.

4.4 Discussion

4.4.1 The expression of the TGF- β superfamily in individual prostate cancer and osteoblastic cell populations and in cultures where these cells are in indirect (i.e. via CM) or in direct contact in a co-culture model

The communication between prostate cancer cells and cells within the bone microenvironment is thought to play an important role in secondary tumour formation and progression as tumour cells need to communicate with local microenvironment physically in order to adhere, invade, survive and proliferate in the metastatic site (Bhattacharyya and Stern 2003).

Co-culturing prostate cancer cells and bone cells is one method for studying the interaction between these cells. In order to investigate the ability of PC3RFP to attach to/grow with bone cells, images were taken after seeding PC3RFP on confluent osteoblast cells (SaOS2/or MG63). PC3RFP was found to form colonies on or with both osteoblast cell types. In this chapter the expression of 43 members of the TGF- β superfamily genes were studied in both prostate cancer (PC3RFP) cells and osteosarcoma (SaOS2, MG63) cells. When grown separately, most of these genes were expressed at the same level in both prostate cancer and osteoblast cells with the following exceptions: BMPs 3, 4 and 6, Noggin, endoglin (ENG), Growth differentiation Factor 1 (GDF1;LASS1), inhibin beta A (INHBA), inhibin beta B (INHBB), TGF- β 1 and TGF- β 2. PC3-RFP was found to express BMP3, BMP6 and the BMP antagonist Noggin at higher levels than osteoblast cells. Similar findings were reported by Masuda and Hamdy, who showed the presence of BMPs in prostate cancer, predominately BMP6 (Hamdy *et al.* 1997; Masuda *et al.* 2003). A model was developed in this study where prostate cancer cell (PC3RFP) were co-cultured with either SaOS2 a mature osteoblast like sarcoma cell line or with MG63 an immature osteoblastic cell type able to differentiate in culture. Once more, the expression of 43 members of the TGF- β superfamily genes were analysed and expression compared between these cells grown alone and when cell were grown together. The levels of expression of these genes were changed when cells become in direct contact with each other in the co-culture model. As mentioned previously, the purity of the cells used after sorting was around 95%. There was a possibility that contaminating SaOS2 cells could 'piggy-back' on top of PC3RFP and visa versa accounting for this 5% contamination. However, the relative expression of Noggin in co-cultured cells was 88.3 times higher than that measured in control SaOS2 cells.

This is a substantial increase and would have required much higher levels of contamination with PC3RFP cells than 5%. In absolute terms, the levels of Noggin expression were higher in the co-cultured SaOS2 cells than in control PC3RFP or co-cultured PC3RFP making it extremely unlikely that the observed increase in Noggin expression in co-cultured SaOS2 cells was a result of contaminating PC3RFP cells. Our results were similar to a study done by Wang et al investigated the molecular mechanisms of prostate cancer bone metastases by creating two models bi-compartmental system where prostate cancer cell (PC3) and bone marrow stromal cells (BMSC) isolated from the calvaria of neonatal mice share the same culturing media but without direct contact and heterotypic contact system gene expression profiles were then analysed and compared between these groups. His results revealed that certain genes were modified only by direct cells contact including collagen III, IV,X,XII, integrin α 1, α 2, MMP-2, MMP-9, uPA, biglycan, osteopontin and raf-1 in PC3, and collagen VIII, IX, BMP6, TGF β 1, Smad6 and Twist in BMSC cells. Other genes were modified only by soluble factors (Wang *et al.* 2006). This was also suggested by another study investigating the effect of PC3 on the bone marrow hMSCs, which indicated that bone metastatic PC3 cells could regulate bone remodelling by altering the expression profile and differentiation ability of hMSCs (Fritz *et al.* 2011). In this study, the expression of Noggin, BMP6 and BMP3 were all changed to be expressed at higher levels in osteoblast (SaOS2 and MG63) when they were co-cultured with PC3RFP cells. This study focused on Noggin expression since Noggin was expressed at moderate levels by prostate cancer cells compared to low levels in osteoblasts grown alone but expression was dramatically induced in the latter when co-cultured with PC3-RFP cells. This finding was confirmed by single assay gene analysis investigating expression of Noggin in osteoblast cells in both mRNA and reflected in Noggin protein level present in cells.

4.4.2 Effect of prostate cancer cells on Noggin expression by osteoblasts

Recently high level of interest has focused on Noggin as bone metastasis promoter (Virk *et al.* 2011). It is well known from previous studies that bone metastasis associated with prostate cancer was characterized by osteoblastic lesions (Keller and Brown 2004). However, many studies showed that prostate cancer related bone metastasis could be a mixture of both osteoblastic and osteolytic lesions with unknown mechanisms or impact on tumour growth/survival (Logothetis and Lin 2005; Secondini *et al.* 2011). To date, studies of how Noggin stimulates such phenotype have commonly focussed on osteolytic lesions in prostate cancer (Secondini *et al.*

2011). A study done by Haudenschild reported that prostate cancer cell LNCaP express both Noggin and BMP6 (Haudenschild *et al.* 2004). The same finding was reported by Laurila, who studied the expression of Noggin in normal prostate tissue biopsies and in prostate cancer tissue samples confirming the expression of Noggin in prostate cancer cells grown alone (Laurila *et al.* 2013). In this study, we aimed to investigate the effect of prostate cancer cells on osteoblast cells either by direct contact or by treating the cells with conditioned media collected over PC3RFP. The use of conditioned media in this study tested the hypothesis that inductive signals regulating Noggin in osteoblasts were soluble. Many studies have assessed the composition of conditioned media and found it to be a rich source of potential signalling molecules, protein and biomarkers (Xue *et al.* 2008; Dowling and Clynes 2011). The ability of prostate cancer cells (PC3RFP) to produce Noggin and secrete it into the media, was tested by measuring Noggin concentration in PC3RFP-CM by ELISA. A detectable and potentially biologically active concentration of Noggin protein was found in the PC3-RFP conditioned media. The expression of mRNA Noggin was significantly increased in co-cultured osteoblasts (SaOS2) and in SaOS2 cells treated with PC3RFP-CM compared to control SaOS2 cells, while the increase in Noggin expression in MG63 cells were less and not significant. These results, obtained from qPCR, were reflected by flow cytometry and immunofluorescence, which detect increased production of Noggin protein in SaOS2 cells associated with PC3-RFP cells and more prominently in SaOS2 treated with PC3RFP-CM. The clear effect of CM may be due to the large number of cells that were used in generating 10 ml of conditioned media, around 100,000cells/cm² in T75 flask. This large number of cells would contribute higher levels of potential mediators regulating cellular behaviour and the expression of Noggin in SaOS2 cells than would be available in the co-culture model, where PC3RFP were seeded in lower numbers: 5000cell/cm² in the T75 flask with SaOS2 cells. These findings do suggest that at least some of the induction of Noggin in SaOS2 cells was mediated by soluble factors derived from PC3-RFP cultures. Although, western blot was conducted several times on co-cultured and conditioned media treated samples we were able to detect increased production of Noggin protein in SaOS2 treated with PC3RFP-CM group only once. This was probably due to inadequate protein concentration in the remaining samples where Noggin levels were below or at the limit of detection of the Western blot analyses.

There were no significant differences in the expression of Noggin at the mRNA level between control PC3RFP grown alone and those co-cultured with SaOS2 cells. However, there were significant decreases in Noggin protein present when the cells came into direct contact with SaOS2, seen by flow cytometry and western blot. As the regulation of protein production can occur at many different levels, there can be a weak or no correlation between mRNA and protein levels (Tian *et al.* 2004). The changes in protein expression in PC3RFP after co-culture may be linked to the proposal that prostate cancer cells have osteomimetic properties making them more osteoblast-like cells and allowing them to metastasis, adhere, survive and grow in bone (Koeneman *et al.* 1999). From our results and other studies BMP6 and Noggin were over expressed in prostate cancer cells (Haudenschild, Palmer *et al.* 2004). BMP6 is associated with the progression of prostate cancer (Dai *et al.* 2005; Darby *et al.* 2008; Yuen *et al.* 2008). Many studies have found that BMP6 is upregulated in prostate cancer compared to nodular hyperplasia and with low-grade prostate cancer (Barnes *et al.* 1995; Hamdy *et al.* 1997). Noggin has been shown to modify BMP signalling in prostate cancer and is upregulated by increased BMP signalling (Sutherland *et al.* 2004). These findings suggest that the activities of BMP6 and Noggin are inter-regulated by this negative feed back loop (Haudenschild *et al.* 2004; Feeley *et al.* 2006) where BMP induces Noggin gene expression by activating signalling cascades involving Smad-1, Smad-5 and Smad-8 as well as the transcription factor Osterix (Ishida *et al.* 2000; Nakashima *et al.* 2002) and secreted Noggin causes an inhibition of BMP action (Wu *et al.* 2003). It may be that the balance between BMP and Noggin is critical in controlling the balance between bone formation/lysis in tumour induced bone disease (Simonet *et al.* 1997).

The Wnt and BMP pathways were also shown to interact in prostate cancer bone metastasis (Schwaninger *et al.* 2007). A study done by Dai showed that treating MC3T3 cells with CM collected from DKK1 pre-treated prostate cancer cell line results in blocking osteoblast differentiation. This was a result of inhibiting both Wnt and BMP activity indicating that BMP activity depends on Wnt. Whereas, treating MC3T3 cells with CM collected from Noggin pre-treated prostate cancer cell line results in loss of BMP activity only. There was no effect on Wnt indicating that Wnt activity does not depend on BMP activity. (Dai *et al.* 2008).

There are other factors that may affect Noggin expression either by enhancing or repressing its expression. For example, both Wnt and Sonic Hedgehog (SHH)

stimulate Noggin expression (Hirsinger *et al.* 1997). FGF18 was found to repress Noggin gene expression and consequently facilitate BMP signalling, which in turn stimulated osteoblast differentiation (Reinhold *et al.* 2004). Moreover, another study done by Fakhry *et al* revealed that FGF2 and FGF9 induce the expression of BMP2 and TGF- β 1 genes in osteoblast while they inhibited Noggin expression thus amplifying BMP effect on osteoblast activity (Fakhry *et al.* 2005).

The presence of Noggin either induced in osteoblasts by interactions with prostate cancer cells or produced directly by the latter would tend to suppress osteoblast differentiation in osteoblastic cell lines. Reduced differentiation would be likely to produce conditions that would favour proliferation. This may account for the effects of PC3-RFP CM on proliferation of SaOS2 cells presented in Chapter 3, where differentiation was suppressed and proliferation increased.

In conclusion the data tends to support the hypothesis posed in the aims section that prostate cancer cells alter the expression of TGF- β family genes in osteoblast cells thus affecting their proliferation and differentiation.

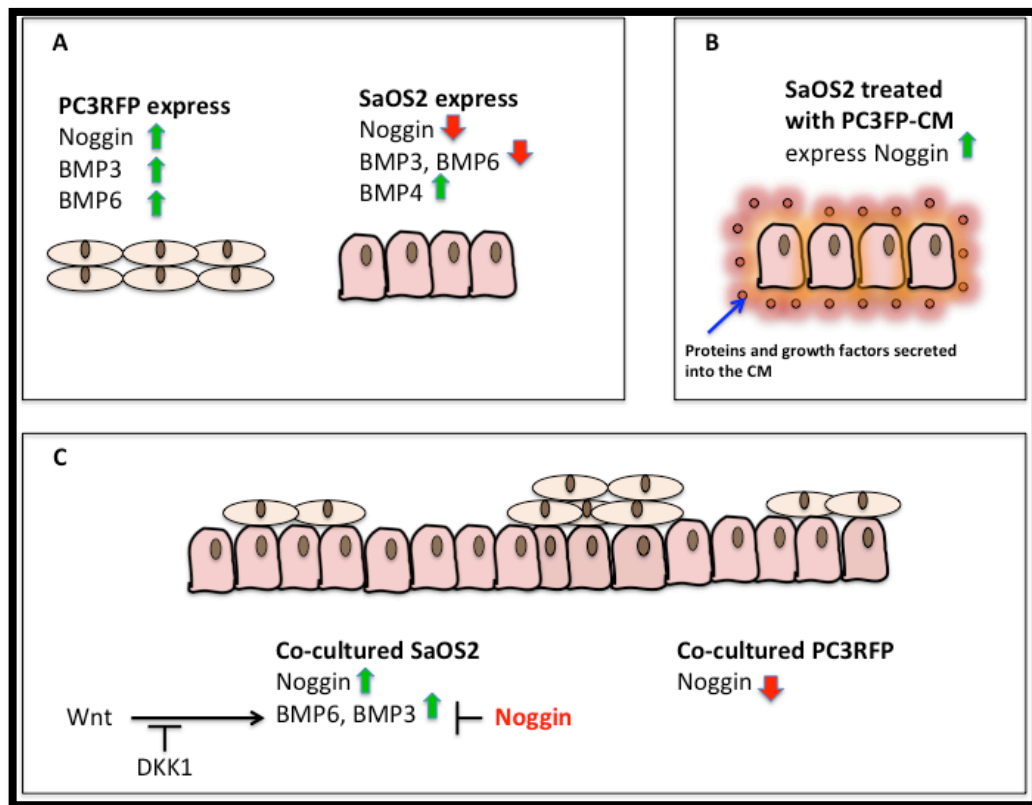


Figure 4.30 diagram summarizing gene expression pattern in prostate cancer cells and osteoblast cells during different experimental condition compared to control cells.

(A) PC3RFP and SaOS2 cells seeded individually in standard DMEM 2% media (Control) (B) Noggin expression was increased in SaOS2 treated with PC3RFP-CM (C) Noggin, BMP3 and BMP6 expressions were increased in co-cultured SaOS2 cells while Noggin expression was decreased in co-cultured PC3RFP cells. This Figure shows that BMP secreted by tumour cells promote organ-specific metastasis to bone stimulus the bone microenvironment through paracrine signalling.

Chapter 5 Noggin knockdown in PC3RFP and the effect of recombinant Noggin on osteoblast proliferation

5 Chapter 5 Noggin knockdown in PC3RFP and the effect of recombinant Noggin on osteoblast proliferation

5.1 Introduction

Metastasis requires the concerted effects of several biological processes in order to enable tumour cells to leave from primary site survive in the circulation and seed and colonize a specific organ. Some of these processes depend upon the tumour characteristics and primary site, while others are supplied by the metastatic niche (Tarragona *et al.* 2012). This phenomenon has highlighted the importance of communication signals that occur between tumour cells and site of metastasis (Morales *et al.* 2011). The interactions between TGF- β and BMP signalling pathways in tumour and non-tumour populations are potentially part of these interactions of biological significance. It has been suggested that disturbances in these signalling pathways are vital to tumourigenesis and tumour progression in cancer cell-dependent and independent manner (Massagué and Gomis 2006). Among the different factors that could control the TGF- β /BMP signalling pathway and its contribution, we focused on Noggin, since, it has been identified as an important player in bone metastasis given its action on bone remodelling processes, as well as in defining the stroma capacity to maintain cancer stem cells and their niche (Tang *et al.* 2007; Mani *et al.* 2008). The Noggin gene resides within a single exon and encodes a polypeptide with a expected molecular weight of 22KDa, however it is secreted as homodimeric glycoprotein with molecular weight of 64KDa (Kavsak *et al.* 2000). Noggin is one of the mediators involved in Spemann organizer activity during embryo development during dorsalization and the formation of neural tissue from ectoderm. However, the expression and function of Noggin is well known and not limited to the brain and Spemann organizer (Valenzuela *et al.* 1995). Although, Noggin expression in osteoblasts is limited, exposing the cells to exogenous BMP2, 4 or 6, can induce its production suggesting that this may be a protective mechanism to prevent excessive exposure of skeletal cells to BMPs (Gazzerro *et al.* 1998). In general, Noggin inhibits the effect of BMPs in both differentiated and undifferentiated cells of osteoblastic lineage. Thus addition of Noggin to osteoblasts in culture, blocks the stimulatory effect of BMPs on collagen, non collagen protein synthesis and alkaline phosphatase activity (Gazzerro *et al.* 1998). Osteoblasts produce and release the receptor activator of nuclear factor- κ B (NF κ B) ligand (RANKL), which binds to its receptor on osteoclast precursors causing them to become mature osteoclast cells. Osteoprotegerin (OPG) is also secreted by osteoblasts and modulates RANKL activity as a decoy receptor. It is clear that the net rate of bone growth/loss is a product of the activities of signalling molecules, their antagonists,

receptors and decoy receptors. BMPs stimulate bone formation by shifting the equilibrium between OPG and RANKL toward the accumulation of OPG. However, Noggin might shift this equilibrium to the opposite direction favouring the accumulation of mature Osteoclast cells (Logothetis and Lin 2005). Noggin over expression in osteoblastic lineage cells reduces their differentiation; while Noggin down regulation in these cells increases the expression of osteogenic differentiation markers (Gazzerro *et al.* 2003; Wan *et al.* 2007). In addition, Noggin down regulation *in vivo* was found to enhance the regeneration of bone defects (Wan *et al.* 2007).

In this Chapter, several trials were done to establish PC3RFP knockdown Noggin (PC3RFP-KD) cells in order to determine the effect of tumour derived Noggin on osteoblast (SaOS2) proliferation. Growth curves were done using conditioned media collected from PC3-KD and from cells transduced to express a non-Noggin targeting shRNA (PC3-mock cells). These growth curves were compared with control medium and with cultures challenged with recombinant Noggin.

Aim

The aim of this study was to evaluate the effect of conditioned media collected from PC3-KD cells on the proliferation of osteoblast (SaOS2) cells compared to conditioned media collected from PC3-mock cells and to determine the effect of exogenous recombinant Noggin on the growth rate of osteoblast cells.

Hypothesis

Noggin a BMP antagonist made by prostate cancer cells that plays an important role in osteoblast proliferation.

Objective

- 1- Establishment of Noggin knockdown and sham/mock knock down PC3RFP cells using shRNA lentivirus.
- 2- Generate SaOS2 growth curves using conditioned media collected over PC3-KD cells and compare these to SaOS2 growth curve using condition media collected over Mock cells.
- 3- Generate SaOS2 growth curves using exogenous recombinant Noggin and compare these to the growth of SaOS2 cells grown in regular DMEM 2% FBS media.

5.2 Material and method

5.2.1 Materials and Disposable Equipment

Item	Supplier
Noggin shRNA (h) Lentiviral	Santa-Cruz SC-42138-V
Polybrene	Santa-Cruz SC-134220
Puromycin	Santa-Cruz SC-108071-A
Recombinant human Noggin	R&D systems

5.2.2 Knockdown Noggin in PC3RFP using Noggin short hairpin RNA (shRNA) Lentiviral

The expression of the Noggin gene was partially blocked in PC3RFP cells using short hairpin RNA (shRNA). Lentiviral vectors were used to infect cells. Vectors contained shRNA targeting sequences for the Noggin transcript or a non-targeting sequence to create both Noggin knockdown (PC3RFP-KD) and a negative control (PC3RFP-Mock) respectively. The stability of the transfected PC3RFP produced was derived by selection with Puromycin. Polybrene was used to increase the cell sensitivity to the virus. Polybrene and Puromycin killing curve were conducted before PC3RFP was transfected with shRNA virus.

5.2.2.1 Polybrene killing curve

Polybrene (Santa-Cruz SC-134220) was used to increase the efficiency of infection of cells with retrovirus in cell culture. The lyophilised powder was re-suspended in 1ml PBS making a stock concentration of 25mg/ml.

Cells were harvested from T75 flask and counted. The same cell density that was used in normal growth curve was used. Cells were seeded in 3x24 well plates and were fed normally with DMEM 10% FBS. After cultures reached 70% confluence, around day6, cells were washed with PBS and the media were changed with DMEM 10% FBS containing different Polybrene concentrations (1µg/ml, 2.5µg/ml, 5µg/ml, 7µg/ml and 10µg/ml). Cells viability was assessed by counting the cells using a Coulter counter and visually by phase contrast microscopy on day 2, day4 and day6. Cells in the first plate were counted after 48h for monitoring the growth. While, the media on the remaining 2 plates were removed and replaced with freshly made Polybrene media.

5.2.2.2 Puromycin killing curve

Puromycin (Santa-Cruz SC-108071A) is used in cell biology as selective agent in cell culture systems. It is toxic but cells infected with either lentiviral vector used would become resistance to puromycin. The recommended dose as a selection agent in cell cultures is within a range of 1-10 µg/ml, although it can be toxic to some cells at concentrations as low as 1 µg/ml. It acts quickly and can kill up to 99% of nonresistant cells within 2 days. The purpose of the experiment was to test different puromycin concentrations on PC3-RFP to select the best concentration to use in the knockdown experiment. The lyophilised powder was re-suspended in 1ml PBS making a stock concentration of 10mg/ml. Cells were harvested from T75 flasks and counted. The same cell density that was used in the normal growth curves was used. Cells were seeded in 3x24 well plates and were fed normally with DMEM 10% FBS. After cultures reached 70% confluence, around day6, the cells were washed with PBS and the media were changed with DMEM 10% FBS containing different Puromycin concentrations (1µg/ml, 2.5µg/ml, 5µg/ml, 7µg/ml and 10µg/ml). The cells viability was assessed by counting the cells using Coulter counter and visually using phase contrast microscopy on day 2, day 4 and day 6. Cells in the first plate were counted after 48h for monitoring the growth. While, the media on the remaining 2 plates were removed and replaced with freshly made Puromycin media.

5.2.2.3 Lentiviral infection/transduction of PC3RFP

PC3RFP were seeded in 48 well plate in a density of around 2500cell/well. After 72h, cells were exposed to the virus supernatant, at multiplicity of infection (MOI) of 20 in the presence of Polybrene (5µg/ml). Cells were incubated for 18h then cells were washed with normal media and the media was replaced with complete media of DMEM 10% FBS. Cells were allowed to grow for 72h then the media were replaced with DMEM 10% FBS containing (1µg/ml) Puromycin. Media were changed every 72h with freshly prepared Puromycin containing media until cells reached confluent. RNA and protein were extracted from part of the cells for the assessment of Noggin knock down in PC3RFP cells remaining cells were sub-cultured and continued to grow.

5.2.3 Detecting the presence of Noggin gene in PC3RFP-KD by QPCR

The stability of Noggin knockdown in PC3RFP cells was measured using Taqman single gene assay of Noggin. RNA was extracted from PC3RFP at different time point after viral transduction and cDNA were synthesized as described previously in chapter

2 section (2.3.5). Noggin expression was measured relative to the expression of a housekeeping gene GAPDH as described earlier in Chapter 2 section (2.3.6).

5.2.4 Detecting the presence of Noggin protein in knockdown PC3RFP by western blot

On the protein level the stability of Noggin knockdown in PC3RFP cells was detected by western blot. Protein was extracted and quantified from 80% confluent PC3RFP cells at different time points after viral infection as described in Chapter 2 section (2.4.1). 30 µg of protein samples were separated on 12% SDS-PAGE, blotted on PVDF membranes and probed with anti-Noggin and anti-GAPDH as described in Chapter 2 section (2.4.2). Noggin band intensity was measured by densitometry (Gel Documentation system, Bio-Rad).

5.2.5 Detecting the presence of Noggin protein in conditioned media collected over knockdown PC3RFP by ELISA

The amount of secreted Noggin protein present in media collected over knockdown cells at various time points was compared to the amount of protein found in control cells, measured by ELISA as described in Chapter 4 section 4.2.8.

5.2.6 Collecting conditioned media from PC3-KD and PC3-Mock cells

PC3-KD and PC3-Mock cells were seeded as described in 3.2.4. Conditioned media were then collected over both cell strains as described in 3.2.4 for the use in further experiments.

5.2.7 Analysing the effects of PC3-KD Condition media on the proliferation of osteoblast (SaOS2) cells

SaOS2 cells were seeded into 24 well plates at the same densities that were used in growth curves previously. Cells were challenged with 50% PC3-KD CM or with 50% PC3-Mock CM as control.

Cells were counted in quadruplicate cultures every 48h until day 12 and the mean cell number was calculated for each day. The media was changed every 4 days during the growth curve in all groups.

5.2.8 Selecting Recombinant Noggin concentrations

Recombinant Noggin was prepared by adding 400µL of 0.1% BSA in PBS to the lyophilized powder to make a final concentration of 250µg/ml stock solution. SaOS2 cells were seeded in the same cell density that was used in previous growth curves.

Cells were fed normally with DMEM 2% FBS containing recombinant Noggin with different concentrations (25ng/ml, 50ng/ml and 100ng/ml). Cells were counted in quadruplicate cultures after 6 days and after 10 days to determine the optimum concentration to be used in further experiments.

5.2.9 Effect of recombinant Noggin on the proliferation of Osteoblast (SaOS2) cells

SaOS2 cells were seeded into 24 well plates at the same densities that were used in previous growth curves. Cells were grown in DMEM 2% FBS containing 100ng/ml recombinant Noggin.

Cells were counted in quadruplicate cultures every 48h until day 12 and the mean cell number was calculated for each day. The media was changed every 4 days during the growth curve in all groups.

5.3 Results

5.3.1 Polybrene and Puromycin killing curve

In order to knockdown Noggin in PC3RFP cells using shRNA lentiviral virus the sensitivity of the cells to Polybrene and Puromycin was tested. The viability of the cells was assessed by counting the cells or by their appearance under the microscope. The growth of PC3RFP was not affected by any of Polybrene concentrations Figure 5.1 (A). 5µg/ml of Polybrene was the recommended concentration to be used according to the kit data sheet and this was subsequently used. PC3RFP cells were highly sensitive to Puromycin. Cells were killed by the lowest concentration of Puromycin (1µg/ml) after the first 48h Figure 5.1 (B).

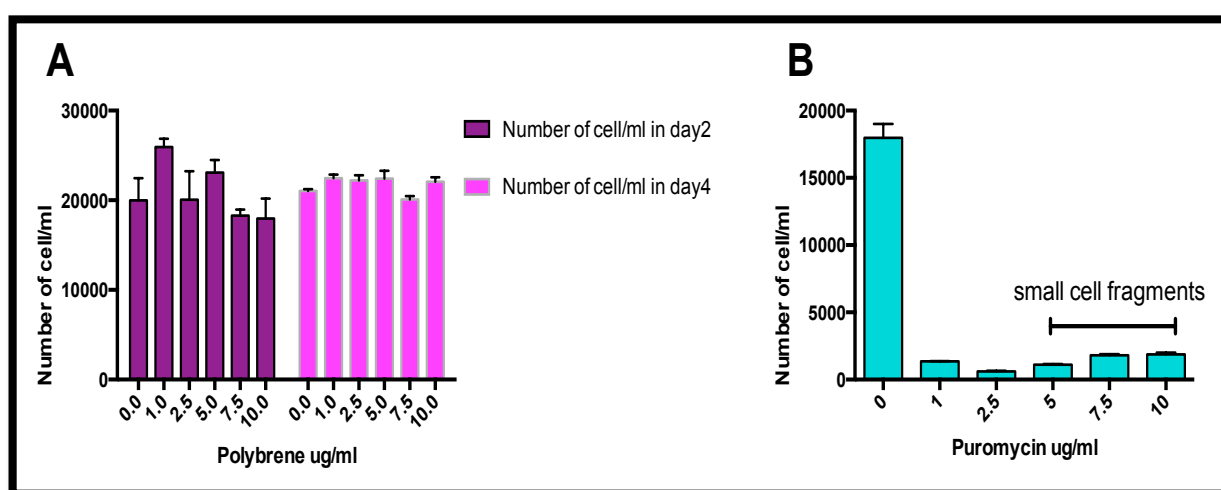


Figure 5.1 Polybrene and Puromycin killing curve.

(A) This illustrates the proliferative effect of Polybrene on the PC3RFP cells. Cells were not affected by any of the concentrations used (1, 2.5, 5, 7.5 and 10) µg/ml. (B) This illustrates the effect of different concentration of Puromycin (1, 2.5, 5, 7.5 and 10) µg/ml on PC3RFP cells. Cells were killed by the lowest concentration 1µg/ml after the first 48 h.

5.3.2 Validation of Noggin knockdown in PC3RFP cells by QPCR

Expression of the Noggin gene in PC3RFP-KD cells produced from our experiment was first measured by QPCR using Noggin single gene assay and this was compared to PC3RFP-Mock cells as controls. Noggin gene was 61% knockdown in PC3RFP-KD cells compared to mock cells. The stability of Noggin knockdown in cells was tested after growing the cells and passaging them twice. Cells were significantly knockdown $P=0.0001$ during the first passage of cells but not after this time (Figure 5.2).

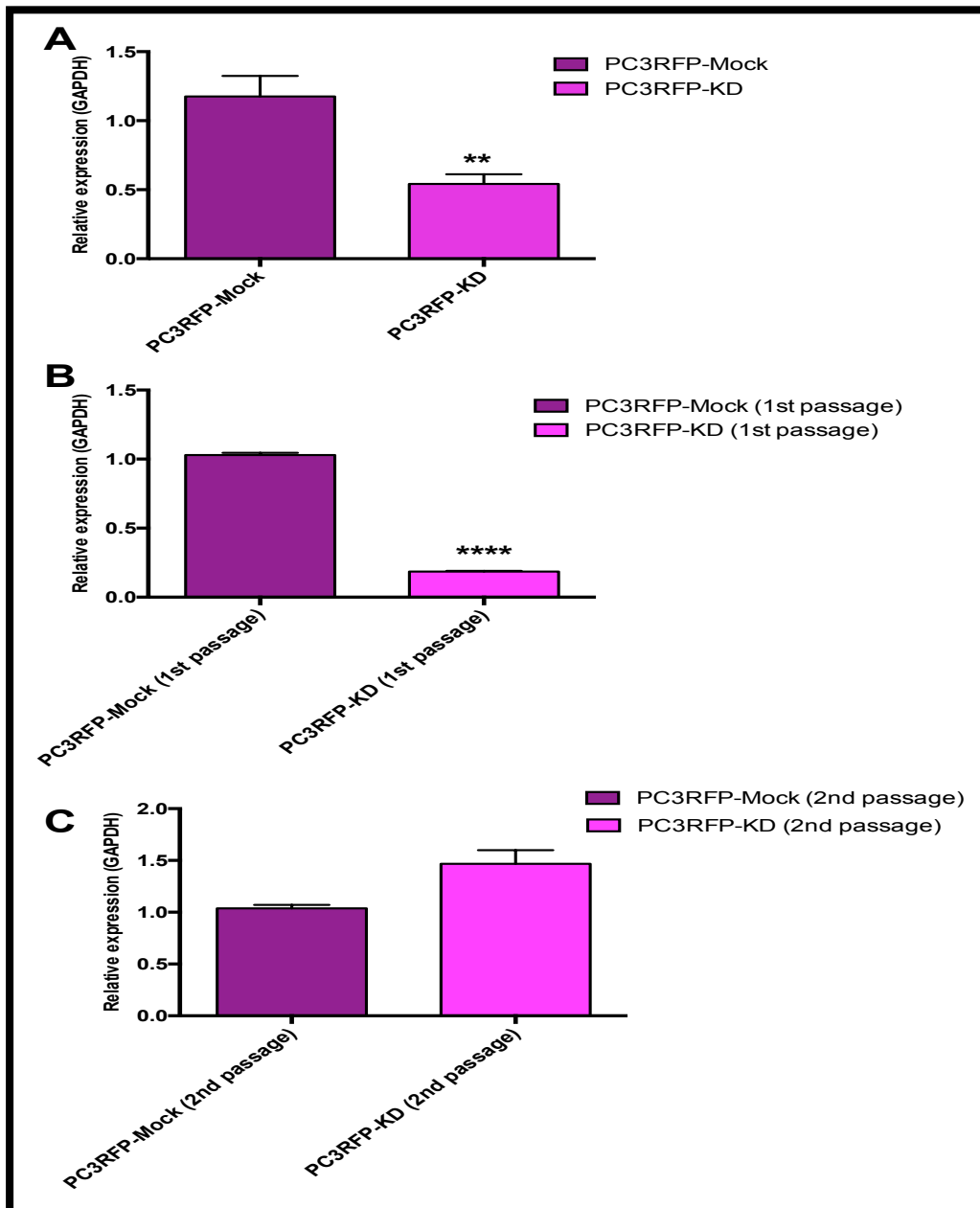


Figure 5.2 Noggin expression in PC3RFP-KD and PC3RFP-Mock.

(A) This shows the reduction in Noggin expression in PC3RFP-KD cells by 61% with P value= 0.009, unpaired t test compared to mock cells. (B) Confirmation of the reduction of Noggin expression in PC3RFP-KD cells during the first passage of cells with P value= 0.0001, unpaired t test. (C) This shows that after passaging the cells twice cells, the expression of Noggin was similar in the KD and Mock cells. Relative expression was calculated after calculating dct and Δdc then Δdc was raised to the square root. All data are displayed with mean \pm SEM of 3 independent experiments.

5.3.3 Validation of Noggin knockdown in PC3RFP cells by ELISA

Noggin protein produced by PC3RFP-KD cells was measured by ELISA compared to the amount of Noggin protein produced by PC3RFP-Mock cells. Conditioned media was collected from both PC3RFP-KD and PC3RFP-Mock cells at the same time point that the levels of expression of the Noggin gene were analysed by QPCR.

Results obtained from the ELISA assay matched the QPCR results. Noggin protein was reduced in KD cells compared to mock cells at the beginning of the experiment (P value = 0.01 and P value= 0.02 respectively) but not after passage 2 (Figure 5.3).

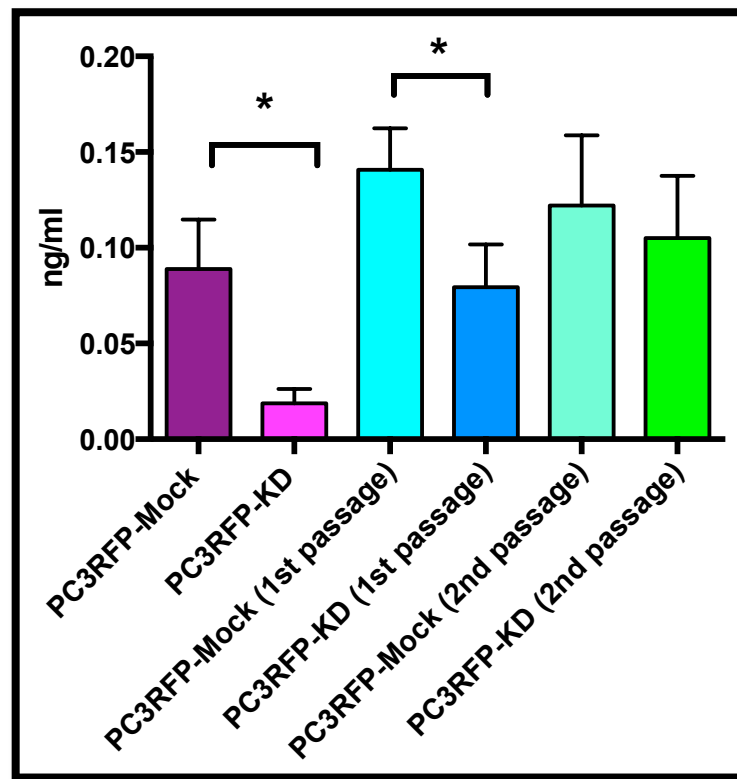


Figure 5.3 Noggin protein levels in PC3RFP-KD and PC3RFP-mock conditioned media.

This Figure illustrates the significant reduction in Noggin protein production in PC3RFP-KD cells at the beginning of the experiment (P value = 0.01 and P value= 0.02 respectively, unpaired t test) compared to mock cells. However, Noggin production was similar in both strains after passaging the cells twice. All data are displayed as means \pm SEM of 3 independent experiments.

5.3.4 Validation of Noggin knockdown in PC3RFP cells by western blot

The expression of Noggin protein was assessed by western blot to validate the stability of the knockdown. Western blot results were with an agreement with previous results of QPCR and ELISA, indicating that Noggin protein expression was only reduced initially but not with further passaging to the cells (Figure 5.4).

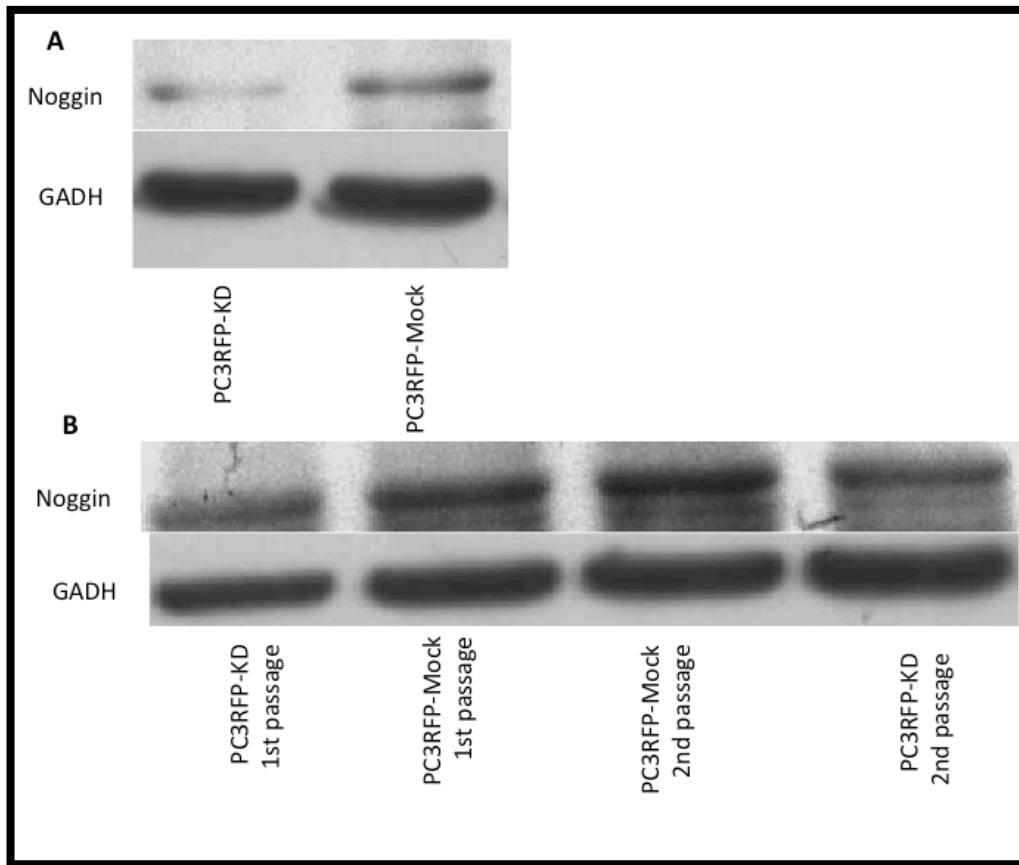


Figure 5.4 Noggin protein production profile in PC3RFP-KD and PC3RFP-mock cells.

The Figure shows western blot analyses of protein production by PC3RFP-KD and PC3RFP-mock cells during different time point (A) illustrates reduction in Noggin expression in PC3RFP-KD cells compared to mock cells during the beginning of the experiment (B) PC3RFP-KD cells retained Noggin expression back to normal after passaging the cells several times. First lane shows Noggin expression and a lane shows GAPDH expression as house keeping protein.

5.3.5 Validation of the stability of Noggin knockdown in PC3-KD Clone 14 cells by QPCR and western blot

The failure to establish a stable PC3RFP Noggin knock down cell strain was a major setback to my work. Even after several attempts I was unable to generate strains that had stable reductions in Noggin production. A stable Noggin knock-down clone, PC3-KD (clone 14) and a mock transfected (random sequence) PC3-mock (clone 4) cells were thankfully given to us by Dr. Marco G. Cecchini from the Urology Research Laboratory University of Bern, Bern Switzerland. The stability of knockdown in PC3-KD cells given by Dr. Marco G. Cecchini were tested by both QRT-PCR and western blot after passaging the cells for several times before using them in the next experiments. PC3-KD cells were stably knocked down for Noggin as shown by QRT-PCR which revealed a significant reduction in Noggin gene expression in PC3-KD cells by 75% (P value= 0.004) compared to mock cells. These results were confirmed by western blot which showed a significant reduction in Noggin protein expression in

PC3-KD cells compared to mock cells with P value= 0.0001 Figure 5.5.

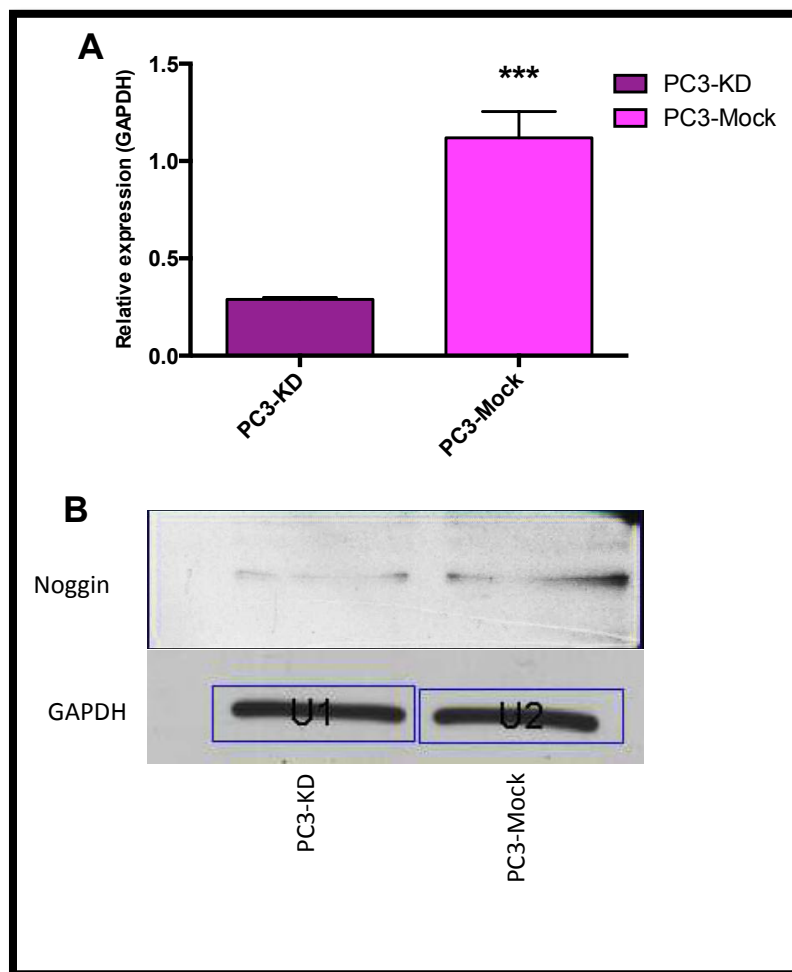


Figure 5.5 Noggin expressions in PC3-KD and PC3-mock cells.

(A) This illustrates 75% reduction in Noggin gene expression in PC3-KD cells compared to mock cells (P value= 0.004, unpaired t test). (B) illustrate a significant reduction in Noggin protein level in PC3-KD cells compared to mock cells (P value= 0.0001, unpaired t test). Relative expression was calculated after calculating dct and Δdc then Δdc was raised to the square root. All data are displayed with $mean \pm SEM$ of 3 independent experiments

5.3.6 Effects of PC3-KD Condition media on the proliferation of osteoblast (SaOS2) cells

Conditioned media was collected from both PC3-KD and PC3-mock cells. The growth rates of Osteoblast (SaOS2) cells were studied when they were seeded in conditioned media from PC3-KD and in PC3-mock cells. Conditioned media collected from PC3-KD cells significantly decreased the proliferation of SaOS2 cells compared to PC3-mock cells with P value= 0.04 Figure 5.6.

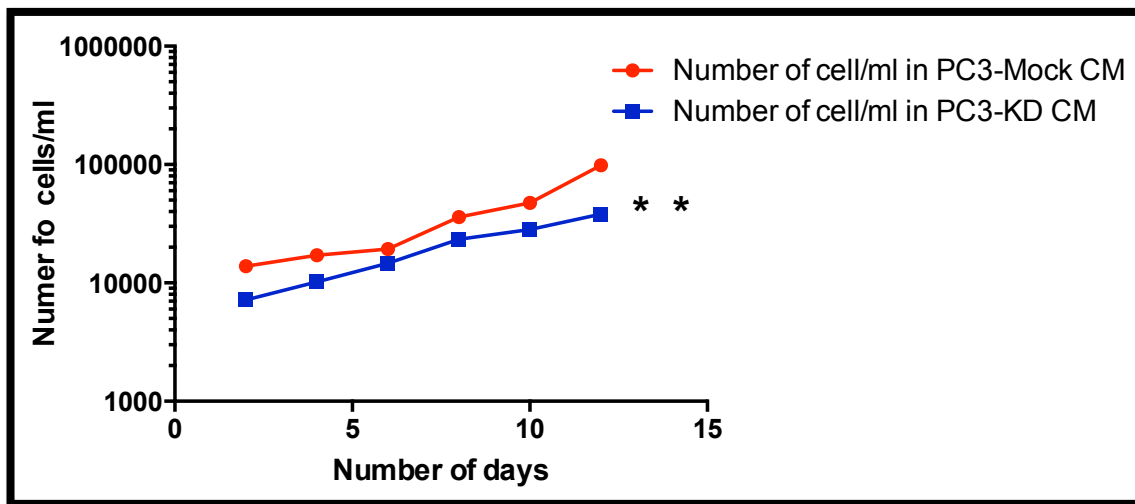


Figure 5.6 Conditioned media from Noggin knockdown PC3-KD cells reduced the proliferation of SaOS2 cells.

This Figure demonstrates that conditioned media from Noggin knockdown PC3 (PC3-KD) caused a significant reduction on the proliferation of SaOS2 cells compared to conditioned media collected from mock cells (PC3-Mock) (P value= 0.006, unpaired t test). All data are displayed with mean \pm SEM of 3 independent experiments.

5.3.7 Selecting Recombinant Noggin concentration

Several recombinant Noggin concentrations (25ng/ml, 50ng/ml and 100ng/ml) were tested in order to select the best concentration to be used with osteoblast (SaOS2) cells. SaOS2 cells were seeded in media containing different concentrations of recombinant Noggin. Cells were counted at two time points, days 6 and 10. 100ng/ml was found to be the dose that stimulated the growth of SaOS2 cells the most Figure 5.7. Therefore 100ng/ml of recombinant Noggin was used in further experiment.

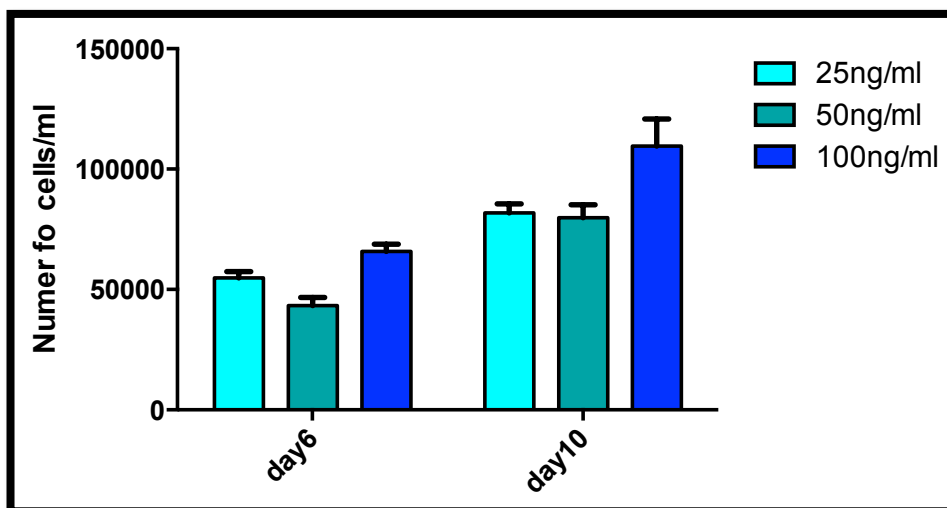


Figure 5.7 The effect of various recombinant Noggin concentrations on the growth of SaOS2 cells.

Different recombinant Noggin concentrations (25ng/ml, 50ng/ml and 100ng/ml) were used to evaluate the optimum dose to be used in further experiment. Osteoblast (SaOS2) cells were counted at two time points day 6 and day 10. 100ng/ml of recombinant Noggin was found to be the optimum concentration and was used in further with SaOS2 cells. All data are displayed with mean \pm SEM of 3 independent experiments.

5.3.8 Effect of recombinant Noggin on the proliferation of Osteoblast (SaOS2) cells

Recombinant Noggin was found to stimulate the growth of osteoblast (SaOS2) cells significantly compared to SaOS2 cells grown in regular DMEM 2%FBS media. This effect was similar to the effect of PC3RFP-CM on the proliferation of osteoblast cells Figure 5.8.

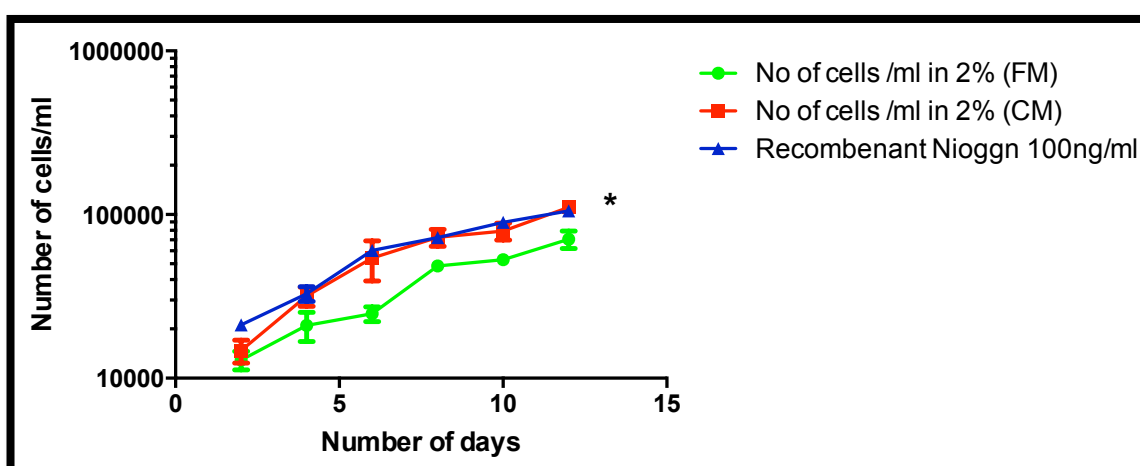


Figure 5.8 Recombinant Noggin stimulates SaOS2 proliferation.

This Figure showed that recombinant Noggin enhanced the proliferation of SaOS2 cells significantly (P value= 0.04, 1 way ANOVA). This increase in proliferation by Noggin was to the same extent caused by PC3RFP-CM. All data are displayed as means \pm SEM of 3 independent experiments.

5.4 Discussion

In this chapter I tried to establish my own knockdown Noggin PC3RFP cells. PC3RFP cells were initially knocked down for Noggin expression by infecting the cells with the Noggin shRNA Lentiviral. At the beginning of the experiment, a 61% reduction in Noggin mRNA levels was observed (determined by QPCR), and a 77% reduction in secreted Noggin as determined by ELISA was demonstrated but knockdown was not stable and after several passages, Noggin expression and protein production were the same in both KD and Mock strains but cells continued to be Puromycin resisted. This was unfortunate and appears to an effect of silencing of at least part of the transduced sequences by the infected cells. This may imply that suppression of Noggin by shRNA induces a growth disadvantage to these cells. More likely is the recognition of viral promoters by the cells led to silencing of sequences regulated.

PC3-KD clone 14 and PC3-mock clone 4 cells were kindly provided by Dr. Marco G. Cecchini. The stability of Noggin knockdown in these cells after several passages was tested before they were used in further experiments. Cells were stably knocked down, with a 75% reduction in Noggin mRNA level this was measured by QRT-PCR and 70% reduction in Noggin protein level as measured by western blot. Conditioned media was collected from both PC3-KD and PC3-mock cells. The effect of these media on the proliferation of SaOS2 was assessed by conducting growth curves in which SaOS2 cells were grown in conditioned media collected over PC3-KD cells and was compared to their growth in PC3-Mock cell conditioned media. Conditioned media collected over PC3-KD cells caused a significant reduction in SaOS2 cells proliferation compared to those grown in PC3-Mock conditioned media. The addition of exogenous recombinant Noggin to the media resulted in significant increased SaOS2 proliferation. My result are in agreement with a study done by Hsu et al that reported Noggin overexpressing melanoma cells showed a growth advantage in response to subsequent BMP7 transduction both *in vitro* and *in vivo*, whereas, Noggin knockdown melanoma cells exhibited a growth inhibition. This result suggested that advanced melanoma cells might escape from BMP7-mediated autocrine growth inhibition through corresponding Noggin upregulation (Hsu *et al.* 2008). Abnormal BMP7 expression during tumour progression is not specific to melanoma. Elevated levels of BMP7 have been associated with bone metastasis of prostate cancer (Masuda *et al.* 2003). The roles of BMP7 on growth regulation have

been studied widely in carcinogenesis since BMP7 has been shown to have divergent effect acting as both growth stimulation and inhibition (Pouliot *et al.* 2003; Baade Ro *et al.* 2004). BMP7 has been shown to either induce apoptosis or inhibit proliferation of androgen insensitive prostate cancer such as PC3 through causing cell cycle arrest in G₀-G₁ phase (Baade Ro *et al.* 2004; Miyazaki *et al.* 2004). In contrast, in androgen sensitive LNCaP prostate cancer cell line, BMP7 seems to promote cell survival suggesting that various cells type respond differently to BMP7 as a result of cross talk with other signalling pathways (Ide *et al.* 1997; Yang *et al.* 2005). Our results was also similar to a study done by Tarragona et al investigating the role of Noggin in breast cancer metastasis to bone which revealed that over expression of Noggin increased the growth rate of bone metastasis in orthotopic mouse model. In the same study it was found that silencing Noggin by using transfection with shRNA targeting Noggin gene caused growth rate reduction of bone metastases (Tarragona *et al.* 2012). These results suggested that Noggin modulates the initiation of breast cancer metastasis through DNA-binding protein inhibitor 2 (ID2) and by altering RANKL levels thus linking the possibility of metastatic cells expressing high level of Noggin with chemotherapy resistance (Schramek *et al.* 2010). Noggin has been linked not only to the ability of metastatic cells to successfully metastasize to the bone but also to the ability of self-renewal activity acquired by metastatic cells (Tarragona *et al.* 2012). This might explain the elevated levels of expression of Noggin mRNA during early phase of fracture healing in mice reported by Yoshimura et al in his study (Yoshimura *et al.* 2001). In another study Canalis *et al.*, the physiological function of Noggin in osteoblasts was determined by generating tissue specific null Noggin mice. This was achieved by mating Noggin conditional knock out mice, where the Noggin allele is flanked by loxP sequences, with mice expressing the Cre recombinase under the control of the Osteocalcin promoter (Oc-Cre). Their study showed that Noggin conditional null mice presented with a decreased in body weight, shorter femoral length and generalized osteopenia. Demonstrating that Noggin inactivation causes osteopenia suggests that excessive exposure to BMP may have detrimental effect in bone (Canalis *et al.* 2012). Wu et al found that overproduction of Noggin by infecting preosteoblastic U-33 cells with a retrovirus containing Noggin gene or in transgenic mice with more Noggin in their mature osteoblast resulted in osteoblast differentiation inhibition and reduced bone formation and net bone loss (Wu *et al.* 2003). In addition, another study investigated the effects of BMP2 on osteoblast apoptosis by using different osteoblast cells with

different degrees of maturation including human mesenchymal stem cells (MSCs) immature osteoblast (MG63 cells), mature normal human osteoblast (HNOst) and MG63 with silenced Noggin (shNog-MG63). Both MSCs and HNOst cells were treated with exogenous BMP2 while, shNOG-MG63 cells were used a model system with increased endogenous BMP signalling as result of Noggin silencing. Apoptosis was higher in mature osteoblast HNOst and in shNOG-MG63. This, suggested that BMP2 induced apoptosis depending on the maturation state of the cells and the effect was under the regulation of Noggin (Hyzy *et al.* 2012). The same finding was reported by other investigators indicating that increased apoptosis was associated with loss of function of Noggin transgenic mice during palatogenesis (He *et al.* 2010). Overexpression of Noggin in transgenic mice resulted in decreased apoptosis in eyelid epithelium (Sharov *et al.* 2003). This was not the case in oesophageal cancer cell line EC109 expressing high level of BMP6 and weak expression of SOST. Knockdown of Noggin in these cells resulted in enhanced non adherent cells growth (Yuen *et al.* 2012).

In this chapter, our results supported the hypothesis that Noggin plays an important role in the regulation of osteoblast cell proliferation. This was shown by increased growth rate when SaOS2 cell were treated with recombinant Noggin. When SaOS2 cells were treated with conditioned media collected over PC3-KD cells, the growth enhancement seen with CM from standard PC3RFP or PC3-Mock cells was reversed, suggesting that Noggin is one of the reasons behind increased proliferation of osteoblast cells when treated with conditioned media collected over PC3RFP cells seen in chapter 3.

However, the amount of recombinant Noggin that were needed to a chive maximum growth in the SaOS2 cells were much higher than the amount of Noggin present in the conditioned medium collected over PC3RFP cells which, was only 0.293 ng/ml. Suggesting that the level of Noggin produced by the SaOS2 cells in response to PC3 conditioned medium is much more important than Noggin produced by the PC3 themselves.

**Chapter 6 Noggin in the interactions of prostate cancer cells with
osteoblasts *in vivo***

6 Chapter 6 Noggin in the interactions of prostate cancer cells with osteoblasts *in vivo*

6.1 Introduction

Bone microenvironment is a rich source of survival and growth signalling molecules for bone cell populations potentially making it a favourable site for the metastasis of cancers, including prostate cancer (Kyle *et al.* 2003; Hess *et al.* 2006). Clinically significant metastases can occur years to decades after the removal of primary tumour after periods where patients appear to be disease free. This phenomenon is observed in clinical cases, but also has parallels in animal experimental studies (Shen *et al.* 2014). Both osteoclast and osteoblast cells that originate from hematopoietic and mesenchymal progenitors respectively play essential role in bone remodelling processes during which renewal of adult human skeleton takes place (Parfitt 1994; Manolagas and Jilka 1995). Skeletal homeostasis requires a continuous and regular supply of these cells therefore; any increase or decrease in the production or any change in the rate of apoptosis or proliferation of these cells may results in imbalance between bone resorption and formation. Such imbalances underlie bone disease including osteoporosis and tumour associated bone disease associated with metastases (Jilka *et al.* 1992; Hughes *et al.* 1996; Weinstein *et al.* 1998). Once cancer reaches the bone it becomes difficult to treat, since bone provides a niche in which cancer cell may lay dormant and as such are resistant to chemotherapies that rely on targeting proliferating cells (Mundy 2002).

A study done by Jung *et al.*, reported that in murine model of prostate cancer most of the lesions were found in the hind limb regions (Jung *et al.* 2012). This suggests that these bones (tibias and femurs) may represent a consistent and relevant model for tumour growth in the skeleton.

From the *in vitro* study in previous chapters, conditioned media collected over PC3RFP cells stimulated the growth rate in the osteoblastic cell line, SaOS2. In addition, the presence of prostate cancer with osteoblast cells (SaOS2) either directly or in direct through conditioned media caused an increase in Noggin expression in mRNA and protein level by osteoblast cells. Treating SaOS2 cells with recombinant Noggin had the same effect of PC3RFP-CM on SaOS2 proliferation while silencing Noggin in PC3 cells, suggested that the effects observed with CM on SaOS2 growth was at least in part mediated by Noggin. This suggests that prostate cancer derived Noggin contributes to the proliferation and differentiation of osteoblastic cells and, *in vivo*, have an effect on bone remodelling and tumour growth. To test this hypothesis, both PC3-mock and PC3-KD described in Chapter 5 were injected intracardiac, into

immunosuppressed BALB/c nude mice to determine their ability to metastases to the bone.

Aim

To determine the tumour take of PC3-Luc (Noggin knockdown/ mock control) prostate cancer cells in the BALB/c mice.

Hypothesis

Knockdown Noggin in PC3 cells reduces tumour metastases to bone.

Objective

1- Evaluate the effects of Noggin knock down compared to controls on:

- a) the total tumour frequency (bioluminescent *in vivo* monitoring and post-mortem histology)
- b) the structure of bone in tumour bearing animals (micro CT)

2- Evaluate the immunolocalisation of Noggin in bones/tumours post-mortem

6.2 Material and method

6.2.1 Materials and Disposable Equipment

Item	Supplier
DiD cell labeling solution	Invitrogen
EDTA	Fisher Scientific
SingleStain Boost IHC detection reagent (HPR, Rabbit) universal secondary antibody	Cell signaling technology
ImmPACT DAB peroxidase substrate	Vector laboratories

6.2.2 Cell lines

The cell lines that were used in the *in vivo* study were the cells thankfully given by Dr. Marco G. Cecchini PC3-KD clone 14 and PC3-mock clone 4 cells. These cells were stably transfected with a luciferase gene Luc and were called PC3-KD and PC3-mock.

6.2.3 Mice

The *in vivo* studies were performed using 20 male BALB/c nude immunocompromised mice aged 12 weeks. These animals were housed in a controlled environment with a 12 h light/dark cycle at 22°C. All procedures complied with the UK animals (scientific procedures) and were reviewed and approved by local Research Ethics Committee of the University of Sheffield (Sheffield, UK).

6.2.4 *In vivo* imaging system (IVIS)

Mice were injected with 30mg/kg D-luciferin (100µl subcutaneously) and were anaesthetised using Isoflurane (3% isoflurane and oxygen 3% in an anaesthesia induction chamber) for 1-2 min. Mice were transferred to the Xenogen IVIS Lumina 11 (California, USA) *in vivo* imaging system. Images were taken 5 min after luciferin injection with the instrument set to automatic exposure for luminescence detection in an area/dimension adjusted for mouse imaging. The duration of acquiring the images varied between 1-2 min at day 0 (injecting day) and few seconds as the tumours grew and signals became stronger. Mice were allowed to recover in an incubator set at 30°C and monitored during recovery from the anaesthetic in line with the Home Office Project License governing the work. The mice were monitored at 4,7,8,9 and 10 weeks after injection of the cells.

6.2.5 PC3-mock and PC3-KD cells labelling with DiD solution

One T75 flask from each PC3-mock and PC3-KD were harvested by trypsinization and were counted. Around 2,000,000 cells from each cell type were taken and were mixed with 14 μ L of DiD cell labelling solution. Cells were covered with foil and incubated for 20 min in the incubator. Cells were centrifuged for 3 min at 500xg in order to remove excess dye; as a result a blue pellet of cells was obtained. The pellet formed was washed twice with PBS. The cells were re-suspended in 2 ml of PBS.

6.2.6 Intra-cardiac injection of PC3-mock and PC3-KD cells into immunosuppressed mice

20 old BALB/c nude male mice aged 12 weeks were divided into two groups 10 mice in each group were Intracardiac injected with 100 μ L of either PC3-mock or PC3-KD cells suspension. Mice were monitored throughout the entire experiment duration; weights and *in vivo* images (IVIS) were taken at the beginning of the experiment and every week until the tumour develops Figure (6.1).

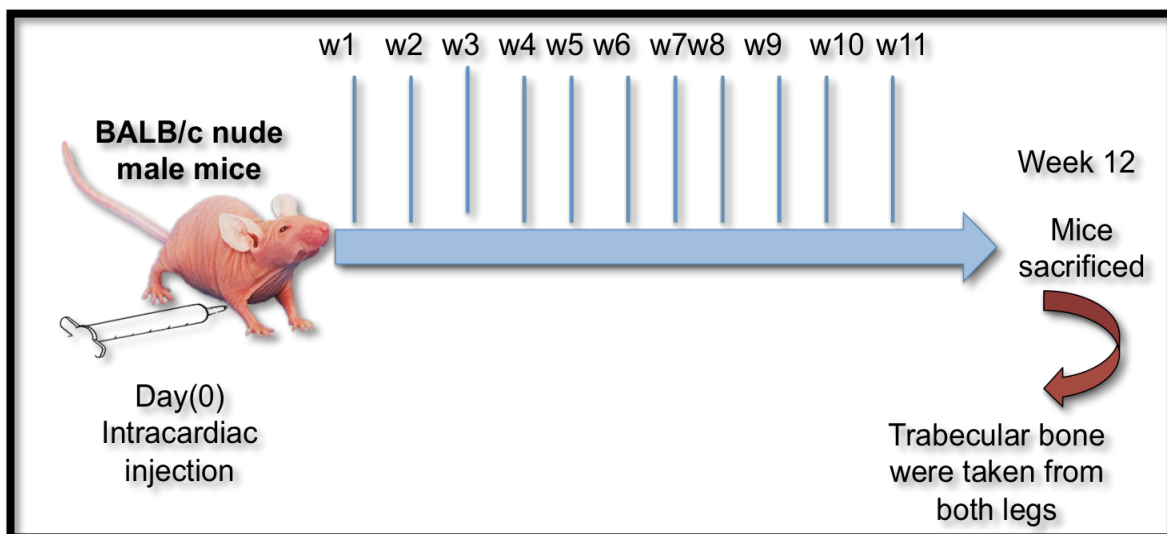


Figure 6.1 Experimental design of the *in vivo* study.

20 BALB/C nude male 12 weeks old mice were Intracardiac injected with approximately 0.1 million of either PC3-mock or PC3-KD cells. Mice were monitored during the entire duration of the experiment by using *in vivo* imaging system (IVIS). At week 12 the mice were sacrificed and trabecular bone were taken from both legs for further investigations.

6.2.7 Harvesting trabecular bone from mice

Trabecular of tibia bones of the mice were taken from both legs. Left leg was snap frozen by dipping in liquid nitrogen. Bone was transferred and stored at -80 °C for high-resolution micro-computed tomography (μ CT) scanner. For

immunohistochemistry right leg were excised carefully and stored in 10% of neutral buffered formalin (NBF) for a minimum of three days and decalcified in EDTA for 14 days. Bones were washed with distilled water to remove EDTA and through graded alcohols to remove water. Sections of tibial trabecular bones were taken every 3 μ M using a Leica microsystems microtome RM 2265. Sections were floated for 30 min in a 45°C water bath, transferred onto glass slides, dried for 30 min on a 45°C hotplate, incubated overnight at 37°C, and stored at 4°C until staining.

6.2.8 High-resolution micro-computed tomography (μ CT)

High-resolution μ CT scanner (model 1172; Skyscan, Belgium) is an imaging technique that uses x-rays to produce cross-sectional images of an object that can be restructured to produce a three-dimensional model. It allows for non-destructive quantitative analysis of the density, geometry and microarchitecture of bone (Bouxsein et al 2010). μ CT scanner was used to scan tibia bones. Image captured every 0.35° through a 360° rotation with 4.1 pixel size. Scanned images were remodeled using Skyscan NRecon software (version 1.5.1.3, Skyscan, Belgium) and analysed using Skyscan CT analysis software (version 1.8.1.2, Skyscan, Belgium). Trabecular volume, trabecular thickness and trabecular number were evaluated in a standardized region of interest. Trabecular bone within this region was quantitated.

6.2.9 Immunohistochemistry detection of Noggin in trabecular bone

Bone sections were dipped twice in xylene for 5 min to remove wax and re-hydrated twice in absolute alcohol, 95% alcohol and 70% alcohol for 5 min and washed briefly in water. Sections were incubated in 3% hydrogen peroxide in water for 15 min to block the endogenous peroxidase activity. Sections were washed in water to stop the enzymatic reaction. Slides were incubated in PT module preheating machine at temperature ranges between 87°C-85°C for 10 min. Sections were kept in warm PBS. Bone sections were blocked with 5% normal donkey serum in 0.1% PBS/Tween for 1 hour at room temperature, and followed by an incubation overnight at 4°C with 100 μ l of anti-Noggin antibody (abcam, UK) (1:500 dilution in PBS/Tween). 100 μ l of normal rabbit IgG antibody (R&D systems, UK) was used as a negative control (1:500 dilution in PBS/Tween). Bone sections were washed 3 times with PBS/Tween at room temperature to remove unbound antibody, and incubated with 100 μ l of SingleStain Boost IHC detection reagent (HRP, Rabbit) secondary antibody, for 30 min at room temperature. The washing steps were repeated again with PBS/Tween as described above, and incubated with 300 μ l of Impact DAB for 3

min at room temperature. Cells washed with water for 5 min, counter stained with haematoxyline for 20 s to stain nuclei, and washed again with water for 5 min. Bone sections were de-hydrated in 70% alcohol for 5 min, 95% alcohol, twice in absolute alcohol for 5 min each and dipped twice in xylene for 5 min to remove alcohol. Slides were mounted and covered using cover slip.

6.3 Result

6.3.1 Effect of knockdown of Noggin in prostate cancer cells on bone and their ability to form tumours

PC3-mock and PC3-KD cells were intra-cardiac injected into BALB/c nude male mice aged 12 weeks. The mice were monitored throughout the experiment period of 12 weeks. Images were taken by *in vivo* imaging system (IVIS) during week 4, 7, 10 and 11 as seen in Figure (6.2) and Table (6.2). On the 12th week the mice were culled and tibiae were carefully dissected. The overall tumour formation rate in animals injected with these cell strains that had been genetically altered and cloned was below that expected with the parental PC3 cell line in 12 week old mice (~30%, in long bones). At the early time points, up to week 7, there were more tumours, when all sites were taken in consideration, in the animals injected with the PC3-mock than with the PC3-KD cells. Only one mouse developed a lesion in the long bones and that was in the PC3-KD group. Trabecular of tibia bones were analysed using a high resolution μ CT scanner (model 1172; Skyscan, Belgium) to determine the effect of injecting PC3-mock and PC3 knockdown Noggin on bone disease Figure (6.3) panel (A) shows bone μ CT images of mice injected with PC3-mock cells as a control panel (B) shows bone μ CT images of mice injected with PC3-Noggin knockdown cells. Figure (6.3) panel (C), (D) and (E) shows that there were no differences in the trabecular bone volume, trabecular number and trabecular thickness of mice injected with PC3-KD cells compared to mice injected with PC3-mock cells as a control respectively.

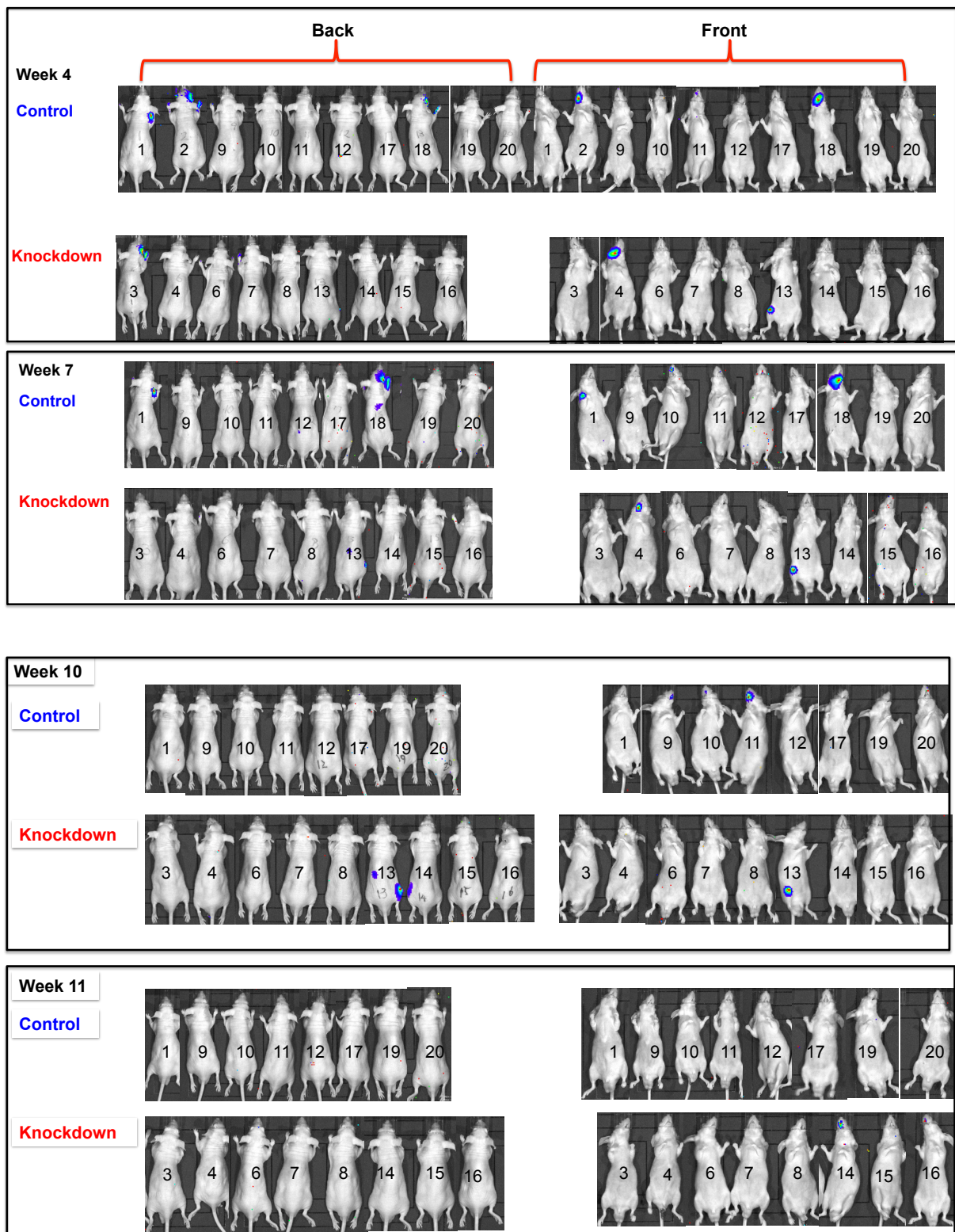


Figure 6.2 In vivo imaging of PC3 mock and PC3KD (Noggin) in cohorts of mice using bioluminescence detected using the IVIS system.

This figure shows images of two groups of mice: the first group was injected with PC3-mock (control) the second group was injected with PC3-KD. Mice in both groups developed tumours mainly in the jaw, right eye, paw and vertebra/hip only one mouse (m13) from the KD group developed a tumour in the right leg and was culled after weeks 10. Animals were assessed from the front and back and whole body mages were taken on week 4, 7, 10 and 11.

Table 6.1 summaries IVIS images of mice in all groups.

control	wk 3	wk 4	wk 7	wk 10	wk 11
m1		Right shoulder	Right shoulder		
m2		Right eye paw and jaw	culled		
m9				jaw	
m10			jaw	jaw	
m11		jaw		jaw	
m12		vertebra/hip	vertebra/hip		
m17					
m18		Right eye paw and jaw	Right eye paw jaw and vert.	culled	
m19					
m20					
		5/10	5/10	3/10	1/10
knockdown					
m3					
m4		Right eye paw and jaw	jaw		
m5	Died (6.7.13)				
m6					
m7					
m8					
m13		Right leg	Right leg and vert	Right leg and vert	culled
m14					jaw
m15					
m16					
		2/10	2/10	1/10	1/10

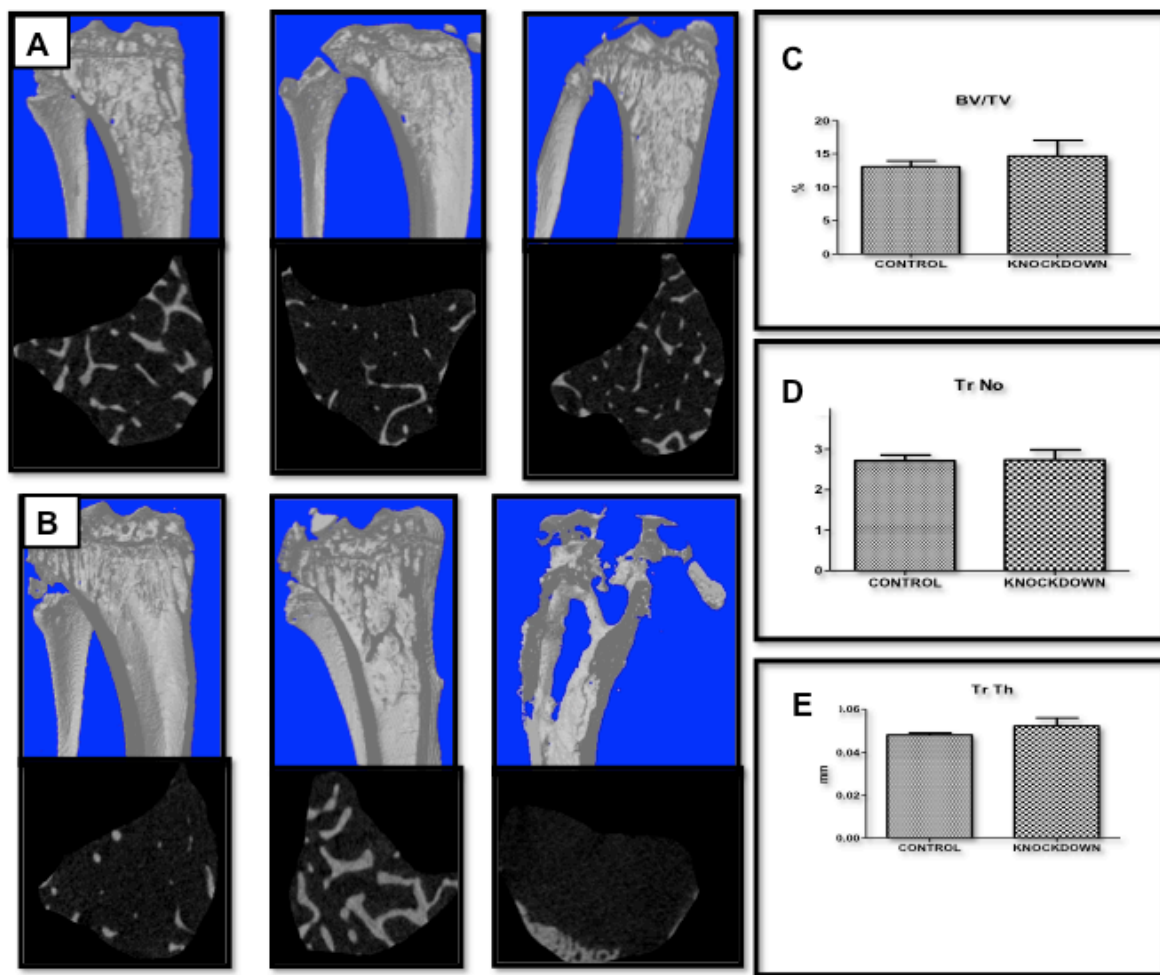


Figure 6.3 Effect of knockdown Noggin in prostate cancer cell line on bone disease in trabecular tibia bone using BALB/C nude male mice aged 12 weeks.

DiD labeled mock and knockdown Noggin PC3-KD cells were Intracardiac injected into BALB/c nude male mice aged 12 weeks. Mice were sacrificed after 12 weeks (24 weeks old) and tibia bone were dissected. Panels A and B show 3D μ CT-reconstructed images of tibias in mice injected with mock cells (but no tumour present) and with Noggin-KD cells only one tumour was present, respectively. White colour shows the trabecular bone. Panel C, D and E shows that there was no difference in the trabecular bone volume (BV/TV), trabecular number (Tr No) and trabecular thickness (Tr Th) between the two groups.

6.3.2 Noggin was expressed on the bone lining cells and bone surface *in vivo* in BALB/C nude male mice

20 BALB/C nude male mice were intra-cardiac injected with either PC3-mock cells or PC3-Noggin knockdown both were DiD labeled. After 12 weeks mice were harvested but only one mouse in the knockdown group developed a tumour in the tibia. Tibia bones were dissected for immunohistochemistry. Several dilutions of anti-Noggin primary antibody were tested to minimize non-specific binding of the antibody Figure (6.4) panel A shows Noggin antibody with different dilution (1/175, 1/500 and 1/2500) panel B shows the corresponding isotype with the same dilution. 1/500 primary antibody dilution was used in all immunohistochemistry slides. Figure (6.5) panel (A) shows strong Noggin staining in osteoblasts in the bone marrow of control mice. Panel (B) shows weak Noggin staining in bone marrow of mice injected with PC3-KD cells. Panel (C) shows strong Noggin staining on the bone lining cells and bone surface where tumour came close to the endosteal bone of control mice. Panel (D) shows very weak Noggin staining on the bone lining cells and bone surface when tumour cells were located close to the endosteal bone surface of mice injected with PC3-KD cells. Panel (E) shows strong Noggin staining in within the tumour cells itself in control mice. Panel (F) there was no Noggin staining presented in the tumour cells in mice injected with PC3-KD cells.

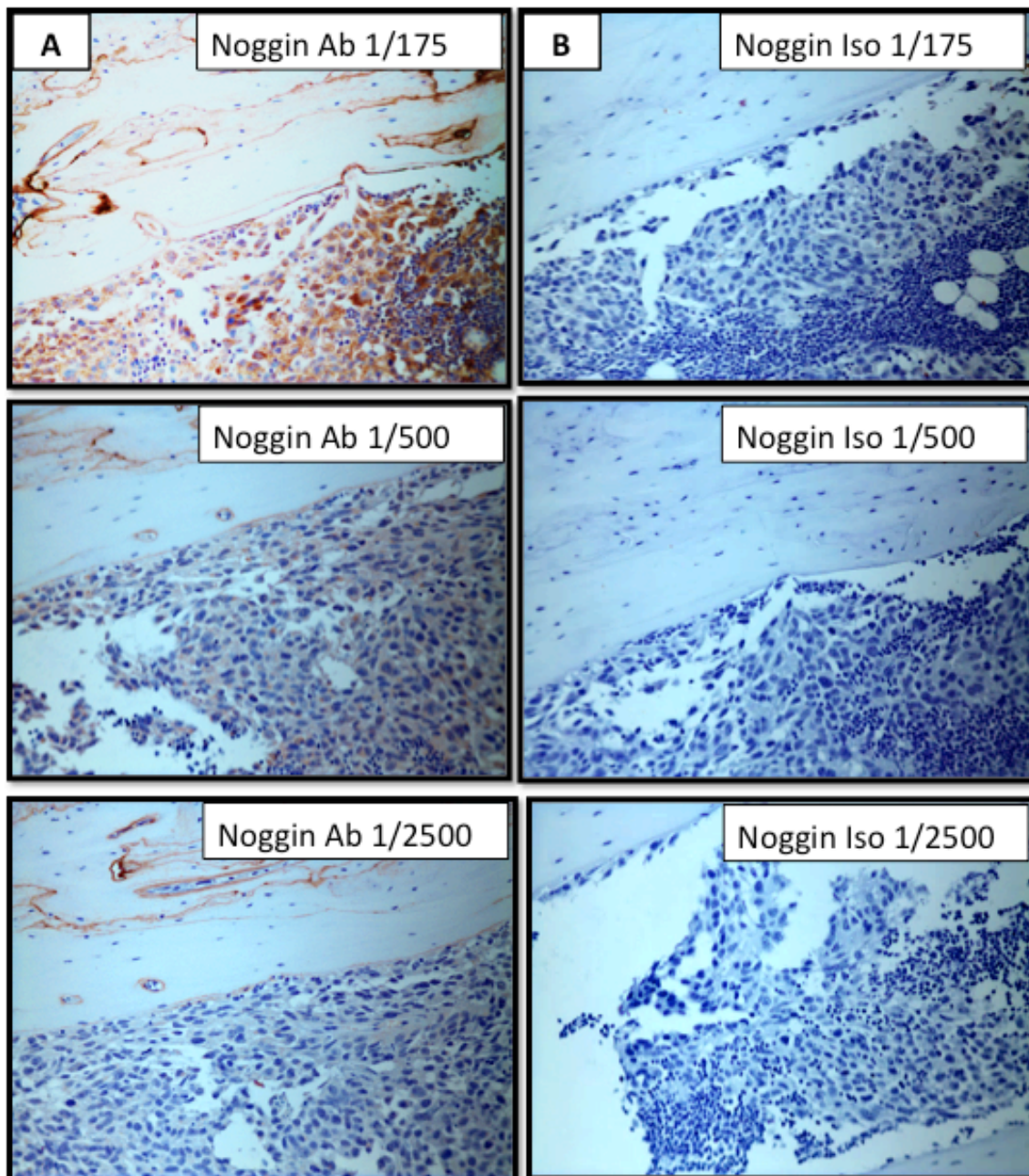


Figure 6.4 Immunohistochemistry optimization of Noggin protein in trabecular tibia bone.

Bone sections were stained with rabbit polyclonal anti- Noggin primary antibody or isotype control, normal rabbit IgG antibody. Nuclei were counterstained with haematoxyline. Cells were examined under microscope with 20x objective. Panel (A) shows Noggin antibody with different dilution (1/175, 1/500 and 1/2500) panel (B) shows the corresponding isotype with the same dilution.

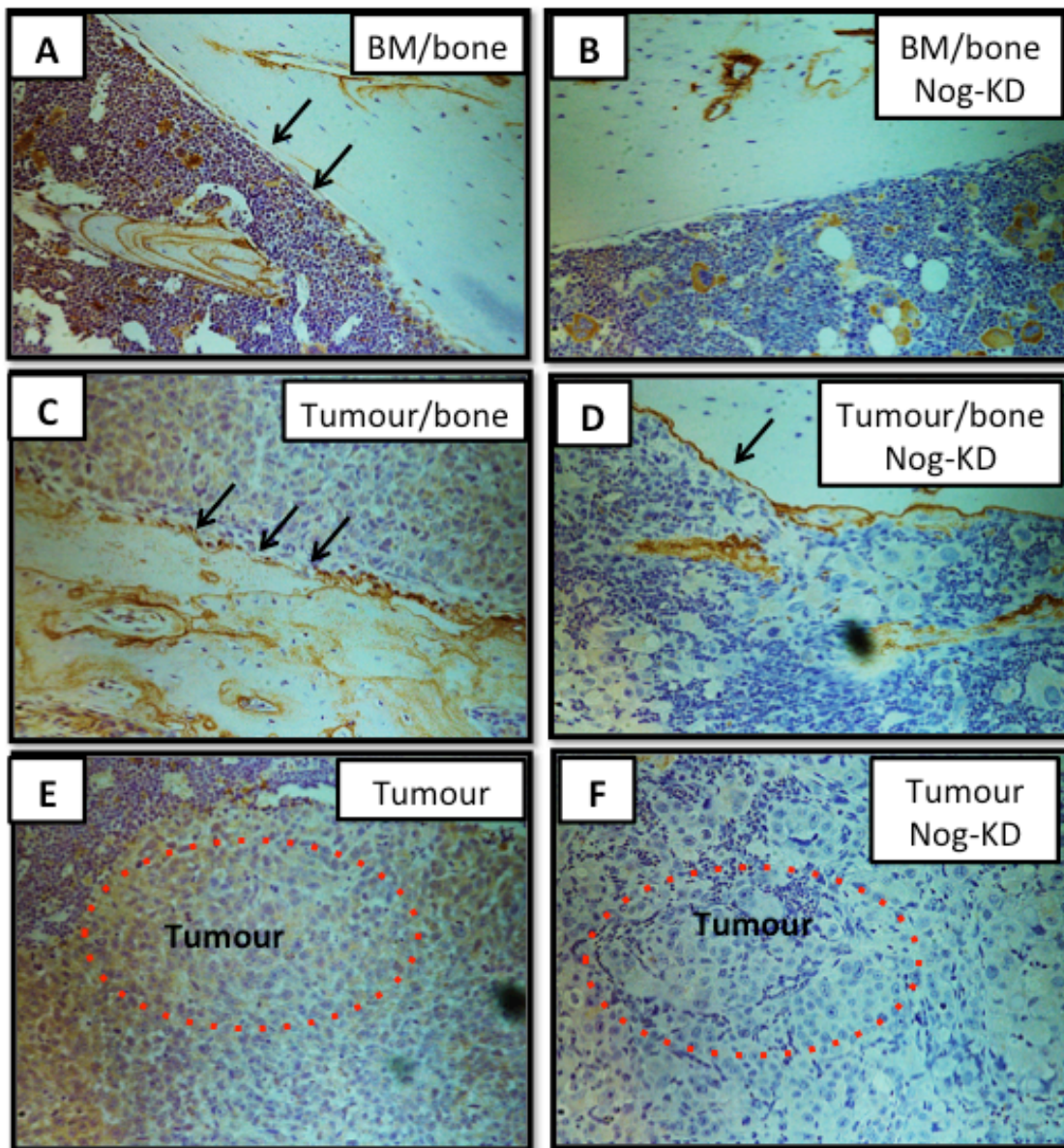


Figure 6.5 Noggin was expressed on the bone lining cells and bone surface in vivo in BALB/C nude male mice.

Illustrate Noggin distribution in bone section from two groups of mice injected with either PC3-mock or PC3-KD cells where arrow indicate dark brown staining of Noggin protein panel (A) shows strong Noggin staining in osteoblasts in bone marrow of control mice. Panel (B) shows weak Noggin staining in bone marrow of mice injected with PC3-KD cells. Panel (C) shows strong Noggin staining on the bone lining cells and bone surface when tumour cells came close to the bone of control mice. Panel (D) shows very weak Noggin staining on the bone lining cells and bone surface when tumour came close to the bone of mice injected with PC3-KD cells. Panel (E) shows strong Noggin staining within the tumour cells in control mice. Panel (F) there was no Noggin staining presented in the tumour cells in mice injected with PC3-KD cells.

6.4 Discussion

Many difficulties have confronted the demonstration of bone homing in prostate cancer preclinical studies due to restriction in available cell lines and to technical problems in reproducing bone metastasis *in vivo* (Rucci and Angelucci 2014). Many prostate cancer cell lines that were used in experimental animals were genetically engineered by either overexpression or by deletion of specific genes prior to use (Kaplan-Lefko *et al.* 2003). These animal models partially demonstrate the progression of human disease and metastases to the bone. (Isaacs *et al.* 1986; Gingrich *et al.* 1996). In this study bone metastases was induced by introducing PC3-mock cells as a control and Noggin knockdown PC3-KD cells into immunocompromised mice through intra-cardiac injection. Direct injection into the left cardiac ventricle has been shown to increase the incidence of bone metastases compared to intravenously injection into the tail (Arguello *et al.* 1988). However, the frequency of tumour development in the two groups throughout the entire duration of the experiment, which was 12 weeks, was below that expected. This difficulty in achieving adequate bone metastases *in vivo* models using tumour cells strains has been reported by others (Rucci and Angelucci 2014). This may be due to several factors including the long latency time in natural development of bone metastases and the phenotypic modification induced by *in vitro* culture of cancer cell lines/strains and their cloning, which may result in reduction in their tumourigenicity (Shevrin *et al.* 1988; Nemeth *et al.* 1999; Rucci and Angelucci 2014). Recent studies in my group suggest that the frequency of tumour formation depends on numbers of metastasis initiating cells (Kang *et al.* 2003) and it is possible that these were not included in the cells selected and cloned during the generation of PC-3Mock or KD cells.

In this study there was no difference in the trabecular bone volume (BV/TV), trabecular number (Tr No) and trabecular thickness (Tr Th) between the two groups. This is different from a study done by Secondini *et al* where she found that the bones of BALB/c nude male mice aged 7-8 weeks xenografted with Noggin silenced PC3 cells were characterized by structural and histological modification: tibia in mice xenografted with Noggin knockdown PC3 had higher BV/TV ratio than those engrafted with mock clones. Moreover, these studies showed that in the xenograft model, silencing Noggin in cancer cells had a moderate impact on their proliferation *in vivo* initially they grow with similar rate compared to xenograft model with mock or control PC3 cells, but tumour growth slowed down in Noggin knockdown group at

later time points. Injecting the PC3 control and mock cells through intra-cardiac injection in mice caused systematic bone metastases mostly to the jaw limiting the duration of the experiment making it difficult to compare between control, mock group and knockdown group (Secondini *et al.* 2011). In a study done by Feeley *et al* it was reported that when PC3 control, PC3 mock and PC3 over expressing Noggin cells were injected directly into the tibiae of SCID mice aged 8 weeks, PC3 control cells implanted into tibia formed osteolytic lesions as early as 2 weeks and completely destroyed the tibia after 8 weeks while, cells over expressing Noggin inhibited the expansion of this lesions (Feeley *et al.* 2006). In another study, Schwaninger *et al* studied the effect of Noggin on the osteoblast response in bone metastases by injecting osteoinductive prostate cancer cells (C4-2B) or the over expressing Noggin clone (C4-2B-Nog) into the tibia of SCID and BALB/c nude mice aged 7 weeks. The tibia inoculated with C4-2B-Nog cells showed a significantly lower expression of the structural parameters of excesses of bone formation, such as high total bone area (TBA), trabecular bone area (TrBA) and content (TrBC) compared with tibia implanted with parental C4-2B or mock cells. He concluded that over expression of Noggin in Prostate cancer cells (C4-2B) cells caused an elimination of their osteoinductive activity (Schwaninger *et al.* 2007). However, a study done by Canalis reported that both male and female Noggin conditional null mice had decreased trabecular bone volume compared to control mice thus inactivation of Noggin in adult male and female mice caused osteopenia, indicating that Noggin is important not only in skeletal development but also in normal postnatal bone remodelling (Canalis *et al.* 2012). In addition Noggin was found to be an essential actor in providing breast metastatic cancer cells with bone colonization capabilities. Following Intra-cardiac injection of breast cancer bone metastatic cell line 1833 and these cells knocked-down for Noggin into nude male BALB/c mice aged 8 weeks, Noggin knockdown cells had dramatically reduced the capacity to form bone metastases as well as reduced metastatic weight after the first week of injecting and continued throughout the entire experiment. On the other hand, forced over expressing Noggin in SKBr3 cells, which normally express low level of Noggin and poorly colonize to bone led to a significant increase in the probability to develop bone metastases and an intense increase in the metastatic weight during the 9 weeks experiment. This suggests that Noggin provides cancer cells with the ability to home, seed and colonize the bone by increasing their self renewal function as well as through altering the bone microenvironment (Tarragona *et al.* 2012).

In this study histologic sections of tibial trabecular bones from both groups were taken after the 12th weeks. Immunohistochemistry using Noggin antibody was used to localize Noggin protein in both bone and tumour. Noggin protein represented by dark brown stain was found to be on the bone surface and bone lining cells when tumour came close to bone. Earlier studies revealed that Noggin was expressed mainly in the osteoblast, chondrocyte, mesenchymal and in macrophages cells (Warren *et al.* 2003; Wu *et al.* 2003). In addition other investigators has detected Noggin by using immunocytochemically techniques at fracture sites and where BMP induced formation is high (Nakase *et al.* 1994; Yoshimura *et al.* 2001).

In conclusion Noggin was found to enhance the growth of osteoblast cells *in vitro*. This was determined by evaluating the effect of conditioned media from both knockdown and mock PC3 cells as well as the effect of supplementing the media with recombinant Noggin on the proliferation of osteoblast cells. However there were no differences between the two groups injected by either PC3-mock or PC3-KD cells *in vivo*. The low take rate in long bones compared to native PC3 cells that had not been genetically manipulated suggests that the experiment may have been compromised by factors associated with the cloning process. The association of Noggin staining with bone surfaces adjacent to tumour foci is an interesting and novel finding.

Chapter 7 General Discussion

7 Chapter 7 General Discussion

7.1 General Discussion

Prostate cancer is one of the most common types of cancer in men worldwide and around 90% of patients with advanced prostate cancer develop bone metastases (Larson *et al.* 2014). Bone metastasis is a key event responsible for the morbidity in these patients since once the tumour reaches the bone (Özdemir *et al.* 2014), the disease is incurable. The formation of metastases is a multistep process. After local invasion of tumour cells in the primary site, metastases proceeds by migration of cancer cells through the surrounding extracellular matrix and intravasation into blood capillaries. Circulating cancer cells have to survive in the blood before they start to colonize and proliferate to the distal organ (Leber and Efferth 2009). In the case of prostate cancer bone is the most common single site of metastasis (Saitoh *et al.* 1984). The bone microenvironment is a rich source of growth factors, cytokines, chemokines and signalling molecules, which potentially aid the survival and growth of tumour cells within the bone (Suva *et al.* 2011). It has been suggested that tumour cells interact with bone microenvironment by enhancing osteoblast and osteoclast activity which in turn stimulates the release of these growth factors from the bone matrix generating a so called “vicious cycle”. This is of great importance in tumour growth and progression. There are other reasons why the bone a special site for metastases: The blood sinusoids are thin walled and easily invaded and the environment also contains specialised ‘niches’ for stem cells (mesenchymal and hematopoietic) as well as a rich milieu of growth factors and cytokines and immune cells located within the bone marrow (Shiozawa *et al.* 2011; Chirgwin 2012). Disseminated tumour cells have been shown to hijack these niches on arrival in bone. The effect of these niches is complex and little understood but they may allow tumour cells to remain dormant within bone or induce the formation of micro-metastases, which afterward progress to clinically detectable lesions (Shiozawa *et al.* 2011; Chirgwin 2012). Thus further research is needed in order to acquire agents that prevent the development of bone metastases by either preventing tumour cell occupancy of niches in bone or by preventing tumour cells escape from dormancy.

Though radical prostatectomy has a significant effect on survival up to 30% of patients may need other treatment in the form of androgen deprivation both by surgical or chemical castration and up to 15% in the form of radiotherapy for local recurrence and previously undetected metastatic disease (Bill-Axelsson *et al.* 2014). This outcome for patients who present with treatable disease initially but who go on

to develop life threatening disease sometimes many years later is direct evidence that the disease can remain dormant for long periods. The problem with systemic treatments is that with time cancer cells become resistant to such therapy (Goktas and Crawford 1999). Therefore further research is needed to define the mechanisms that are involved in the initiation and progression of metastatic growth in order to help in the development of new therapeutic targets for the prevention and treating cancer metastases.

The aim of this study was to investigate the interaction between the osteolytic prostate cancer cells (PC3RFP) and osteoblastic cells with different degrees of maturation (SaOS2 and MG63) either through direct (co-culture) or indirect contact (treating the cells with PCRFP-CM) and to determine how members of the TGF- β superfamily contributed to the modification of the bone microenvironment. This study will test the hypothesis that tumour derived TGF- β signalling is an important component of the signalling between prostate cancer and bone cells.

This study started by determining general growth characteristics of all the cell lines used, since generating this type of information is an essential prerequisite before undertaking further experiments. In this study, the expression of 43 members of the TGF- β superfamily genes were studied in both prostate cancer (PC3RFP) cells and osteosarcoma (SaOS2, MG63) cells grown in isolation, in co-cultures where osteoblastic cells came to direct contact with PC3RFP and in experiment were these cells were treated with PC3RFP- conditioned medium (CM). PC3RFP was found to express Noggin, which was detectible in conditioned media and also BMP3 at elevated levels compared to osteoblastic cells while SaOS2 was found to express TGF- β 1, TGF- β 2 and BMP4 at higher levels than prostate cancer cells. This expression pattern changed when these cells came into direct contact with each other, where SaOS2 cells expressed more Noggin, BMP3 and BMP6 than when these cells were grown alone. Noggin was the only gene in SAOS2 cells where expression was affected by treating cells with PC3RFP-CM. **PC3RFP conditioned media (PC3RFP-CM) was found to enhance the proliferation of SaOS2 especially when cells become close to confluence and decreased their early differentiation stage by decreasing alkaline phosphatase level but with increased level of mineralization.** This diverse effect of conditioned media on the differentiation of osteoblasts cells were reported by other researchers and could be related to fundamental difference in the types of bone cells used or might be due to

different experimental conditions in each model system (Eaton and Coleman 2003). The effect of PC3RFP-CM on the rate of proliferation was only seen in SaOS2 cells and not in the MG63. This difference in osteoblast lineage cell responses to conditioned media collected over prostatic cancer cells did not appear to be due to differences in their native differentiation status, since differentiation of MG63 cells to more a osteoblastic phenotype did not alter responses to CM. The transforming growth factor beta superfamily which plays an important roles in early development, homeostasis is also involved in the pathogenesis of many disease including bone metastases. More over, this superfamily is essential in the differentiation of mesenchymal stem cells (MSCs) into osteoblasts (Maeda *et al.* 2004; Janssens *et al.* 2005). Some of these factors are produced at higher levels by bone cells while others are expressed more highly by prostate cancer cells. For example TGF- β is abundant in bone matrix and contribute to osteoblastic bone formation (Wrana *et al.* 1988). TGF- β family members have been associated with tumour progression in many types of cancer including prostate cancer and breast cancer. Human prostate cancer including PC3 cells is characterized by high-affinity TGF- β receptors (Wilding *et al.* 1989; Barrack 1997). A previous study showed that osteoblasts can regulate prostate cancer migration and invasion *in vitro* by producing several factors including TGF- β 1, which contributes to the increase invasion capacity (Festuccia *et al.* 1999).

TGF- β is present in bone matrix in an inactive form thus can be activated upon bone resorption through the osteolytic activity of osteoclasts (Oursler 1994; Janssens *et al.* 2005). The activated TGF- β stimulates migration of bone mesenchymal stem cells (MSCs) to bone-resorptive surface where BMPs induce their differentiation toward osteoblast lineage (Tang *et al.* 2009). De Gorter *et al* reported that the effect of TGF- β on BMP-induced osteoblast differentiation depended on timing thus during early differentiation stage recruited MSCs respond to both BMP and TGF- β signals that enhance the differentiation process. During later stages of differentiation the concentration of cytokines found in the bone microenvironment and the responses of the differentiated cells changes to a point where TGF- β is likely to have an inhibitory effects on BMP induced signal transduction and osteoblast differentiation. It was found in the same study done by De Gorter et al that basal mineralization of hMSCs were enhanced through the short term stimulation of TGF- β and this could be blocked by Noggin, suggesting that TGF- β stimulates osteoblast differentiation induced by BMP produced by the cells themselves. This might explain the inhibitory effects of TGF- β that have been reported (de Gorter *et al.* 2011). Furthermore, Runt-

related transcription factor 2 (Runx2) and Osterix act via two important pathways, Wnt and BMP signalling, that are involved in the early step of differentiation, converting MSCs towards an osteo/chondroprogenitor and then toward an osteoblastic phenotype (Del Fattore *et al.* 2012). Deregulation of these two pathways has been associated in prostate cancer bone metastases. Both BMP2 and Runx2 have overlapping and different effects to promote osteoblast differentiation (Ogasawara *et al.* 2004). It was reported in a previous study that Runx2 were underexpressed in many osteosarcoma cell lines including SaOS2 cells compared to osteoblast-like reference cells and that SaOS2 cells express the osteoblast-specific MASN isoform of Runx2 which have the ability to stimulate osteocalcin, expression the gene product responsible for mineralization but not ALP (Harada *et al.* 1999; Thomas *et al.* 2004).

The TGF- β superfamily including BMPs and their antagonists contribute to the pathogenesis of carcinomas at different stages. At an early stage of cancer TGF- β acts as tumour suppressor arresting the growth of many cell types, while, at later stages these growth factors contribute to cancer progression and tumour invasiveness. As tumours progress cancer cells tend to lose the tumour –suppressive response to TGF- β (Buijs *et al.* 2012) acquiring somatic mutations in components of the TGF- β -Smad signal transduction pathway allowing cancer cells to escape the TGF- β anti-proliferative response. TGF- β in these cells acts as an oncogenic/tumour progression factor by inducing their proliferation, angiogenesis, invasion and metastases (Seoane 2006). In tumours where TGF- β does not directly inhibit growth, tumour cells express high levels of TGF- β , which may be a result of induction of its own expression, creating a malignant autocrine positive feedback loop (Seoane 2006). TGF- β also enhanced tumour progression by suppressing the anti-tumour immune response by inhibiting the proliferation and differentiation of immune cells, specifically T cells, in tumours that are resistant to the anti proliferative effect of this growth factor (Weinberg 2007).

Mitotic dormancy is a key feature of tumour cells that take up residency in metastatic sites in bone (Willis RA 1934; Banyas *et al.* 2012). This may be a survival mechanism that allows tumour cells to establish themselves in a new location before being activated to divide. The tumour cells that enter the premetastatic niche express surface ligands and receptors (integrins, cadherins and fibronectin), which facilitate interaction with an accommodating environment for migrating tumour cells (Kaplan *et*

al. 2005). The interaction between receptors in the bone marrow stroma such as urokinase receptor, vascular cell adhesion molecule-1, fibronectin and the ligands for the latter over-expressed on the tumour cells including β_1 , $\alpha_4 \beta_1$ and $\alpha_5 \beta_1$ integrin, cadherin-11 and CXCR4 facilitates the colonization of circulating cancer cells in the bone marrow (Mastro *et al.* 2003; Yoneda and Hiraga 2005). Growth factors such as TGF- β s and BMPs that are stored in the bone matrix are released during bone remodelling may aid cancer cell colonization of bone as well as enhancing their proliferation (Hauschka *et al.* 1986; Feeley *et al.* 2005).

There are two general histological types of bone metastases classified as either osteolytic or osteoblastic but it is generally accepted that patients can have both osteolytic and osteoblastic components in their metastases (Coleman 1997; Mundy 2002). It has been demonstrated that osteoblastic metastases occurring in prostate cancer also involve considerable osteolysis since blood and urinary samples from these patients contains high levels of bone resorption markers (Garnero *et al.* 2000). Studies showed that BMPs are involved in prostate carcinogenesis (Ide *et al.* 1997; Tamada *et al.* 2001; Ye *et al.* 2007). In a study done by Kim *et al.* investigating the role of BMPs and their receptors and their correlation with the grade of prostate cancer showed that high grade prostate cancer cells lose BMP receptors and this also correlated with high frequency of prostate cancer metastases to bone (Kim *et al.* 2000). It was reported by a previous study that TGF- β had a significant effects on PC3 adhesion to bone endothelial cells. Cooper *et al.* showed that different BMPs have different effect on PC3 cell adhesion to bone marrow endothelium and specifically that BMP4 increased adhesion (Cooper *et al.* 2003). It is also reported that BMP2 aids the migration of prostate cancer cells through the activation of Akt and ERK, which in turn activate NF- κ B thus activating β_1 and β_3 integrins (Lai *et al.* 2008). A study done by Buijs *et al.* suggested a cross talk between BMP7, BMP6 and TGF- β signalling regulated epithelial to mesenchymal transition (EMT) in tumour cells and facilitated their migration into new microenvironments. TGF- β_1 and BMP6 were found to induce EMT while BMP7 treatment significantly inhibited EMT, inducing the reverse process MET and inhibiting bone metastases by breast and prostate cancer cells *in vivo* (Buijs *et al.* 2007). This results was supported by further investigation indicating that BMP7 and its receptor BMP7R are important in suppressing the growth of prostate cancer cells in bone and induce senescence in these cells however this effect was reversible upon withdrawal of BMP7. This results suggest that BMP7 and its receptor plays essential role in dormancy and recurrent of the

disease (Kobayashi *et al.* 2011). This may be related to tumour cell interaction with the metastatic niche: EMT is required to enter the niche in a dormant state and MET required to activate proliferation via altered interactions in the niche or exit from this structure.

A recent study done by Naber *et al* concluded that BMP-7 inhibit bone metastases in both breast and prostate cancer and it is able to inhibit the tumour-promoting effect of TGF- β through either Smad and non-Smad mechanisms depending on the type of cell. He showed that the inhibitory effect of BMP-7 on breast cancer invasion can be explained by the inhibition of TGF- β which induced the expression of integrin β 3 and enhanced EMT (Naber *et al.* 2012). However, Noggin inhibits BMP-7 but have no effect on BMP-6 (Song *et al.* 2010). It is now clear that the metastatic process in epithelial cancers requires both EMT and MET to be sequentially induced: EMT is needed to allow tumour cells to escape the primary tumour and MET is required to establish growing lesions in the metastatic site (Chaffer *et al.* 2007; Polyak and Weinberg 2009; van der Pluijm 2011). In order for cancer cell to leave its primary site cancer cells must shed many of their epithelial characteristics and acquire a mesenchymal migratory phenotype thus increasing their motility and invasiveness (Thiery 2002; Kalluri and Weinberg 2009). During cancer progression the expression of E-cadherin which are normally expressed by epithelial cells, are either be functionally inactive or silenced by many suppressors such as Snail1 and Snail2 (Thiery 2002). Thus cancer cells switches from E-cadherin to N-cadherin and initiates EMT (Chaffer *et al.* 2007; Kalluri and Weinberg 2009). There are many pathways that are involved in the regulation of EMT processes including TGF- β , Notch, Wnt and IGF many of these factors are involved in bone metastases. In addition there are other factors that are also involved including cell-cell adhesion and others such as hypoxia and the effects microRNAs (Chaffer *et al.* 2007; Dunn *et al.* 2009; Kalluri and Weinberg 2009). On the other hand some BMPs can oppose factors that stimulate EMT in many cell types and induce MET (Buijs *et al.* 2007; Scheel *et al.* 2011; Buijs *et al.* 2012). BMP expression in this case could be considered to be an important protective mechanism preventing tumour cells from further colonization. Conversely overexpression of the BMP antagonist Noggin could suppress this control and enhance metastatic activity (Gao *et al.* 2012; Tarragona *et al.* 2012) Figure 1.7 summarizes the role of TGF- β , BMP7 and its antagonist Noggin in tumour invasion and colonization into the bone. A study done by Van den Hoogen reported the association of α v integrin with the invasion and migration capability of prostate cancer

cells since silencing this receptors resulted in a decreased stem/progenitor cell characteristic and a decreased in the expression of invasion associated genes Snail1, Snail2 and Twist (van den Hoogen *et al.* 2011). This again highlights the significance of cellular attachment and EMT/MET status in the metastatic process.

Among all TGF- β superfamily and their antagonists analysed in this study I focused on Noggin as a BMP antagonist as a potential regulator of bone metastasis. In this study I found that treating osteoblasts (SaOS2) cells with conditioned media collected over PC3RFP cells stimulated the expression of Noggin by SaOS2 cells.

Noggin is a secreted glycoprotein monomer but normally occurs as a homodimer and has a cysteine-rich C-terminal region (Yanagita 2005; Krause *et al.* 2011). It was reported that Noggin bound with different affinities to different BMPs. Noggin binds strongly to BMP2 and BMP4 and with lower affinity to BMP6 and BMP7 (Krause *et al.* 2011). Sclerostin (SOST) another BMP antagonist has the ability to also bind Noggin limiting the inhibitory effect of Noggin and increasing BMP availability (Winkler *et al.* 2004). It was reported in an *in vivo* study using a bone tumour model, that exposing the tumour to Noggin reduced the size of bone lesions by a mechanism that involve both osteoblastic and osteolytic processes (Ye *et al.* 2007). Both Noggin and follistatin determine cell responses to BMPs, however, the expression of these antagonists can be controlled by BMPs themselves via an autocrine or paracrine feedback loop (Ye *et al.* 2007). In an agreement with our results, a study done by Yoshimura *et al.* 2001 reported that osteoblast do not normally express Noggin, suggesting that the amplified Noggin mRNA signal in osteoblastic cells in this study may be as a result of enhanced expression of BMPs and BMP receptors (Gazzerro *et al.* 1998). Therefore growth factors and BMPs BMP2, BMP4, BMP6 and TGF- β produced from prostate cancer cells (PC3RFP) may be responsible from stimulated Noggin expression in osteoblasts cells (SaOS2) found in my study. A study done by Hsu *et al.* reported that Noggin overexpressing melanoma cells showed a growth advantage in response to subsequent BMP7 transduction both *in vitro* and *in vivo*, whereas, Noggin knockdown melanoma cells exhibited a growth inhibition. This implies that Noggin up regulation may cause advanced melanoma cells to escape from BMP7-mediated autocrine growth inhibition (Hsu *et al.* 2008). Noggin may have a similar the role in breast cancer metastasis to bone since over expression of Noggin increased the growth rate of bone metastasis in an orthotopic mouse model. Moreover in the same study it was found that silencing Noggin (shRNA targeting

Noggin gene) caused growth rate reduction of bone metastases (Tarragona *et al.* 2012). Noggin is suggested to modulate cancer cells through stimulating ID2 and subsequently may increase the level of RANK expression which is linked to chemotherapy resistance (Schramek *et al.* 2010). It has been suggested that Noggin compromised BMP signaling in turn results in the activation of stem cell self-renewal pathways (Wakefield and Hill 2013). This may open the possibility of Noggin being linked not only to the ability of metastatic cells to successfully metastasize to the bone but also to the ability of self-renewal activity acquired by metastatic cells and to acquiring chemotherapy resistant (Tarragona *et al.* 2012). Schwaninger et al reported that forced Noggin expression in an osteoinductive prostate cancer cell line suppressed the osteoblastic response observed when these cells were injected into bone *in vivo*, suggesting that lack of Noggin production by cancer cells is part of the mechanism controlling the balance between osteolytic and osteoblastic responses in bone metastases (Schwaninger *et al.* 2007).

In conclusion the *in vitro* results obtained from this study showed that growth factors and other molecules produced by prostate cancer cells affected both proliferation and initial differentiation of SaOS2 cells. In addition it showed that prostate cancer cells affect the gene expression of TGF- β superfamily genes during their interaction with SaOS2 cells either directly or indirect. More attention was given to Noggin, a BMP antagonist that was expressed and secreted by PC3RFP cells while being expressed in a very low level by SaOS2. This pattern of Noggin gene expression changed after treating the cells with conditioned media derived from PC3RFP cells leading to enhanced expression of this gene by osteoblastic cells. The effect of Noggin on the proliferation of osteoblastic cells was also assessed by either treating the cells with PC3-KD conditioned media or by media supplemented with recombinant Noggin. Silencing Noggin in PC3 cells inhibited the growth of SaOS2 cells while media containing recombinant Noggin stimulated its growth. However the amount of recombinant Noggin that were required to increase the growth of SaOS2 cells were much higher than the amount of Noggin present in the condition media. This result suggests that the enhanced growth of osteoblasts cells may not be due to Noggin secreted from prostate cancer cells but due to the stimulated expression of Noggin by osteoblast cells themselves. Induced autocrine or even intracrine Noggin activity in osteoblasts would be dependent on local levels surrounding or inside cells that could reach those present in medium supplemented with recombinant Noggin.

In this study, mice injected with either PC3-Mock or with PC3-KD cells did not develop the numbers of bone metastases expected for PC3 cells. These cells were injected into left cardiac ventricle so it was expected that not all of these cells would home to bone and establish metastatic lesions, but it was expected that around 20% of controls would develop long bone tumours in 12 week old animals. The problem encountered here may be due to clonal selection after genetic manipulation. Difficulty in achieving adequate bone metastases *in vivo* models using tumour cells strains that have been genetically modified has been reported by others (Rucci and Angelucci 2014). This may be due to many different factors including the long latency time in natural development of bone metastases and the phenotypic modification induced by *in vitro* culture of cancer cell lines/strains and their cloning, which may result in reduction in their tumorigenicity (Shevrin *et al.* 1988; Nemeth *et al.* 1999; Rucci and Angelucci 2014). Recent studies in my group suggest that the frequency of tumour formation depends on numbers of metastasis initiating cells (Kang *et al.* 2003) and it is possible that these were not included in the cells selected and cloned during the generation of PC-3Mock or KD cells.

In this study histologic sections of tibial trabecular bones were taken from both groups and Noggin protein was localized in both bone and tumour. Noggin protein represented by dark brown stain was found to be on the bone surface and bone lining cells when tumour came close to bone. Moreover, other investigators have detected Noggin by using immunocytochemically techniques at fracture sites and where BMP induced formation is high (Nakase *et al.* 1994; Yoshimura *et al.* 2001).

The *in vitro* data suggested that Noggin regulates osteoblastic cell differentiation/proliferation and it would be predicted that this would result in the formation of osteolytic lesions *in vivo*. This may also enhance the growth of PC3 cells in bone via release of factors sequestered in bone. Conversely, knock down of Noggin would result in more osteoblastic lesions and possibly reduced tumorigenicity. This will have to be retested in better knock down/knock-out models made without clonal selection.

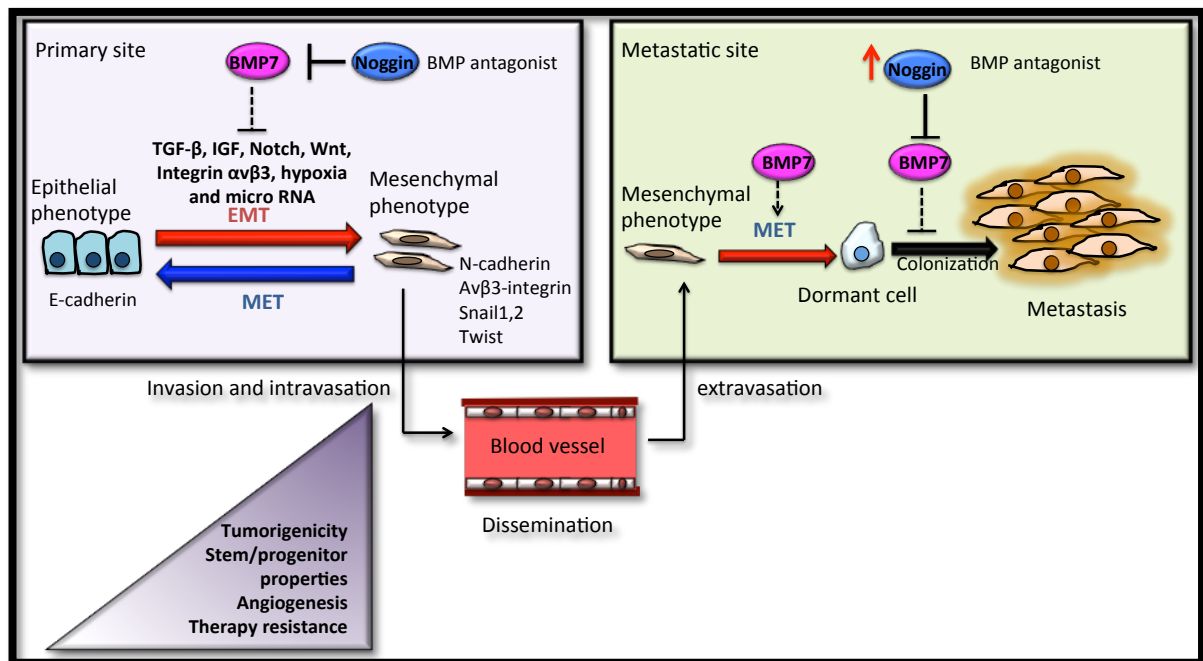


Figure 7.1 Scheme showing the role of TGF- β , BMP7 and Noggin in cancer invasion and colonization.

Many EMT effectors are identified including TGF- β , IGF, Notch, Wnt, integrin $\alpha\beta 3$ and other microRNA that stimulate EMT processes and make cancer cells lose their epithelial characteristics such as E-cadherin and acquiring mesenchymal phenotype. This process could be either blocked by BMP7 or enhanced under the influence of BMP antagonist (Noggin). Cancer cells with mesenchymal phenotype have the ability to invade and enter the blood vessels and disseminated in distal organ most commonly the bone in case of prostate cancer. Bone express normally high level of endogenous BMP, which may promote a mesenchymal to epithelial transition, MET in the newly arrived tumour cells. They also may maintain the disseminated tumour cells in dormant state this could be overcome in tumour cells expressing high level of BMP antagonists Noggin.

7.2 Future work

Metastasis is responsible for the majority of prostate cancer deaths and the primary site for metastatic lesions in this disease is the skeleton. Understanding mechanisms that facilitate the formation of metastases to the bone is needed if drugs are to be designed to prevent or interfere with prostate cancer metastasis. It is known that once prostate cancer cells disseminated in the bone, a cross talk between the bone microenvironment factors and factors produced from prostate cancer cells contribute to the establishment of lesions (Ganguly *et al.* 2014). In this study most focus has been given toward one of the BMP antagonist, Noggin. Noggin is known to play role in prostate cancer bone metastases. The finding that tumour cells can induce the expression of this potentially autocrine factor in bone cells is an important novel finding of the study. Further investigation of factors that regulate the expression of this protein is required for better understand this interaction. In addition it may be useful to study microRNAs, which, are highly conserved small RNAs molecules that regulate gene expression. A study done by Peng *et al* Compared arrays-based miRNA profiles of human primary prostate tumours and matched bone metastases and showed that expression levels of miRNA-145, -143, -33a, -100 and -508-5p were the most highly down regulated in bone metastases specimen. It was reported in the same study that ectopic expression of miRNA-143 and miRNA-145 in the aggressive and androgen insensitive PC3 prostate cancer cell line reduced the migratory and invasive capacities of these tumour cells *in vitro* and their tendency to metastasise to bone *in vivo* (Peng *et al.* 2011). Another study done by Pollari *et al* identified certain types of miRNAs that down regulate a set of genes involved in TGF- β signalling (Pollari *et al.* 2012).

The host environmental factors play a major role in prostate cancer metastases to bone understanding these factors require the use of animal model. The most commonly used model is the immunosuppressed mouse, which differ significantly from humans in both the structure and physiology of prostate gland and in the support of tumour growth (Ganguly *et al.* 2014). Adding to this the difficulty of initiating bone metastases in mouse model when using genetically modified prostate cancer cell lines. These cells were used in *in vitro* culture where their activity appeared to support a role for Noggin but their cloning, may have resulted in a reduction in their tumourigenicity. Developing a wider range of Noggin-KD or knock out models that have not been cloned would be helpful here. However my own

experience attempting to make Noggin-KD models and the difficulties I know others have had in generating these cells may mean that this will be a challenge. The foregoing certainly suggests that there is a need to develop a better tumour/animal models that fully recapitulate the metastatic process as seen in human disease and retain tumourogenicity *in vivo* after manipulation in order to investigate the molecular events associated with prostate cancer metastases further. It may then be possible to repeat the experiments presented here to more definitively evaluate the effects of TGF β 1, BMPs and Noggin on prostate cancer metastasis.

Reference

- Abdollah, S., M. Macías-Silva, T. Tsukazaki, H. Hayashi, L. Attisano and J. L. Wrana (1997). "T β RI Phosphorylation of Smad2 on Ser465 and Ser467 Is Required for Smad2-Smad4 Complex Formation and Signaling." Journal of Biological Chemistry **272**(44): 27678-27685.
- Ahrens, M., T. Ankenbauer, D. Schroder, A. Hollnagel, H. Mayer and G. Gross (1993). "Expression of human bone morphogenetic proteins-2 or -4 in murine mesenchymal progenitor C3H10T1/2 cells induces differentiation into distinct mesenchymal cell lineages." DNA Cell Biol **12**(10): 871-880.
- Alarmo, E. L., R. Kuukasjarvi T Fau - Karhu, A. Karhu R Fau - Kallioniemi and A. Kallioniemi (2006). "A comprehensive expression survey of bone morphogenetic proteins in breast cancer highlights the importance of BMP4 and BMP7." Breast Cancer reaserch Treatment **103**(0167-6806 (Print)): 239-246.
- An, D. S., Y. Xie, S. H. Mao, K. Morizono, S. K. Kung and I. S. Chen (2003). "Efficient lentiviral vectors for short hairpin RNA delivery into human cells." Hum Gene Ther **14**(12): 1207-1212.
- Anderson, H. C. (2003). "Matrix vesicles and calcification." Current Rheumatology Reports **5**(3): 222-226.
- Aono, A., M. Hazama, K. Notoya, S. Taketomi, H. Yamasaki, R. Tsukuda, S. Sasaki and Y. Fujisawa (1995). "Potent Ectopic Bone-Inducing Activity of Bone Morphogenetic Protein-4/7 Heterodimer." Biochemical and Biophysical Research Communications **210**(3): 670-677.
- Arguello, F., R. B. Baggs and C. N. Frantz (1988). "A Murine Model of Experimental Metastasis to Bone and Bone Marrow." Cancer Research **48**(23): 6876-6881.
- Arteaga, C. L. (2006). "Inhibition of TGF[beta] signaling in cancer therapy." Current Opinion in Genetics & Development **16**(1): 30-37.
- Asahina, I., T. K. Sampath, I. Nishimura and P. V. Hauschka (1993). "Human osteogenic protein-1 induces both chondroblastic and osteoblastic differentiation of osteoprogenitor cells derived from newborn rat calvaria." The Journal of Cell Biology **123**(4): 921-933.
- Attisano, L., J. Cárcamo, F. Ventura, F. M. B. Weis, J. Massagué and J. L. Wrana (1993). "Identification of human activin and TGF 2 type I receptors that form heteromeric kinase complexes with type II receptors." Cell **75**(4): 671-680.
- Attisano, L., J. Wrana, E. Montalvo and J. Massague (1996). "Activation of signalling by the activin receptor complex." Mol. Cell. Biol. **16**(3): 1066-1073.
- Autzen, P., C. N. Robson, A. Bjartell, A. J. Malcolm, M. I. Johnson, D. E. Neal and F. C. Hamdy (1998). "Bone morphogenetic protein 6 in skeletal metastases from prostate cancer and other common human malignancies." Br J Cancer **78**(9): 1219-1223.
- Baade Ro, T., R. Utne Holt, A.-T. Brenne, H. Hjorth-Hansen, A. Waage, O. Hjertner, A. Sundan and M. Borset (2004). "Bone morphogenetic protein-5, -6 and -7 inhibit growth and induce apoptosis in human myeloma cells." Oncogene **23**(17): 3024-3032.
- Banys, M., A. D. Hartkopf, N. Krawczyk, T. Kaiser, F. Meier-Stiegen, T. Fehm and H. Neubauer (2012). "Dormancy in breast cancer." Breast Cancer : Targets and Therapy **4**: 183-191.

- Barnes, J., N. Anthony Ct Fau - Wall, M. S. Wall N Fau - Steiner and M. S. Steiner (1995). "Bone morphogenetic protein-6 expression in normal and malignant prostate." World journal of urology **13**(0724-4983 (Print)): 337-343.
- Barrack, E. R. (1997). "TGF β in prostate cancer: A growth inhibitor that can enhance tumourigenicity." The Prostate **31**(1): 61-70.
- Bei, M. and R. Maas (1998). "FGFs and BMP4 induce both Msx1-independent and Msx1-dependent signaling pathways in early tooth development." Development **125**(21): 4325-4333.
- Bello-DeOcampo, D. and D. J. Tindall (2003). "TGF-beta1/Smad signaling in prostate cancer." curr Drug Targets **4**(1389-4501 (Print)).
- Bentley, H., K. A. Hamdy Fc Fau - Hart, J. M. Hart Ka Fau - Seid, J. L. Seid Jm Fau - Williams, D. Williams JI Fau - Johnstone, R. G. Johnstone D Fau - Russell and R. G. Russell (1992). "Expression of bone morphogenetic proteins in human prostatic adenocarcinoma and benign prostatic hyperplasia." Br J Cancer **66**(0007-0920 (Print)): 1159-1163.
- Bhattacharyya, R. S. and P. H. Stern (2003). "IGF-I and MAP kinase involvement in the stimulatory effects of LNCaP prostate cancer cell conditioned media on cell proliferation and protein synthesis in MC3T3-E1 osteoblastic cells." Journal of Cellular Biochemistry **90**(5): 925-937.
- Bhola, N. E., J. M. Balko, T. C. Dugger, M. Kuba, xEd, G. a, xE, V. nchez, M. Sanders, J. Stanford, R. S. Cook and C. L. Arteaga (2013). "TGF- β inhibition enhances chemotherapy action against triple-negative breast cancer." The Journal of Clinical Investigation **123**(3): 1348-1358.
- Bhowmick, N. A., M. Ghiassi, M. Aakre, K. Brown, V. Singh and H. L. Moses (2003). "TGF-beta-induced RhoA and p160ROCK activation is involved in the inhibition of Cdc25A with resultant cell-cycle arrest." Proc Natl Acad Sci U S A **100**(26): 15548-15553.
- Bierie, B. and H. L. Moses (2006). "Tumour microenvironment: TGF[beta]: the molecular Jekyll and Hyde of cancer." Nat Rev Cancer **6**(7): 506-520.
- Bill-Axelson, A., L. Holmberg, H. Garmo, J. R. Rider, K. Taari, C. Busch, S. Nordling, M. Häggman, S.-O. Andersson, A. Spångberg, O. Andrén, J. Palmgren, G. Steineck, H.-O. Adami and J.-E. Johansson (2014). "Radical Prostatectomy or Watchful Waiting in Early Prostate Cancer." New England Journal of Medicine **370**(10): 932-942.
- Blair, H. C. and N. A. Athanasou (2004). "Recent advances in osteoclast biology and pathological bone resorption." histology and histopathology **19**(0213-3911 (Print)): 189-199.
- Bollard, C. M., C. Rossig, M. J. Calonge, M. H. Huls, H.-J. Wagner, J. Massague, M. K. Brenner, H. E. Heslop and C. M. Rooney (2002). "Adapting a transforming growth factor beta -related tumour protection strategy to enhance antitumour immunity." Blood **99**(9): 3179-3187.
- Bonewald, L. F. and G. R. Mundy (1990). "Role of Transforming Growth Factor-Beta in Bone Remodeling." Clinical Orthopaedics and Related Research **250**: 261-276.

- Bonewald, L. F. and M. L. Johnson (2008). "Osteocytes, Mechanosensing and Wnt Signaling." Bone **42**(4): 606-615.
- Botchkarev, V. A. (2003). "Bone Morphogenetic Proteins and Their Antagonists in Skin and Hair Follicle Biology[ast]." J Investig Dermatol **120**(1): 36-47.
- Boyce, B. F., D. E. Hughes, K. R. Wright, L. Xing and A. Dai (1999). "Recent advances in bone biology provide insight into the pathogenesis of bone diseases." Lab Invest **79**(2): 83-94.
- Boyde, A., E. Maconnachie, S. A. Reid, G. Delling and G. R. Mundy (1986). "Scanning electron microscopy in bone pathology: review of methods, potential and applications." Scanning electron microscopy(Pt 4): 1537-1554.
- Boyle, W. J., W. S. Simonet and D. L. Lacey (2003). "Osteoclast differentiation and activation." Nature **423**(6937): 337-342.
- Bretland, A. J., S. V. Reid, C. R. Chapple and C. L. Eaton (2001). "Role of endogenous transforming growth factor β (TGF β) 1 in prostatic stromal cells*." The Prostate **48**(4): 297-304.
- Brunet, L. J., J. A. McMahon, A. P. McMahon and R. M. Harland (1998). "Noggin, Cartilage Morphogenesis, and Joint Formation in the Mammalian Skeleton." Science **280**(5368): 1455-1457.
- Bubendorf, L., A. Schöpfer, U. Wagner, G. Sauter, H. Moch, N. Willi, T. C. Gasser and M. J. Mihatsch (2000). "Metastatic patterns of prostate cancer: An autopsy study of 1,589 patients." Human Pathology **31**(5): 578-583.
- Buijs, J. T., C. A. Rentsch, G. van der Horst, P. G. M. van Overveld, A. Wetterwald, R. Schwaninger, N. V. Henriquez, P. ten Dijke, F. Borovecki, R. Markwalder, G. N. Thalmann, S. E. Papapoulos, R. C. M. Pelger, S. Vukicevic, M. G. Cecchini, C. W. G. M. Löwik and G. van der Pluijm (2007). "BMP7, a Putative Regulator of Epithelial Homeostasis in the Human Prostate, Is a Potent Inhibitor of Prostate Cancer Bone Metastasis in Vivo." The American Journal of Pathology **171**(3): 1047-1057.
- Buijs, J. T., G. van der Horst, C. van den Hoogen, H. Cheung, B. de Rooij, J. Kroon, M. Petersen, P. G. M. van Overveld, R. C. M. Pelger and G. van der Pluijm (2012). "The BMP2/7 heterodimer inhibits the human breast cancer stem cell subpopulation and bone metastases formation." Oncogene **31**(17): 2164-2174.
- Buijs, J. T., K. R. Stayrook and T. A. Guise (2012). "The role of TGF- β in bone metastasis: novel therapeutic perspectives." BoneKEy reports **1**: 96.
- Buijs, J., N. Henriquez, P. M. van Overveld, G. van der Horst, P. ten Dijke and G. van der Pluijm (2007). "TGF- β and BMP7 interactions in tumour progression and bone metastasis." Clinical & Experimental Metastasis **24**(8): 609-617.
- Burr, D. B. (2002). "Targeted and nontargeted remodeling." Bone **30**(1): 2-4.

- Canalis, E., et al. (2012). "Conditional Inactivation of Noggin in the Postnatal Skeleton Causes Osteopenia." Endocrinology **153**(4): 1616-1626.
- Cancer Research UK. (2011). "Cancer State report-most common cancer in male, percentages of all cancer." Retrieved 3 March 2015, 2015, from <http://www.cancerresearchuk.org/cancer-info/cancerstats/incidence/commoncancers/Ten>.
- Cao, X. and D. Chen (2005). "The BMP signaling and in vivo bone formation." Gene **357**(1): 1-8.
- Chaffer, C. L., E. W. Thompson and E. D. Williams (2007). "Mesenchymal to Epithelial Transition in Development and Disease." Cells Tissues Organs **185**(1-3): 7-19.
- Chang, H.-L., N. Gillett, I. Figari, A. R. Lopez, M. A. Palladino and R. Derynck (1993). "Increased Transforming Growth Factor β Expression Inhibits Cell Proliferation in Vitro, yet Increases Tumourigenicity and Tumour Growth of Meth A Sarcoma Cells." Cancer Research **53**(18): 4391-4398.
- Chang, H., C. W. Brown and M. M. Matzuk (2002). "Genetic Analysis of the Mammalian Transforming Growth Factor- β Superfamily." Endocr Rev **23**(6): 787-823.
- Charhon, S. A., M. C. Chapuy, E. E. Delvin, A. Valentin-Opran, C. M. Edouard and P. J. Meunier (1983). "Histomorphometric analysis of sclerotic bone metastases from prostatic carcinoma with special reference to osteomalacia." Cancer **51**(5): 918-924.
- Chen, M. L., M. J. Pittet, L. Gorelik, R. A. Flavell, R. Weissleder, H. von Boehmer and K. Khazaie (2005). "Regulatory T cells suppress tumour-specific CD8 T cell cytotoxicity through TGF- β signals in vivo." Proc Natl Acad Sci U S A **102**(2): 419-424.
- Chen, Y.-G., A. Hata, R. S. Lo, D. Wotton, Y. Shi, N. Pavletich and J. Massagué (1998). "Determinants of specificity in TGF- β signal transduction." Genes & Development **12**(14): 2144-2152.
- Chichester, C. O., M. Fernández and J. J. Minguell (1993). "Extracellular Matrix Gene Expression by Human Bone Marrow Stroma and by Marrow Fibroblasts." Cell Communication and Adhesion **1**(2): 93-99.
- Chirgwin, J. M. (2012). "The stem cell niche as a pharmaceutical target for prevention of skeletal metastases." Anticancer Agents Med Chem **12**(1875-5992 (Electronic)): 187-193.
- Clarke, B. (2008). "Normal Bone Anatomy and Physiology." Clinical Journal of the American Society of Nephrology **3**(Supplement 3): S131-S139.
- Clines, G. A. and T. A. Guise (2008). "Molecular mechanisms and treatment of bone metastasis." Expert Reviews in Molecular Medicine **10**: null-null.
- Coleman, R. E. (1997). "Skeletal complications of malignancy." Cancer **80**(8 Suppl): 1588-1594.

- Coleman, R. E. (2001). "Metastatic bone disease: clinical features, pathophysiology and treatment strategies." Cancer treatment reviews **27**(3): 165-176.
- Condeelis, J. and J. E. Segall (2003). "Intravital imaging of cell movement in tumours." Nat Rev Cancer **3**(12): 921-930.
- Conery, A. R., Y. Cao, E. A. Thompson, C. M. Townsend, Jr., T. C. Ko and K. Luo (2004). "Akt interacts directly with Smad3 to regulate the sensitivity to TGF-beta induced apoptosis." Nat Cell Biol **6**(4): 366-372.
- Cooper, C. R., C. H. Chay, J. D. Gendernalik, H.-L. Lee, J. Bhatia, R. S. Taichman, L. K. McCauley, E. T. Keller and K. J. Pienta (2003). "Stromal factors involved in prostate carcinoma metastasis to bone." Cancer **97**(S3): 739-747.
- Cordenonsi, M., S. Dupont, S. Maretto, A. Insinga, C. Imbriano and S. Piccolo (2003). "Links between Tumour Suppressors: p53 Is Required for TGF- β Gene Responses by Cooperating with Smads." Cell **113**(3): 301-314.
- Cramer, S. D., Z. Chen and D. M. Peehl (1996). "Prostate Specific Antigen Cleaves Parathyroid Hormone-Related Protein in the PTH-like Domain: Inactivation of PTHrP-Stimulated cAMP Accumulation in Mouse Osteoblasts." The Journal of urology **156**(2): 526-531.
- Crockett, J. C., M. J. Rogers, F. P. Coxon, L. J. Hocking and M. H. Helfrich (2011). "Bone remodelling at a glance." Journal of Cell Science **124**(7): 991-998.
- DaCosta Byfield, S., C. Major, N. J. Laping and A. B. Roberts (2004). "SB-505124 Is a Selective Inhibitor of Transforming Growth Factor- β Type I Receptors ALK4, ALK5, and ALK7." Molecular Pharmacology **65**(3): 744-752.
- Dai, J., J. Hall Ci Fau - Escara-Wilke, A. Escara-Wilke J Fau - Mizokami, J. M. Mizokami A Fau - Keller, E. T. Keller Jm Fau - Keller and E. T. Keller (2008). "Prostate cancer induces bone metastasis through Wnt-induced bone morphogenetic protein-dependent and independent mechanisms." Cancer Research **68**(1538-7445 (Electronic)): 5785-5794
- Dai, J., J. Keller J Fau - Zhang, Y. Zhang J Fau - Lu, Z. Lu Y Fau - Yao, E. T. Yao Z Fau - Keller and E. T. Keller (2005). "Bone morphogenetic protein-6 promotes osteoblastic prostate cancer bone metastases through a dual mechanism." Cancer Research **65**(0008-5472 (Print)): 8274-8285.
- Darby, S., N. J. Cross Ss Fau - Brown, F. C. Brown Nj Fau - Hamdy, C. N. Hamdy Fc Fau - Robson and C. N. Robson (2008). "BMP-6 over-expression in prostate cancer is associated with increased Id-1 protein and a more invasive phenotype." Journal of Pathology **214**(0022-3417 (Print)): 394-404.
- Datta, P. K., M. C. Blake and H. L. Moses (2000). "Regulation of Plasminogen Activator Inhibitor-1 Expression by Transforming Growth Factor- β -induced Physical and Functional Interactions between Smads and Sp1." Journal of Biological Chemistry **275**(51): 40014-40019.

Datto, M. B., Y. Yu and X.-F. Wang (1995). "Functional Analysis of the Transforming Growth Factor β Responsive Elements in the WAF1/Cip1/p21 Promoter." Journal of Biological Chemistry **270**(48): 28623-28628.

Day, T. F., X. Guo, L. Garrett-Beal and Y. Yang (2005). "Wnt/ β -Catenin Signaling in Mesenchymal Progenitors Controls Osteoblast and Chondrocyte Differentiation during Vertebrate Skeletogenesis." Developmental Cell **8**(5): 739-750.

de Gorter, D. J. J., M. van Dinther, O. Korchyński and P. ten Dijke (2011). "Biphasic effects of transforming growth factor β on bone morphogenetic protein-induced osteoblast differentiation." Journal of Bone and Mineral Research **26**(6): 1178-1187.

De Pinieux, G., et al. (2001). "Bone sialoprotein, bone morphogenetic protein 6 and thymidine phosphorylase expression in localized human prostatic adenocarcinoma as predictors of clinical outcome: a clinicopathological and immunohistochemical study of 43 cases." Journal of Urology **166**(0022-5347 (Print)): 1924-1930.

Defetos, L. J. (2000). "Prostate carcinoma: production of bioactive factors." Cancer **88**(12 Suppl): 3002-3008.

Del Fattore, A., N. Teti A Fau - Rucci and N. Rucci (2012). "Bone cells and the mechanisms of bone remodelling." Frontiers in Bioscience **4**(1945-0508 (Electronic)): 2302-2321.

Delaissé, J.-M., T. L. Andersen, M. T. Engsig, K. Henriksen, T. Troen and L. Blavier (2003). "Matrix metalloproteinases (MMP) and cathepsin K contribute differently to osteoclastic activities." Microscopy Research and Technique **61**(6): 504-513.

Derynck, R. and R. J. Akhurst (2007). "Differentiation plasticity regulated by TGF- β family proteins in development and disease." Nat Cell Biol **9**(9): 1000-1004.

Derynck, R. and Y. E. Zhang (2003). "Smad-dependent and Smad-independent pathways in TGF- β family signalling." Nature **425**(6958): 577-584.

Derynck, R., R. J. Akhurst and A. Balmain (2001). "TGF- β signaling in tumour suppression and cancer progression." Nat Genet **29**(2): 117-129.

Dickson, M. C., J. S. Martin, F. M. Cousins, A. B. Kulkarni, S. Karlsson and R. J. Akhurst (1995). "Defective haematopoiesis and vasculogenesis in transforming growth factor-beta 1 knock out mice." Development **121**(6): 1845-1854.

Dobnig, H. and R. T. Turner (1995). "Evidence that intermittent treatment with parathyroid hormone increases bone formation in adult rats by activation of bone lining cells." Endocrinology **136**(8): 3632-3638.

Dowling, P. and M. Clynes (2011). "Conditioned media from cell lines: A complementary model to clinical specimens for the discovery of disease-specific biomarkers." PROTEOMICS **11**(4): 794-804.

Dubois, C. M., M.-H. Laprise, F. Blanchette, L. E. Gentry and R. Leduc (1995). "Processing of Transforming Growth Factor 1 Precursor by Human Furin Convertase." Journal of Biological Chemistry **270**(18): 10618-10624.

- Ducy, P. and G. Karsenty (2000). "The family of bone morphogenetic proteins." Kidney Int **57**(6): 2207-2214.
- Ducy, P., R. Zhang, V. Geoffroy, A. L. Ridall and G. Karsenty (1997). "Osf2/Cbfa1: A Transcriptional Activator of Osteoblast Differentiation." Cell **89**(5): 747-754.
- Ducy, P., T. Schinke and G. Karsenty (2000). "The Osteoblast: A Sophisticated Fibroblast under Central Surveillance." Science **289**(5484): 1501-1504.
- Dunn, L. K., K. S. Mohammad, P. G. J. Fournier, C. R. McKenna, H. W. Davis, M. Niewolna, X. H. Peng, J. M. Chirgwin and T. A. Guise (2009). "Hypoxia and TGF- β Drive Breast Cancer Bone Metastases through Parallel Signaling Pathways in Tumour Cells and the Bone Microenvironment." PLoS ONE **4**(9): e6896.
- Eastham, J. A., L. D. Truong, E. Rogers, M. Kattan, K. C. Flanders, P. T. Scardino and T. C. Thompson (1995). "Transforming growth factor-beta 1: comparative immunohistochemical localization in human primary and metastatic prostate cancer." Lab Invest **73**(5): 628-635.
- Eaton, C. L. and R. E. Coleman (2003). "Pathophysiology of bone metastases from prostate cancer and the role of bisphosphonates in treatment." Cancer Treatment Reviews **29**(3): 189-198.
- Economides, A., N. E. Stahl and R. M. Harland (2000). Modified noggin polypeptide and compositions, Google Patents.
- Edlund, S., S. Bu, N. Schuster, P. Aspenstrom, R. Heuchel, N.-E. Heldin, P. ten Dijke, C.-H. Heldin and M. Landstrom (2003). "Transforming Growth Factor-beta 1 (TGF-beta 1)-induced Apoptosis of Prostate Cancer Cells Involves Smad7-dependent Activation of p38 by TGF-beta 1 -activated Kinase 1 and Mitogen-activated Protein Kinase Kinase 3." Mol. Biol. Cell **14**(2): 529-544.
- Eriksen EF, A. D., Melsen F (1994). Bone Histomorphometry. New York, Raven Press.
- Eriksen, E. F. (1986). "Normal and Pathological Remodeling of Human Trabecular Bone: Three Dimensional Reconstruction of the Remodeling Sequence in Normals and in Metabolic Bone Disease." Endocrine Reviews **7**(4): 379-408.
- Fakhry, A., C. Ratisoontorn, C. Vedhachalam, I. Salhab, E. Koyama, P. Leboy, M. Pacifici, R. E. Kirschner and H.-D. Nah (2005). "Effects of FGF-2/-9 in calvarial bone cell cultures: differentiation stage-dependent mitogenic effect, inverse regulation of BMP-2 and noggin, and enhancement of osteogenic potential." Bone **36**(2): 254-266.
- Fan, J., H. Park, S. Tan and M. Lee (2013). "Enhanced Osteogenesis of Adipose Derived Stem Cells with Noggin Suppression and Delivery of BMP-2." PLoS ONE **8**(8): e72474.
- Feeley, B. T., L. Krenek, N. Liu, W. K. Hsu, S. C. Gamradt, E. M. Schwarz, J. Huard and J. R. Lieberman (2006). "Overexpression of noggin inhibits BMP-mediated growth of osteolytic prostate cancer lesions." Bone **38**(2): 154-166.

Feeley, B. T., S. C. Gamradt, W. K. Hsu, N. Liu, L. Krenek, P. Robbins, J. Huard and J. R. Lieberman (2005). "Influence of BMPs on the Formation of Osteoblastic Lesions in Metastatic Prostate Cancer." Journal of Bone and Mineral Research **20**(12): 2189-2199.

Festuccia, C., M. Bologna, G. L. Gravina, F. Guerra, A. Angelucci, I. Villanova, D. Millimaggi and A. Teti (1999). "Osteoblast conditioned media contain TGF- β 1 and modulate the migration of prostate tumour cells and their interactions with extracellular matrix components." International Journal of Cancer **81**(3): 395-403.

Foletta, V. C., M. A. Lim, J. Soosairajah, A. P. Kelly, E. G. Stanley, M. Shannon, W. He, S. Das, J. Massagué and O. Bernard (2003). "Direct signaling by the BMP type II receptor via the cytoskeletal regulator LIMK1." The Journal of Cell Biology **162**(6): 1089-1098.

Friese, M. A., J. Wischhusen, W. Wick, M. Weiler, G. Eisele, A. Steinle and M. Weller (2004). "RNA Interference Targeting Transforming Growth Factor- β Enhances NKG2D-Mediated Antiglioma Immune Response, Inhibits Glioma Cell Migration and Invasiveness, and Abrogates Tumourigenicity In vivo." Cancer Research **64**(20): 7596-7603.

Fritz, V., et al. (2011). "Bone-metastatic prostate carcinoma favors mesenchymal stem cell differentiation toward osteoblasts and reduces their osteoclastogenic potential." Journal of Cellular Biochemistry **112**(1097-4644 (Electronic)): 3234-3245.

Gallea, S., F. Lallemand, A. Atfi, G. Rawadi, V. Ramez, S. Spinella-Jaegle, S. Kawai, C. Faucheu, L. Huet, R. Baron and S. Roman-Roman (2001). "Activation of mitogen-activated protein kinase cascades is involved in regulation of bone morphogenetic protein-2-induced osteoblast differentiation in pluripotent C2C12 cells." Bone **28**(5): 491-498.

Gamer, L. W., M. Nove J Fau - Levin, V. Levin M Fau - Rosen and V. Rosen (2005). "BMP-3 is a novel inhibitor of both activin and BMP-4 signaling in *Xenopus* embryos." Dev Biol **285**(0012-1606 (Print)): 156-168.

Ganguly, S. S., X. Li and C. K. Miranti (2014). "The Host Microenvironment Influences Prostate Cancer Invasion, Systemic Spread, Bone Colonization, and Osteoblastic Metastasis." Frontiers in Oncology **4**: 364.

Gao, H., G. Chakraborty, A. P. Lee-Lim, Q. Mo, M. Decker, A. Vonica, R. Shen, E. Brogi, A. H. Brivanlou and F. G. Giancotti (2012). "The BMP Inhibitor Coco Reactivates Breast Cancer Cells at Lung Metastatic sites." Cell **150**(4): 764-779.

Garnero, P., N. Buchs, J. Zekri, R. Rizzoli, R. E. Coleman and P. D. Delmas (2000). "Markers of bone turnover for the management of patients with bone metastases from prostate cancer." British Journal of Cancer **82**(4): 858-864.

Gazzerro, E., E. Gangji V Fau - Canalis and E. Canalis (1998). "Bone morphogenetic proteins induce the expression of noggin, which limits their activity in cultured rat osteoblasts." J Clin Invest **102**(0021-9738 (Print)): 2106-2114.

Gazzerro, E., Z. Du, R. D. Devlin, S. Rydziel, L. Priest, A. N. Economides and E. Canalis (2003). "Noggin arrests stromal cell differentiation in vitro." Bone **32**(2): 111-119.

Gentry, L. E., M. N. Liubin, A. F. Purchio and H. Marquardt (1988). "Molecular events in the processing of recombinant type 1 pre-pro-transforming growth factor beta to the mature polypeptide." Mol. Cell. Biol. **8**(10): 4162-4168.

Gingrich, J. R., R. J. Barrios, R. A. Morton, B. F. Boyce, F. J. DeMayo, M. J. Finegold, R. Angelopoulou, J. M. Rosen and N. M. Greenberg (1996). "Metastatic Prostate Cancer in a Transgenic Mouse." Cancer Research **56**(18): 4096-4102.

Goktas, S. and E. D. Crawford (1999). "Optimal hormonal therapy for advanced prostatic carcinoma." Seminars in oncology **26**(2): 162-173.

Goltzman, D., S. A. Bolivar I Fau - Rabbani and S. A. Rabbani (1992). "Studies on the pathogenesis of osteoblastic metastases by prostate cancer." Adv Exp Med Biol **324**(0065-2598 (Print)): 165-171.

Gorelik, L. and R. A. Flavell (2001). "Immune-mediated eradication of tumours through the blockade of transforming growth factor-[beta] signaling in T cells." Nat Med **7**(10): 1118-1122.

Gotzmann, J., M. Mikula, A. Eger, R. Schulte-Hermann, R. Foisner, H. Beug and W. Mikulits (2004). "Molecular aspects of epithelial cell plasticity: implications for local tumour invasion and metastasis." Mutation Research/Reviews in Mutation Research **566**(1): 9-20.

Goustin, A. S., E. B. Leof, G. D. Shipley and H. L. Moses (1986). "Growth Factors and Cancer." Cancer Research **46**(3): 1015-1029.

Griffith, D. L., P. C. Keck, T. K. Sampath, D. C. Rueger and W. D. Carlson (1996). "Three-dimensional structure of recombinant human osteogenic protein 1: structural paradigm for the transforming growth factor beta superfamily." Proc Natl Acad Sci U S A **93**(2): 878-883.

Grimm, D., K. Pandey and M. A. Kay (2005). Adeno-Associated Virus Vectors for Short Hairpin RNA Expression. Methods in Enzymology. R. E. David and J. R. John, Academic Press. Volume **392**: 381-405.

Grishin, N. V. (2001). "MH1 domain of Smad is a degraded homing endonuclease." Journal of Molecular Biology **307**(1): 31-37.

Groppe, J., J. Greenwald, E. Wiater, J. Rodriguez-Leon, A. N. Economides, W. Kwiatkowski, M. Affolter, W. W. Vale, J. C. I. Belmonte and S. Choe (2002). "Structural basis of BMP signalling inhibition by the cystine knot protein Noggin." Nature **420**(6916): 636-642.

Guise, T. A., J. J. Yin, S. D. Taylor, Y. Kumagai, M. Dallas, B. F. Boyce, T. Yoneda and G. R. Mundy (1996). "Evidence for a causal role of parathyroid hormone-related protein in the pathogenesis of human breast cancer-mediated osteolysis." J Clin Invest **98**(7): 1544-1549.

Hall, C. L., A. Bafico, J. Dai, S. A. Aaronson and E. T. Keller (2005). "Prostate Cancer Cells Promote Osteoblastic Bone Metastases through Wnts." Cancer Research **65**(17): 7554-7560.

Hall, C. L., S. Kang, O. A. MacDougald and E. T. Keller (2006). "Role of wnts in prostate cancer bone metastases." Journal of Cellular Biochemistry **97**(4): 661-672.

Hamdy, F. C., P. Autzen, M. C. Robinson, C. H. Horne, D. E. Neal and C. N. Robson (1997). "Immunolocalization and messenger RNA expression of bone morphogenetic protein-6 in human benign and malignant prostatic tissue." Cancer Res **57**(19): 4427-4431.

Harada, H., S. Tagashira, M. Fujiwara, S. Ogawa, T. Katsumata, A. Yamaguchi, T. Komori and M. Nakatsuka (1999). "Cbfa1 Isoforms Exert Functional Differences in Osteoblast Differentiation." Journal of Biological Chemistry **274**(11): 6972-6978.

Haudenschild, D. R., S. M. Palmer, T. A. Moseley, Z. You and A. H. Reddi (2004). "Bone Morphogenetic Protein (BMP)-6 Signaling and BMP Antagonist Noggin in Prostate Cancer." Cancer Research **64**(22): 8276-8284.

Hauschka, P. V., A. E. Mavrakos, M. D. Iafrati, S. E. Doleman and M. Klagsbrun (1986). "Growth factors in bone matrix. Isolation of multiple types by affinity chromatography on heparin-Sepharose." Journal of Biological Chemistry **261**(27): 12665-12674.

He, F., W. Xiong, Y. Wang, M. Matsui, X. Yu, Y. Chai, J. Klingensmith and Y. Chen (2010). "Modulation of BMP signaling by Noggin is required for the maintenance of palatal epithelial integrity during palatogenesis." Developmental biology **347**(1): 109-121.

He, W., D. C. Dorn, H. Erdjument-Bromage, P. Tempst, M. A. S. Moore and J. Massagué (2006). "Hematopoiesis Controlled by Distinct TIF1³ and Smad4 Branches of the TGF² Pathway." Cell **125**(5): 929-941.

Hess, K. R., G. R. Varadhachary, S. H. Taylor, W. Wei, M. N. Raber, R. Lenzi and J. L. Abbruzzese (2006). "Metastatic patterns in adenocarcinoma." Cancer **106**(7): 1624-1633.

Hirsinger, E., D. Duprez, C. Jouve, P. Malapert, J. Cooke and O. Pourquie (1997). "Noggin acts downstream of Wnt and Sonic Hedgehog to antagonize BMP4 in avian somite patterning." Development **124**(22): 4605-4614.

HOCK, J. M., M. CENTRELLA and E. CANALIS (1988). "Insulin-Like Growth Factor I Has Independent Effects on Bone Matrix Formation and Cell Replication." Endocrinology **122**(1): 254-260.

Hofmann, T. G., N. Stollberg, M. L. Schmitz and H. Will (2003). "HIPK2 Regulates Transforming Growth Factor- β -Induced c-Jun NH2-Terminal Kinase Activation and Apoptosis in Human Hepatoma Cells." Cancer Research **63**(23): 8271-8277.

Hogan, B. L. (1996). "Bone morphogenetic proteins: multifunctional regulators of vertebrate development." Genes & Development **10**(13): 1580-1594.

Holtrop, M. (1990). Light and electron microscopic structure of bone forming cells Bone. H. BK, Telford Press Inc. **1**: 1-39.

Hsu, M.-Y., S. Rovinsky, C.-Y. Lai, S. Qasem, X. Liu, J. How, J. F. Engelhardt and G. F. Murphy (2008). "Aggressive melanoma cells escape from BMP7-mediated autocrine growth inhibition through coordinated Noggin upregulation." Lab Invest **88**(8): 842-855.

Hughes-Fulford, M. and C.-F. Li (2011). "The role of FGF-2 and BMP-2 in regulation of gene induction, cell proliferation and mineralization." J Orthop Surg Res **6**(8).

Hughes, D. E., J. C. Dai A Fau - Tiffée, H. H. Tiffée Jc Fau - Li, G. R. Li Hh Fau - Mundy, B. F. Mundy Gr Fau - Boyce and B. F. Boyce (1996). "Estrogen promotes apoptosis of murine osteoclasts mediated by TGF-beta." Nat Med **2**(1078-8956 (Print)): 1132-1136.

Hyzy, S. L., R. Olivares-Navarrete, Z. Schwartz and B. D. Boyan (2012). "BMP2 induces osteoblast apoptosis in a maturation state and noggin-dependent manner." Journal of Cellular Biochemistry **113**(10): 3236-3245.

Ide, H., M. Katoh, H. Sasaki, T. Yoshida, K. Aoki, Y. Nawa, Y. Osada, T. Sugimura and M. Terada (1997). "Cloning of human bone morphogenetic protein type IB receptor (BMPR-IB) and its expression in prostate cancer in comparison with other BMPRs." Oncogene **14**(11): 1377-1382.

Ide, H., T. Yoshida, N. Matsumoto, K. Aoki, Y. Osada, T. Sugimura and M. Terada (1997). "Growth Regulation of Human Prostate Cancer Cells by Bone Morphogenetic Protein-2." Cancer Research **57**(22): 5022-5027.

Iemura, S., T. S. Yamamoto, C. Takagi, H. Uchiyama, T. Natsume, S. Shimasaki, H. Sugino and N. Ueno (1998). "Direct binding of follistatin to a complex of bone-morphogenetic protein and its receptor inhibits ventral and epidermal cell fates in early *Xenopus* embryo." Proc Natl Acad Sci U S A **95**(16): 9337-9342.

Ilka, R. L., G. Hangoc G Fau - Girasole, G. Girasole G Fau - Passeri, D. C. Passeri G Fau - Williams, J. S. Williams Dc Fau - Abrams, B. Abrams Js Fau - Boyce, H. Boyce B Fau - Broxmeyer, S. C. Broxmeyer H Fau - Manolagas and S. C. Manolagas (1992). "Increased osteoclast development after estrogen loss: mediation by interleukin-6." Science **257**(0036-8075 (Print)): 88-91.

Inagaki, M., A. Moustakas, H. Y. Lin, H. F. Lodish and B. I. Carr (1993). "Growth inhibition by transforming growth factor beta (TGF-beta) type I is restored in TGF-beta-resistant hepatoma cells after expression of TGF-beta receptor type II cDNA." Proc Natl Acad Sci U S A **90**(11): 5359-5363.

International Agency for Research on Cancer. (2015). "GLOBOCAN 2012:Estimated Cancer Incidence Mortality and Prevalence worldwide in 2012." 2015, from <http://globocan.iarc.fr/Default.aspx>.

Isaacs Jt Fau - Isaacs, W. B., W. F. Isaacs Wb Fau - Feitz, J. Feitz Wf Fau - Scheres and J. Scheres (1986). "Establishment and characterization of seven Dunning rat prostatic cancer cell lines and their use in developing methods for predicting metastatic abilities of prostatic cancers." The Prostate **9**(0270-4137 (Print)): 261-281.

Israel, D. I., J. Nove, K. M. Kerns, R. J. Kaufman, V. Rosen, K. A. Cox and J. M. Wozney (1996). "Heterodimeric bone morphogenetic proteins show enhanced activity in vitro and in vivo." Growth Factors **13**(3-4): 291-300.

Iwamura, M., J. Hellman, A. T. K. Cockett, H. Lilja and S. Gershagen (1996). "Alteration of the hormonal bioactivity of parathyroid hormone-related protein (PTHrP) as a result of limited proteolysis by prostate-specific antigen." Urology **48**(2): 317-325.

Iwasaki, S., N. Tsuruoka, A. Hattori, M. Sato, M. Tsujimoto and M. Kohno (1995). "Distribution and Characterization of Specific Cellular Binding Proteins for Bone Morphogenetic Protein-2." Journal of Biological Chemistry **270**(10): 5476-5482.

Jacobs, C. R., A. B. Temiyasathit S Fau - Castillo and A. B. Castillo (2010). "Osteocyte mechanobiology and pericellular mechanics." Annu. Rev. Biomed. Eng **12**(1545-4274 (Electronic)): 369-400.

- Janssens, K., P. t. Dijke, S. Janssens and W. V. Hul (2005). "Transforming Growth Factor- β 1 to the Bone." Endocrine Reviews **26**(6): 743-774.
- Javelaud, D., J. Laboureau, E. Gabison, F. Verrecchia and A. Mauviel (2003). "Disruption of Basal JNK Activity Differentially Affects Key Fibroblast Functions Important for Wound Healing." Journal of Biological Chemistry **278**(27): 24624-24628.
- Jemal, A., R. Siegel, E. Ward, T. Murray, J. Xu and M. J. Thun (2007). "Cancer Statistics, 2007." CA: A Cancer Journal for Clinicians **57**(1): 43-66.
- Jennings, M. T. and J. A. Pietsenpol (1998). "The role of transforming growth factor B in glioma progression." Journal of Neuro-Oncology **36**(2): 123-140.
- Jung, K., M. Lein, C. Stephan, K. Von Hösslin, A. Semjonow, P. Sinha, S. A. Loening and D. Schnorr (2004). "Comparison of 10 serum bone turnover markers in prostate carcinoma patients with bone metastatic spread: Diagnostic and prognostic implications." International Journal of Cancer **111**(5): 783-791.
- Jung, Y., Y. Shiozawa, J. Wang, N. McGregor, J. Dai, S. I. Park, J. E. Berry, A. M. Havens, J. Joseph, J. K. Kim, L. Patel, P. Carmeliet, S. Daignault, E. T. Keller, L. K. McCauley, K. J. Pienta and R. S. Taichman (2012). "Prevalence of Prostate Cancer Metastases after Intravenous Inoculation Provides Clues into the Molecular Basis of Dormancy in the Bone Marrow Microenvironment." Neoplasia (New York, N.Y.) **14**(5): 429-439.
- Kaartinen, V., J. W. Voncken, C. Shuler, D. Warburton, D. Bu, N. Heisterkamp and J. Groffen (1995). "Abnormal lung development and cleft palate in mice lacking TGF-beta 3 indicates defects of epithelial-mesenchymal interaction." Nat Genet **11**(4): 415-421.
- Kahn, D., G. Weiner, S. Ben-Haim, L. Ponto, M. Madsen, D. Bushnell, G. Watkins, E. Argenyi and R. Hichwa (1994). "Positron emission tomographic measurement of bone marrow blood flow to the pelvis and lumbar vertebrae in young normal adults [published erratum appears in Blood 1994 Nov 15;84(10):3602]." Blood **83**(4): 958-963.
- Käkönen, S.-M., K. S. Selander, J. M. Chirgwin, J. J. Yin, S. Burns, W. A. Rankin, B. G. Grubbs, M. Dallas, Y. Cui and T. A. Guise (2002). "Transforming Growth Factor- β Stimulates Parathyroid Hormone-related Protein and Osteolytic Metastases via Smad and Mitogen-activated Protein Kinase Signaling Pathways." Journal of Biological Chemistry **277**(27): 24571-24578.
- Kalluri, R. and R. A. Weinberg (2009). "The basics of epithelial-mesenchymal transition." The Journal of Clinical Investigation **119**(6): 1420-1428.
- Kamaraju, A. K. and A. B. Roberts (2005). "Role of Rho/ROCK and p38 MAP Kinase Pathways in Transforming Growth Factor- β -mediated Smad-dependent Growth Inhibition of Human Breast Carcinoma Cells in Vivo." Journal of Biological Chemistry **280**(2): 1024-1036.
- Kaminska, B., A. Wesolowska and M. Danilkiewicz (2005). "TGF beta signalling and its role in tumour pathogenesis." Acta Biochim Pol **52**(2): 329-337.
- Kang, Y., P. M. Siegel, W. Shu, M. Drobnjak, S. M. Kakonen, C. Cordón-Cardo, T. A. Guise and J. Massagué (2003). "A multigenic program mediating breast cancer metastasis to bone." Cancer cell **3**(6): 537-549.

- Kang, Y., W. He, S. Tulley, G. P. Gupta, I. Serganova, C. R. Chen, K. Manova-Todorova, R. Blasberg, W. L. Gerald and J. Massague (2005). "Breast cancer bone metastasis mediated by the Smad tumour suppressor pathway." Proc Natl Acad Sci U S A **102**(39): 13909-13914.
- Kaplan-Lefko, P. J., T.-M. Chen, M. M. Ittmann, R. J. Barrios, G. E. Ayala, W. J. Huss, L. A. Maddison, B. A. Foster and N. M. Greenberg (2003). "Pathobiology of autochthonous prostate cancer in a pre-clinical transgenic mouse model." The Prostate **55**(3): 219-237.
- Kaplan, R. N., R. D. Riba, S. Zacharoulis, A. H. Bramley, L. Vincent, C. Costa, D. D. MacDonald, D. K. Jin, K. Shido, S. A. Kerns, Z. Zhu, D. Hicklin, Y. Wu, J. L. Port, N. Altorki, E. R. Port, D. Ruggero, S. V. Shmelkov, K. K. Jensen, S. Rafii and D. Lyden (2005). "VEGFR1-positive haematopoietic bone marrow progenitors initiate the pre-metastatic niche." Nature **438**(7069): 820-827.
- Kasperk, C., J. Wergedal, D. Strong, J. Farley, K. Wangerin, H. Gropp, R. Ziegler and D. J. Baylink (1995). "Human bone cell phenotypes differ depending on their skeletal site of origin." The Journal of Clinical Endocrinology & Metabolism **80**(8): 2511-2517.
- Kavsak, P., R. K. Rasmussen, C. G. Causing, S. Bonni, H. Zhu, G. H. Thomsen and J. L. Wrana (2000). "Smad7 Binds to Smurf2 to Form an E3 Ubiquitin Ligase that Targets the TGF β Receptor for Degradation." Molecular Cell **6**(6): 1365-1375.
- Kawabata, M., T. Imamura and K. Miyazono (1998). "Signal transduction by bone morphogenetic proteins." Cytokine & growth factor reviews **9**(1): 49-61.
- Keller, E. T. and J. Brown (2004). "Prostate cancer bone metastases promote both osteolytic and osteoblastic activity." J Cell Biochem **91**(0730-2312 (Print)): 718-729.
- Killian, C. S., D. A. Corral, E. Kawinski and R. I. Constantine (1993). "Mitogenic Response of Osteoblast Cells to Prostate-Specific Antigen Suggests an Activation of Latent TGF-[beta] and a Proteolytic Modulation of Cell Adhesion Receptors." Biochemical and Biophysical Research Communications **192**(2): 940-947.
- Kim, I. Y., D.-H. Lee, H.-J. Ahn, H. Tokunaga, W. Song, L. M. Devereaux, D. Jin, T. K. Sampath and R. A. Morton (2000). "Expression of Bone Morphogenetic Protein Receptors Type-IA, -IB, and -II Correlates with Tumour Grade in Human Prostate Cancer Tissues." Cancer Research **60**(11): 2840-2844.
- Kim, I. Y., H. J. Ahn, D. J. Zelner, J. W. Shaw, S. Lang, M. Kato, M. G. Oefelein, K. Miyazono, J. A. Nemeth, J. M. Kozlowski and C. Lee (1996). "Loss of expression of transforming growth factor beta type I and type II receptors correlates with tumour grade in human prostate cancer tissues." Clinical Cancer Research **2**(8): 1255-1261.
- Kim, I. Y., H.-J. Ahn, D. J. Zelner, J. W. Shaw, J. A. Sensibar, J.-H. Kim, M. Kato and C. Lee (1996). "Genetic Change in Transforming Growth Factor β (TGF- β) Receptor Type I Gene Correlates with Insensitivity to TGF- β 1 in Human Prostate Cancer Cells." Cancer Research **56**(1): 44-48.
- Kim, S. G., H.-S. Jong, T.-Y. Kim, J. W. Lee, N. K. Kim, S. H. Hong and Y.-J. Bang (2004). "Transforming Growth Factor- β 1 Induces Apoptosis through Fas Ligand-independent Activation of the Fas Death Pathway in Human Gastric SNU-620 Carcinoma Cells." Mol. Biol. Cell **15**(2): 420-434.

Kim, S. J., Y. H. Im, S. D. Markowitz and Y. J. Bang (2000). "Molecular mechanisms of inactivation of TGF- β receptors during carcinogenesis." Cytokine and Growth Factor Reviews **11**(1): 159-168.

Kimura, G., Y. Sugisaki, Y. Masugi and N. Nakazawa (1992). "Calcification in human osteoblasts cultured in medium conditioned by the prostatic cancer cell line PC-3 and prostatic acid phosphatase." Urol Int **48**(1): 25-30.

Kingsley, D. M. (1994). "The TGF-beta superfamily: new members, new receptors, and new genetic tests of function in different organisms." Genes & Development **8**(2): 133-146.

Kingsley, L. A., P. G. J. Fournier, J. M. Chirgwin and T. A. Guise (2007). "Molecular Biology of Bone Metastasis." Molecular Cancer Therapeutics **6**(10): 2609-2617.

Kitazawa, S. and R. Kitazawa (2002). "RANK ligand is a prerequisite for cancer-associated osteolytic lesions." The Journal of Pathology **198**(2): 228-236.

Knaus, P. I., D. Lindemann, J. F. DeCoteau, R. Perlman, H. Yankelev, M. Hille, M. E. Kadin and H. F. Lodish (1996). "A dominant inhibitory mutant of the type II transforming growth factor beta receptor in the malignant progression of a cutaneous T-cell lymphoma." Molecular and Cellular Biology **16**(7): 3480-3489.

Kobayashi, A., H. Okuda, F. Xing, P. R. Pandey, M. Watabe, S. Hirota, S. K. Pai, W. Liu, K. Fukuda, C. Chambers, A. Wilber and K. Watabe (2011). "Bone morphogenetic protein 7 in dormancy and metastasis of prostate cancer stem-like cells in bone." The Journal of Experimental Medicine **208**(13): 2641-2655.

Kobayashi, S., H. E. Takahashi, A. Ito, N. Saito, M. Nawata, H. Horiuchi, H. Ohta, A. Ito, R. Iorio, N. Yamamoto and K. Takaoka (2003). "Trabecular minimodeling in human iliac bone." Bone **32**(2): 163-169.

Koeneman, K. S., L. W. Yeung F Fau - Chung and L. W. Chung (1999). "Osteomimetic properties of prostate cancer cells: a hypothesis supporting the predilection of prostate cancer metastasis and growth in the bone environment." Prostate **39**(0270-4137 (Print)): 246-261.

Kogawa, K., T. Nakamura, K. Sugino, K. Takio, K. Titani and H. Sugino (1991). "Activin-Binding Protein Is Present in Pituitary." Endocrinology **128**(3): 1434-1440.

Koutsilieris, M., S. A. Rabbani and D. Goltzman (1987). "Effects of human prostatic mitogens on rat bone cells and fibroblasts." Journal of Endocrinology **115**(3): 447-NP.

Kowanetz, M., U. Valcourt, R. Bergstrom, C.-H. Heldin and A. Moustakas (2004). "Id2 and Id3 Define the Potency of Cell Proliferation and Differentiation Responses to Transforming Growth Factor {beta} and Bone Morphogenetic Protein." Mol. Cell. Biol. **24**(10): 4241-4254.

Kozlow, W. and T. A. Guise (2005). "Breast Cancer Metastasis to Bone: Mechanisms of Osteolysis and Implications for Therapy." Journal of Mammary Gland Biology and Neoplasia **10**(2): 169-180.

- Krause, C., A. Guzman and P. Knaus (2011). "Noggin." The International Journal of Biochemistry & Cell Biology **43**(4): 478-481.
- Kulkarni, A. B., C. G. Huh, D. Becker, A. Geiser, M. Lyght, K. C. Flanders, A. B. Roberts, M. B. Sporn, J. M. Ward and S. Karlsson (1993). "Transforming growth factor beta 1 null mutation in mice causes excessive inflammatory response and early death." Proc Natl Acad Sci U S A **90**(2): 770-774.
- Kutz, S. M., J. Hordines, P. J. McKeown-Longo and P. J. Higgins (2001). "TGF- β 1-induced PAI-1 gene expression requires MEK activity and cell-to-substrate adhesion." J Cell Sci **114**(21): 3905-3914.
- Kyle, R. A., M. A. Gertz, T. E. Witzig, J. A. Lust, M. Q. Lacy, A. Dispenzieri, R. Fonseca, S. V. Rajkumar, J. R. Offord, D. R. Larson, M. E. Plevak, T. M. Therneau and P. R. Greipp (2003). "Review of 1027 Patients With Newly Diagnosed Multiple Myeloma." Mayo Clinic Proceedings **78**(1): 21-33.
- Lai, C.-F. and S.-L. Cheng (2002). "Signal Transductions Induced by Bone Morphogenetic Protein-2 and Transforming Growth Factor- β in Normal Human Osteoblastic Cells." Journal of Biological Chemistry **277**(18): 15514-15522.
- Lai, T.-H., Y.-C. Fong, W.-M. Fu, R.-S. Yang and C.-H. Tang (2008). "Osteoblasts-derived BMP-2 enhances the motility of prostate cancer cells via activation of integrins." The Prostate **68**(12): 1341-1353.
- Larson, S., J. Chin, X. Zhang, L. Brown, I. Coleman, B. Lakely, M. Tenniswood, E. Corey, P. Nelson, R. Vessella and C. Morrissey (2014). "Prostate cancer derived prostatic acid phosphatase promotes an osteoblastic response in the bone microenvironment." Clinical & Experimental Metastasis **31**(2): 247-256.
- Laurila, R., S. Parkkila, J. Isola, A. Kallioniemi and E.-L. Alarmo (2013). "The expression patterns of gremlin 1 and noggin in normal adult and tumour tissues." International Journal of Clinical and Experimental Pathology **6**(7): 1400-1408.
- Lawson, R. K. (1990). "Benign prostatic hyperplasia and growth factors." Der Urologe. Aug. A **29**(1): 5-7.
- Leber, M. F. and T. Efferth (2009). "Molecular principles of cancer invasion and metastasis (review)." International journal of oncology **34**(4): 881-895.
- Lee, K. S., S. H. Hong and S. C. Bae (2002). "Both the Smad and p38 MAPK pathways play a crucial role in Runx2 expression following induction by transforming growth factor-beta and bone morphogenetic protein." Oncogene **21**(47): 7156-7163.
- Lee, M. S., S. G. Ko, H. P. Kim, Y. B. Kim, S. Y. Lee, S. G. Kim, H. S. Jong, T. Y. Kim, J. W. Lee and Y. J. Bang (2004). "Smad2 mediates Erk1/2 activation by TGF-beta1 in suspended, but not in adherent, gastric carcinoma cells." Int J Oncol **24**(5): 1229-1234.
- Li, M. O. and R. A. Flavell (2008). "TGF- β 2: A Master of All T Cell Trades." Cell **134**(3): 392-404.

- Lin, S. J., T. F. Lerch, R. W. Cook, T. S. Jardetzky and T. K. Woodruff (2006). "The structural basis of TGF- β , bone morphogenetic protein, and activin ligand binding." Reproduction **132**(2): 179-190.
- Lindholm, D., E. Castrén, R. Kiefer, F. Zafra and H. Thoenen (1992). "Transforming growth factor-beta 1 in the rat brain: increase after injury and inhibition of astrocyte proliferation." The Journal of Cell Biology **117**(2): 395-400.
- Lindsay, R., F. Cosman, H. Zhou, M. P. Bostrom, V. W. Shen, J. D. Cruz, J. W. Nieves and D. W. Dempster (2006). "A Novel Tetracycline Labeling Schedule for Longitudinal Evaluation of the Short-Term Effects of Anabolic Therapy With a Single Iliac Crest Bone Biopsy: Early Actions of Teriparatide." Journal of Bone and Mineral Research **21**(3): 366-373.
- Liu, F., F. Ventura, J. Doody and J. Massague (1995). "Human type II receptor for bone morphogenic proteins (BMPs): extension of the two-kinase receptor model to the BMPs." Mol. Cell. Biol. **15**(7): 3479-3486.
- Locklin, R. M., J. T. Oreffo Ro Fau - Triffitt and J. T. Triffitt (1999). "Effects of TGFbeta and bFGF on the differentiation of human bone marrow stromal fibroblasts." Cell Biol Int **23**(1065-6995 (Print)): 185-194.
- Loeys, B. L., U. Schwarze, T. Holm, B. L. Callewaert, G. H. Thomas, H. Pannu, J. F. De Backer, G. L. Oswald, S. Symoens, S. Manouvrier, A. E. Roberts, F. Faravelli, M. A. Greco, R. E. Pyeritz, D. M. Milewicz, P. J. Coucke, D. E. Cameron, A. C. Braverman, P. H. Byers, A. M. De Paepe and H. C. Dietz (2006). "Aneurysm Syndromes Caused by Mutations in the TGF- β Receptor." New England Journal of Medicine **355**(8): 788-798.
- Logothetis, C. J. and S. H. Lin (2005). "Osteoblasts in prostate cancer metastasis to bone." Nature review cancer **5**(1474-175X (Print)): 21-28.
- Luo, G., C. Hofmann, A. L. Bronckers, M. Sohocki, A. Bradley and G. Karsenty (1995). "BMP-7 is an inducer of nephrogenesis, and is also required for eye development and skeletal patterning." Genes & Development **9**(22): 2808-2820.
- Lyon, P. B., W. A. See, Y. Xu and M. B. Cohen (1995). "Diversity and modulation of plasminogen activator activity in human prostate carcinoma cell lines." Prostate **27**(4): 179-186.
- Maeda, H., H. Kuwahara, Y. Ichimura, M. Ohtsuki, S. Kurakata and A. Shiraishi (1995). "TGF-beta enhances macrophage ability to produce IL-10 in normal and tumour-bearing mice." The Journal of Immunology **155**(10): 4926-4932.
- Maeda, S., M. Hayashi, S. Komiya, T. Imamura and K. Miyazono (2004). "Endogenous TGF- β signaling suppresses maturation of osteoblastic mesenchymal cells." The EMBO Journal **23**(3): 552-563.
- Mani, S. A., W. Guo, M.-J. Liao, E. N. Eaton, A. Ayyanan, A. Y. Zhou, M. Brooks, F. Reinhard, C. C. Zhang, M. Shipitsin, L. L. Campbell, K. Polyak, C. Brisken, J. Yang and R. A. Weinberg (2008). "The epithelial-mesenchymal transition generates cells with properties of stem cells." Cell **133**(4): 704-715.
- Manolagas, S. C. and R. L. Jilka (1995). "Bone Marrow, Cytokines, and Bone Remodeling — Emerging Insights into the Pathophysiology of Osteoporosis." New England Journal of Medicine **332**(5): 305-311.

- Marcelle, C., M. R. Stark and M. Bronner-Fraser (1997). "Coordinate actions of BMPs, Wnts, Shh and noggin mediate patterning of the dorsal somite." Development **124**(20): 3955-3963.
- Markowitz, S., J. Wang, L. Myeroff, R. Parsons, L. Sun, J. Lutterbaugh, R. S. Fan, E. Zborowska, K. W. Kinzler, B. Vogelstein and et al. (1995). "Inactivation of the type II TGF-beta receptor in colon cancer cells with microsatellite instability." Science **268**(5215): 1336-1338.
- Marks, S. C., Jr. and S. N. Popoff (1988). "Bone cell biology: the regulation of development, structure, and function in the skeleton." American journal of anatomy **183**(0002-9106 (Print)): 1-44.
- Marks, S.C and Paul R. Odgren (1996). The structure and development of the skeleton Principles of bone biology. Bilezikian JP, Raisz LG and Rodman GA. SanDiego, Clifornia Academic Press. **1**: 3-14.
- Martin, T. J., E. H. Allan, P. W. M. Ho, J. H. Gooi, J. M. W. Quinn, M. T. Gillespie, V. Krasnoperov and N. A. Sims (2010). Communication Between EphrinB2 and EphB4 Within the Osteoblast Lineage. Osteoimmunology. Y. Choi, Springer US. **658**: 51-60.
- Martínez Winkler, J., S. Silva and J. F. Santibáñez (1996). "Prostate-derived soluble factors block osteoblast differentiation in culture." Journal of Cellular Biochemistry **61**:18-25.
- Massague, J. (2004). "G1 cell-cycle control and cancer." Nature **432**(7015): 298-306.
- Massagué, J. (2008). "TGF² in Cancer." Cell **134**(2): 215-230.
- Massagué, J. and R. R. Gomis (2006). "The logic of TGFβ signaling." FEBS Letters **580**(12): 2811-2820.
- Massagué, J. and Y.-G. Chen (2000). "Controlling TGF-β signaling." Genes & Development **14**(6): 627-644.
- Mastro, A. M., D. R. Gay Cv Fau - Welch and D. R. Welch (2003). "The skeleton as a unique environment for breast cancer cells." Clinical & Experimental Metastasis **20**(0262-0898 (Print)): 275-284.
- Masuda, H., K. Fukabori Y Fau - Nakano, Y. Nakano K Fau - Takezawa, T. Takezawa Y Fau - Csuzuki, H. Csuzuki T Fau - Yamanaka and H. Yamanaka (2003). "Increased expression of bone morphogenetic protein-7 in bone metastatic prostate cancer." Prostate **54**(0270-4137 (Print)).
- Matsuo, K. (2010). Eph and Ephrin Interactions in Bone. Osteoimmunology. Y. Choi, Springer US. **658**: 95-103.
- McMahon, J. A., S. Takada, L. B. Zimmerman, C.-M. Fan, R. M. Harland and A. P. McMahon (1998). "Noggin-mediated antagonism of BMP signaling is required for growth and patterning of the neural tube and somite." Genes & Development **12**(10): 1438-1452.
- Miyazaki, H., T. Watabe T Fau - Kitamura, K. Kitamura T Fau - Miyazono and K. Miyazono (2004). "BMP signals inhibit proliferation and in vivo tumour growth of androgen-insensitive prostate carcinoma cells." Oncogen **23**(0950-9232 (Print)): 9326-9335

- Miyazono, K., S. Maeda and T. Imamura (2004). "Coordinate regulation of cell growth and differentiation by TGF-beta superfamily and Runx proteins." Oncogene **23**(24): 4232-4237.
- Miyazono, K., Y. Kamiya and M. Morikawa (2010). "Bone morphogenetic protein receptors and signal transduction." Journal of Biochemistry **147**(1): 35-51.
- Mohan, S. and D. J. Baylink (1991). "Bone growth factors." Clin Orthop Relat Res(263): 30-48.
- Morales, M., E. Planet, A. Arnal-Estape, M. Pavlovic, M. Tarragona and R. R. Gomis (2011). "Tumour-stroma interactions a trademark for metastasis." The Breast **20**, Supplement **3**(0): S50-S55.
- Morton, D. M. and E. R. Barrack (1995). "Modulation of Transforming Growth Factor β Effects on Prostate Cancer Cell Proliferation by Growth Factors and Extracellular Matrix." Cancer Research **55**(12): 2596-2602.
- Moses, H. and M. H. Barcellos-Hoff (2011). "TGF-beta biology in mammary development and breast cancer." Microscopy Research and Technique **52**(1943-0264 (Electronic)).
- Moul, J. W. and D. R. Lipo (1999). "Prostate cancer in the late 1990s: hormone refractory disease options." Urol Nurs **19**(2): 125-131; quiz 132-123.
- Moustakas, A. and C.-H. Heldin (2003). "Ecsit-ement on the crossroads of Toll and BMP signal transduction." Genes & Development **17**(23): 2855-2859.
- Moustakas, A. and C.-H. Heldin (2005). "Non-Smad TGF- β signals." J Cell Sci **118**(16): 3573-3584.
- Moustakas, A., S. Souchelnytskyi and C.-H. Heldin (2001). "Smad regulation in TGF- β signal transduction." J Cell Sci **114**(24): 4359-4369.
- Mundy, G. R. (2002). "Metastasis: Metastasis to bone: causes, consequences and therapeutic opportunities." Nat Rev Cancer **2**(8): 584-593.
- Munger, J. S., X. Huang, H. Kawakatsu, M. J. D. Griffiths, S. L. Dalton, J. Wu, J.-F. Pittet, N. Kaminski, C. Garat, M. A. Matthay, D. B. Rifkin and D. Sheppard (1999). "A Mechanism for Regulating Pulmonary Inflammation and Fibrosis: The Integrin α v β 6 Binds and Activates Latent TGF β 1." Cell **96**(3): 319-328.
- Muraoka, R. S., N. Dumont, C. A. Ritter, T. C. Dugger, D. M. Brantley, J. Chen, E. Easterly, L. R. Roebuck, S. Ryan, P. J. Gotwals, V. Koteliansky and C. L. Arteaga (2002). "Blockade of TGF-beta inhibits mammary tumour cell viability, migration, and metastases." J Clin Invest **109**(12): 1551-1559.

Naber, H. H., E. Wiercinska, E. Pardali, T. van Laar, E. Nirmala, A. Sundqvist, H. van Dam, G. van der Horst, G. van der Pluijm, B. Heckmann, E. J. Danen and P. ten Dijke (2012). "BMP-7 inhibits TGF- β -induced invasion of breast cancer cells through inhibition of integrin β 3 expression." Cellular Oncology **35**(1): 19-28.

Nakase, T., S. Nomura, H. Yoshikawa, J. Hashimoto, S. Hirota, Y. Kitamura, S. Oikawa, K. Ono and K. Takaoka (1994). "Transient and localized expression of bone morphogenetic protein 4 messenger RNA during fracture healing." Journal of Bone and Mineral Research **9**(5): 651-659.

Nakashima, K., G. Zhou X Fau - Kunkel, Z. Kunkel G Fau - Zhang, J. M. Zhang Z Fau - Deng, R. R. Deng Jm Fau - Behringer, B. Behringer Rr Fau - de Crombrugge and B. de Crombrugge (2002). "The novel zinc finger-containing transcription factor osterix is required for osteoblast differentiation and bone formation." Cell **108**(0092-8674 (Print)): 17-29.

Nemeth, J. A., J. F. Harb, U. Barroso, Z. He, D. J. Grignon and M. L. Cher (1999). "Severe Combined Immunodeficient-hu Model of Human Prostate Cancer Metastasis to Human Bone." Cancer Research **59**(8): 1987-1993.

Nieto, M. A. (2002). "The snail superfamily of zinc-finger transcription factors." Nat Rev Mol Cell Biol **3**(3): 155-166.

Nishimori, H., S. Ehata, H. I. Suzuki, Y. Katsuno and K. Miyazono (2012). "Prostate Cancer Cells and Bone Stromal Cells Mutually Interact with Each Other through Bone Morphogenetic Protein-mediated Signals." Journal of Biological Chemistry **287**(24): 20037-20046.

Oft, M., K.-H. Heider and H. Beug (1998). "TGF² signaling is necessary for carcinoma cell invasiveness and metastasis." Current biology : CB **8**(23): 1243-1252.

Ogasawara, T., H. Kawaguchi, S. Jinno, K. Hoshi, K. Itaka, T. Takato, K. Nakamura and H. Okayama (2004). "Bone Morphogenetic Protein 2-Induced Osteoblast Differentiation Requires Smad-Mediated Down-Regulation of Cdk6." Molecular and Cellular Biology **24**(15): 6560-6568.

Ogawa, K., S. Ishihara, Y. Saito, K. Mineta, M. Nakazawa, K. Ikeo, T. Gojobori, K. Watanabe and K. Agata (2002). "Induction of a noggin-Like Gene by Ectopic DV Interaction during Planarian Regeneration." Developmental Biology **250**(1): 59-70.

Oursler, M. J. (1994). "Osteoclast synthesis and secretion and activation of latent transforming growth factor β ." Journal of Bone and Mineral Research **9**(4): 443-452.

Ozdamar, B., R. Bose, M. Barrios-Rodiles, H. R. Wang, Y. Zhang and J. L. Wrana (2005). "Regulation of the polarity protein Par6 by TGFbeta receptors controls epithelial cell plasticity." Science **307**(5715): 1603-1609.

Özdemir, B. C., J. Hensel, C. Secondini, A. Wetterwald, R. Schwaninger, A. Fleischmann, W. Raffelsberger, O. Poch, M. Delorenzi, R. Temanni, I. G. Mills, G. van der Pluijm, G. N. Thalmann and M. G. Cecchini (2014). "The Molecular Signature of the Stroma Response in Prostate Cancer-Induced Osteoblastic Bone Metastasis Highlights Expansion of Hematopoietic and Prostate Epithelial Stem Cell Niches." PLoS ONE **9**(12): e114530.

Paine-Saunders, S., B. L. Viviano, A. N. Economides and S. Saunders (2002). "Heparan Sulfate Proteoglycans Retain Noggin at the Cell Surface: A POTENTIAL MECHANISM FOR SHAPING BONE MORPHOGENETIC PROTEIN GRADIENTS." Journal of Biological Chemistry **277**(3): 2089-2096.

Parfitt, A. M. (1994). "Osteonal and hemi-osteonal remodeling: the spatial and temporal framework for signal traffic in adult human bone." Journal of Cell Biochemistry **55**(0730-2312 (Print)): 273-276.

Parfitt, A. M. (2002). "Targeted and nontargeted bone remodeling: relationship to basic multicellular unit origination and progression." Bone **30**(1): 5-7.

Patterson, G. I. and R. W. Padgett (2000). "TGF[beta]-related pathways: roles in *Caenorhabditis elegans* development." Trends in Genetics **16**(1): 27-33.

Pautke, C., M. Schieker, T. Tischer, A. Kolk, P. Neth, W. Mutschler and S. Milz (2004). "Characterization of Osteosarcoma Cell Lines MG-63, Saos-2 and U-2 OS in Comparison to Human Osteoblasts." Anticancer Research **24**(6): 3743-3748.

Peinado, H., M. Quintanilla and A. Cano (2003). "Transforming Growth Factor β -1 Induces Snail Transcription Factor in Epithelial Cell Lines." Journal of Biological Chemistry **278**(23): 21113-21123.

Peng, X., W. Guo, T. Liu, X. Wang, X. a. Tu, D. Xiong, S. Chen, Y. Lai, H. Du, G. Chen, G. Liu, Y. Tang, S. Huang and X. Zou (2011). "Identification of miRs-143 and -145 that Is Associated with Bone Metastasis of Prostate Cancer and Involved in the Regulation of EMT." PLoS ONE **6**(5): e20341.

Pereira, R. C., S. Rydziel and E. Canalis (2000). "Bone morphogenetic protein-4 regulates its own expression in cultured osteoblasts." Journal of Cellular Physiology **182**(2): 239-246.

Perkel, V. S., S. Mohan, S. J. Herring, D. J. Baylink and T. A. Linkhart (1990). "Human Prostatic Cancer Cells, PC3, Elaborate Mitogenic Activity Which Selectively Stimulates Human Bone Cells." Cancer Research **50**(21): 6902-6907.

Perlman, R., W. P. Schiemann, M. W. Brooks, H. F. Lodish and R. A. Weinberg (2001). "TGF-beta-induced apoptosis is mediated by the adapter protein Daxx that facilitates JNK activation." Nat Cell Biol **3**(8): 708-714.

Piccolo, S., Y. Sasai, B. Lu and E. M. De Robertis (1996). "Dorsoventral Patterning in *Xenopus*: Inhibition of Ventral Signals by Direct Binding of Chordin to BMP-4." Cell **86**(4): 589-598.

Platten, M., W. Wick and M. Weller (2001). "Malignant glioma biology: Role for TGF- β in growth, motility, angiogenesis, and immune escape." Microscopy Research and Technique **52**(4): 401-410.

Plotkin, L. I., S. C. Manolagas and T. Bellido (2002). "Transduction of Cell Survival Signals by Connexin-43 Hemichannels." Journal of Biological Chemistry **277**(10): 8648-8657.

Pollari, S., S.-K. Leivonen, M. Perälä, V. Fey, S.-M. Käkönen and O. Kallioniemi (2012). "Identification of MicroRNAs Inhibiting TGF- β -Induced IL-11 Production in Bone Metastatic Breast Cancer Cells." PLoS ONE **7**(5): e37361.

Pollock, J. H., M. J. Blaha, S. A. Lavish, S. Stevenson and E. M. Greenfield (1996). "In vivo demonstration that parathyroid hormone and parathyroid hormone-related protein stimulate expression by osteoblasts of interleukin-6 and leukemia inhibitory factor." Journal of Bone and Mineral Research **11**(6): 754-759.

Polyak, K. and R. A. Weinberg (2009). "Transitions between epithelial and mesenchymal states: acquisition of malignant and stem cell traits." Nat Rev Cancer **9**(4): 265-273.

Pouliot, F., A. Blais and C. Labrie (2003). "Overexpression of a Dominant Negative Type II Bone Morphogenetic Protein Receptor Inhibits the Growth of Human Breast Cancer Cells." Cancer Research **63**(2): 277-281.

Prasanna Bukka, M. D. M., and Andrew C. Karaplis (2004). Molecular regulation of osteoblast differentiation. Bone formation. F. B. a. M. C. Farach-Carson. London Springer. **1**: 1-14.

Proetzel, G., S. A. Pawlowski, M. V. Wiles, M. Yin, G. P. Boivin, P. N. Howles, J. Ding, M. W. Ferguson and T. Doetschman (1995). "Transforming growth factor-beta 3 is required for secondary palate fusion." Nat Genet **11**(4): 409-414.

Qing, J., Y. Zhang and R. Derynck (2000). "Structural and Functional Characterization of the Transforming Growth Factor- β -induced Smad3/c-Jun Transcriptional Cooperativity." Journal of Biological Chemistry **275**(49): 38802-38812.

Rabbani, S. A., J. Desjardins, A. W. Bell, D. Banville, A. Mazar, J. Henkin and D. Goltzman (1990). "An amino-terminal fragment of urokinase isolated from a prostate cancer cell line (PC-3) is mitogenic for osteoblast-like cells." Biochemical and Biophysical Research Communications **173**(3): 1058-1064.

Raftopoulou, M. and A. Hall (2004). "Cell migration: Rho GTPases lead the way." Developmental Biology **265**(1): 23-32.

Ranges, G. E., I. S. Figari, T. Espevik and M. A. Palladino, Jr. (1987). "Inhibition of cytotoxic T cell development by transforming growth factor beta and reversal by recombinant tumour necrosis factor alpha." J Exp Med **166**(4): 991-998.

Reddi, A. H. (1997). "Bone morphogenetic proteins: An unconventional approach to isolation of first mammalian morphogens." Cytokine & growth factor reviews **8**(1): 11-20.

Reddy, S. V. (2004). "Regulatory Mechanisms Operative in Osteoclasts." Critical Reviews in Eukaryotic Gene Expression **14**(4): 16.

Reinhold, M. I., M. Abe, R. M. Kapadia, Z. Liao and M. C. Naski (2004). "FGF18 Represses Noggin Expression and Is Induced by Calcineurin." Journal of Biological Chemistry **279**(37): 38209-38219.

Remy, I., A. Montmarquette and S. W. Michnick (2004). "PKB/Akt modulates TGF-[beta] signalling through a direct interaction with Smad3." Nat Cell Biol **6**(4): 358-365.

Rodan, S. B., Y. Imai, M. A. Thiede, G. Wesolowski, D. Thompson, Z. Bar-Shavit, S. Shull, K. Mann and G. A. Rodan (1987). "Characterization of a Human Osteosarcoma Cell Line (Saos-2) with Osteoblastic Properties." Cancer Research **47**(18): 4961-4966.

- Roodman, G. D. (1999). "Cell biology of the osteoclast." Experimental Hematology **27**(8): 1229-1241.
- Roodman, G. D. (2004). "Mechanisms of Bone Metastasis." New England Journal of Medicine **350**(16): 1655-1664.
- Rucci, N. and A. Angelucci (2014). "Prostate Cancer and Bone: The Elective Affinities." BioMed Research International **2014**: 14.
- Saitoh H Fau - Hida, M., T. Hida M Fau - Shimbo, K. Shimbo T Fau - Nakamura, J. Nakamura K Fau - Yamagata, T. Yamagata J Fau - Satoh and T. Satoh (1984). "Metastatic patterns of prostatic cancer. Correlation between sites and number of organs involved." Cancer **54**(0008-543X (Print)): 3078.
- Sandberg, M. M. (1991). "Matrix in Cartilage and Bone Development: Current Views on the Function and Regulation of Major Organic Components." Annals of Medicine **23**(3): 207-217.
- Sanford, L. P., I. Ormsby, A. C. Gittenberger-de Groot, H. Sariola, R. Friedman, G. P. Boivin, E. L. Cardell and T. Doetschman (1997). "TGFbeta2 knockout mice have multiple developmental defects that are non-overlapping with other TGFbeta knockout phenotypes." Development **124**(13): 2659-2670.
- Scheel, C., E. N. Eaton, S. H.-J. Li, C. L. Chaffer, F. Reinhardt, K.-J. Kah, G. Bell, W. Guo, J. Rubin, A. L. Richardson and R. A. Weinberg (2011). "Paracrine and autocrine signals induce and maintain mesenchymal and stem cell states in the breast." Cell **145**(6): 926-940.
- Schiller, M., D. Javelaud and A. Mauviel (2004). "TGF- β -induced SMAD signaling and gene regulation: consequences for extracellular matrix remodeling and wound healing." Journal of dermatological science **35**(2): 83-92.
- Schlunegger, M. P. and M. G. Grutter (1992). "An unusual feature revealed by the crystal structure at 2.2 [angst] resolution of human transforming growth factor β 2." Nature **358**(6385): 430-434.
- Schmierer, B. and C. S. Hill (2007). "TGF[β]-SMAD signal transduction: molecular specificity and functional flexibility." Nat Rev Mol Cell Biol **8**(12): 970-982.
- Schramek, D., A. Leibbrandt, V. Sigl, L. Kenner, J. A. Pospisilik, H. J. Lee, R. Hanada, P. A. Joshi, A. Aliprantis, L. Glimcher, M. Pasparakis, R. Khokha, C. J. Ormandy, M. Widschwendter, G. Schett and J. M. Penninger (2010). "Osteoclast differentiation factor RANKL controls development of progestin-driven mammary cancer." Nature **468**(7320): 98-102.
- Schultz-Cherry, S., J. Lawler and J. E. Murphy-Ullrich (1994). "The type 1 repeats of thrombospondin 1 activate latent transforming growth factor-beta." Journal of Biological Chemistry **269**(43): 26783-26788.
- Schultz-Cherry, S., S. Ribeiro, L. Gentry and J. E. Murphy-Ullrich (1994). "Thrombospondin binds and activates the small and large forms of latent transforming growth factor-beta in a chemically defined system." Journal of Biological Chemistry **269**(43): 26775-26782.

Schwaninger, R., A. Rentsch Ca Fau - Wetterwald, G. Wetterwald A Fau - van der Horst, R. L. van der Horst G Fau - van Bezooijen, G. van Bezooijen RI Fau - van der Pluijm, C. W. G. M. van der Pluijm G Fau - Lowik, K. Lowik Cw Fau - Ackermann, W. Ackermann K Fau - Pyerin, F. C. Pyerin W Fau - Hamdy, G. N. Hamdy Fc Fau - Thalmann, M. G. Thalmann Gn Fau - Cecchini and M. G. Cecchini (2007). "Lack of noggin expression by cancer cells is a determinant of the osteoblast response in bone metastases." Am J pathol **170**(0002-9440 (Print)): 160-175.

Scott Sawyer, J., D. W. Beight, K. S. Britt, B. D. Anderson, R. M. Campbell, T. Goodson, D. K. Herron, H.-Y. Li, W. T. McMillen, N. Mort, S. Parsons, E. C. R. Smith, J. R. Wagner, L. Yan, F. Zhang and J. M. Yingling (2004). "Synthesis and activity of new aryl- and heteroaryl-substituted 5,6-dihydro-4H-pyrrolo[1,2-b]pyrazole inhibitors of the transforming growth factor-[beta] type I receptor kinase domain." Bioorganic & Medicinal Chemistry Letters **14**(13): 3581-3584.

Sebald, W., J. Nickel, J. L. Zhang and T. D. Mueller (2004). "Molecular recognition in bone morphogenetic protein (BMP)/receptor interaction." Biol Chem **385**(8): 697-710.

Secondini, C., A. Wetterwald, R. Schwaninger, G. N. Thalmann and M. G. Cecchini (2011). "The role of the BMP signaling antagonist noggin in the development of prostate cancer osteolytic bone metastasis." PloS one **6**(1): e16078.

Seoane, J. (2006). "Escaping from the TGF β anti-proliferative control." Carcinogenesis **27**(11): 2148-2156.

Seoane, J., H.-V. Le, L. Shen, S. A. Anderson and J. Massagué (2004). "Integration of Smad and Forkhead Pathways in the Control of Neuroepithelial and Glioblastoma Cell Proliferation." Cell **117**(2): 211-223.

Shah, A. H., W. B. Tabayoyong, S. D. Kundu, S.-J. Kim, L. Van Parijs, V. C. Liu, E. Kwon, N. M. Greenberg and C. Lee (2002). "Suppression of Tumour Metastasis by Blockade of Transforming Growth Factor β Signaling in Bone Marrow Cells through a Retroviral-mediated Gene Therapy in Mice." Cancer Research **62**(24): 7135-7138.

Sharov, A. A., L. Weiner, T. Y. Sharova, F. Siebenhaar, R. Atoyan, A. M. Reginato, C. A. McNamara, K. Funa, B. A. Gilchrest, J. L. Brisette and V. A. Botchkarev (2003). "Noggin overexpression inhibits eyelid opening by altering epidermal apoptosis and differentiation." The EMBO Journal **22**(12): 2992-3003.

Shen, W., Y. Niu and H. Zhang (2014). "The Bone Microenvironmental Effect in the Dormancy of Cancer." Journal of Cancer Therapy **2014**: 315-322.

Shevrin, D. H., L. Kukreja Sc Fau - Ghosh, T. E. Ghosh L Fau - Lad and T. E. Lad (1988). "Development of skeletal metastasis by human prostate cancer in athymic nude mice." Clinical and experimental metastasis **6**(0262-0898 (Print)): 401-409.

Shi, Y. (2001). "Structural insights on Smad function in TGF β signaling." BioEssays **23**(3): 223-232.

Shi, Y. and J. Massagué (2003). "Mechanisms of TGF- β Signaling from Cell Membrane to the Nucleus." Cell **113**(6): 685-700.

shida, W., K. Hamamoto T Fau - Kusanagi, K. Kusanagi K Fau - Yagi, M. Yagi K Fau - Kawabata, K. Kawabata M Fau - Takehara, T. K. Takehara K Fau - Sampath, M. Sampath Tk Fau - Kato, K. Kato M Fau - Miyazono and K. Miyazono (2000). "Smad6 is a Smad1/5-induced smad inhibitor. Characterization of bone morphogenetic protein-responsive element in the mouse Smad6 promoter." Journal of biological chemistry **275**(0021-9258 (Print)): 6075-6078.

Shimonaka, M., S. Inouye, S. Shimasaki and N. Ling (1991). "Follistatin Binds to both Activin and Inhibin through the Common Beta-Subunit." Endocrinology **128**(6): 3313-3315.

Shiozawa, Y., E. A. Pedersen, A. M. Havens, Y. Jung, A. Mishra, J. Joseph, J. K. Kim, L. R. Patel, C. Ying, A. M. Ziegler, M. J. Pienta, J. Song, J. Wang, R. D. Loberg, P. H. Krebsbach, K. J. Pienta and R. S. Taichman (2011). "Human prostate cancer metastases target the hematopoietic stem cell niche to establish footholds in mouse bone marrow." The Journal of Clinical Investigation **121**(4): 1298-1312.

Shull, M. M., I. Ormsby, A. B. Kier, S. Pawlowski, R. J. Diebold, M. Yin, R. Allen, C. Sidman, G. Proetzel, D. Calvin, N. Annunziata and T. Doetschman (1992). "Targeted disruption of the mouse transforming growth factor- β 1 gene results in multifocal inflammatory disease." Nature **359**(6397): 693-699.

Siegel, P. M. and J. Massague (2003). "Cytostatic and apoptotic actions of TGF- β in homeostasis and cancer." Nat Rev Cancer **3**(11): 807-820.

Silver, I. A., D. J. Murrills Rj Fau - Etherington and D. J. Etherington (1988). "Microelectrode studies on the acid microenvironment beneath adherent macrophages and osteoclasts." Experimental Cell Research **175**(0014-4827 (Print)): 266-276.

Simonet, W. S., C. R. Lacey DI Fau - Dunstan, M. Dunstan Cr Fau - Kelley, M. S. Kelley M Fau - Chang, R. Chang Ms Fau - Luthy, H. Q. Luthy R Fau - Nguyen, S. Nguyen Hq Fau - Wooden, L. Wooden S Fau - Bennett, T. Bennett L Fau - Boone, G. Boone T Fau - Shimamoto, M. Shimamoto G Fau - DeRose, R. DeRose M Fau - Elliott, A. Elliott R Fau - Colombero, H. L. Colombero A Fau - Tan, G. Tan Hl Fau - Trail, J. Trail G Fau - Sullivan, E. Sullivan J Fau - Davy, N. Davy E Fau - Bucay, L. Bucay N Fau - Renshaw-Gegg, T. M. Renshaw-Gegg L Fau - Hughes, D. Hughes Tm Fau - Hill, W. Hill D Fau - Pattison, P. Pattison W Fau - Campbell, S. Campbell P Fau - Sander, G. Sander S Fau - Van, J. Van G Fau - Tarpley, P. Tarpley J Fau - Derby, R. Derby P Fau - Lee, W. J. Lee R Fau - Boyle and W. J. Boyle (1997). "Osteoprotegerin: a novel secreted protein involved in the regulation of bone density." Cell **89**(0092-8674 (Print)): 309-319.

Sitaras, N. M., E. Sariban, M. Bravo, P. Pantazis and H. N. Antoniades (1988). "Constitutive Production of Platelet-derived Growth Factor-like Proteins by Human Prostate Carcinoma Cell Lines." Cancer Research **48**(7): 1930-1935.

Smith, P. K., Krohn, R. I., Hermanson, G. T., Mallia, A. K., Gartner, F. H., Provenzano, M. D., Fujimoto, E. K., Goetze, N. M., Olson, B. J. & Klenk, D. C. (1985). Measurement of protein using bicinchoninic acid. Anal Biochem, **150**, 76-85.

- Smith, W. C. and R. M. Harland (1992). "Expression cloning of noggin, a new dorsalizing factor localized to the Spemann organizer in *Xenopus* embryos." *Cell* **70**(5): 829-840.
- Soda, H., E. Raymond, S. Sharma, R. Lawrence, C. Cerna, L. Gomez, G. A. Timony, D. D. Von Hoff and E. Izbicka (1998). "Antiproliferative effects of recombinant human bone morphogenetic protein-2 on human tumour colony-forming units." *Anticancer Drugs* **9**(4): 327-331.
- Soff, G. A., J. Sanderowitz, S. Gately, E. Verrusio, I. Weiss, S. Brem and H. C. Kwaan (1995). "Expression of plasminogen activator inhibitor type 1 by human prostate carcinoma cells inhibits primary tumour growth, tumour-associated angiogenesis, and metastasis to lung and liver in an athymic mouse model." *J Clin Invest* **96**(6): 2593-2600.
- Song, K., C. Krause, S. Shi, M. Patterson, R. Suto, L. Grgurevic, S. Vukicevic, M. van Dinther, D. Falb, P. ten Dijke and M. H. Alaoui-Ismaili (2010). "Identification of a Key Residue Mediating Bone Morphogenetic Protein (BMP)-6 Resistance to Noggin Inhibition Allows for Engineered BMPs with Superior Agonist Activity." *Journal of Biological Chemistry* **285**(16): 12169-12180.
- Sorrentino, A., N. Thakur, S. Grimsby, A. Marcusson, V. von Bulow, N. Schuster, S. Zhang, C. H. Heldin and M. Landstrom (2008). "The type I TGF-beta receptor engages TRAF6 to activate TAK1 in a receptor kinase-independent manner." *Nat Cell Biol* **10**(10): 1199-1207.
- STEIN, G. S. and J. B. LIAN (1993). "Molecular Mechanisms Mediating Proliferation/Differentiation Interrelationships During Progressive Development of the Osteoblast Phenotype." *Endocrine Reviews* **14**(4): 424-442.
- Steiner, M. S., D. C. Zhou Zz Fau - Tonb, E. R. Tonb Dc Fau - Barrack and E. R. Barrack (1994). "Expression of transforming growth factor-beta 1 in prostate cancer." *Endocrinology* **135**(0013-7227_(Print)).
- Sutherland, M. K., J. C. Geoghegan, C. Yu, D. G. Winkler and J. A. Latham (2004). "Unique regulation of SOST, the sclerosteosis gene, by BMPs and steroid hormones in human osteoblasts." *Bone* **35**(2): 448-454.
- Suva, L. J., C. Washam, R. W. Nicholas and R. J. Griffin (2011). "Bone metastasis: mechanisms and therapeutic opportunities." *Nature reviews. Endocrinology* **7**(4): 208-218.
- Taichman, R. S. (2005). "Blood and bone: two tissues whose fates are intertwined to create the hematopoietic stem-cell niche." *Blood* **105**(7): 2631-2639.
- Tamada, H., R. Kitazawa, K. Gohji and S. Kitazawa (2001). "Epigenetic Regulation of Human Bone Morphogenetic Protein 6 Gene Expression in Prostate Cancer." *Journal of Bone and Mineral Research* **16**(3): 487-496.
- Tang, B., N. Yoo, M. Vu, M. Mamura, J.-S. Nam, A. Ooshima, Z. Du, P.-Y. Desprez, M. R. Anver, A. M. Michalowska, J. Shih, W. T. Parks and L. M. Wakefield (2007). "Transforming Growth Factor- β Can Suppress Tumourigenesis through Effects on the Putative Cancer Stem or Early Progenitor Cell and Committed Progeny in a Breast Cancer Xenograft Model." *Cancer Research* **67**(18): 8643-8652.

Tang, Y., X. Wu, W. Lei, L. Pang, C. Wan, Z. Shi, L. Zhao, T. R. Nagy, X. Peng, J. Hu, X. Feng, W. Van Hul, M. Wan and X. Cao (2009). "TGF- β 1-induced Migration of Bone Mesenchymal Stem Cells Couples Bone Resorption and Formation." Nature medicine **15**(7): 757-765.

Tarragona, M., M. Pavlovic, A. Arnal-Estapé, J. Urosevic, M. Morales, M. Guiu, E. Planet, E. González-Suárez and R. R. Gomis (2012). "Identification of NOG as a Specific Breast Cancer Bone Metastasis-supporting Gene." Journal of Biological Chemistry **287**(25): 21346-21355.

ten Dijke, P., K. Miyazono and C.-H. Heldin (2000). "Signaling inputs converge on nuclear effectors in TGF- β signaling." Trends in Biochemical Sciences **25**(2): 64-70.

Ten Dijke, P., M.-J. Goumans, F. Itoh and S. Itoh (2002). "Regulation of cell proliferation by Smad proteins." Journal of Cellular Physiology **191**(1): 1-16.

Tenenbaum, H. C. (1987). "Levamisole and inorganic pyrophosphate inhibit beta-glycerophosphate induced mineralization of bone formed in vitro." Bone Mineral **2**(0169-6009 (Print)): 13-26.

Tenenbaum, H. C., C. McCulloch Ca Fau - Fair, C. Fair C Fau - Birek and C. Birek (1989). "The regulatory effect of phosphates on bone metabolism in vitro." Cell tissue research **257**(0302-766X (Print)): 555-563.

Theriault, R. L. and R. L. Theriault (2012). "Biology of bone metastases." Cancer control : journal of the Moffitt Cancer Center **19**(2): 92-101.

Thiery, J. P. (2002). "Epithelial-mesenchymal transitions in tumour progression." Nat Rev Cancer **2**(6): 442-454.

Thiery, J. P. (2003). "Epithelial-mesenchymal transitions in development and pathologies." Current Opinion in Cell Biology **15**(6): 740-746.

Thomas, D. M., S. A. Johnson, N. A. Sims, M. K. Trivett, J. L. Slavin, B. P. Rubin, P. Waring, G. A. McArthur, C. R. Walkley, A. J. Holloway, D. Diyagama, J. E. Grim, B. E. Clurman, D. D. L. Bowtell, J.-S. Lee, G. M. Gutierrez, D. M. Piscopo, S. A. Carty and P. W. Hinds (2004). "Terminal osteoblast differentiation, mediated by runx2 and p27KIP1, is disrupted in osteosarcoma." The Journal of Cell Biology **167**(5): 925-934.

Thompson, T. C., L. D. Truong, T. L. Timme, D. Kadmon, B. K. McCune, K. C. Flanders, P. T. Scardino and S. H. Park (1993). "Transgenic models for the study of prostate cancer." Cancer **71**(3 Suppl): 1165-1171.

Tian, Q., S. B. Stepaniants, M. Mao, L. Weng, M. C. Feetham, M. J. Doyle, E. C. Yi, H. Dai, V. Thorsson, J. Eng, D. Goodlett, J. P. Berger, B. Gunter, P. S. Linseley, R. B. Stoughton, R. Aebersold, S. J. Collins, W. A. Hanlon and L. E. Hood (2004). "Integrated Genomic and Proteomic Analyses of Gene Expression in Mammalian Cells." Molecular & Cellular Proteomics **3**(10): 960-969.

Tonegawa, A. and Y. Takahashi (1998). "Somitogenesis Controlled by Noggin." Developmental Biology **202**(2): 172-182.

- Tosh, D. and J. M. W. Slack (2002). "How cells change their phenotype." Nat Rev Mol Cell Biol **3**(3): 187-194.
- Tu, W. H., T. Z. Thomas, N. Masumori, N. A. Bhowmick, A. E. Gorska, Y. Shyr, S. Kasper, T. Case, R. L. Roberts, S. B. Shappell, H. L. Moses and R. J. Matusik (2003). "The loss of TGF-beta signaling promotes prostate cancer metastasis." Neoplasia **5**(3): 267-277.
- Tylzanowski, P., L. Mebis and F. P. Luyten (2006). "The Noggin null mouse phenotype is strain dependent and haploinsufficiency leads to skeletal defects." Developmental Dynamics **235**(6): 1599-1607.
- Ubara, Y., T. Fushimi, T. Tagami, N. Sawa, J. Hoshino, M. Yokota, H. Katori, F. Takemoto and S. Hara (2003). "Histomorphometric features of bone in patients with primary and secondary hypoparathyroidism." Kidney Int **63**(5): 1809-1816.
- Ubara, Y., T. Tagami, S. Nakanishi, N. Sawa, J. Hoshino, T. Suwabe, H. Katori, F. Takemoto, S. Hara and K. Takaichi (2005). "Significance of minimodeling in dialysis patients with adynamic bone disease." Kidney Int **68**(2): 833-839.
- Uzel, M. I., I. C. Scott, H. Babakhanlou-Chase, A. H. Palamakumbura, W. N. Pappano, H.-H. Hong, D. S. Greenspan and P. C. Trackman (2001). "Multiple Bone Morphogenetic Protein 1-related Mammalian Metalloproteinases Process Pro-lysyl Oxidase at the Correct Physiological Site and Control Lysyl Oxidase Activation in Mouse Embryo Fibroblast Cultures." Journal of Biological Chemistry **276**(25): 22537-22543.
- Valcourt, U., M. Kowanzetz, H. Niimi, C.-H. Heldin and A. Moustakas (2005). "TGF- β and the Smad Signaling Pathway Support Transcriptomic Reprogramming during Epithelial-Mesenchymal Cell Transition." Mol. Biol. Cell **16**(4): 1987-2002.
- Valenzuela, D. M., E. Economides An Fau - Rojas, T. M. Rojas E Fau - Lamb, L. Lamb Tm Fau - Nunez, P. Nunez L Fau - Jones, N. Y. Jones P Fau - Lp, R. Lp Ny Fau - Espinosa, 3rd, C. I. Espinosa R 3rd Fau - Brannan, D. J. Brannan Ci Fau - Gilbert, D. J. Gilbert and et al. (1995). "Identification of mammalian noggin and its expression in the adult nervous system." Journal of Neurosci **15**(0270-6474 (Print)).
- van den Hoogen, C., G. van der Horst, H. Cheung, J. T. Buijs, R. C. M. Pelger and G. van der Pluijm (2011). "Integrin α v Expression Is Required for the Acquisition of a Metastatic Stem/Progenitor Cell Phenotype in Human Prostate Cancer." The American Journal of Pathology **179**(5): 2559-2568.
- van der Pluijm, G. (2011). "Epithelial plasticity, cancer stem cells and bone metastasis formation." Bone **48**(1): 37-43.
- Van Der Pluijm, G., B. Sijmons, H. Vloedgraven, M. Deckers, S. Papapoulos and C. Löwik (2001). "Monitoring Metastatic Behavior of Human Tumour Cells in Mice with Species-Specific Polymerase Chain Reaction: Elevated Expression of Angiogenesis and Bone Resorption Stimulators by Breast Cancer in Bone Metastases." Journal of Bone and Mineral Research **16**(6): 1077-1091.
- Vardouli, L., A. Moustakas and C. Stournaras (2005). "LIM-kinase 2 and Cofilin Phosphorylation Mediate Actin Cytoskeleton Reorganization Induced by Transforming Growth Factor- β ." Journal of Biological Chemistry **280**(12): 11448-11457.

- Verrecchia, F. and A. Mauviel (2002). "Control of connective tissue gene expression by TGF beta: role of Smad proteins in fibrosis." Curr Rheumatol Rep **4**(2): 143-149.
- Virk, M. S., F. Alaei, F. A. Petrigliano, O. Sugiyama, A. F. Chatziioannou, D. Stout, W. C. Dougall and J. R. Lieberman (2011). "Combined inhibition of the BMP pathway and the RANK-RANKL axis in a mixed lytic/blastic prostate cancer lesion." Bone **48**(3): 578-587.
- Voegelé, T. J., M. Voegelé-Kadletz, V. Esposito, K. Macfelda, U. Oberndorfer, V. Vecsei and R. Schabus (2000). "The effect of different isolation techniques on human osteoblast-like cell growth." Anticancer research **20**(5B): 3575-3581.
- Wakefield, L. M. and C. S. Hill (2013). "Beyond TGF[beta]: roles of other TGF[beta] superfamily members in cancer." Nat Rev Cancer **13**(5): 328-341.
- Wakefield, L. M., D. M. Smith, T. Masui, C. C. Harris and M. B. Sporn (1987). "Distribution and modulation of the cellular receptor for transforming growth factor-beta." The Journal of Cell Biology **105**(2): 965-975.
- Walsh, D. W., D. P. Godson C Fau - Brazil, F. Brazil Dp Fau - Martin and F. Martin (2010). "Extracellular BMP-antagonist regulation in development and disease: tied up in knots." Trends Cell Biol **20**(1879-3088 (Electronic)): 244-256.
- Wan, D. C., J. H. Pomerantz, L. J. Brunet, J.-B. Kim, Y.-F. Chou, B. M. Wu, R. Harland, H. M. Blau and M. T. Longaker (2007). "Noggin Suppression Enhances in Vitro Osteogenesis and Accelerates in Vivo Bone Formation." Journal of Biological Chemistry **282**(36): 26450-26459.
- Wang, E. A., V. Rosen, J. S. D'Alessandro, M. Bauduy, P. Cordes, T. Harada, D. I. Israel, R. M. Hewick, K. M. Kerns, P. LaPan and et al. (1990). "Recombinant human bone morphogenetic protein induces bone formation." Proc Natl Acad Sci U S A **87**(6): 2220-2224.
- Wang, J., L. Sun, L. Myeroff, X. Wang, L. E. Gentry, J. Yang, J. Liang, E. Zborowska, S. Markowitz, J. K. V. Willson and M. G. Brattain (1995). "Demonstration That Mutation of the Type II Transforming Growth Factor β Receptor Inactivates Its Tumour Suppressor Activity in Replication Error-positive Colon Carcinoma Cells." Journal of Biological Chemistry **270**(37): 22044-22049.
- Wang, J., R. L. Levenson As Fau - Satcher, Jr. and R. L. Satcher, Jr. (2006). "Identification of a unique set of genes altered during cell-cell contact in an in vitro model of prostate cancer bone metastasis." Int J Mol Med **17**(1107-3756 (Print)): 849-856.
- Warren, S. M., L. J. Brunet, R. M. Harland, A. N. Economides and M. T. Longaker (2003). "The BMP antagonist noggin regulates cranial suture fusion." Nature **422**(6932): 625-629.
- Weilbaecher, K. N., T. A. Guise and L. K. McCauley (2011). "Cancer to bone: a fatal attraction." Nat Rev Cancer **11**(6): 411-425.
- Weinberg, R. A. (1989). "Positive and negative controls on cell growth." Biochemistry **28**(21): 8263-8269.

- Weinberg, R. A. (2007). The biology of cancer Garland Science, Taylor and Francis Group.
- Weinstein, R. S., R. L. Jilka, A. M. Parfitt and S. C. Manolagas (1998). "Inhibition of osteoblastogenesis and promotion of apoptosis of osteoblasts and osteocytes by glucocorticoids. Potential mechanisms of their deleterious effects on bone." The Journal of Clinical Investigation **102**(2): 274-282.
- Welch, D. R., A. Fabra and M. Nakajima (1990). "Transforming growth factor beta stimulates mammary adenocarcinoma cell invasion and metastatic potential." Proc Natl Acad Sci U S A **87**(19): 7678-7682.
- Whitman, M. (1998). "Smads and early developmental signaling by the TGF β superfamily." Genes & Development **12**(16): 2445-2462.
- Wick, W., M. Platten and M. Weller (2001). "Glioma Cell Invasion: Regulation of Metalloproteinase Activity by TGF- β ." Journal of Neuro-Oncology **53**(2): 177-185.
- Wikström, P., J.-E. Damber and A. Bergh (2001). "Role of transforming growth factor- β 1 in prostate cancer." Microscopy Research and Technique **52**(4): 411-419.
- Wilding, G. (1991). "Response of prostate cancer cells to peptide growth factors: transforming growth factor-beta." Cancer Surv **11**: 147-163.
- Wilding, G., G. Zugmeier, C. Knabbe, K. Flanders and E. Gelmann (1989). "Differential effects of transforming growth factor β on human prostate cancer cells in vitro." Molecular and Cellular Endocrinology **62**(1): 79-87.
- Willis RA (1934). The spread of tumours in the human body. London, J&A Churchill.
- Wingo, P. A., T. Tong and S. Bolden (1995). "Cancer statistics, 1995." CA: A Cancer Journal for Clinicians **45**(1): 8-30.
- Winkler, D. G., C. Yu, J. C. Geoghegan, E. W. Ojala, J. E. Skonier, D. Shpektor, M. K. Sutherland and J. A. Latham (2004). "Noggin and Sclerostin Bone Morphogenetic Protein Antagonists Form a Mutually Inhibitory Complex." Journal of Biological Chemistry **279**(35): 36293-36298.
- Wozney, J. M. (2002). "Overview of bone morphogenetic proteins." Spine (Phila Pa 1976) **27**(16 Suppl 1): S2-8.
- Wozney, J. M. and V. Rosen (1998). "Bone morphogenetic protein and bone morphogenetic protein gene family in bone formation and repair." Clin Orthop Relat Res(346): 26-37.

Wozney, J. M., A. J. Rosen V Fau - Celeste, L. M. Celeste Aj Fau - Mitscock, M. J. Mitscock Lm Fau - Whitters, R. W. Whitters Mj Fau - Kriz, R. M. Kriz Rw Fau - Hewick, E. A. Hewick Rm Fau - Wang and E. A. Wang (1998). "Novel regulators of bone formation: molecular clones and activities." Science **242**(0036-8075

Wrana, J. L., M. Maeno, B. Hawrylyshyn, K. L. Yao, C. Domenicucci and J. Sodek (1988). "Differential effects of transforming growth factor-beta on the synthesis of extracellular matrix proteins by normal fetal rat calvarial bone cell populations." The Journal of Cell Biology **106**(3): 915-924.

Wrzesinski, S. H., Y. Y. Wan and R. A. Flavell (2007). "Transforming growth factor-beta and the immune response: implications for anticancer therapy." Clin Cancer Res **13**(18 Pt 1): 5262-5270.

Wu, X.-B., Y. Li, A. Schneider, W. Yu, G. Rajendren, J. Iqbal, M. Yamamoto, M. Alam, L. J. Brunet, H. C. Blair, M. Zaidi and E. Abe (2003). "Impaired osteoblastic differentiation, reduced bone formation, and severe osteoporosis in noggin-overexpressing mice." The Journal of Clinical Investigation **112**(6): 924-934.

Xiao, G., R. Gopalakrishnan, D. Jiang, E. Reith, M. D. Benson and R. T. Franceschi (2002). "Bone Morphogenetic Proteins, Extracellular Matrix, and Mitogen-Activated Protein Kinase Signaling Pathways Are Required for Osteoblast-Specific Gene Expression and Differentiation in MC3T3-E1 Cells." Journal of Bone and Mineral Research **17**(1): 101-110.

Xiao, Z., Zhang, S., Mahlios, J., Zhou, G., Magenheimer, B. S., Guo, D., Dallas, S. L., Maser, R., Calvet, J. P., Bonewald, L. & Quartes, L. D. 2006. Cilia-like structures and polycystin-1 in osteoblasts/osteocytes and associated abnormalities in skeletogenesis and Runx2 expression. J Biol Chem **281**:30884-95.

Xu, J., K. Matsuzaki, K. McKeehan, F. Wang, M. Kan and W. L. McKeehan (1994). "Genomic structure and cloned cDNAs predict that four variants in the kinase domain of serine/threonine kinase receptors arise by alternative splicing and poly(A) addition." Proc Natl Acad Sci U S A **91**(17): 7957-7961.

Xue, H., B. Lu and M. Lai (2008). "The cancer secretome: a reservoir of biomarkers." J Transl Med **6**(1): 6-52.

Yamaguchi, K., S.-i. Nagai, J. Ninomiya-Tsuji, M. Nishita, K. Tamai, K. Irie, N. Ueno, E. Nishida, H. Shibuya and K. Matsumoto (1999). "XIAP, a cellular member of the inhibitor of apoptosis protein family, links the receptors to TAB1-TAK1 in the BMP signaling pathway." EMBO J **18**(1): 179-187.

Yamashita, H., P. ten Dijke, D. Huylebroeck, T. K. Sampath, M. Andries, J. C. Smith, C. H. Heldin and K. Miyazono (1995). "Osteogenic protein-1 binds to activin type II receptors and induces certain activin-like effects." The Journal of Cell Biology **130**(1): 217-226.

Yamashita, M., K. Fatyol, C. Jin, X. Wang, Z. Liu and Y. E. Zhang (2008). "TRAF6 Mediates Smad-Independent Activation of JNK and p38 by TGF-²." Molecular cell **31**(6): 918-924.

Yan, X., Z. Liu and Y. Chen (2009). "Regulation of TGF-beta signaling by Smad7." Acta Biochim Biophys Sin (Shanghai) **41**(4): 263-272.

- Yanagisawa, M., K. Nakashima, K. Takeda, W. Ochiai, T. Takizawa, M. Ueno, M. Takizawa, H. Shibuya and T. Taga (2001). "Inhibition of BMP2-induced, TAK1 kinase-mediated neurite outgrowth by Smad6 and Smad7." Genes to Cells **6**(12): 1091-1099.
- Yanagita, M. (2005). "BMP antagonists: Their roles in development and involvement in pathophysiology." Cytokine & Growth Factor Reviews **16**(3): 309-317.
- Yang, S., C. Zhong, B. Frenkel, A. H. Reddi and P. Roy-Burman (2005). "Diverse Biological Effect and Smad Signaling of Bone Morphogenetic Protein 7 in Prostate Tumour Cells." Cancer Research **65**(13): 5769-5777.
- Ye, L., J. M. Lewis-Russell, H. G. Kyanaston and W. G. Jiang (2007). "Bone morphogenetic proteins and their receptor signaling in prostate cancer." Histol Histopathol **22**(10): 1129-1147.
- Ye, L., J. M. Lewis-Russell, H. Kynaston and W. G. Jiang (2007). "Endogenous Bone Morphogenetic Protein-7 Controls the Motility of Prostate Cancer Cells Through Regulation of Bone Morphogenetic Protein Antagonists." The Journal of Urology **178**(3): 1086-1091.
- Yin, J. J., K. Selander, J. M. Chirgwin, M. Dallas, B. G. Grubbs, R. Wieser, J. Massague, G. R. Mundy and T. A. Guise (1999). "TGF-beta signaling blockade inhibits PTHrP secretion by breast cancer cells and bone metastases development." J Clin Invest **103**(2): 197-206.
- Yoneda, T. and T. Hiraga (2005). "Crosstalk between cancer cells and bone microenvironment in bone metastasis." Biochemical and Biophysical Research Communications **328**(3): 679-687.
- Yoshimura, Y., S. Nomura, S. Kawasaki, T. Tsutsumimoto, T. Shimizu and K. Takaoka (2001). "Colocalization of Noggin and Bone Morphogenetic Protein-4 During Fracture Healing." Journal of Bone and Mineral Research **16**(5): 876-884.
- Yu, P. B., H. Beppu, N. Kawai, E. Li and K. D. Bloch (2005). "Bone Morphogenetic Protein (BMP) Type II Receptor Deletion Reveals BMP Ligand-specific Gain of Signaling in Pulmonary Artery Smooth Muscle Cells." Journal of Biological Chemistry **280**(26): 24443-24450.
- Yuen, H. F., W.-L. Chan Yp Fau - Cheung, Y.-C. Cheung Wl Fau - Wong, X. Wong Yc Fau - Wang, K.-W. Wang X Fau - Chan and K. W. Chan (2008). "The prognostic significance of BMP-6 signaling in prostate cancer." Modern Pathology **21**(1530-0285 (Electronic)): 1436-1443.
- Yuen, H.-F., C. M. McCrudden, C. Grills, S.-D. Zhang, Y.-H. Huang, K.-K. Chan, Y.-P. Chan, M. L.-Y. Wong, S. Law, G. Srivastava, D. A. Fennell, G. Dickson, M. El-Tanani and K.-W. Chan (2012). "Combinatorial use of bone morphogenetic protein 6, noggin and SOST significantly predicts cancer progression." Cancer Science **103**(6): 1145-1154.
- Zagzag, D., K. Salnikow, L. Chiriboga, H. Yee, L. Lan, M. A. Ali, R. Garcia, S. Demaria and E. W. Newcomb (2005). "Downregulation of major histocompatibility complex antigens in invading glioma cells: stealth invasion of the brain." Lab Invest **85**(3): 328-341.
- Zaidi, M., A. M. Inzerillo, B. S. Moonga, P. J. R. Bevis and C. L. H. Huang (2002). "Forty years of calcitonin—where are we now? A tribute to the work of Iain Macintyre, FRS." Bone **30**(5): 655-663.

Zavadil, J., M. Bitzer, D. Liang, Y. C. Yang, A. Massimi, S. Kneitz, E. Piek and E. P. Bottinger (2001). "Genetic programs of epithelial cell plasticity directed by transforming growth factor-beta." Proc Natl Acad Sci U S A **98**(12): 6686-6691.

Zehentner, B. K., A. Haussmann and H. Burtscher (2002). "The bone morphogenetic protein antagonist Noggin is regulated by Sox9 during endochondral differentiation." Development, Growth & Differentiation **44**(1): 1-9.

Zhang, H. and A. Bradley (1996). "Mice deficient for BMP2 are nonviable and have defects in amnion/chorion and cardiac development." Development **122**(10): 2977-2986.

Zhao, G.-Q. (2003). "Consequences of knocking out BMP signaling in the mouse." genesis **35**(1): 43-56.

Zhao, X., J. M. Nicholls and Y.-G. Chen (2008). "Severe Acute Respiratory Syndrome-associated Coronavirus Nucleocapsid Protein Interacts with Smad3 and Modulates Transforming Growth Factor- β Signaling." Journal of Biological Chemistry **283**(6): 3272-3280.

Zhu, W., J. Kim, C. Cheng, B. A. Rawlins, O. Boachie-Adjei, R. G. Crystal and C. Hidaka (2006). "Noggin regulation of bone morphogenetic protein (BMP) 2/7 heterodimer activity in vitro." Bone **39**(1): 61-71.

Zimmerman, L. B., J. M. De Jesús-Escobar and R. M. Harland (1996). "The Spemann Organizer Signal noggin Binds and Inactivates Bone Morphogenetic Protein 4." Cell **86**(4): 599-606.

Appendix A

Table 1A Express plate gene expression in exponential and confluent SaOS2 cells.

Gene Name	SaOS2 (exponential) Mean ct Value	GAPDH Mean ct Value	SaOS2 (confluent) Mean ct Value	GAPDH Mean ct Value	Δ dct
ACVR1	28.72608693	20.94892438	29.27659035	20.79617182	0.703256
ACVR1B	31.714077	20.94892438	31.86755816	20.79617182	0.306234
ACVR2A	30.74973933	20.94892438	30.89818891	20.79617182	0.301202
ACVR2A	30.8026975	20.94892438	30.70807838	20.79617182	0.058133
ACVR2B	30.95208041	20.94892438	31.12030538	20.79617182	0.320978
BMP10	37.21621323	20.94892438	36.63376427	20.79617182	-0.4297
BMP2	30.93817711	20.94892438	31.26523209	20.79617182	0.479808
BMP3	33.85720189	20.94892438	35.26694616	20.79617182	1.562497
BMP4	23.51956177	20.94892438	24.28214836	20.79617182	0.915339
BMP5	36.98243078	20.94892438	35.69938914	20.79617182	-1.13029
BMP6	30.92572403	20.94892438	31.77471161	20.79617182	1.00174
BMP7	34.81692123	20.94892438	34.62957382	20.79617182	-0.03459
BMP8B;BMP8A	31.77512105	20.94892438	32.31136322	20.79617182	0.688995
BMPR1A	29.50725492	20.94892438	29.27017148	20.79617182	-0.08433
BMPR1B	30.83174769	20.94892438	30.7936751	20.79617182	0.11468
BMPR2	26.96928914	20.94892438	27.14547729	20.79617182	0.328941
CER1	undetermined	20.94892438	undetermined	20.79617182	#VALUE!
CHRD	36.29343033	20.94892438	36.04893112	20.79617182	-0.09175
ENG	27.95445506	20.94892438	28.04511897	20.79617182	0.243416
FST	31.3014946	20.94892438	31.18039767	20.79617182	0.031656
GDF11	29.91272418	20.94892438	30.27658081	20.79617182	0.516609
GDF1;LASS1	31.92202314	20.94892438	32.21234194	20.79617182	0.443071
GDF2	undetermined	20.94892438	undetermined	20.79617182	#VALUE!
GDF3	undetermined	20.94892438	undetermined	20.79617182	#VALUE!
GDF6	32.50665283	20.94892438	33.42245674	20.79617182	1.068556
GDF7	35.64224243	20.94892438	36.16138713	20.79617182	0.671897
GDF9	34.76025772	20.94892438	35.30661774	20.79617182	0.699113
GREM1	25.53823471	20.94892438	26.31441498	20.79617182	0.928933
INHA	35.81718953	20.94892438	36.58116913	20.79617182	0.916732
INHBA	27.47245407	20.94892438	27.27426974	20.79617182	-0.04543
INHBB	30.44009717	20.94892438	30.29593849	20.79617182	0.008594

Gene Name	SaOS2 (exponential) Mean ct Value	GAPDH Mean ct Value	SaOS2 (confluent) Mean ct Value	GAPDH Mean ct Value	Δ dct
INHBC	36.32163493	20.94892438	36.23087438	20.79617182	0.061992
INHBE	33.41264852	20.94892438	32.29367383	20.79617182	-0.96622
LEFTY2	37.05011113	20.94892438	35.69972356	20.79617182	-1.19764
LTBP1	28.53319105	20.94892438	28.28687859	20.79617182	-0.09356
NBL1	27.86512693	20.94892438	27.53838603	20.79617182	-0.17399
NOG	32.84244665	20.94892438	34.09048971	20.79617182	1.400796
SOST	34.70230484	20.94892438	36.6013298	20.79617182	2.051778
TGFB1	23.80765279	20.94892438	24.289608	20.79617182	0.634708
TGFB2	28.61895116	20.94892438	28.49724706	20.79617182	0.031048
TGFB3	28.80683517	20.94892438	29.29043706	20.79617182	0.636354
TGFBR1	28.02592913	20.94892438	28.23258909	20.79617182	0.359413
TGFBR2	27.77650452	20.94892438	27.9066143	20.79617182	0.282862
TGFBR3	30.98367246	20.94892438	31.18359121	20.79617182	0.352671

This Table represents the ct values and the differences in Δ dct value between SaOS2 cells during exponential growth and SaOS2 cells during Confluent Phase. The dct was calculated by subtracting the gene of interest from the house keeping gene GAPDH for each cell type. The Δ dct value was calculated by subtracting dct value of SaOS2 exponential from the dct value of the SaOS2 confluent cells. Data expressed as mean of 3 independent experiments.

Table 2A Express plate gene expression in exponential PC3RFP and confluent PC3RFP cells.

Gene Name	PC3RFP (exponential) Mean ct Value	GAPDH Mean ct Value	PC3RFP (confluent) Mean ct Value	GAPDH Mean ct Value	Δ dct
ACVR1	28.67760	19.71322	29.61977	20.51371	0.14168
ACVR1B	30.37804	19.71322	31.23541	20.51371	0.05688
ACVR2A	30.06857	19.71322	30.92702	20.51371	0.05796
ACVR2A	30.17434	19.71322	30.73866	20.51371	-0.23617
ACVR2B	31.74068	19.71322	32.49391	20.51371	-0.04726
BMP10	undetermined	19.71322	undetermined	20.51371	#VALUE!
BMP2	30.54163	19.71322	30.93080	20.51371	-0.41133
BMP3	27.92534	19.71322	28.39143	20.51371	-0.33440
BMP4	31.23007	19.71322	31.89929	20.51371	-0.13126
BMP5	36.90198	19.71322	37.14349	20.51371	-0.55898
BMP6	29.72940	19.71322	30.11338	20.51371	-0.41651
BMP7	38.09402	19.71322	36.89372	20.51371	-2.00078
BMP8B;BMP8A	30.59572	19.71322	31.34903	20.51371	-0.04717
BMPR1A	30.25607	19.71322	30.30324	20.51371	-0.75331
BMPR1B	29.93496	19.71322	30.65239	20.51371	-0.08306
BMPR2	28.33518	19.71322	28.94415	20.51371	-0.19153
CER1	37.24395	19.71322	37.24757	20.51371	-0.79687
CHRD	37.01204	19.71322	undetermined	20.51371	#VALUE!
ENG	36.30861	19.71322	37.03303	20.51371	-0.07607
FST	31.81458	19.71322	32.73969	20.51371	0.12461
GDF11	27.29718	19.71322	27.84155	20.51371	-0.25611
GDF1;LASS1	35.20585	19.71322	35.94738	20.51371	-0.05896
GDF2	undetermined	19.71322	undetermined	20.51371	#VALUE!
GDF3	undetermined	19.71322	undetermined	20.51371	#VALUE!
GDF6	undetermined	19.71322	undetermined	20.51371	#VALUE!
GDF7	undetermined	19.71322	37.05927	20.51371	#VALUE!
GDF9	35.23329	19.71322	35.75269	20.51371	-0.28108
GREM1	undetermined	19.71322	undetermined	20.51371	#VALUE!
INHA	34.25590	19.71322	34.67130	20.51371	-0.38508
INHBA	31.53516	19.71322	32.60780	20.51371	0.27215
INHBB	36.78977	19.71322	37.59675	20.51371	0.00649
INHBC	35.37048	19.71322	35.62355	20.51371	-0.54742
INHBE	32.47049	19.71322	33.93227	20.51371	0.66129

Gene Name	PC3RFP (exponential) Mean ct Value	GAPDH Mean ct Value	PC3RFP (confluent) Mean ct Value	GAPDH Mean ct Value	Δ dct
LEFTY2	38.16286	19.71322	37.92624	20.51371	-1.03710
LTBP1	26.31649	19.71322	27.29221	20.51371	0.17523
NBL1	26.88291	19.71322	27.63373	20.51371	-0.04967
NOG	26.88119	19.71322	27.32347	20.51371	-0.35821
SOST	undetermined	19.71322	undetermined	20.51371	#VALUE!
TGFB1	26.55849	19.71322	27.31067	20.51371	-0.04831
TGFB2	31.15269	19.71322	31.91540	20.51371	-0.03777
TGFB3	28.83040	19.71322	29.63135	20.51371	0.00046
TGFBR1	27.90963	19.71322	28.60142	20.51371	-0.10869
TGFBR2	28.34935	19.71322	28.88057	20.51371	-0.26927
TGFBR3	29.51358	19.71322	30.19828	20.51371	-0.11579

This Table shows the ct values and the differences in Δ dct value between PC3RFP cells during exponential growth and PC3RFP cells during Confluent Phase. The dct was calculated by subtracting the gene of interest from the house keeping gene GAPDH for each cell type. The Δ dct value was calculated by subtracting dct value of PC3RFP exponential from the dct value of the PC3RFP confluent cells. Data expressed as mean of 3 independent experiments.

Table 3A Express plate gene expression in confluent PC3RFP and SaOS2 cells.

Gene Name	SaOS2 (Confluent) Mean ct Value	GADH Mean ct Value	PC3RFP (Confluent) Mean ct Value	GADH Mean ct Value	Δ dct
ACVR1	29.27659	20.79617	29.61977	20.51371	0.62564
ACVR1B	31.86756	20.79617	31.23541	20.51371	-0.34968
ACVR2A	30.89819	20.79617	30.92702	20.51371	0.31130
ACVR2A	30.70808	20.79617	30.73866	20.51371	0.31304
ACVR2B	31.12031	20.79617	32.49391	20.51371	1.65607
BMP10	36.63376	20.79617	undetermined	20.51371	#VALUE!
BMP2	31.26523	20.79617	30.93080	20.51371	-0.05197
BMP3	35.26695	20.79617	28.39143	20.51371	-6.59305
BMP4	24.28215	20.79617	31.89929	20.51371	7.89961
BMP5	35.69939	20.79617	37.14349	20.51371	1.72656
BMP6	31.77471	20.79617	30.11338	20.51371	-1.37887
BMP7	34.62957	20.79617	36.89372	20.51371	2.54661
BMP8B;BMP8A	32.31136	20.79617	31.34903	20.51371	-0.67987
BMPR1A	29.27017	20.79617	30.30324	20.51371	1.31553
BMPR1B	30.79368	20.79617	30.65239	20.51371	0.14118
BMPR2	27.14548	20.79617	28.94415	20.51371	2.08113
CER1	undetermined	20.79617	37.24757	20.51371	#VALUE!
CHRD	36.04893	20.79617	undetermined	20.51371	#VALUE!
ENG	28.04512	20.79617	37.03303	20.51371	9.27038
FST	31.18040	20.79617	32.73969	20.51371	1.84175
GDF11	30.27658	20.79617	27.84155	20.51371	-2.15256
GDF1;LASS1	32.21234	20.79617	35.94738	20.51371	4.01750
GDF2	undetermined	20.79617	undetermined	20.51371	#VALUE!
GDF3	undetermined	20.79617	undetermined	20.51371	#VALUE!
GDF6	33.42246	20.79617	undetermined	20.51371	#VALUE!
GDF7	36.16139	20.79617	37.05927	20.51371	1.18034
GDF9	35.30662	20.79617	35.75269	20.51371	0.72854
GREM1	26.31441	20.79617	undetermined	20.51371	#VALUE!
INHA	36.58117	20.79617	34.67130	20.51371	-1.62740

Gene Name	SaOS2 (Confluent) Mean ct Value	GADH Mean ct Value	PC3RFP (Confluent) Mean ct Value	GADH Mean ct Value	Δ dct
INHBA	27.27427	20.79617	32.60780	20.51371	5.61599
INHBB	30.29594	20.79617	37.59675	20.51371	7.58327
INHBC	36.23087	20.79617	35.62355	20.51371	-0.32487
INHBE	32.29367	20.79617	33.93227	20.51371	1.92106
LEFTY2	35.69972	20.79617	37.92624	20.51371	2.50898
LTBP1	28.28688	20.79617	27.29221	20.51371	-0.71221
NBL1	27.53839	20.79617	27.63373	20.51371	0.37781
NOG	34.09049	20.79617	27.32347	20.51371	-6.48456
SOST	36.60133	20.79617	undetermined	20.51371	#VALUE!
TGFB1	24.28961	20.79617	27.31067	20.51371	3.30353
TGFB2	28.49725	20.79617	31.91540	20.51371	3.70062
TGFB3	29.29044	20.79617	29.63135	20.51371	0.62337
TGFBR1	28.23259	20.79617	28.60142	20.51371	0.65130
TGFBR2	27.90661	20.79617	28.88057	20.51371	1.25641

This Table shows the ct values and the differences in Δ dct value between PC3RFP cells compared to the SaOS2 cells during the Confluent Phase. The dct was calculated by subtracting the gene of interest from the house keeping gene GAPDH for each cell type. The Δ dct value was calculated by subtracting dct value of PC3RFP confluent from the dct value of the saOs2 cells. Highlighted value represents more than 10 fold change in gene expression. Data expressed as mean of 3 independent experiments.

Table 4A Express plate gene expression in confluent PC3RFP and MG63 cells.

Gene Name	PC3RFP (Confluent) Mean ct Value	GAPDH Mean ct Value	MG63 (Confluent) Mean ct Value	GAPDH Mean ct Value	Δ dct
ACVR1	29.61976751	20.51370811	27.45970345	22.97153473	-4.617890676
ACVR1B	31.2354126	20.51370811	31.9857645	22.97153473	-1.707474709
ACVR2A	30.92702103	20.51370811	30.46175385	22.97153473	-2.923093796
ACVR2A	30.73865573	20.51370811	30.46175385	22.97153473	-2.734728495
ACVR2B	32.49391492	20.51370811	34.45285702	22.97153473	-0.498884519
BMP10	#DIV/0!	20.51370811	#DIV/0!	22.97153473	#DIV/0!
BMP2	30.93079694	20.51370811	33.9507122	22.97153473	0.562088648
BMP3	28.39143181	20.51370811	37.18087006	22.97153473	6.331611633
BMP4	31.8992939	20.51370811	29.96717453	22.97153473	-4.389945984
BMP5	37.14348984	20.51370811	31.46509647	22.97153473	-8.136219978
BMP6	30.11337789	20.51370811	35.45298004	22.97153473	2.881775538
BMP7	36.89372444	20.51370811	29.96841526	22.97153473	-9.383135796
BMP8B;BMP8A	31.34903208	20.51370811	31.95696354	22.97153473	-1.849895159
BMPR1A	30.30324173	20.51370811	31.45823956	22.97153473	-1.302828789
BMPR1B	30.65238698	20.51370811	#DIV/0!	22.97153473	#DIV/0!
BMPR2	28.94414584	20.51370811	27.97273445	22.97153473	-3.429238002
CER1	37.24756622	20.51370811	36.50650787	22.97153473	-3.198884964
CHRD	#DIV/0!	20.51370811	33.97208977	22.97153473	#DIV/0!
ENG	37.03303146	20.51370811	24.9516983	22.97153473	-14.53915977
FST	32.73968506	20.51370811	32.96305561	22.97153473	-2.234456062
GDF11	27.84155464	20.51370811	30.45579052	22.97153473	0.156409264
GDF1;LASS1	35.94737625	20.51370811	26.95148277	22.97153473	-11.45372009
GDF2	#DIV/0!	20.51370811	#DIV/0!	22.97153473	#DIV/0!
GDF3	#DIV/0!	20.51370811	37.08481598	22.97153473	#DIV/0!
GDF6	#DIV/0!	20.51370811	31.43332863	22.97153473	#DIV/0!
GDF7	37.05926704	20.51370811	34.47594261	22.97153473	-5.041151047
GDF9	35.75269318	20.51370811	33.96159649	22.97153473	-4.248923302
GREM1	#DIV/0!	20.51370811	34.4677639	22.97153473	#DIV/0!
INHA	34.67130407	20.51370811	33.45564842	22.97153473	-3.673482259
INHBA	32.60780017	20.51370811	32.9467535	22.97153473	-2.118873278
INHBB	37.59674581	20.51370811	36.96137238	22.97153473	-3.093200048
INHBC	35.62354533	20.51370811	37.00120544	22.97153473	-1.080166499
INHBE	33.93226624	20.51370811	31.45604229	22.97153473	-4.93405056
LEFTY2	37.92624474	20.51370811	36.50269127	22.97153473	-3.881380081

Gene Name	PC3RFP (Confluent) Mean ct Value	GAPDH Mean ct Value	MG63 (Confluent) Mean ct Value	GAPDH Mean ct Value	Δ dct
LTBP1	27.29220645	20.51370811	27.45436859	22.97153473	-2.295664469
NBL1	27.63373184	20.51370811	26.47146511	22.97153473	-3.620093346
NOG	27.32346916	20.51370811	34.46164322	22.97153473	4.680347443
SOST	#DIV/0!	20.51370811	#DIV/0!	22.97153473	#DIV/0!
TGFB1	27.31066958	20.51370811	26.46272373	22.97153473	-3.305772463
TGFB2	31.91540209	20.51370811	34.45627117	22.97153473	0.083042463
TGFB3	29.63134766	20.51370811	32.96736717	22.97153473	0.878192902
TGFBR1	28.6014239	20.51370811	28.43787479	22.97153473	-2.62137572
TGFBR2	28.88056501	20.51370811	26.45248508	22.97153473	-4.885906537
TGFBR3	30.19827906	20.51370811	28.95666027	22.97153473	-3.699445407

This Table shows the ct values and the differences in Δ dct value between MG63 cells and PC3-RFP cells during the Confluent Phase. The dct was calculated by subtracting the gene of interest from the house keeping gene GAPDH for each cell type. The Δ dct value was calculated by subtracting dct value of PC3RFP confluent from the dct value of the MG63 cells. Highlighted value represents more than 10 fold change in gene expression. Data expressed as mean of 3 independent experiments.

Table 5A TGF β superfamily gene expression in co-culture SaOS2 compared to control SaOS2 cells.

Gene Name	SaOS2 (Control) ct Value	GAPDH ct Value	SaOS2 (Co-cultured) ct value	GAPDH ct Value	Δ dct
ACVR1	29.27659035	20.79617182	28.9532299	20.9656105	-0.492799123
ACVR1B	31.86755816	20.79617182	31.980299	20.9656105	-0.056697845
ACVR2A	30.89818891	20.79617182	29.95549583	20.9656105	-1.112131755
ACVR2A	30.70807838	20.79617182	29.95549583	20.9656105	-0.92202123
ACVR2B	31.12030538	20.79617182	29.97760201	20.9656105	-1.312142054
BMP10	36.63376427	20.79617182	Undetermined	20.9656105	#VALUE!
BMP2	31.26523209	20.79617182	31.93518066	20.9656105	0.500509898
BMP3	35.26694616	20.79617182	30.94885635	20.9656105	-4.487528483
BMP4	24.28214836	20.79617182	24.94000626	20.9656105	0.488419215
BMP5	35.69938914	20.79617182	35.94908905	20.9656105	0.08026123
BMP6	31.77471161	20.79617182	28.93636894	20.9656105	-3.007781347
BMP7	34.62957382	20.79617182	33.95807648	20.9656105	-0.840936025
BMP8B;BMP8A	32.31136322	20.79617182	30.97959328	20.9656105	-1.501208623
BMPR1A	29.27017148	20.79617182	29.9485302	20.9656105	0.508920034
BMPR1B	30.7936751	20.79617182	33.9930954	20.9656105	3.029981613
BMPR2	27.14547729	20.79617182	26.96865082	20.9656105	-0.346265157
CER1	#DIV/0!	20.79617182	Undetermined	20.9656105	#DIV/0!
CHRD	36.04893112	20.79617182	36.98843765	20.9656105	0.770067851
ENG	28.04511897	20.79617182	28.95251274	20.9656105	0.737955093
FST	31.18039767	20.79617182	30.96162796	20.9656105	-0.388208389
GDF11	30.27658081	20.79617182	28.94433784	20.9656105	-1.501681646
GDF1;LASS1	32.21234194	20.79617182	31.95088196	20.9656105	-0.430898666
GDF2	#DIV/0!	20.79617182	Undetermined	20.9656105	#DIV/0!
GDF3	#DIV/0!	20.79617182	Undetermined	20.9656105	#DIV/0!
GDF6	33.42245674	20.79617182	34.91986084	20.9656105	1.327965418
GDF7	36.16138713	20.79617182	35.96345139	20.9656105	-0.36737442

Gene Name	SaOS2 (Control) ct Value	GAPDH ct Value	SaOS2 (Co-cultured) ct value	GAPDH ct Value	Δ dct
GDF9	35.30661774	20.79617182	35.95517349	20.9656105	0.479117076
GREM1	26.31441498	20.79617182	30.96870232	20.9656105	4.484848658
INHA	36.58116913	20.79617182	34.96567917	20.9656105	-1.78492864
INHBA	27.27426974	20.79617182	26.95631599	20.9656105	-0.487392426
INHBB	30.29593849	20.79617182	30.96619797	20.9656105	0.500820796
INHBC	36.23087438	20.79617182	35.9522934	20.9656105	-0.448019663
INHBE	32.29367383	20.79617182	31.95554733	20.9656105	-0.50756518
LEFTY2	35.69972356	20.79617182	36.97317886	20.9656105	1.104016622
LTBP1	28.28687859	20.79617182	26.94904137	20.9656105	-1.507275899
NBL1	27.53838603	20.79617182	27.96681404	20.9656105	0.258989334
NOG	34.09048971	20.79617182	27.94402695	20.9656105	-6.315901438
SOST	36.6013298	20.79617182	35.99904633	20.9656105	-0.771722158
TGFB1	24.289608	20.79617182	23.96656036	20.9656105	-0.492486318
TGFB2	28.49724706	20.79617182	29.95263672	20.9656105	1.285950979
TGFB3	29.29043706	20.79617182	29.96563911	20.9656105	0.505763372
TGFBR1	28.23258909	20.79617182	28.93655777	20.9656105	0.534530004
TGFBR2	27.9066143	20.79617182	27.95667267	20.9656105	-0.119380315
TGFBR3	31.18359121	20.79617182	30.95687294	20.9656105	-0.396156947

This Table shows the ct values and the differences in Δ dct value between co-cultured SaOS2 cells and control SaOS2 cells during the Confluent Phase. The dct was calculated by subtracting the gene of interest from the house keeping gene GAPDH for each cell type. The Δ dct value was calculated by subtracting dct value of control from the dct value of the co-cultured SaOS2 cells. Highlighted value represents more than 10 fold change in gene expression. Data expressed as mean of 3 independent experiments.

Table 6A TGF β superfamily gene expression in co-cultured PC3RFP with SaOS2 compared to control PC3RFP cells.

Gene Name	PC3 (control) ct value	GADH ct value	PC3/SaOS2 (co-cultured) Ct value	GADH ct value	Δ dct
ACVR1	29.61976751	20.51371	27.96547699	19.95773315	-0.99360466
ACVR1B	31.2354126	20.51371	30.9859333	19.95773315	1.01010704
ACVR2A	30.92702103	20.51371	30.95611763	19.95773315	1.021625519
ACVR2A	30.73865573	20.51371	30.95611763	19.95773315	1.120658875
ACVR2B	32.49391492	20.51371	31.98219109	19.95773315	0.157283783
BMP10	#DIV/0!	20.51371	Undetermined	19.95773315	#VALUE!
BMP2	30.93079694	20.51371	30.95896149	19.95773315	1.035814285
BMP3	28.39143181	20.51371	29.9454174	19.95773315	2.211952209
BMP4	31.8992939	20.51371	30.95910645	19.95773315	0.010868073
BMP5	37.14348984	20.51371	37.07818604	19.95773315	0.950033188
BMP6	30.11337789	20.51371	28.97106934	19.95773315	0.051765442
BMP7	36.89372444	20.51371	37.01209259	19.95773315	1.203203201
BMP8B;BMP8A	31.34903208	20.51371	30.97738266	19.95773315	0.736444473
BMPR1A	30.30324173	20.51371	31.94968796	19.95773315	2.65476799
BMPR1B	30.65238698	20.51371	33.00383759	19.95773315	3.037137985
BMPR2	28.94414584	20.51371	27.96653938	19.95773315	0.007659912
CER1	37.24756622	20.51371	Undetermined	19.95773315	#VALUE!
CHRD	#DIV/0!	20.51371	Undetermined	19.95773315	#VALUE!
ENG	37.03303146	20.51371	36.94768524	19.95773315	0.83490181
FST	32.73968506	20.51371	29.96795845	19.95773315	-1.975879669
GDF11	27.84155464	20.51371	26.95577049	19.95773315	-0.00038147
GDF1;LASS1	35.94737625	20.51371	34.95160294	19.95773315	0.020875931
GDF2	#DIV/0!	20.51371	Undetermined	19.95773315	#VALUE!
GDF3	#DIV/0!	20.51371	Undetermined	19.95773315	#VALUE!
GDF6	#DIV/0!	20.51371	Undetermined	19.95773315	#VALUE!
GDF7	37.05926704	20.51371	Undetermined	19.95773315	#VALUE!
GDF9	35.75269318	20.51371	35.97348022	19.95773315	1.016462326
GREM1	#DIV/0!	20.51371	Undetermined	19.95773315	#VALUE!
INHA	34.67130407	20.51371	32.95661545	19.95773315	-0.998556137
INHBA	32.60780017	20.51371	30.9564724	19.95773315	-0.993232727
INHBB	37.59674581	20.51371	37.01879883	19.95773315	-0.601884842
INHBC	35.62354533	20.51371	35.96622086	19.95773315	1.01067543

Gene Name	PC3 (control) ct value	GADH ct value	PC3/SaOS2 (co-cultured) Ct value	GADH ct value	Δ dct
INHBE	33.93226624	20.51371	31.95113182	19.95773315	-1.012889862
LEFTY2	37.92624474	20.51371	37.06781387	19.95773315	#VALUE!
LTBP1	27.29220645	20.51371	26.95423508	19.95773315	1.011125565
NBL1	27.63373184	20.51371	28.97649002	19.95773315	2.018360138
NOG	27.32346916	20.51371	25.96490479	19.95773315	-0.420198441
SOST	#DIV/0!	20.51371	37.05952454	19.95773315	#VALUE!
TGFB1	27.31066958	20.51371	26.9741497	19.95773315	1.012626648
TGFB2	31.91540209	20.51371	32.96443558	19.95773315	2.149311066
TGFB3	29.63134766	20.51371	31.96960831	19.95773315	3.00856781
TGFBR1	28.6014239	20.51371	28.93507767	19.95773315	1.006612778
TGFBR2	28.88056501	20.51371	27.94732666	19.95773315	-0.011320114
TGFBR3	30.19827906	20.51371	29.94961548	19.95773315	1.013208389

This Table shows the ct values and the differences in Δ dct value the estimated fold change between co-cultured PC3RFP/with SaOS2 cells and control PC3RFP cells during the Confluent Phase. The Δ dct was calculated by subtracting the gene of interest from the house keeping gene GAPDH for each cell type. The ddct value was calculated by subtracting Δ dct value of control from the dct value of the co-cultured PC3RFP/with SaOS2 cells. Data expressed as mean of 3 independent experiments.

Table 7A TGF β superfamily gene expression in co-culture MG63 compared to control MG63 cells.

Gene Name	MG63 (control) ct Value	GAPDH ct Value	MG63 (Co-cultured) ct Value	GAPDH ct Value	Δ dct
ACVR1	27.45970345	22.97153473	27.55764008	22.96488571	0.104585648
ACVR1B	31.9857645	22.97153473	31.67817497	22.96488571	-0.300940514
ACVR2A	30.46175385	22.97153473	36.96150589	22.96488571	6.506401062
ACVR2B	34.45285702	22.97153473	30.74513245	22.96488571	-3.701075554
BMP10	#DIV/0!	22.97153473	Undetermined	22.96488571	#DIV/0!
BMP2	33.9507122	22.97153473	33.95262527	22.96488571	0.008562088
BMP3	37.18087006	22.97153473	34.94942856	22.96488571	-2.22479248
BMP4	29.96717453	22.97153473	29.96358109	22.96488571	0.003055573
BMP5	31.46509647	22.97153473	31.99669647	22.96488571	0.538249016
BMP6	35.45298004	22.97153473	34.03453827	22.96488571	-1.411792755
BMP7	29.96841526	22.97153473	30.89259148	22.96488571	0.930825233
BMP8B;BMP8A	31.95696354	22.97153473	32.98453522	22.96488571	1.034220695
BMPR1A	31.45823956	22.97153473	30.94623184	22.96488571	-0.505358696
BMPR1B	#DIV/0!	22.97153473	Undetermined	22.96488571	#DIV/0!
BMPR2	27.97273445	22.97153473	27.83947182	22.96488571	-0.126613617
CER1	36.50650787	22.97153473	36.98629379	22.96488571	0.486434937
CHRD	33.97208977	22.97153473	30.43661118	22.96488571	-3.528829575
ENG	24.9516983	22.97153473	24.95506859	22.96488571	0.010019302
FST	32.96305561	22.97153473	31.77300835	22.96488571	-1.183398247
GDF11	30.45579052	22.97153473	29.44002342	22.96488571	-1.00911808
GDF1;LASS1	26.95148277	22.97153473	27.34437943	22.96488571	0.39954567
GDF2	#DIV/0!	22.97153473	Undetermined	22.96488571	#DIV/0!
GDF3	37.08481598	22.97153473	Undetermined	22.96488571	#VALUE!
GDF6	31.43332863	22.97153473	29.7163887	22.96488571	-1.710290909
GDF7	34.47594261	22.97153473	35.96851349	22.96488571	1.499219894
GDF9	33.96159649	22.97153473	33.49467468	22.96488571	-0.460272789
GREM1	34.4677639	22.97153473	30.62531471	22.96488571	-3.835800171
INHA	33.45564842	22.97153473	31.95536613	22.96488571	-1.49363327
INHBA	32.9467535	22.97153473	32.61723328	22.96488571	-0.322871208
INHBB	36.96137238	22.97153473	37.03042984	22.96488571	0.075706482

Gene Name	MG63 (control) ct Value	GAPDH ct Value	MG63 (Co-cultured) ct Value	GAPDH ct Value	Δ dct
INHBC	37.00120544	22.97153473	36.96479797	22.96488571	-0.029758453
INHBE	31.45604229	22.97153473	31.71233749	22.96488571	0.262944221
LEFTY2	36.50269127	22.97153473	Undetermined	22.96488571	#VALUE!
LTBP1	27.45436859	22.97153473	26.56694794	22.96488571	-0.880771637
NBL1	26.47146511	22.97153473	25.97489738	22.96488571	-0.489918709
NOG	34.46164322	22.97153473	31.98920059	22.96488571	-2.46579361
SOST	#REF!	22.97153473	Undetermined	22.96488571	#REF!
TGFB1	26.46272373	22.97153473	26.31716919	22.96488571	-0.138905525
TGFB2	34.45627117	22.97153473	34.63266373	22.96488571	0.183041573
TGFB3	32.96736717	22.97153473	31.81608772	22.96488571	-1.144630432
TGFBR1	28.43787479	22.97153473	28.2257843	22.96488571	-0.205441475
TGFBR2	26.45248508	22.97153473	26.95654869	22.96488571	0.510712624
TGFBR3	28.95666027	22.97153473	29.66415405	22.96488571	0.714142799

This Table shows the ct values and the differences in Δ dct between the co-cultured MG63 cells and the control MG63 cells during the Confluent Phase. The dct was calculated by subtracting the gene of interest from the house keeping gene GAPDH for each cell type. The Δ dct value was calculated by subtracting dct value of control from the dct value of the co-cultured MG63 cells. Highlighted value represents approximant 10 fold change in gene expression. Data expressed as mean of 3 independent experiments.

Table 8A TGF β superfamily gene expression in co-cultured PC3RFP with MG63 compared to control PC3RFP cells.

Gene Name	PC3 (Control) ct value	GADH ct value	PC3/MG63 (Co-cultured) Ct value	GADH ct value	Δ dct
ACVR1	29.61976751	20.51370811	28.97067451	22.26200676	-2.397391637
ACVR1B	31.2354126	20.51370811	30.99282837	22.26200676	-1.990882874
ACVR2A	30.92702103	20.51370811	Undetermined	22.26200676	#VALUE!
ACVR2A	30.73865573	20.51370811	Undetermined	22.26200676	#VALUE!
ACVR2B	32.49391492	20.51370811	31.97089386	22.26200676	-2.271319707
BMP10	#DIV/0!	20.51370811	Undetermined	22.26200676	#DIV/0!
BMP2	30.93079694	20.51370811	32.17337799	22.26200676	-0.505717595
BMP3	28.39143181	20.51370811	31.51320839	22.26200676	1.373477936
BMP4	31.8992939	20.51370811	32.49723053	22.26200676	-1.150362015
BMP5	37.14348984	20.51370811	36.97239685	22.26200676	-1.919391632
BMP6	30.11337789	20.51370811	31.93276978	22.26200676	0.071093241
BMP7	36.89372444	20.51370811	35.96075439	22.26200676	-2.681268692
BMP8B;BMP8A	31.34903208	20.51370811	32.85150909	22.26200676	-0.245821635
BMPR1A	30.30324173	20.51370811	32.5143013	22.26200676	0.462760925
BMPR1B	30.65238698	20.51370811	33.99121857	22.26200676	1.590532939
BMPR2	28.94414584	20.51370811	28.98261261	22.26200676	-1.709831874
CER1	37.24756622	20.51370811	Undetermined	22.26200676	#VALUE!
CHRD	#DIV/0!	20.51370811	37.004776	22.26200676	#DIV/0!
ENG	37.03303146	20.51370811	30.94250298	22.26200676	-7.838827133
FST	32.73968506	20.51370811	32.9630661	22.26200676	-1.524917603
GDF11	27.84155464	20.51370811	27.95772743	22.26200676	-1.632125854
GDF1;LASS1	35.94737625	20.51370811	32.95769882	22.26200676	-4.737976074
GDF2	#DIV/0!	20.51370811	Undetermined	22.26200676	#DIV/0!
GDF3	#DIV/0!	20.51370811	Undetermined	22.26200676	#DIV/0!
GDF6	#DIV/0!	20.51370811	35.94604111	22.26200676	#DIV/0!
GDF7	37.05926704	20.51370811	Undetermined	22.26200676	#VALUE!
GDF9	35.75269318	20.51370811	36.96233368	22.26200676	-0.538658142
GREM1	#DIV/0!	20.51370811	37.06842041	22.26200676	#DIV/0!
INHA	34.67130407	20.51370811	34.91033554	22.26200676	-1.509267171
INHBA	32.60780017	20.51370811	30.95749855	22.26200676	-3.39860026
INHBB	37.59674581	20.51370811	39.07902908	22.26200676	-0.266015371
INHBC	35.62354533	20.51370811	35.305233	22.26200676	-2.066610972
INHBE	33.93226624	20.51370811	30.96523857	22.26200676	-4.715326309

Gene Name	PC3 (Control) ct value	GADH ct value	PC3/MG63 (Co-cultured) Ct value	GADH ct value	Δ dct
LEFTY2	37.92624474	20.51370811	Undetermined	22.26200676	#VALUE!
LTBP1	27.29220645	20.51370811	27.95863914	22.26200676	-1.081865946
NBL1	27.63373184	20.51370811	28.77157402	22.26200676	-0.610456467
NOG	27.32346916	20.51370811	28.9696579	22.26200676	-0.102109909
SOST	#DIV/0!	20.51370811	Undetermined	22.26200676	#DIV/0!
TGFB1	27.31066958	20.51370811	26.9671917	22.26200676	-2.09177653
TGFB2	31.91540209	20.51370811	34.96070862	22.26200676	1.297007879
TGFB3	29.63134766	20.51370811	29.97441864	22.26200676	-1.405227661
TGFBR1	28.6014239	20.51370811	32.97459793	22.26200676	2.624875387
TGFBR2	28.88056501	20.51370811	27.96858025	22.26200676	-2.660283407
TGFBR3	30.19827906	20.51370811	31.95786476	22.26200676	0.011287053

This Table represents the ct value and the differences in Δ dct between co-cultured PC3RFP/with MG63 cells and control PC3RFP cells during the Confluent Phase. The dct was calculated by subtracting the gene of interest from the house keeping gene GAPDH for each cell type. The Δ dct value was calculated by subtracting dct value of control from the dct value of the co-cultured PC3RFP/with MG63 cells. Highlighted value represents more than 10 fold change in gene expression. Data expressed as mean of 3 independent experiments.

Table 9A Expressed plate gene expression in confluent SaOS2 compared to SaOS2 treated with PC3RFP-CM.

Gene Name	SaOS2 in 2%DMEM ct value	GAPDH ct value	SaOS2 treated with CM ct value	GAPDH ct value	Δ dct
ACVR1	29.9361897	21.9097481	29.7593397	22.6219705	-0.88907241
ACVR1B	32.9362526	21.9097481	35.0935148	22.6219705	1.44503975
ACVR2A	31.8985271	21.9097481	32.0458132	22.6219705	-0.56493632
ACVR2B	31.7777367	21.9097481	32.6348483	22.6219705	0.1448892
BMP10	36.3345566	21.9097481	undetermined	22.6219705	#VALUE!
BMP2	31.9093113	21.9097481	33.7084211	22.6219705	1.08688736
BMP3	35.96268845	21.90974808	36.7482605	22.6219705	0.07334964
BMP4	24.9498692	21.9097481	26.0465806	22.6219705	0.38448906
BMP5	36.6571846	21.9097481	36.9717407	22.6219705	-0.39766629
BMP6	32.7582245	21.9097481	34.4436061	22.6219705	0.97315916
BMP7	35.3900375	21.9097481	34.8728905	22.6219705	-1.22936948
BMP8B;BMP8A	32.7899208	21.9097481	35.0839691	22.6219705	1.5818259
BMPR1A	29.9286213	21.9097481	32.8083452	22.6219705	2.16750146
BMPR1B	30.9656487	21.9097481	undetermined	22.6219705	#VALUE!
BMPR2	27.6560421	21.9097481	28.9718819	22.6219705	0.60361736
CER1	Undetermined	21.9097481	undetermined	22.6219705	#VALUE!
CHRD	37.0776863	21.9097481	undetermined	22.6219705	#VALUE!
ENG	28.6491699	21.9097481	28.6326841	22.6219705	-0.72870826
FST	31.8238277	21.9097481	33.6058566	22.6219705	1.06980642
GDF11	30.9474697	21.9097481	31.2135086	22.6219705	-0.44618351
GDF1;LASS1	32.846386	21.9097481	32.9003754	22.6219705	-0.658233
GDF2	Undetermined	21.9097481	undetermined	22.6219705	#VALUE!
GDF3	Undetermined	21.9097481	undetermined	22.6219705	#VALUE!
GDF6	33.9198875	21.9097481	34.9344215	22.6219705	0.30231158
GDF7	37.1187057	21.9097481	undetermined	22.6219705	#VALUE!
GDF9	35.9574242	21.9097481	35.0351753	22.6219705	-1.63447126
GREM1	26.9796486	21.9097481	28.3748976	22.6219705	0.68302664
INHA	36.9917336	21.9097481	35.9733238	22.6219705	-1.73063214
INHBA	27.9405727	21.9097481	28.2518749	22.6219705	-0.40092023
INHBB	30.9800072	21.9097481	31.9825058	22.6219705	0.29027622
INHBC	36.9617653	21.9097481	35.9407425	22.6219705	-1.73324521
INHBE	32.964592	21.9097481	32.2814961	22.6219705	-1.39531834
LEFTY2	37.0844574	21.9097481	undetermined	22.6219705	#VALUE!
LTBP1	28.9520969	21.9097481	30.9648317	22.6219705	1.30051232
NBL1	27.9620457	21.9097481	28.3815346	22.6219705	-0.2927335
NOG	34.96133041	21.90974808	32.1427184	22.62197049	-3.530834426

Gene Name	SaOS2 in 2%DMEM ct value	GAPDH ct value	SaOS2 treated with CM ct value	GAPDH ct value	Δ dct
SOST	36.9237061	21.9097481	35.9734052	22.6219705	-1.66252327
TGFB1	24.9865398	21.9097481	24.093015	22.6219705	-1.60574722
TGFB2	29.5937691	21.9097481	31.7834988	22.6219705	1.47750727
TGFB3	29.9523315	21.9097481	31.3046659	22.6219705	0.64011192
TGFBR1	28.8648186	21.9097481	30.9559104	22.6219705	1.37886937
TGFBR2	28.7812004	21.9097481	29.4020443	22.6219705	-0.09137852
TGFBR3	31.6579971	21.9097481	31.8710289	22.6219705	-0.49919064

This Table shows the ct values and the differences in Δ dct between confluent SaOS2 cells and SaOS2 treated with PC3RFP-CM. The dct was calculated by subtracting the gene of interest from the house keeping gene GAPDH for each cell type. The Δ dct value was calculated by subtracting dct value of confluent SaOS2 from the dct value of the treated SaOS2 cells. Highlighted value represents more than 10 fold change in gene expression. Data expressed as mean of 3 independent experiments.

Table 10A TGF β superfamily gene expression in confluent MG63 compared to MG63 treated with PC3RFP-CM.

Gene Name	MG63 in 4%DMEM ct value	GADH ct value	MG63 treated with CM ct value	GADH ct value	Δ dct
ACVR1	27.45970345	22.97153473	29.36	21.3249569	3.54687439
ACVR1B	31.9857645	22.97153473	32.2369	21.3249569	1.89771334
ACVR2A	30.46175385	22.97153473	29.18759	21.3249569	0.37241399
ACVR2B	34.45285702	22.97153473	33.1367	21.3249569	0.33042082
BMP10	#DIV/0!	22.97153473	undetermined	21.3249569	#DIV/0!
BMP2	33.9507122	22.97153473	35.2566	21.3249569	2.95246564
BMP3	37.18087006	22.97153473	38.5057	21.3249569	2.97140778
BMP4	29.96717453	22.97153473	30.5732	21.3249569	2.25260331
BMP5	31.46509647	22.97153473	33.58139	21.3249569	3.76287137
BMP6	35.45298004	22.97153473	35.77146	21.3249569	1.9650578
BMP7	29.96841526	22.97153473	32.2354	21.3249569	3.91356258
BMP8B;BMP8A	31.95696354	22.97153473	32.63694	21.3249569	2.3265543
BMPR1A	31.45823956	22.97153473	30.1761888	21.3249569	0.36452707
BMPR1B	#DIV/0!	22.97153473	undetermined	21.3249569	#DIV/0!
BMPR2	27.97273445	22.97153473	27.2886569	21.3249569	0.96250026
CER1	36.50650787	22.97153473	37.09848	21.3249569	2.23854997
CHRD	33.97208977	22.97153473	35.6306597	21.3249569	3.30514781
ENG	24.9516983	22.97153473	28.6288312	21.3249569	5.32371077
FST	32.96305561	22.97153473	34.4833489	21.3249569	3.16687108
GDF11	30.45579052	22.97153473	32.7764193	21.3249569	3.96720664
GDF1;LASS1	26.95148277	22.97153473	28.0790685	21.3249569	2.77416357
GDF2	#DIV/0!	22.97153473	undetermined	21.3249569	#DIV/0!
GDF3	37.08481598	22.97153473	undetermined	21.3249569	#VALUE!
GDF6	31.43332863	22.97153473	33.523049	21.3249569	3.73629825
GDF7	34.47594261	22.97153473	35.9563777	21.3249569	3.1270129
GDF9	33.96159649	22.97153473	35.682586	21.3249569	3.36756738

Gene Name	MG63 in 4%DMEM ct value	GADH ct value	MG63 treated with CM ct value	GADH ct value	Δ dct
GREM1	34.4677639	22.97153473	34.9466026	21.3249569	2.12541652
INHA	33.45564842	22.97153473	34.4658814	21.3249569	2.65681077
INHBA	32.9467535	22.97153473	32.4657466	21.3249569	1.1655709
INHBB	36.96137238	22.97153473	37.0014827	21.3249569	1.68668811
INHBC	37.00120544	22.97153473	34.6946348	21.3249569	-0.65999285
INHBE	31.45604229	22.97153473	29.0104961	21.3249569	-0.79896831
LEFTY2	36.50269127	22.97153473	36.6241201	21.3249569	1.76800665
LTBP1	27.45436859	22.97153473	26.37953	21.3249569	0.5717392
NBL1	26.47146511	22.97153473	28.5694281	21.3249569	3.74454086
NOG	34.46164322	22.97153473	34.0599168	21.3249569	1.24485143
SOST	undetermined	22.97153473	undetermined	21.3249569	undetermined
TGFB1	26.46272373	22.97153473	26.1342055	21.3249569	1.31805961
TGFB2	34.45627117	22.97153473	31.5706183	21.3249569	-1.23907502
TGFB3	32.96736717	22.97153473	31.7616317	21.3249569	0.44084232
TGFBR1	28.43787479	22.97153473	31.9628773	21.3249569	5.17158031
TGFBR2	26.45248508	22.97153473	29.1504873	21.3249569	4.34458001
TGFBR3	28.95666027	22.97153473	31.8689219	21.3249569	4.55883949

This Table shows the ct values and the differences in Δ dct between confluent MG63 and MG63 treated with PC3RFP-CM. The dct was calculated by subtracting the gene of interest from the house keeping gene GAPDH for each cell type. The Δ dct value was calculated by subtracting dct value of control from the dct value of the co-cultured PC3RFP/with MG63 cells. Highlighted value represents more than 10 fold change in gene expression. Data expressed as mean of 3 independent experiments.